

**BIOGAS PRODUCTION FROM KITCHEN WASTE CO-DIGESTED WITH
SELECTED MUNICIPAL SOLID WASTE AND ITS PURIFICATION USING
SODA ASH FROM LAKE NATRON AND EGGSHELL WASTE**

BY

REGISTER W. MROSSO

**A Thesis Submitted to the School of Engineering, Department of Mechanical,
Production, and Energy Engineering in Partial Fulfilment of the
Requirements for the Award of the Degree of
Doctor of Philosophy in Energy Studies**

Moi University

2023

DECLARATION

Declaration by Candidate

I hereby declare that this thesis entitled “**Biogas production from kitchen waste co-digested with some selected municipal solid waste and its purification using soda ash from Lake Natron and eggshells waste**” is my work and has not been presented for a degree in any other university. No part of this thesis may be reproduced without the prior written permission of the author and/or Moi University.

Signature:  Date: 15-11-2023

Register Mrosso

PhD/ES/5731/21

Declaration by Supervisors

We declare that this thesis has been submitted for examination with our approval as University Supervisors.

Signature:  Date: 15-11-2023

Dr. Cleophas Achisa Mecha

Department of Chemical and Process Engineering

School of Engineering

Moi University, Eldoret, Kenya

Signature:  Date: 15-11-2023

Dr. Joseph Kiplagat

Department of Mechanical, Production, and Energy Engineering

School of Engineering

Moi University, Eldoret, Kenya

DEDICATION

The current work is dedicated to my beloved husband Dr. Eusebi Romwald Goima, who has always believed in me and provided encouragement, especially during coursework moment and data collection. This also goes to my beloved children Philipina, Ian, and Ezra, for their encouragement, care, love, support, and patience.

ACKNOWLEDGEMENT

I would like to thank the almighty God for his endless boundaries of keeping my healthy and mental state fit to undertake studies at Moi University, School of Engineering.

I am immensely indebted to my supervisors Dr. Cleophas Achisa and Joseph Kiplagat for their active supervision and upkeep through this research work.

I gratefully acknowledge the Mobility for Innovative Renewable Energy Technologies (MIRET) [grant number 614658-1-2018-1-KE-PANAF-MOBAF] via the African Center of Excellence in Phytochemical, Textile, and Renewable Energy (ACE II PTRE) for the financial provision without which the current study could not be possible. I am grateful to the School of Engineering for allowing me to use their school laboratory facilities from mechanical, chemistry, and biological laboratories. I thank Dr. Stephen Talai, Prof. Ambrose Kiprop, and Madam Irene for their guidance, support, and encouragement in completing this study. Additionally, I am thankful to the lab technicians and the Department of Mechanical, Production, and Engineering colleagues for their advice and technical support during lab work preparation.

I am thankful to Mr. Sengwer from Kesses, Eldoret, for providing an opportunity for me to conduct sorption experiments within his residence house, Prof Karol Njau from Nelson Mandela African Institution of Science and Technology, and Center for Agricultural Mechanization and Rural Technology institution in Tanzania for their instrumental support during sorption experiment. Moreover, I am very thankful to my lovely husband Dr. Eusebi Romwald Goima, for taking care of the family in my absence. I thank my beloved kids Philipina, Ian, and Ezra for their encouragement and prayers and I thank them for their patience when they missed my parental care, especially during lab work moments. Lastly, I acknowledge my parents for their schooling.

ABSTRACT

The amount of kitchen and municipal waste increases along with consumption standards and urbanization, thus, most cities face the problem of managing it. It can be transformed into energy, addressing the twin challenges of waste management and energy insecurity. The presence of impurities in biogas limits its application hence purification needed. This study investigated the potential of kitchen waste co-digested with municipal solid waste for biogas production and purification using soda ash and eggshells. The specific objectives were to: characterize kitchen waste and municipal solid waste for biogas production; optimize the biogas production through co-digestion; assess the adsorption ability of soda ash and eggshells sorbents; evaluate their regeneration and reuse; and modeling of fixed bed adsorption studies. Standard methods characterized kitchen and municipal solid waste for moisture content, volatile solids, and total solids. Biogas was collected via water displacement method, and digestion temperatures were 20-40°C. Brunauer-Emmett-Teller, Barrett-Joyner-Halenda, and quanta chrome NOVA 4200 methods were used for sorbent characterization. Biogas purification was conducted using soda ash from Lake Natron and eggshell waste. The effect of particle size (280-400 μm), sorbent mass (25-75g), flow rate (0.03-0.04 m^3/h), and calcination temperature (750-900°C) for eggshells was studied. Regeneration was done via soda ash exposure in air, for 1, 5, and 7 days, eggshells were re-calcinated under 750°C. The data were fitted into kinetic and breakthrough models. The results indicated that cabbage contained 96.36 \pm 1.73% volatile solid produced a biogas yield of 800 \pm 8.8mL within 10 days, while cooked rice had an 83.00 \pm 1.49% volatile solid, produced biogas 2821 \pm 31.03mL within 28 days. Furthermore, co-digestion of kitchen and municipal solid waste showed that a mixing ratio of 1:1 produced the highest biogas yield (2907 \pm 32mL). The lowest yield of 2907 \pm 32mL was obtained at 20°C while the highest yield of 4963 \pm 54.6mL was obtained at 40°C. Regarding pH, the yield was 2808 \pm 31mL at pH 6.5 and 7810 \pm 86mL at pH 7.3, indicating a 178.1% increase in biogas yield. Samples sieved at 280 μm , 75g, and a flow rate of 0.03 m^3/h perform best with a removal efficiency of 94%, and sorption capacity (SC) of 0.02g/100g for soda ash while eggshells calcined at 850°C, had a RE of 83%, SC of 5.0g/100g. Regeneration for 7 days of exposure showed the highest RE of 90%. Meanwhile, in the first cycle, regenerated eggshells showed a RE of 79.8% and an SC of 4.97g/100g. The experimental data fitted well to the Freundlich for both H₂S and CO₂ removal with a range of 0<1/n<1. Breakthrough studies showed that the data for carbon dioxide was best fitted to the Thomas model with R² 0.94-0.99 while for H₂S removal Yoon-Nelson model was the best with R² 0.93-0.98. The CO₂ and H₂S uptake were fitted well to the intra-particle model. In conclusion, cooked rice waste could be mono-digested while others require co-digestion to increase yield. The high RE and SC obtained show that soda ash and eggshells are promising materials for biogas purification. The study recommends the use of bio-waste in biogas production to address the twin challenges of waste management and energy insecurity.

TABLE OF CONTENTS

DECLARATION	ii
DEDICATION	iii
ACKNOWLEDGEMENT	iv
ABSTRACT.....	v
TABLE OF CONTENTS.....	vi
LIST OF TABLES	xii
LIST OF FIGURES	xv
ABBREVIATIONS	xix
CHAPTER ONE	1
INTRODUCTION.....	1
1.1 Background of the Study	1
1.2 Statement of the Problem.....	8
1.3 Objectives	9
1.3.1 General objective	9
1.3.2 Specific objectives	9
1.4 Research Questions.....	10
1.5 Significance of the Study	10
1.6 Delineation of the Study	11
CHAPTER TWO	12
LITERATURE REVIEW	12
2.1 General Overview	12
2.2 Biogas Production Technology.....	13
2.3 Kitchen Waste and Municipal Solid Waste for Biogas Production.....	14
2.4 Characterization of Kitchen Waste and Municipal Solid Waste for Biogas Production	15
2.5 Feedstock Selection for Biogas Production	17
2.6 Anaerobic Digestion	19
2.6.1 Hydrolysis	20
2.6.2 Acidogenesis	21
2.6.3 Acetogenesis	21
2.6.4 Methanogenesis.....	22
2.7 Mono-digestion of Different Food Waste and Municipal Solid Waste	22

2.8 Co-digestion.....	23
2.9 Synergic Effect.....	26
2.10 Pre-treatment Methods.....	27
2.10.1 Physical pre-treatment	28
2.10.2 Chemical pre-treatment.....	29
2.10.3 Biological pre-treatment	29
2.11 Biogas Digesters and Process	30
2.11.1 Batch and Continuous anaerobic digestion processes	30
2.11.2 Single-stage and two-stage anaerobic digestion processes.....	31
2.11.3 Liquid and Solid anaerobic digestion process	32
2.12 Variation in Operational Parameters.....	33
2.13 Limitations and Benefits of the Anaerobic Digestion Process	33
2.14 Factors Affecting Biogas Production.....	35
2.14.1 Volatile Fatty acid (VFA)	36
2.14.2 Biodegradability.....	37
2.14.3 Organic loading time (OLR).....	38
2.14.4 Hydraulic retention time (HRT).....	40
2.14.5 Temperature	41
2.14.6 Operating pH.....	43
2.14.7 Particle size	44
2.14.8 Carbon to nitrogen ratio (CN).....	46
2.14.9 Presence of heavy metals in the feedstock for biogas production	47
2.15 Effect of Design of a Digester on Biogas Production.....	49
2.16 Inoculum	50
2.17 Mathematical Modeling and Simulation in Adsorption.....	51
2.17.1 Adsorption modeling	51
2.17.1.1 Adams-Bohart model	51
2.17.1.2 Thomas model.....	52
2.17.1.3 Yoon-Nelson model	53
2.17.2 Adsorption Isotherms.....	54
2.17.2.1 The Langmuir isotherm.....	55
2.17.2.2 The Freundlich isotherm	58
2.17.2.3 The Jovanovich isotherm	59
2.17.3 Adsorption kinetics	60

2.18 Presence of Impurities in Biogas	61
2.19 Methods for Purification	62
2.19.1 Chemical methods.....	62
2.19.2 Physical methods	66
2.19.3 Water scrubbing methods method	67
2.19.4 Biological Method or Chemoautotrophic	68
2.19.5 Cryogenic upgrading method.....	69
2.19.6 Pressure swing adsorption (PSA).....	70
2.19.7 Membrane upgrading method	72
2.20 Regeneration of the Spent Sorbent	74
CHAPTER THREE	77
MATERIALS AND METHODS	77
3.1 Material Used.....	77
3.2 Equipment.....	78
3.3 Methods.....	78
3.3.1 Determination of moisture content	78
3.3.2 Determination of total solid (TS).....	79
3.3.3 Determination of total volatile solid (TVS)	79
3.4 Experimental Setup for Mono-Digestion.....	80
3.5 Experimental Setup for Co-digestion.....	81
3.5.1 Experimental setup for co-digestion on the effect of mixing ratio	83
3.5.2 Experimental setup for co-digestion on the effect of temperature.....	83
3.5.3 Experimental setup for co-digestion on the effect of pH.....	84
3.6 The Quantification of Lab-Scale Biogas.....	85
3.7 Sorbent Preparation for Biogas Purification	85
3.7.1 Eggshells collection and calcination.....	85
3.7.2 Soda ash collection and preparation	86
3.8 Material Characterization.....	87
3.9 Purification Experiments	87
3.9.1 Adsorption and performance evaluation using soda ash from Lake Natron... 88	
3.9.2 Adsorption of carbon dioxide and performance evaluation using eggshell waste.....	90
3.10 Regeneration Process	90
3.10.1 Regeneration of spent soda ash.....	90

3.10.2	Regeneration of spent eggshells waste	91
3.11	Adsorption Isotherms	91
3.11.1	Langmuir Isotherm.....	91
3.11.2	Freundlich isotherm	92
3.11.3	Jovanovich	93
3.12	Adsorption Modeling	94
3.12.1	Adams-Bohart model.....	94
3.12.2	Thomas model.....	95
3.12.3	Yoon-Nelson	96
3.13	Adsorption Kinetics	96
3.13.1	Pseudo-first-order kinetics (PFO)	96
3.13.2	Pseudo-sec-order kinetics (PSO)	97
3.13.3	Elovich adsorption kinetics.....	98
3.13.4	Intra particles diffusion.....	98
CHAPTER FOUR.....		100
RESULTS AND DISCUSSIONS		100
4.1	Characterization of Kitchen Waste and Municipal Solid Waste for Biogas Production	100
4.2	Physical-chemical Analysis	106
4.3	Mono-digestion of Kitchen Waste and Municipal Solid Waste Substrates	107
4.3.1	Biogas yield from different substrates	108
4.3.2	Effect of total solid content on biogas yield	111
4.3.3	Effect of total volatile solids on biogas yield.....	112
4.4	Co-digestion of Different Substrates	113
4.4.1	Effect of substrate mixing ratios	115
4.4.2	Effect of temperature on biogas yield.....	118
4.4.3	Effect of pH on biogas yield	120
4.5	Synergy Effect of Anaerobic co-digestion.....	122
4.6	Biogas Composition from Onsite Digesters	123
4.7	Characterization of the sorbents.....	124
4.7.1	Textural properties of the soda ash adsorbent.....	124
4.7.2	Sorbent morphology/Soda ash morphological structure.....	125
4.8	Mineral composition and pH of soda ash sorbent.....	127
4.9	Adsorption Ability of Soda Ash	128

4.9.1 Effect of adsorbent mass	128
4.9.2 Effect of particle size	130
4.9.3 Effect of biogas flow rate.....	132
4.10 A comparison of soda ash with other sorbent materials used in literature	133
4.11 Textural properties of the eggshell waste	134
4.12 The Surface Morphological Studies of Calcined Eggshell Waste	137
4.13 Mineral Composition and Eggshell Sorbent	138
4.14 Adsorption Ability of Calcined Eggshells Sorbent.....	139
4.14.1 Effect of particle size	139
4.14.2 Effect of mass of CaO derived from eggshells on the adsorption ability ...	141
4.14.3 Effect of biogas flow rate on the adsorption process	141
4.14.4. Effect of calcination temperature on the adsorption process	143
4.15 A Comparison of Eggshell Waste with Other Sorbent used in Literature	145
4.16 Sorbent Regeneration.....	145
4.16.1 Regeneration of soda ash sorbent for hydrogen sulfide removal.....	145
4.16.2 Regeneration of eggshell waste sorbent for carbon dioxide removal	148
4.17 Equilibrium Adsorption Isotherms	149
4.17.1 The Langmuir isotherm.....	149
4.17.2 The Freundlich adsorption isotherm	150
4.17.3 The Jovanovich adsorption isotherm	151
4.18 Adsorption Modeling	153
4.18.1 Adams–Bohart model for the removal of carbon dioxide from biogas	153
4.18.2 Adams–Bohart model for the removal of hydrogen sulfide from biogas ...	156
4.18.3 Thomas model for carbon dioxide removal from biogas	158
4.18.4 Thomas model for hydrogen sulfide removal from biogas.....	160
4.18.5 Yoon Nelson model for carbon dioxide removal from biogas	162
4.18.6 Yoon Nelson model for hydrogen sulfide removal from biogas	164
4.19 Effect of adsorbent mass on the removal of both carbon dioxide and hydrogen sulfide from biogas using the Adam-Bohart model.....	166
4.20 Effect of Adsorbent Mass on the Removal of Both Carbon Dioxide and Hydrogen Sulfide from Biogas using the Thomas Model	167
4.21 Effect of Adsorbent Mass on the Removal of Both Carbon Dioxide and Hydrogen Sulfide from Biogas using the Yoon -Nelson model	168
4.22 Adsorption Kinetics	170

4.22.1 Pseudo-first order for carbon dioxide and hydrogen sulfide removal from biogas.....	170
4.22.2 Pseudo-second order for carbon dioxide and hydrogen sulfide removal from biogas.....	171
4.22.3 Elovich model for carbon dioxide and hydrogen sulfide removal from biogas	173
4.22.4 Intra-particle diffusion model for carbon dioxide and hydrogen sulfide removal from biogas.....	174
CHAPTER FIVE	177
CONCLUSIONS AND RECOMMENDATIONS.....	177
5.1 Conclusion	177
5.2 The Environmental Benefits of Biogas Purification	181
5.3 Recommendations for Further Research Work.....	182
REFERENCES	184
APPENDICES	207
Appendix I: Research Output.....	207
Appendix II: Plagiarism Certificate	208

LIST OF TABLES

Table 2.1: Limitations and benefits of the anaerobic digestion process	35
Table 2.2: Recommended design retention times for anaerobic digestion	41
Table 2.3: Temperature ranges and corresponding retention time for AD	43
Table 2.4: Fixed bed column model used in the current study	54
Table 2.5: The meaning of m and $1/n$ and n parameters as used in Freundlich isotherm.	59
Table 2.6: Four types of adsorption kinetic models in non-linear form.	61
Table 3.1: Research run design for co-digestion	82
Table 3.2: A summary of the four types of adsorption kinetic models in linear form.	99
Table 4.1: Moisture content, total solid, volatile solid, and ash content of pineapple peels	100
Table 4.2: Moisture content, total solid, volatile solid, and ash content of banana peels	101
Table 4.3: Moisture content, total solid, volatile solid, and ash content of Irish potato peels	101
Table 4.4: Moisture content, total solid, volatile solid, and ash content of cooked rice	101
Table 4.5: Moisture content, total solid, volatile solid, and ash content of ugali	102
Table 4.6: Moisture content, total solid, volatile solid, and ash content of cooked beans	102
Table 4.7: Moisture content, total solid, volatile solid, and ash content of cooked banana	102
Table 4.8: Moisture content, total solid, volatile solid, and ash content of cooked Irish potatoes	102
Table 4.9: Moisture content, total solid, volatile solid, and ash content of cabbage .	103
Table 4.10: Moisture content, total solid, volatile solid, and ash content of african nightshades.....	103
Table 4.11: Moisture content, total solid, volatile solid, and ash content of spinach waste	103
Table 4.12: Moisture content, total solid, volatile solid, and ash content of kale waste	104

Table 4.13: Moisture content, total solid, volatile solid, and ash content of tomato waste	104
Table 4.14: Moisture content, total solid, volatile solid, and ash content of carrot peels	104
Table 4.15: Physical-chemical analysis of selected substrates	106
Table 4.16: SI for co-digestion of tuber waste (Irish potato peels) and fruit waste (banana peels).	122
Table 4.17: Biogas composition from the two working digesters	123
Table 4.18: Multipoint BET data for unspent sample (S_1), spent sample (S_2), and regenerated sample (S_3) with 280 μ m particle size.....	124
Table 4.19: Composition of soda ash from XRF analysis	127
Table 4.20: A comparison between soda ash sorbent with the literature studies	134
Table 4.21: Multipoint BET summary for calcined unspent sample (E_1), calcined spent sample (E_2), and regenerated sample (E_3) with 280 μ m particle size.	136
Table 4.22: XRF analysis for calcined eggshells showing the chemical composition	138
Table 4.23: A comparison of eggshell wastes with the previous adsorbent on CO ₂ removal	145
Table 4.24: Summarized isotherm parameters for the adsorption of hydrogen sulfide and carbon dioxide from biogas during on-site experiments.....	153
Table 4.25: Parameters of the Adams–Bohart model under different conditions using linear regression analysis	158
Table 4.26: Parameters of Thomas model under different conditions using linear regression analysis.	162
Table 4.27: Yoon Nelson Model for the removal of CO ₂ and H ₂ S from biogas	166
Table 4.28: Effect of mass on the removal of CO ₂ and H ₂ S from the biogas Adam-Bohart model.....	167
Table 4.29: Effect of mass on the removal of CO ₂ and H ₂ S from biogas - Thomas model.....	167
Table 4.30: Effect of adsorbent mass on the removal of CO ₂ and H ₂ S from biogas Yoon model.....	168
Table 4.31: Adsorption kinetics model parameters for the four models on CO ₂ removal	176

Table 4.32: Adsorption kinetics model parameters for the four models on H ₂ S removal	
.....	176

LIST OF FIGURES

Figure 2.1: Flow chart of anaerobic digestion	20
Figure 2.2: Anaerobic digestion system (a) single stage (b) Two-stage system.....	32
Figure 2.3: Operational parameters for the biogas power plants.....	50
Figure 2.4: Chemical scrubbing method using amine scrubber. Adapted from Bauer et al. (2013).	66
Figure 2.5: Cryogenic separation diagram. Adapted from (Persson 2003).	70
Figure 2.6: PSA unit. Adapted from Kadam and Panwar (2017).	71
Figure 2.7: Biogas upgrading process using a membrane. Adapted from Khan et al. (2017).	73
Figure 2.8: A pathway showing ways of biogas utilization.....	74
Figure 3.1: (a) Weighing balance, (b) oven, and (c) muffle furnace used in the characterization of KW and MSW samples.	80
Figure 3.2: (a) schematic diagram (b) Lab-scale setup for mono-digestion for 10 substrates in duplicate	81
Figure 3.3: (a) schematic diagram (b) Lab-scale setup for co-digestion of Irish potato peels and banana peels in duplicate.....	82
Figure 3.4: Lab-scale setup for co-digestion for different ratios for the 15 days	83
Figure 3.5: Lab-scale setup for co-digestion of TW: FrW on the effect of temperature	84
Figure 3.6: Lab-scale setup for co-digestion of TW: FrW on the effect of pH variation	85
Figure 3.7: Lab scale biogas sampling equipment (a) sampling bag (b) biogas analyzer	85
Figure 3.8: Eggshells preparation for adsorption experiment: (a) raw eggshells (b) grinder (c) sieving machines (d) working particle size 280 μ m.....	86
Figure 3.9: Soda ash preparation for adsorption experiment: (a) Large particle size (b) grinder (c) working particle size (d) packed column bed reactor.....	86
Figure 3.10: Schematic diagram for both hydrogen sulfide and carbon dioxide purification unit	88
Figure 3.11: On-site experiment purification: (a) schematic diagram (b) photo	89
Figure 4.1: A graph of biogas yield against (a) kitchen waste and (b) municipal solid waste substrates	108

Figure 4.2: Biogas yield against TS for (a) KW and (b) MSW	111
Figure 4.3: Biogas yield against TVS for different feedstock (a) KW and (b) MSW	112
Figure 4.4: Biogas yield versus co-digestion of different feedstock	113
Figure 4.5: Daily biogas yield against retention time in various ratios for TW: FrW	116
Figure 4.6: Biogas yield per retention time on the effect of temperature (a) daily (b) cumulative	119
Figure 4.7: Biogas yield per retention time on the effect of pH (a) daily (b) cumulative	120
Figure 4.8: (a) Nitrogen adsorption/desorption isotherms. (b) Pore size distribution was calculated from desorption isotherm using the BJH method.	125
Figure 4.9 (a): SEM micrograph images of the adsorbent S ₁ (a) 10 KX (b) 25 KX..	126
Figure 4.10: SEM micrograph images of the adsorbent S ₂ (a) 10 KX (b) 25 KX.....	126
Figure 4.11: SEM micrograph images of the adsorbent S ₃ (a) 10 KX (b) 25 KX	126
Figure 4.12: Effect of adsorbent mass on the performance of soda ash (a) Removal efficiency (b) Sorption capacity. Test condition: Flow rate =0.03m ³ /h, particle size 280 μm and Co=1227ppm.....	129
Figure 4.13: Effect of particle size on the performance of soda ash (a) Removal efficiency, (b) Sorption capacity. Test condition: Flow rate 0.03m ³ /h and Co =1228 ppm	131
Figure 4.14: Effect of flow rate on the performance of soda ash (a) Removal efficiency, (b) Sorption capacity. Test condition: Particle size 280 μm and Co =1480ppm	132
Figure 4.15: (a) Nitrogen adsorption/desorption isotherms. (b) Pore size distribution was calculated from desorption isotherm using the BJH method.	135
Figure 4.16: SEM micrograph images of the adsorbent E ₁ (a) 10 KX (b) 25 KX.....	137
Figure 4.17: SEM micrograph images of the adsorbent E ₂ (a) 10 KX (b) 25 KX	137
Figure 4.18: SEM micrograph images of the adsorbent E ₃ (a) 25 KX (b) 50 KX	138
Figure 4.19: Effect of particle size on the performance of CaO derived from eggshells (a) Removal efficiency (b) Sorption capacity. Test condition: Flow rate =0.03m ³ /h, temperature 850°C and Co=30.8%.....	140
Figure 4.20: Effect of adsorbent mass on the performance of CaO derived from eggshells (a) Removal efficiency (b) Sorption capacity. Test condition: Flow rate =0.03, particle size 280 μm, 850°C and Co=30.8%.....	141

Figure 4.21: Effect of flow rate on the performance of CaO derived from eggshells (a) Removal efficiency (b) Sorption capacity. Test condition: Flow rate =0.03&0.04m ³ /h, particle size 280 μm, 850°C and Co=30.8%.	142
Figure 4.22: Effect of temperature on the achievement of CaO derived from eggshells (a) RE (b) SC. Condition for testing: Flow rate (FR) = 0.03, size 280μm, 850°C, sorbent mass 75g, and Co=30.8%.	144
Figure 4.23: Removal efficiency and adsorption capacity of regenerated soda ash: Particle size 280 μm, Flow rate 0.03m ³ /h, exposure days 7.	146
Figure 4.24: Removal efficiency and adsorption capacity of regenerated soda ash: Particle size 280 μm, Flow rate 0.03m ³ /h, exposure days 5.	147
Figure 4.25: Removal efficiency and adsorption capacity of regenerated soda ash: Particle size 280 μm, Flow rate 0.03m ³ /h, exposure days 1.	148
Figure 4.26: A comparison between removal efficiency of original and regenerated eggshells: Particle size 280 μm, Flow rate 0.03m ³ /h, temperature 850°C.	148
Figure 4.27: Langmuir isotherm plots for (a) H ₂ S and (b) CO ₂ removal.	150
Figure 4.28: Freundlich adsorption isotherm plots for (a) H ₂ S and (b) CO ₂ removal.	151
Figure 4.29: Jovanovich adsorption isotherm plots for (a) H ₂ S and (b) CO ₂ removal.	152
Figure 4.30: Breakthrough curve for carbon dioxide removal (a) 10, (b) 7, and, (c) 4cm	154
Figure 4.31: Breakthrough curve for hydrogen sulfide from biogas (a) 10, (b) 7, and, (c) 4cms	157
Figure 4.32: Breakthrough curve for CO ₂ from biogas (a) 10, (b) 7, and, (c) 4cm ...	159
Figure 4.33: Breakthrough curve for hydrogen sulfide removal from biogas (a) 10, (b) 7, and, (c) 4cm.....	161
Figure 4.34: Breakthrough curve for CO ₂ removal from biogas (a) 10, (b) 7, and, (c) 4cm	163
Figure 4.35: Breakthrough curve for hydrogen sulfide removal from biogas (a) 10, (b) 7, and, (c) 4cm.....	165
Figure 4.36: Effect of adsorbent mass on the removal of carbon dioxide from biogas a) 75 g (b) 25 g.	166

Figure 4.37: Effect of adsorbent mass on the removal of hydrogen sulfide from biogas.....	167
Figure 4.38: Effect of adsorbent mass on the removal of CO ₂ from biogas.....	168
Figure 4.39: Effect of adsorbent mass on the removal of H ₂ S from biogas	168
Figure 4.40: Effect of adsorbent mass on the removal of CO ₂ from biogas.....	169
Figure 4.41: Effect of adsorbent mass on the removal of H ₂ S from biogas.	169
Figure 4.42: First-order adsorption kinetics model for biogas purification (a) CO ₂ (b) H ₂ S removal	171
Figure 4.43: Pseudo sec-order adsorption kinetics model for biogas purification (a) CO ₂ (b) H ₂ S removal.....	172
Figure 4.44: Elovich adsorption kinetics model for biogas purification (a) CO ₂ removal (b) H ₂ S removal.....	173
Figure 4.45: Intra-particle diffusion kinetics model for biogas purification (a) CO ₂ removal (b) H ₂ S removal.....	175

ABBREVIATIONS

ACD	Anaerobic co-digestion
AD	Anaerobic digestion
BET	Brunauer-Emmett-Teller
BI	Biodegradability Index
Bio-CNG	Bio-compressed natural gas
BOD	Biological oxygen demand
BP	Banana peels
C	Carbon
°C	Degree Celsius
C/N	Carbon to Nitrogen ratio
CaO	Calcium Oxide
CB	Cooked beans
CBG	Cabbage
CBN	Cooked banana
CH ₄	Methane
CIP	Cooked Irish potatoes
CO ₂	Carbon dioxide
COD	Chemical oxygen demand
CP	Carrot peels
CR	Cooked rice
EC	Electrical conductivity
EHS	Environmental, Health, and Safety
FrW	Fruit waste
GHG	Greenhouse gasses
H	Hydrogen

H ₂ O ₂	Hydrogen peroxide
H ₂ S	Hydrogen sulfide
H ₂ SO ₄	Sulphuric acid
HCl	Hydrochloric acid
HRT	Hydraulic retention time
HVFA	High volatile fatty acid
IPP	Irish potato peel
K ₂ CO ₃	Potassium carbonate
Kg	Kilogram
KOH	Potassium Hydroxide
KW	Kitchen waste
L	Litre
LBG	Liquefied biogas
MC	Moisture content
mg/L	milligram per Liter
MgO	Magnesium oxide
mL	millilitre
MSW	Municipal solid waste
MSWM	Municipal solid waste management
MW	Mega Watt
N	Nitrogen
N ₂	Nitrogen gas
NaCO ₃	Sodium carbonate
NaOH	Sodium hydroxide
NH ₃	Ammonia
O ₂	Oxygen gas

O ₃	Ozone
OLR	Organic loading rate
PFO	Pseudo-first-order kinetics
pH	Potential Hydrogen
PNP	Pineapple peels
ppm	Part per million
PSA	Pressure swing adsorption
PSO	Pseudo sec-order kinetics
S	Sulphur
SCCA	Short-chain carboxylic acids
SEM	Scanning Electron Microscope
SO ₂	Sulfur dioxide
SSA	Sub- Saharan Africa
SSAD	Single- stage anaerobic digester
SW	Spinach
SWW	Kale
TAD	Two-Stage anaerobic digester
TDS	Total dissolved solids
TS	Total solid
TVS	Total volatile solid
TW	Rotten tomatoes
UG	<i>Ugali</i>
VFA	Volatile fatty acid
XRF	X-ray Fluorescence

CHAPTER ONE

INTRODUCTION

1.1 Background of the Study

Worldwide, the production of municipal solid waste is rising annually because of consumerization and the urbanization process the threat climate, and the environment in general. Meanwhile, energy is an essential commodity for any society to meet its basic needs such as boiling water, cooking, heating, and lighting (Felix & Gheewala, 2011). Globally, more than 2.4 billion people rely on solid biofuels such as charcoal, firewood, dung, and crop residues for their daily energy (Muala et al., 2015). Most of these solid fuel leads to incomplete combustion, which can lead to the production of different poisonous gases, which lead to acute cardiovascular effects. Air pollution from solid biomass/fuel has become a major issue to human health and is estimated to be one of the top five risk factors worldwide as it contributed to 3.9 million premature deaths (Smith et al., 2014).

On the other hand, there is some direct significance of having forest and woodland. They provide direct benefits such as timber, animal food, conserving soil and water resources as well as being habitual for some animals (Hafner et al., 2018). Despite continuous conversations on forest conservation dating back to the 1950s, deforestation remains a significant challenge in Sub-Saharan Africa, Tanzania included (Luswaga & Nuppenau, 2020). Most Tanzanians depend on biomass as a source of energy by burning firewood in three-stone fire stoves (Hafner et al., 2020) charcoal, and other traditional fuels. Therefore, there is a need to educate people about the importance of having clean and sustainable energy like biogas.

Considering the detrimental environmental effects caused by conventional sources of energy such as fossil fuels and their rapid depletion, biogas as a sustainable and clean energy source could be used. Biogas use will help in achieving sustainability by providing access to modern, clean energy that is less expensive, conserving the environment, and reducing climate change and its effects by limiting greenhouse gas emissions. Anaerobic digestion of biomass especially food waste and some selected municipal solid waste for biogas production and bio fertilizers is a good way of treating waste (Mshandete et al., 2004). Anaerobic digestion (AD) has been widely utilized by modern society as a solution to organic waste management in households, industries, and urban areas (Orhororo et al., 2017). It reduces greenhouse gas emissions by collecting all kitchen remains and municipal solid waste for biogas production which is almost associated with nutrient recycling and energy recovery from digested biomass in agricultural areas (Motte et al., 2013). It also protects the environment, improves the ecology, eradicates pathogenic microorganisms, and safeguards human and animal health.

The composition of municipal solid waste at a point of generation and collection consists of a large part of an organic fraction like cabbage leftover, kale, spinach, Irish potato peels, and banana peels of about 40-60%, papers (3–6%), plastics, metals, and glasses with less than 1%. Kitchen waste consists of food remains from households, cafeterias, and restaurants such as remains from ugali, cooked rice, cooked bananas, and cooked beans. The disposal methods include incineration, open dumping, landfilling composting. These methods are not recommended as they contribute to environmental pollution and global warming.

Wastes such as kitchen waste and municipal solid waste that are normally viewed as low-valued substances are increasing annually meanwhile all these organic wastes from kitchen waste (KW) and municipal solid waste (MSW) have a great potential for biogas production. In modern society organic waste is seen as a valuable commodity, which can provide renewable energy such as biogas, and it is an ecologically friendly and sustainable energy source. In recent years, different studies have explored some ways of converting organic waste into biogas. This will also be used to revolutionize our resources, protect our environment, and preserve the earth from the effects of global warming. During anaerobic digestion, bacteria decompose the organic matter like KW and MSW to produce the energy required for their metabolism and survival at the same time biogas. The anaerobic digestion technology paves the way for both environmental and agricultural sustainability as it represents an effective method for waste stabilization in converting bio-waste sustainable energy with many nutrients rich. Literature shows that different waste from the kitchen and municipal will not produce the same quantity of biogas as each differs in total volatile solids, moisture content, and total solid and ash contents (Yavini et al., 2014a). It is now necessary to determine the amount of biogas produced from each kitchen waste and solid municipal waste by looking at their moisture content, total solid, and total volatile solid. Biogas technologies have been developed and proven environmentally favorable in these circumstances and are a solution to waste management and energy insecurity. Bioconversion processes are suitable for the substrate that contains moisture contents of more than 50%.

A major problem of the anaerobic digestion of pineapple peels is the rapid acidification due to low pH and higher production of Volatile Fatty acids, which therefore limits the methanogenic activities in the digester. The efficiency of the process and the amount of biogas produced depends on the moisture content, total solids, total volatile solids, type

of substrate used, hydraulic retention time, pH, CN ratio of the substrate, and the presence of toxic metal in the substrate. Mono digestion of different feedstock from kitchen waste and municipal solid waste leads to the accumulation of inhibitors that are toxic and therefore low yields (Li et al., 2019). To overcome the problems associated with low yield, the formation of toxic compounds and the accumulation of volatile fatty acid co-digestion have been adopted.

Co-digestion is the process of using different feedstock for anaerobic digestion. Co-digestion of a low CN ratio substrate selected from municipal solid waste such as Tuber waste (TW) with a high CN ratio substrate such as fruit waste (FrW) has been shown to enhance biomethane production. It has been discovered that using the co-digestion principle to produce biogas from a variety of organic wastes is an efficient way to maximize the amount of biogas produced. It increases the amount of food accessible for digestion while stabilizing nutrients in the digester. Tuber waste and fruit waste contain a high cellulose content, low lignin, and high carbon-to-nitrogen (CN) ratio, and are readily and abundantly available. Therefore, most countries worldwide produce large amounts of food waste and municipal solid waste; they are readily available, affordable, and sustainable alternatives, the successful utilization of FW and MSW to make biomethane in AD may have significant advantages.

Globally, municipal solid waste production per annum exceeds 2 billion tons, which threatens the environment. Developing nations produce 109.5-525.6 kg per individual annually while developed countries generally produce about 521.95-759.2 kg of MSW per individual annually (Karak et al., 2012). In Kenya, according to Muniafu et al. (2010), the total solid generated in the city of Nairobi was about 2,680 tons per day in 2002, equivalent to 0.714 kg per single person per day (Muniafu & Otiato, 2010). The

analysis of municipal waste generated in Thika (a town in Kenya) for six months in 2014 shows that organic solid waste was about 68% (Ephantus et al., 2021). All these wastes are biodegradable and therefore can be transformed into renewable and sustainable energy products thus a solution to waste disposal and management. Anaerobic digestion is a vital way of utilizing waste, generating high-efficiency energy via the utilization of biogas technology, protecting the environment, improving the ecology, eradicating pathogenic microbes, and safeguarding animal health and human health.

Biogas constituents vary depending on what was used in the digester but mainly consist of CH₄ (55–77%), and CO₂ (30–45%), although it contains a small number of some other gases such as ammonia (NH₃), nitrogen (N₂), hydrogen sulfide (H₂S) and some siloxane compounds (Harun et al., 2019). Kitchen waste, fresh manure, and decaying plant organic matter are easily degradable by microorganisms; therefore, biogas production using this material is not complex (Patel & Pamnani, 2017). Characterization of the feedstock before biogas production is very important. Moisture content enhances the growth of methanogenic bacteria and facilitates their movement and transportation of nutrients. Total volatile solids and total solids give useful details regarding the amount of biogas, that will be produced, and the efficiency of the anaerobic process. High volatile solid content may not necessarily be transformed into high biogas yield as there is the presence of non-available volatile solids of lignin material (Yavini et al., 2014b). The CN ratio, biodegradability index, and alkalinity among others are important parameters that should be considered in biogas production (Koniuszewska et al; Bhatt & Tao, 2020). Nitrogen is a vital constituent for the establishment of the cell structure while carbon acts as an energy-giving for the microbes (Tripathi et al., 2021).

In Kenya, the Irish potato contributes to a third of overall energy consumption and is the second major crop (Wakaba et al., 2022). It grows better in elevated areas than grain crops. The production of Irish potatoes in Kenya was 2.1 million tons in 2021 which is a 40% increase from 1.5 million tons in 2017 (Wang'ombe & van Dijk, 2015). The increase in demand for Irish potatoes in Kenya has forced consumption to rise from 35kg per single person in 2019 to 63kg in 2021 (Wakaba et al., 2022), which indicates that waste is highly generated as consumerization increases. The production of bananas in 2012 constituted 38% of all the fruit produced in Kenya (Karienyé & Kamiri, 2020). It generates income for households especially in Tharaka (19%), Kirinyaga (21%), and Mt. Kenya (40) % at the same time achievement of food security (Mbaka et al., 2008). Therefore, bananas and Irish potatoes are widely grown and utilized in Kenya among other foods.

Banana peels and Irish potato peels contain high volatile solids and low ash content and are locally available in abundance for biogas production. Banana peels contain excessive nutrients (Barua et al., 2019) while Irish potato peels do not release an excess volatile fatty acid (VFA). The anaerobic co-digestion of fruit waste and tuber waste accelerates the hydrolysis process, dilutes the inhibitory substance as it balances the nutrients, maintains the reactor equilibrium, and improves the yield. The synergistic effect of co-digested food waste has also been reported (Ebner et al., 2016; Kim et al., 2017). It is determined by dividing the yield obtained from co-digestion by the yield obtained from individual substrates during mono-digestion under the same conditions. A synergy index below 1 indicates an antagonistic effect while above 1 shows a synergistic effect (Kim et al., 2019).

The presence of hydrogen sulfide in biogas is a major concern, especially in metal parts, the engines of machinery (Kundu & Sahoo, 2019), and human health (Andriani et al., 2020). Hydrogen sulfide in humans at a concentration of 1000-3000ppm may cause instantaneous death as it reacts with enzymes in the blood and inhibits cellular respiration that leads to pulmonary paralysis, sudden collapse, and death (Khoshnevisan et al., 2017). Sulfur compounds in combustible fuels such as biogas a subject to progressively stringent constraints for environmental issues while carbon dioxide's lower calorific value of the energy content of methane in biogas is 36 MJ/m³ or 50.4MJ/kg methane (Angelidaki et al., 2018). The presence of a high amount of carbon dioxide increases the break-specific fuel consumption that decreases the temperature hence incomplete combustion (Mulu et al., 2022). It may reduce the laminar speed and delay of ignition (Pizzuti et al., 2016). In addition to that, the presence of carbon dioxide contributes to global warming which is now an agenda worldwide, and health problems, therefore purification technologies are required for the safe application of biogas on a large and small scale.

Different adsorbents have been discovered for the purification of biogas like Oldonyo Lengai ash (Kandola et al., 2018), water hyacinth (Makauki et al., 2017b), sludge-derived material (Mkoma & Mabiki, 2012), sweet potato leaves (Juma et al., 2020) red rock material (Mrosso et al., 2020). The drawback of the mentioned adsorbents is that most of them are not locally available and others like sweet potato depend on the climate conditions. Lake Natron is located at 2.3436°S; 36.0458° E in Northern Tanzania, which is a small-localized Lakes that contain sodium carbonate (soda ash) which can be used as a potential adsorbent for hydrogen sulfide removal from biogas. The adsorbent pH is an important parameter to be considered before the sorption process as H₂S is an acidic gas in nature. The sorbent with acidic pH is mostly like to be influenced by

hydrogen ions (H^+) on its surface that will unflavored H_2S adsorption due to either competition of adsorption surface on the adsorbent or the repelling force. Therefore, the dissociation of H_2S will be limited by acidic pH and automatically limit the oxidation of elemental sulfur (Shang et al., 2013). Lake Natron contains extensive salt deposits with a pH of 12 (exceptional alkaline lake) having huge sodium carbonate salt flats capable of purifying hydrogen sulfide from biogas. (Nyakeri et al., 2018; Scoon & Scoon, 2018).

Eggshells are wastes from chicken eggs that contain a high amount of calcium and carbonate and are mainly disposed of in landfills in most countries in the world. It contains about 1% magnesium carbonate, 90–95% calcium carbonate in the form of calcite, 1% calcium phosphate, and some organic compounds (Baláž, 2018). Most of these materials are discarded although it has multidisciplinary application like purification (Pliya & Cree, 2015).

This study aimed at producing biogas from kitchen waste and municipal solid waste as mono-digestion substrate, followed by a co-digestion process, purify and regeneration process using soda ash collected from Lake Natron and calcium oxide from eggshells and fitting the onsite experimental data to the models for sustainable development.

1.2 Statement of the Problem

The amount of kitchen waste and municipal solid waste increases annually along with consumption standards and urbanization (Idris et al., 2004), and most cities in developing countries face the problem of managing it. Therefore, biogas production can provide a solution to organic waste management by providing green and sustainable energy that will help to reduce greenhouse gas emissions. Co-digestion of kitchen waste and municipal solid waste increases methane production from low-yielding or difficult-

to-digest feedstock due to the balancing of nutrients like CN ratio and COB: BOD. The presence of pollutants in biogas reduces its calorific value and, therefore limits its application in machines by causing corrosion, and wear in metallic parts. These pollutants including hydrogen sulfide, ammonia, and carbon dioxide cause corrosion, erosion, and fouling of cooking utensils. Similarly, the hydrogen sulfide in biogas irritates mucous membranes, detrimental to the ecosystem due to the formation of sulfur dioxide during ignition, nausea, dizziness, and sudden death. Therefore, there is a need to purify biogas before using it. There are some materials and methods that were reported for biogas purification but the drawback is that they are expensive in processing and some of them are difficult to obtain like water hyacinth. Soda ash is locally available and less expensive to purchase while eggshells are available in different cafeterias and restaurants including households.

Therefore, this study aimed at the production and purification of biogas from kitchen waste co-digested with municipal solid waste.

1.3 Objectives

1.3.1 General objective

To investigate the potential of kitchen waste co - digested with municipal solid waste for biogas production and further purification using soda ash and eggshells.

1.3.2 Specific objectives

- i. To characterize kitchen waste and municipal solid waste for biogas production.
- ii. To optimize biogas produced from kitchen remains, municipal waste, and their co-digestion.
- iii. To assess the adsorption ability of soda ash and eggshells for biogas purification.

- iv. To evaluate the regeneration and use of the soda ash and eggshells.
- v. To perform modeling studies on biogas purification.

1.4 Research Questions

- i. What are the characteristics of kitchen waste and municipal solid waste?
- ii. What are the optimal conditions that affect biogas produced from kitchen waste, municipal waste, and their co-digestion?
- iii. What is the adsorption ability of the soda ash and eggshell materials?
- iv. What is the regenerative ability of the soda ash sample and eggshells?
- v. What is the best model that can fit lab work data obtained during the purification stage?

1.5 Significance of the Study

The world is currently shifting from non-renewable energy to renewable one, on the other hand the amount of kitchen waste and municipal solid waste is increasing along with consumption standards and urbanization. Such wastes contain abundant organic matter that can be converted into energy, which will address the twin challenges of waste management and energy insecurity. Thus; the study will have a positive impact on society in different ways; converting kitchen waste and municipal solid waste into biogas will not only reduce environmental pollution but also bring about sustainability and suitability of the renewable energy industry. Results proved that there was a high biogas and methane potential from the anaerobic co-digestion of Tuber waste (TW) and fruit waste (FrW). Biogas generation can be enhanced by optimizing various parameters such as temperature, pH, mixing ratio, and the amount of inoculum. Reduction of particle size via blending helps to increase the surface area to volume ratio of the feedstock resulting in a high biogas generation. Upgrading and desulfurization

processes proved to increase calorific value and reduce health problems for biogas users respectively. Therefore, this study aimed at the characterization of the feedstock, biogas production using kitchen and municipal solid waste, and its purification using soda ash and calcined eggshell waste, which are locally available and less expensive.

1.6 Delineation of the Study

The delineation of this study is in the area of kitchen waste and municipal solid waste characterization, biogas production, purification, and regeneration using soda ash collected from Lake Natron and eggshells. The study evaluates the effects of operating conditions such as mixing ration, temperature, and pH on biogas production and finds out the optimal ratio for maximum biogas yield. Regarding purification, the project evaluated the effect of adsorbent particle size, biogas flow rate, adsorbent mass, and calcination temperature for eggshell waste on the removal efficiency and adsorption capacity of the sorbents. The production part was conducted within university laboratories while purification was done around Kesses center.

CHAPTER TWO

LITERATURE REVIEW

2.1 General Overview

The chapter generally discussed the characterization of kitchen waste and municipal solid waste for biogas production and its co-digestion. To enhance biogas production pretreatment of the feedstock and inoculum is required. Different treatment methods were discussed; and was noted that various factors affect biogas generation including pH, temperature, volatile acids, particle size, and hydraulic retention time, The presence of impurities in biogas lowers its energy value hence the purification process included in this chapter. The isotherms and adsorption kinetics for testing the validity of the adsorbent material for the adsorption process were included in this chapter.

Energy consumption increases day to day due to population (Ramaraj & Dussadee, 2015). Different energy sources are currently used but most of them are not environmentally friendly. Biomass is the major form of energy for most people (90%) in sub-Saharan Africa (Kusekwa et al., 2007). In most sub-Saharan countries like Tanzania and Kenya, forests are unnecessarily threatened by increasing charcoal production and firewood use for energy purposes, which results in leaving bare land that leads to soil erosion (Msuya et al., 2011). Kitchen waste and municipal solid waste are increasing annually which may result in the source for the spreading of diseases in humans, as well as polluting drinking water. To avoid unnecessary deforestation and health problems because of the accumulation of KW and MSW biogas as a renewable and sustainable energy through an anaerobic digestion process can be generated. These wastes constituents a range of energy-contained food inform of proteins, volatile fatty acid, carbohydrates and lipids. Kitchen waste has high calorific value, is easily degradable, and provides nutritive value to microbes during methanogenic process.

Biogas is an alternative source of energy, which is, belongs to the category of biofuel, which is produced by anaerobic digestion in the absence of oxygen. The main components are methane and carbon dioxide, although there are some trace amounts of water vapor, siloxanes, hydrogen sulfide, hydrocarbon, oxygen, ammonia, nitrogen, and carbon monoxide (Uhunamure, Nethengwe, & Tinarwo, 2019). The presence of these impurities brought hazardous effects to living organisms and machinery. Therefore, soda ash and calcined eggshell waste are promising absorbents for purifying the biogas before use.

2.2 Biogas Production Technology

Promoting organic waste-to-energy and other low-carbon technologies in small, medium, and micro-scale enterprises including household promises is an agenda worldwide; advanced in biogas market development and empowerment for domestic and household biogas digesters (Uhunamure et al., 2019). Biogas technologies provide a means of transforming municipal organic solid waste and kitchen waste into energy. This is an important technology as it creates renewable, and clean which addresses the twin challenges of waste management and energy insecurity. Biogas is a result of microbial anaerobic digestion of an organic food waste substrate. It was recognized as a substitute for fossil fuels and may be utilized to address issues with waste treatment and management, rising energy costs, and fostering sustainable growth. It mainly consists of methane and carbon dioxide, and some trace amounts of other gases like nitrogen, ammonia, and hydrogen sulfide (Mrosso et al., 2023).

Biogas is an important non-conventional biomass energy that can replace traditional biomass energy, such as firewood, straws, charcoal, and conventional energy sources like fossil fuel and coal. Biogas technology provides a clean energy source for farmers; ecological and environmental protection especially vegetation and forest; poor

environmental hygiene of villages, ameliorates the dirty, and lifestyle conditions of farmers; messy, and improving the agricultural product quality via the provision of digestate that can be used as natural and amazing fertilizers. Renewable energy technologies especially biogas technology provide sustainable solutions for non-renewable energy problems at the same time address environmental issue (Lu & Gao, 2021). Biogas technology gives various advantages in terms of gas generation, electricity generation, bio-fertilizer, and environmental preservation because biogas does not produce air contaminants like carbon dioxide, sulfur oxide, nitrogen oxide, and other harmful fumes and socioeconomic uplift (Wang et al., 2020).

It can be used as fuel for machines and automobiles as well as for lighting, cooking, heating, and other household and industrial purposes. For the safety and effective use of biogas, a purification process is required; and it can be compressed and stored similarly to natural gas. The presence of carbon dioxide in biogas lowers its energy value and density while hydrogen sulfide is hazardous to humans, and corrodes motors and pipes, its removal is crucial. The carbon dioxide and other biogas impurities can be eliminated by passing through different adsorbents for purification purposes.

2.3 Kitchen Waste and Municipal Solid Waste for Biogas Production

Kitchen waste is the best feedstock for biogas production because it is easily degradable. Improper disposal of kitchen waste can cause secondary pollution like mosquito breeding and odor pollution. Increased urbanization and consumerism have resulted in the excessive release of food waste and municipal solid waste. Such wastes contain abundant organic matter that can be transformed into energy, addressing the twin challenges of waste management and energy insecurity. Therefore, to comply with environmental, Health, and Safety (EHS) policies and regulations the disposal of kitchen waste (KW) is required through sterilization and resource recovery like an

energy waste. Biological waste contains a high level of hemicellulose, cellulose, starch, lignin material, lipid, and protein that are a good alternative to biotechnological production of biofuel like biogas. Additional to methane content in biogas some impurities are present like hydrogen sulfide, ammonia, and carbon dioxide. The presence of contaminants in biogas limits its application in engines by reducing its energy value and density and causing corrosion on machine parts.

Municipal solid waste (MSW) has become an increasingly public and environmental health problem around the world, especially in developing countries due to population increase and urbanization issues (Mrosso et al., 2023). Unfortunately, poor management of these solid wastes in most cities in developing countries can lead to land pollution, air pollution, and water pollution because of greenhouse gases emissions (GHG). Energy insecurity and municipal solid waste management (MSWM) are among the most challenging problems globally. Rapid urbanization leads to a rise in municipal solid waste (MSW) generation that has created big problems regarding waste management and disposal. Currently, the effect brought by conventional energy resources has led to a large effort in promoting renewable energy resources. In most industrialized countries, the conversion of municipal solid waste to produce biogas has become increasingly in recent years (Getahun et al., 2014).

2.4 Characterization of Kitchen Waste and Municipal Solid Waste for Biogas Production

The main reason for performing the characterization of the feedstock is to determine the physical-chemical properties of the feedstock that are used and create a reference point for the experiment purposes. The feedstock substrate needs to be characterized in terms of the ultimate and proximate analysis. The proximate analysis includes physiochemical characteristics in terms of its total solids, moisture content, pH value,

total carbon volatile solid total, nitrogen, and ash. On the other hand, ultimate analysis means parameters like elemental hydrogen (H), carbon (C), nitrogen (N), sulfur (S) oxygen (O). Total volatile solid and total solid provide useful information about the amount of biogas that will be produced and the efficiency of the anaerobic process. High volatile solid content may not necessarily transform into high biogas yield as non-available volatile solid information of lignin material (Yavini et al., 2014b). There is a decrease in yield as there is an increase in total solids. (Sajeena et al., 2013). The above literature shows that the maximum yield was obtained when total solid and moisture content was 9% and 91% respectively. Other literature shows the maximum yield was obtained when TS was 20% (3983 mL), 25% (3679 mL), 10% (3166 mL), and 15% (3545 mL) (Deepanraj et al., 2021). Moisture content is one of the significant parameters that affect biogas production enhances the growth of methanogenic bacteria and facilitates their movement and transportation of nutrients (Mecha & Kiplagat, 2023b). The enzymic activity in the high solid sludge digestion process increases as moisture content raises from 90-96% in a mesophilic climate. Moreover, lower volatile solids have been reported in some feedstock as when moisture content is higher there is an addition of water into the bio - digesters which causes the wash out of some nutrients from microorganisms. Total volatile solids and total solids give useful details regarding the amount of biogas, that will be produced, and the efficiency of the anaerobic process. High volatile solid content may not necessarily be transformed into high biogas yield as there is the existence of inadequate volatile solids of lignin material (Yavini et al., 2014b). For instance, a study by (Sajeena et al., 2013) reported a maximum biogas yield when TS is about 10% and moisture content of about 90% while (Yavini et al., 2014b) reported a high yield of 9% total solids and moisture content of 91%. Anaerobic digestion plays an important role in environmental and agricultural sustainability as an

effective method for waste stabilization in converting bio-waste into sustainable energy and nutrients rich digestate. Biogas is produced in bio-waste digesters, sewage sludge, and landfills during the anaerobic breakdown of organic matter (Karthikeyan & Visvanathan, 2013). Biogas contains methane (55–77 %), carbon dioxide (30-45%), hydrogen (0–1%), nitrogen (0-1 %), hydrogen sulfide (1–2 %), siloxanes, water vapor, a trace of oxygen, and carbon monoxide (Harun et al., 2019). Therefore, degradation efficiency is a crucial factor to be considered when examining anaerobic digestion performance. Not all wastes are suitable for biogas production, and sometimes yield might not be viable, therefore in evaluating the feasibility of the feedstock for biogas yield, characterization is necessary.

2.5 Feedstock Selection for Biogas Production

Kitchen waste and municipal solid waste are the most attractive and preferred feedstock for biogas production. The selection of feedstock needs to be done before biogas production and sorting out of the food waste needs to be done as the food waste is collected directly from the primary sources such as canteens, and restaurants that almost contain cardboard, plastics, and paper cups. Therefore, the primary stage of screening is very crucial for the anaerobic digestion process and enhances biogas yield. The variation in the composition of the food waste needs to be examined at a certain time interval. Kitchen waste includes uneaten foods, vegetable waste, uneaten meats, and rotten foods; therefore, the food waste characteristics may highly vary as they depend on the sources and the specific day of collection. The nutrients present in the feedstock or food waste determine the essential nutrients for the anaerobic digestion process. The volatile solids, total solids, and the nutrients present in the feedstock used in the digester must be examined to understand exactly the nature of the feedstock. Different researchers find that a mixture of different feedstock would lead to higher production

and efficiency as it balances the nutrients in the digester. Moreover, precise preparation and use of the feedstock is an important issue for the biogas digester to run beneficiary and at its maximum potential in the production process. All varieties of biomass can be used as feedstock for biogas generation regardless they have cellulose, proteins, carbohydrates, and hemicellulose and, fats. Nevertheless, depending on the amount of organic matter, the quantity and quality of methane released varies from one feedstock to another feedstock.

The content of methane in the biogas indicates the energy value of the fuel thus; the quality of selected feed substrates plays an important part in terms of biogas generation. A low amount of biogas yield may suggest a low concentration of methane in the biogas, which means a low energy value (NNFCC, 2016). For instance, Dussadee et al. (2016), prove that maize feedstock generates more methane as compared to livestock dung, while livestock dung generates more amount of methane as compared to human waste. Classification and selection of biogas feedstock can assist in the construction of a database to decide the biogas generation and the rate at which it is produced. The following factors are important to be considered.

- i. The selected feedstock for biogas should be available in a sufficient amount for the biogas plant to be feasible for a 10-20-year lifespan.
- ii. Biogas feedstock should have sufficient potential to add value to the energy sector
- iii. Feedstock should be fresh and contain some amount of water content for easy degradation of the feedstock by microorganisms. Therefore, biogas feedstock left in the sun for a while could not be appropriate for biogas generation, as it has lost its water content.

- iv. The amount of starch content in the feedstock should be acceptable for optimal biogas regeneration, apart from that co-digestion process should be considered.

Municipal solid waste, agricultural, and kitchen remains are considered as the highest potential feedstock for biogas production in most of the countries in the world including Kenya. Kenya has different climatic conditions and different temperatures increase the production of various fruits such as pineapple, banana, and oranges, watermelon few to mention. Some energy crops like cassava are agricultural traditional crops that are mostly planted for food purposes. However, because of its high-energy properties, it has been considered as biogas production crop (López-Bellido et al., 2014).

2.6 Anaerobic Digestion

The amount of waste generation is increasing annually due to daily human activities and the progress of the industry. Municipal organic solid waste is approximately to increase to 2.2 billion tons worldwide by 2025 (Hoornweg & Bhada-Tata, 2012). For a variety of biodegradable wastes, such as animal manures, vegetable residues, energy crops, industry waste, sludge from industrial waste, municipal residues, aquatic biomass, food waste, and other types of organic waste, anaerobic digestion is an effective and desirable alternative for waste management and disposal. During the anaerobic digestion process, microorganisms degrade organic matter as a feedstock in the absence of oxygen to generate biogas. The benefits of anaerobic digestion make it the most efficient, cost-effective, and environmentally friendly source of renewable energy. It is widely investigated that the anaerobic digestion process is the most cost-effective technology and sustainable for waste treatment and recovery in the form of biofuel. When purified, biogas replaces non-renewable energy like fossil fuels that release greenhouse gases through combustion in households, transportation, and industries. Moreover, the digestate from anaerobic digestion can be used as a good and

amazing nutrient for the growing of our crop hence maximizing yield. The anaerobic digestion process is classified into four stages that are hydrolysis, acidogenesis, acetogenesis, and methanogenesis (Li et al., 2019). Every stage depends on the metabolic state of the different bacteria **Figure 1.1**.

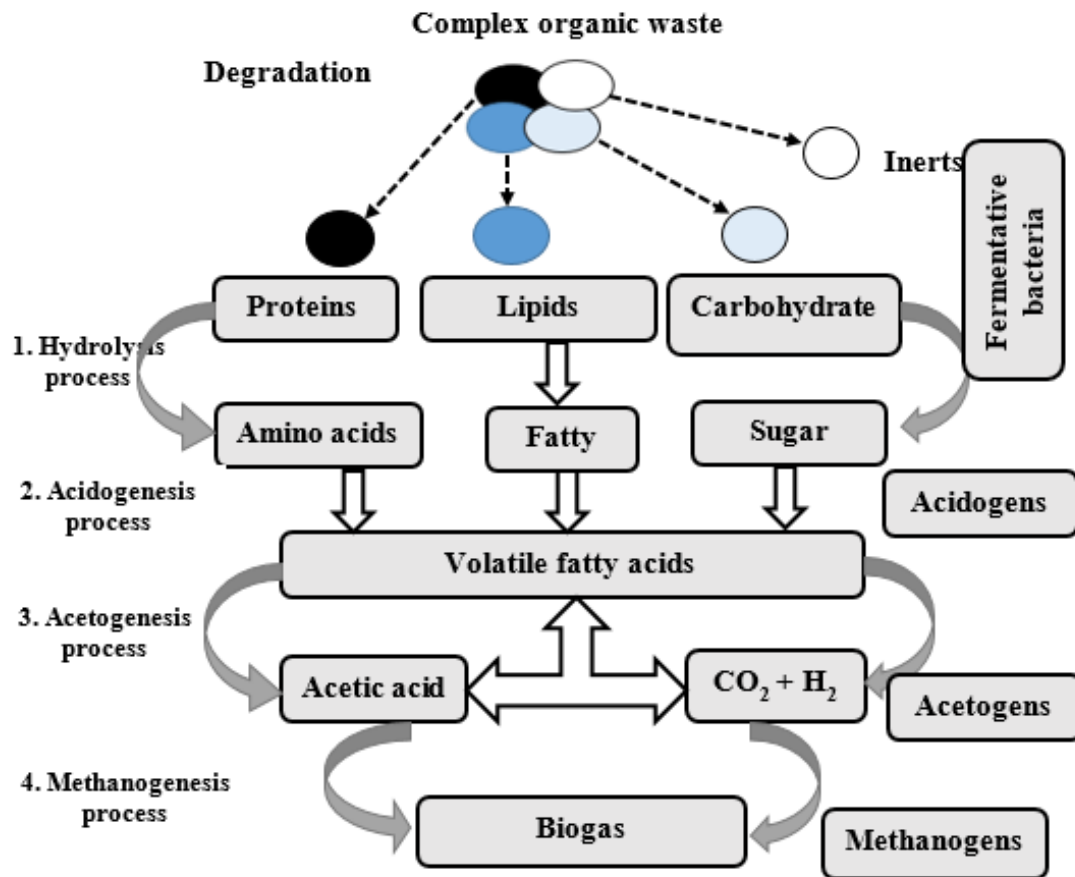


Figure 2.1: Flow chart of anaerobic digestion

2.6.1 Hydrolysis

Hydrolysis is the step in the anaerobic digestion process where complex organic substances that cannot be used by bacteria directly are broken down into soluble molecules with the effect of fermentative bacteria acts as an agent (Li et al., 2019). Complex organic materials are broken down into smaller components and hydrolyzed to soluble compounds during the hydrolysis stage, making them available for biological degradation. These smaller components and hydrolyzed compounds include

carbohydrates, lipids, and proteins. Bacteria such as proteases, cellulase, and lipases, which are extracellular enzymes, degrade proteins, carbohydrates, and lipids, into amino acids sugars, and fatty acids respectively. During this stage, organic loading rate, particle size, pH, temperature, retention time, dilution, mixing ratio, and inoculum concentration, can all affect the hydrolysis stage. Therefore, for an effective and efficiency biogas power plant to perform well, the hydrolysis stage is very important to be considered.

2.6.2 Acidogenesis

During this stage, amino acids, fatty acids, and sugar molecules are converted mainly to alcohol and short-chain carboxylic acids (SCCA). The fatty acids, sugars, and amino acids of the hydrolysis stage are used in the acidogenesis process or acidification to form alcohols, carbon dioxide (CO₂), ammonia (NH₃), volatile fatty acids (VFA), and hydrogen (H₂) gases. This is carried out by acidogenic bacteria and is the quickest response in the anaerobic digestion process of organic matter. Among these steps, slow syntrophic metabolism of fermentative intermediates by acetogens leads to the accumulation of volatile fatty acids, mainly butyric acids and propionic. The imbalance between methanogens and acetogens leads to low methane yield.

2.6.3 Acetogenesis

During this stage, the volatile fatty acids (VFAs) formed during the acidogenesis stage are converted into carbon dioxide (CO₂), hydrogen (H₂), and acetic acid. The hydrogen-producing acetogens bacteria act as an agent at this phase stage (Boe & Angelidaki, 2012). A small number of homo-acetogenic bacteria utilize hydrogen and carbon dioxide as substrates informing acetic acid compounds.

2.6.4 Methanogenesis

Finally, the products from acidification like formic acid, acetic acid, carbon dioxide, and hydrogen (CO_2/H_2) are converted into methane by anaerobic methanogens microbes. The methanogenesis process is a complex situation that is accomplished by the synergistic action of different mesophilic microbes. The methanogenesis process and microorganisms' development are normally affected by different factors such as temperature, pH, mixing ratio, retention time, CN ratio, organic, substrate concentration, and digester configuration, are primarily influenced by different variables including temperature, dilution of the feedstock, pH, retention time, CN ratio, digester configuration, substrate concentration, and organic retention time.

2.7 Mono-digestion of Different Food Waste and Municipal Solid Waste

Anaerobic digestion (AD) is widely utilized to address organic waste management in households, industries, and urban areas (Orhorhoro et al., 2017) thus; addressing the twin challenges of waste management and energy insecurity. The stated literature suggests that biogas generation was noted to increase as total volatile solid increased up to 91.1%, However, it is crucial to critically assess other parameters that affect biogas generation rather than relying on a single parameter. The anaerobic digestion process is an environmentally friendly technology and low-cost for non-conventional energy production as compared with composting processes, landfills, and incineration. The remaining digestate is turned into a nutrient-rich sludge that can be sold as fertilizer. The application of AD reduces greenhouse gas emissions by utilizing municipal solid waste and kitchen waste for biogas production, nutrient recycling, and energy recovery from digested biomass (Motte et al., 2013). During anaerobic digestion, bacteria degrade the organic matter found in kitchen waste (KW), and municipal solid waste (MSW) to generate the energy required for their consumption, survival, and biogas.

Many solid wastes such as Irish potato peels, cabbage waste, and cooked rice waste are produced and their effectual getting rid of is a matter of concern. Meanwhile, these organic wastes from KW and MSW have great potential for biogas production. Kitchen waste and municipal solid waste can be efficiently converted into methane in a mono-digestion digester with the addition of inoculum used as a catalyst for biodegradation process and without the addition of any other nutrients.

Bioconversion processes are suitable for the substrate that contains a moisture content of more than 50%. A major problem of AD in fruit and vegetable waste is the speedy acidification due to low pH and a higher level of producing volatile fatty acid, which therefore limits methanogenesis in the digester. The efficiency of the process and the amount of biogas generated depends on total solids (TS), total volatile solids (TVS), moisture content (MC), type of substrate used, hydraulic retention time (HRT), pH, carbon-nitrogen (CN) ratio of the substrate, and the presence of toxic metals in the substrate (Ebunilo et al., 2015).

2.8 Co-digestion

Anaerobic digestion has been widely studied in the past years, and most of the studies have focused on assessing the performance of different feedstock and identifying the appropriate mixing ratios to improve biogas production. Generally, various organic feedstock are mixed using a series of total solid and volatile solid ratios. Co-digestion refers to the simultaneous anaerobic digestion of multiple organic wastes in one digester. The potential benefits that can be achieved in a co-digestion process among others have increased load of biodegradable organic matter, dilution of toxic compounds, improved balance of nutrients, better biogas yield, and synergistic effect of microorganisms (Ebner et al., 2016; Kim et al., 2017). The anaerobic co-digestion (ACD) process of food waste with other substrates like municipal solid wastes is

suggested to compensate for the problems associated with mono-digestion of food waste alone. ACD is used widely in most of the industry to prevent the low buffer capacity and the high carbon-to-nitrogen ratio (CN) problem associated with the mono-digestion of Food waste. Co-digestion stabilizes the feedstock to the bioreactors thereby decreasing the concentration of nitrogen and hence improving the CN ratio of the substrate in the digester. The use of co-substrate in biogas production with low lipid content and nitrogenous waste increases the biogas production due to complementary characteristics of both substrates and therefore, reduces problems associated with the accumulation of intermediate compounds like high ammonia concentrations and volatile organic compounds. The co-digestion of industrial sludge and municipal solid waste in the ratio of 1:2 provides the highest amount of methane gas, compared to municipal solid waste alone. On the other hand, a two-phase anaerobic digestion system (Fezzani & Cheikh, 2010) recorded the highest biogas production when olive mill solid waste was co-digested with a mixture of olive mill wastewater. (Mehariya et al., 2018) reported that the best co-substrate for food waste in anaerobic digestion is sewage sludge. Sewage sludge is rich in nitrogen molecules and trace nutrients but low in biodegradable organic matter thus; mono-digestion of sewage sludge leads to low biogas production and methane in general. Sewage sludge is an essential co-substrate used in the anaerobic co-digestion of food waste as it can provide alkalinity conditions and essential nutrients in the digestion process to improve and balance the acid during the anaerobic digestion of food waste in the bio-digester. Sewage sludge has high content of active microbes that make it a favorable co-substrate to the formation of microorganisms in the anaerobic process. It has low carbon to nitrogen ratio of 6 – 10 (Cheong et al., 2022) that needs to be co-digested with other substrate with high carbon

to nitrogen ratio like kitchen waste to compensate the nutrients and prevention of inhibition process.

Banana peels and Irish potato peels contain high volatile solids and low ash content and are locally available in abundance for biogas production. Banana peels contain excessive nutrients while Irish potato peels do not release an excess VFA. The anaerobic co-digestion of fruit waste and tuber waste accelerates the hydrolysis process, dilutes the inhibitory substance as it balances the nutrients, maintains the reactor equilibrium, and improves the yield. Therefore, mixed feedstock from municipal solid waste and kitchen wastes was found to be the best in the whole process of biogas production as production rates are influenced by the balance of carbon and nitrogen in the feeding material that is 25:1 and 30:1 (Fezzani & Cheikh, 2010). Cassava products when co-digested with other feedstock could be an alternative feeding substrate for various societies for the production of biogas in most of the developing countries. Cattle manure, cassava, vegetables, and fruits, as co-substrate can be selected depending on their availability, quantity, and quantity of biogas production potential. Most cattle dung ends up in landfills as manure or fertilizer and therefore the use of cattle as a feedstock for biogas production gives an alternative option for waste management and disposal.

Literature shows that cattle dung is rich in organic matter and nutrients and for this reason it is mostly used as an agricultural fertilizer in farms. Some studies showed that cattle manure could be co-digested by mixing the cattle manure with other organic waste such as household and industrial waste. The co-digestion of cow dung has shown to have an important role in the anaerobic digestion process which has resulted in several economic benefits and environmental. Research on analysis of the microbial available in cattle manure indicated that Firmicutes (29.8%), Bacteroides (38.3%), Verrucommicrobia (2%), and Proteobacteria (21.3%) were the microorganisms present

in the dung. They facilitated the breakdown of complex organic content of chitin, lignocelluloses, cellulose, and xylose present in food substrate, and therefore the use of cattle dung is a justification that it can be used as inoculum for anaerobic digester or feedstock in the digester. However, it is important to critically assess the availability and effectiveness of these microbes especially in the inoculum used in this study.

2.9 Synergic Effect

A synergistic effect is an increased hydrolysis rate constant rather than an increase in specific biogas yield from co-digested feedstock material. Biogas yield from co-digested feedstock is expected to be higher than the mono-digested feedstock as it is determined from the methane yield of each feedstock used in a co-digestion process because of synergetic effects in the bio-digester. Co-digestion boosts the biological breakdown of each food substrate in the digester. Specifically, the addition of co-substrate resulted in synergistic effects, which comes because of either a boost in methane yield of a specific substrate in the mixture or an increase in biogas production kinetics. Varying from the additive effect where a rise in methane yield is due to a higher mass of available biodegradable organic matter per unit volume from co-substrate addition (Xie et al., 2017). Some researchers have found evident that not all feedstock used in co-digestion can lead to synergic effects rather others can bring about antagonistic effects (Silvestre et al., 2015), and sometimes there is no clear effect of the co-digestion process as compared to mono-digestion. It is widely believed that the co-digestion process can improve process performance as it balances carbon to nitrogen ratio (CN), micronutrients and macronutrients. Provide higher and readily biodegradable feedstock and lastly give a good buffering capacity in the digester. All these factors accredit to the synergistic effects are fundamentally related with co-

substrate composition and properties. For example, a low carbon to nitrogen ratio can be co-digested with higher carbon to nitrogen ratio to optimize the CN ratio as 20-30:1. Different literature has reported different syngeneic values depending on the feedstock used in the anaerobic digestion process. These effects can be considered as quickening the degradation of feedstock matter, increasing biogas production, and sometimes the combination of the two. Researchers point out a synergy effect when performing an anaerobic co-digestion of pure and slaughterhouse, lipid, protein, and, carbohydrate as a way of enhancing the kinetics of the anaerobic digestion and then increase in ultimate biodegradability of the feedstock. This is because the rate-limiting step in anaerobic co-digestion is the hydrolysis of the complex molecules. It is now important to assess synergistic effects during anaerobic co-digestion on both process kinetics and the specific methane production.

Different techniques have been applied to evaluate the synergistic effects in the literature. Yun et al., (2015) defined the synergistic effects as an increased biogas yield from waste sludge and evaluated a synergetic effect during co-digestion of food waste while presuming a full altering of food waste (1 g COD = 350 mL methane), and employed a chemical oxygen demand balance approach to quantify the extent of synergistic effect. It was worth the choice of a full conversion rate that enables a simplified quantitative analysis of synergistic effects from sludge.

2.10 Pre-treatment Methods

Pre-treatment methods are the major steps of concern in the process of biogas production. It involves the breakdown of the complex organic matter into simpler molecules. The pre-treatment of the feedstock can improve the biodigestibility of kitchen wastes and municipal solid waste, and the accessibility of microbes could be

much simpler. It speeds up the hydrolysis of the substrate, and facilitates the digestive process, thus increasing the biogas yield in the anaerobic digestion system (Aslanzadeh, 2014). The main effects of pre-treatment technologies on feedstock for biogas generation include (i) reduction of particle size, (ii) solubilization, (iii) removal of structural barriers to the hydrolysis stage, (iv) enhancement of the hydrolysis rate (v) enhancement of biodegradability, and (vi) an increase in biogas and methane production. There are different categories of pre-treatment techniques that exist during the anaerobic digestion process including.

2.10.1 Physical pre-treatment

The physical pre-treatment method aims to reduce the substrate's particle size to increase its surface area biodegradability and digestibility for enzymatic degradation. The following are examples of physical pre-treatment technologies steam explosion, liquid hot water pre-treatment, milling and grinding specifically for particle size reduction, and irradiation such as microwave, and gamma-ray (Xu et al., 2019). Particle size reduction is typically the pre-treatment technique used most frequently, and it is always the first stage in the entire biomethane manufacturing process. By reducing the particle size, more biogas would be produced. Milling and gridding of the feedstock can reduce the viscosity inside the digester, which makes the mixing easier and avoids floating. However, too much particle size reduction could lead to inhibitors and reduced biogas generation. It has been found that the production of biogas was raised by 10%, as the size was 0.5 mm compared to 20–30 mm (Menind & Normak, 2009), while sisal fibers milling from 100 mm² was able to achieve an efficiency of up to 20–25% of biogas yield. Knife mills and hammer mills can be applied to biomass, which is dry with a moisture content of up to 15%, meanwhile, hammer mills are cost-effective and easy to operate.

2.10.2 Chemical pre-treatment

The kitchen waste and municipal solid waste are pretreated with alkali and acid. The pre-treatment of feedstock using acid and base will improve energy efficiency. Literature shows that a higher amount of methane was found when wheat was used as a feedstock and pre-treated with hydrochloric acid for 120 minutes (Vijayakumar et al., 2022). The pre-treatment of feedstock with hydrogen peroxide (H_2O_2) and ozone (O_3) will affect ligno cellulose to degrade lignin material that has doubled biogas effect on biogas generation. The lignin material of the feedstock material is an important component in enhancing biogas and methane generation in general. The pre-treated feedstock using sodium hydroxide (NaOH) for about 21 days at the maximum temperature was found to increase biogas yield from 27.3 to 64.54% (Gunaseelan, 2007). Variations of alkaline concentrations can be used to find out the best concentration for the maximum biogas and methane yield, which can be lime, soda ash, ammonia, ammonium sulfate, or caustic soda. On the other hand, acids can also be used as a pre-treatment agent for the feedstock used in biogas generation. This can either be hydrochloric acid HCL, or Sulphuric acid (H_2SO_4). A treatment approach that combines both physical and chemical approaches is called physicochemical pretreatment. Examples include steam explosions, explosions caused by steam containing SO_2 and ammonia fibers, liquid hot water treatment.

2.10.3 Biological pre-treatment

The treatment of the feedstock using biological pre-treatment technology is the most cost-effective technology, environmentally friendly, and a promising method for biogas generation. Three technologies are available under this method such as anaerobic, aerobic, and enzymatic. Aerobic pretreatment technology is carried out via a pure culture of hydrolytic microorganisms. Under aerobic pretreatment, the white-rot fungi

are the most preferred microorganism for degradation due to their high ability to break lignin polymer content. This technology has made other technologies out of fashion due to low by-product formation and cost efficiency. The higher efficiency of biogas yield was linked to increased deterioration by microorganisms. The anaerobic digestion process gives a better yield than all pretreatment technologies and was noted to be cost-effective, promising, and easy to implement worldwide. The lignocellulose material is biologically degraded and transformed into residue using fungi; the oxidative system and hydraulic system are the two types of microbes used in the biodegradation of feedstock. The pre-treatment method may provide a negative or positive effect based on the choice of pre-treatment technology used.

2.11 Biogas Digesters and Process

Anaerobic digestion can use different kinds of digesters and processes, which are normally classified as batch and continuous processes; single, and two-stage processes and liquid-solid-state processes. The description for each type of digester is explained in the following sections.

2.11.1 Batch and Continuous anaerobic digestion processes

A batch digester is a one-stage digestion process in which all stages occur in the same digester. In a batch process, feedstock is fed into the digester once the process starts, then the digester is kept closed during the whole process of digestion and removed as an amazing fertilizer anaerobic digestion process ends. In a batch digestion process, food substrate is generally mixed up with the inoculum while outside the bio-digester to have microbes' communities for the reaction. The digestate is then removed from the biodigester using a front-end loader. The Percolate is collected from the bottom of the digester and circulated via the top for biodigester for improving contact between substrate and microorganism and thus increasing the moisture content in the

digester. The batch digester is the most used which provides data on a substrate's methane yield and digestibility and it is appropriate for small-scale production. The following are some of the advantages of having a batch anaerobic digestion process; low operating costs, ease of design, often lower cost of digestion, and need for less equipment while its disadvantage is that it has high energy consumption and high maintenance costs. For batch reactors TS content, substrate ratio to inoculum ratio (I:S), or the amount of percolate recirculate is the focus (Rocamora et al., 2022).

Continuous digestion systems generate biogas continuously by continuously feeding organic matter into the reactor or adding it to the digester in phases. Products are routinely or continuously eliminated at the end of processes, resulting in a consistent biogas yield. Continuous digesters, as opposed to batch-type digesters, produce biogas continuously while new feedstock is added and digestate is removed. Production of biogas is reliable and consistent, in most cases; continuous digestion is chosen for large-scale production.

2.11.2 Single-stage and two-stage anaerobic digestion processes

In single-stage digestive processes, all anaerobic digestion steps or processes occur in a single closed biogas power plant such as hydrolysis, Acidogenesis, Acetogenesis, and methanogenesis and it is the simplest system as compared to the rest **Figure 2.2a**. Nevertheless, the microorganism characteristics in these steps differ from one other step. Facultative microbes carry out hydrolysis and acidogenesis steps within the short time of 30 minutes, and pH of 5.5–6.5 while Acetogenesis and Methanogenesis are performed by obligate anaerobes within several days with and pH of 7-8 (Pham Van et al., 2020). The obligate anaerobes are very sensitive to volatile fatty acid that is produced during the first step of anaerobic digestion. Therefore, at a high loading rate, it is very difficult to maintain the balance of microorganism growth. To overcome this

problem associated with the single-stage anaerobic digestion process the idea of a two-stage anaerobic digestion process has been suggested.

The two-stage anaerobic digestion processes differentiate the hydrolysis and acidogenesis from Acetogenesis and methanogenesis in two different reactors **Figure 2.2b**. With the introduction of this two-stage anaerobic digestion process, the system can attain higher organic loading capacity, more stable operation, and a higher resistance concerning inhibition and toxicant substances which results in high methane yield. Two-stage anaerobic digestion (TAD) techniques require very high operation and investment costs and therefore, for small-scale domestic digesters, a two-stage process is neither practical nor advantageous.

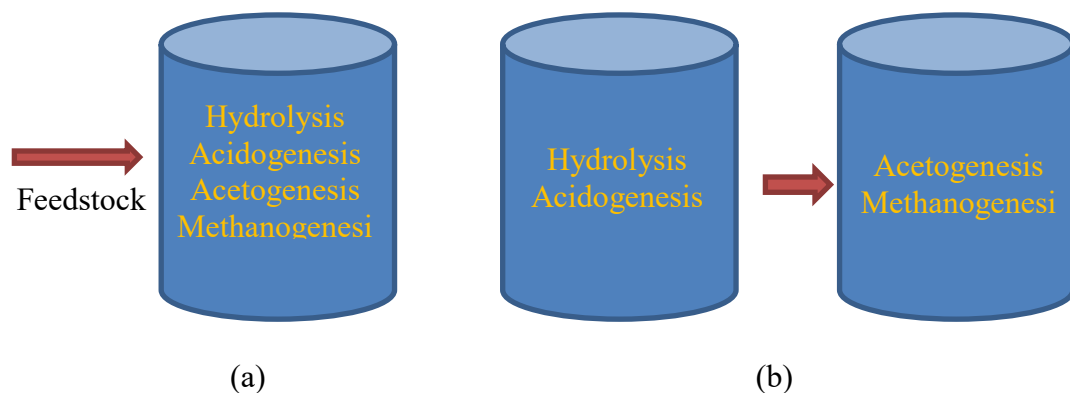


Figure 2.2: Anaerobic digestion system (a) single stage (b) Two-stage system

2.11.3 Liquid and Solid anaerobic digestion process

There are two types of anaerobic digestion processes described via anaerobic digesters total solid contents as wet-anaerobic digestion or liquid that possesses a total solid concentration of less than 15% and a dry-anaerobic digestion/ solid process with a total solid $\geq 15\%$ (Jansson et al., 2019). For those feedstock with high moisture content liquid anaerobic digestion is preferred as compared to solid anaerobic digestion and therefore

solid anaerobic digestion is superior in comparison to the liquid digestion process, as it requires a small amount of water and therefore a high amount of biogas.

2.12 Variation in Operational Parameters

It has been utilized to operate biogas plants efficiently to various factors including particle size, pH, temperature, loading rate, dilution, substrate concentration or ratio, inoculum concentration, agitation, Volatile solid, and total solid. Controlling and observing certain variables within the desired range can affect the biogas production rate (Kumar et al., 2013). Literature shows that biogas generation from kitchen waste municipal solid waste by investigating the impact of substrate concentration 5-30 g/l and incubation 1-6 days, where the highest methane yield was found to be 72.53% generated within 5 days. Angulo et al., (2018) researched alkaline pre-treatment effects on biogas generation from corn crop residue by varying inoculum to feed ratio of 1:1, 2:1, and 3:1 and the particle size between 0.5-2 mm. The maximum biogas yield 392.75 mL was produced from the digestion of corn stalk without pre-treatment. The current study assess, evaluate the quantity and quality of biogas generated through varying mixing ratio, and explore a concrete explanation on effect of mixing ratios.

2.13 Limitations and Benefits of the Anaerobic Digestion Process

Methane from biogas generated during the anaerobic digestion process when burned releases heat and power energy used for cooking, lighting, and as a fuel for vehicles and machines. The use of methane will reduce the dependence on fossil fuel consumption and thus reduce greenhouse gas emissions that lead to global warming. This is brought about by the presence of carbon in the organic feedstock, which is the component of the carbon cycle. **Table 2.1** illustrates the general limitations and benefits of the anaerobic digestion process (AD). To avoid the drawback optimization of the anaerobic digestion process is important. It can be converted into heat and electricity via combined heat

and power technology with 45% thermal conversional efficiency and 35% electricity (Labatut & Pronto, 2018). Biogas gives a high way of sustainable development by converting organic waste substrate into an amazing renewable energy. Thus, it is important to approximate the quantity of biogas and non-conventional energy converted from food waste and municipal solid waste worldwide, which can additionally estimate the advantages of the anaerobic digestion process. The total heat generation potential, biogas generation potential, heat generation potential, and power generation potential, can be obtained using **equations** 2.1, 2.2, 2.3, and 2.4 respectively.

$$H_{AD} = V_{CH_4} \cdot Q_{CH_4} \quad (2.1)$$

$$V_{CH_4} = q \cdot f_{vs} \cdot b \cdot g \cdot C_{CH_4} \quad (2.2)$$

$$H_{CHP} = V_{CH_4} \cdot Q_{CH_4} \cdot \eta_h \quad (2.3)$$

$$E_{CHP} = \frac{1}{3600} \cdot V_{CH_4} \cdot Q_{CH_4} \cdot \eta_e \quad (2.4)$$

Where H_{AD} : the total heating potential (MJ/ year); V_{CH_4} : the volume of CH_4 produced (m^3); H_{CHP} : the CHP heating potential (MJ year⁻¹); E_{CHP} : the CHP electric energy potential

(MWh/year); q annual available resource of feedstock substrate (tonne/year); b volatile solid biodegradability for food waste/ feedstock; f_{vs} ; the ratio of volatile solid to total solid. CH_4 ; the volume of methane in biogas ($m^3 m^{-3}$); g ; biogas yield (m^3 tonne); Q_{CH_4} : the volumetric heating value of methane ($MJ m^{-3}$); η_h ; CHP engine-generator efficiency on biogas; and η_e : CHP engine-generator efficiency on biogas.

Table 2.1: Limitations and benefits of the anaerobic digestion process

Advantages
<ol style="list-style-type: none"> 1. Organic waste management and treatment system is carried out 2. Reuse, reduction, and recycling are improved 3. Neutralization of waste is adopted 4. Dependence on fossil fuels is reduced 5. Modern, clean, and renewable fuel is produced 6. Reduction in the production of odorous gases 7. Less land is used 8. Greenhouse gas emissions are reduced 9. Reduction in the need for inorganic fertilizers 10. The Source of electricity and heat is generated by biogas and 11. The prevention of the spread of pathogens
Disadvantages
<ol style="list-style-type: none"> 1. Start-up times are lengthy 2. High capital expense 3. Production rate may be long according to the substrate characteristics 4. Environmental changes may cause the process to fail 5. The additive may be necessary 6. Changes in operational parameters may cause the production of biogas to fail 7. Needs additional treatments 8. Corrosive and odor gases may be available. 9. High explosion risk

2.14 Factors Affecting Biogas Production

Anaerobic digestion can be influenced by numerous factors that contributed to the increase of the biogas yield including temperature (Toutian et al., 2020), carbon-to-nitrogen ratio (Naik et al., 2014) pH (Budiyono et al., 2013). On the other hand, organic loading rate (OLR), hydraulic retention time (HRT) (Rincón et al., 2009), totally solid and particle size of the substrate (Nalinga & Legonda, 2016) as well as the digester configuration (Liu et al., 2006), volatile fatty acid, nutrients substrate, and feedstock characteristics. The inoculum sources used in the digestion process should be in

consideration as a variable parameter. All factors that affect biogas production must be present in their optimal ranges for efficient biogas production. The optimization of anaerobic digestion parameters for effective biogas production is a paramount and it based on kind of wastes used in the bio-digester. To maximize microbial activity and the effectiveness of anaerobic degradation, the operational factors of the reactor can be controlled or adjusted. This is because the microorganisms' growth rate is crucial to the anaerobic digestion process. These variables are recognized to have an important impact on the effectiveness of the digestion system, biogas quality and quantity, and the cost-effectiveness of running the biogas power plant.

2.14.1 Volatile Fatty acid (VFA)

Volatile fatty acid in biogas digester is an important factor in determining the stability of the anaerobic digestion process. VFA concentration is the most delicate operational parameter to watch as a process performance indicator. The high accumulation of volatile fatty acid in the biogas digester is due to the overloading of the organic substrate in the digester or due to the presence of some inhibitors in the digesters. This will hinder the methanogenic bacteria from utilizing the VFA as they are produced during anaerobic digestion, resulting in decreasing buffering capacity and accumulation of more acids that inhibit the hydrolysis process of the feedstock used in the digester. The most common VFA in biogas digesters are propionic acid, acetic acid, and butyric acid that are produced during the anaerobic digestion process. Acetic acid is a byproduct of the anaerobic process that is eventually digested to produce methane and carbon dioxide. The accumulation of the VFA can be counterbalanced by the level of basicity in the biogas digester that will cause the pH level to decrease. When the level of VFA to alkalinity ratio is below 0.4 the anaerobic process is considered as a very stable process, and a high amount of biogas production can be observed. On the other hand,

when VFA is between 0.4-0.8 there may be some instability reactions while when it is above 0.8 the production ceases due to the accumulation of more fatty acid that can induce systemic discomfort and hence failure of the methanogenic bacteria to work on the substrate available in the digester (Kameswari et al., 2012).

2.14.2 Biodegradability

This is the ability of the materials to be decomposed by the action of microorganisms such as fungi or bacteria with or without the presence of oxygen while being assimilated into the natural environment. However, its significance is in the relative rates of such processes such as the number of days, weeks, years, or centuries. In practice, kitchen waste and municipal solid wastes can be subjected to a biodegradation process to release biogas from them. The rate at which the materials undergo degradation can be measured in several ways like the amount of methane or alloy that they can produce. The degradation of kitchen waste co-digested with solid municipal waste can be affected by the contents that are contained in the substrate that can be degraded either chemically or biologically. The rapid degradation of volatile solids in the food waste resulted in rapid acid formation and volatile fatty acids accumulation.

COD is a good indication of the degree of completeness of the degradation process, as any indigestible material will require oxygen to complete the degradation process (Ward et al., 2008). During anaerobic digestion, COD is used as a control tool for the whole process. It is used to determine the organic matter contents that are present in the substrate that is used in the anaerobic digestion process. A study done on the impact of the substrate-to-inoculum ratio in anaerobic digestion of swine slurry shows that soluble COD profile initially was 1830, 3380, 4789 mg/L but as the process continues the COD rises due to hydrolysis of complex compounds by acidogenesis (González-Fernández & García-Encina, 2009). Soluble COD is due to the presence of VFAs.

The ratio of chemical oxygen demand and biochemical oxygen demand (COD: BOD) can be used to determine the biodegradability which is called a biodegradability index. The biodegradability index can be used to assist the toxicity and the presence of non-biodegradable contents in the substrates in the biogas digester. Before choosing the biological waste for biogas production, it is important to know the biodegradability index of the raw influent waste. When the BOD/COD is greater than 0.6 then the waste is moderately biodegradable, when it is between 0.3-0.6 some treatment is required before the biodegradability of the substrate because the process will be relatively slow, as the acclimatization of the microorganisms that help in the degradation process takes time. Similarly, when the BOD/COD is less than 0.3 then the process cannot be a procedure (Abdalla & Hammam, 2014).

2.14.3 Organic loading time (OLR)

The organic loading rate is an important parameter to archive an optimized anaerobic co-digestion process and determine the effectiveness of biogas production. Biogas production in a power plant will be higher when the loading rate is minimal. The organic loading rate will be decided by the size of the biogas power plant and can be calculated as per **equation 2.5**. The organic loading rate that is applied in co-digestion is often higher than the one that can be applied in mono-digestion. It is important to understand that biodegradable organic matter like volatile content and dry solids optimize the loading rate of the substrate in an anaerobic digester (Ndiweni et al., 2017). The loading rate is inversely proportional to methane production, especially in co-digester. An increase in substrate than the number of microbial available results in the failure of bacteria to decompose the substrate. A higher loading rate in the digester affects the methanogenic bacteria and thus affects the biogas generation. A higher amount of feedstock can be attained by the right organic loading rate that will lead to a rise in the

number of microbial and hence increase in microbial activities. The hydraulic retention time of the biogas plant will be mainly based on the type of feedstock. This results in the accumulation of indigestible material such as fatty acid, which results in an acidic environment and lowers pH, which leads to an unstable decomposition process (Jabeen et al., 2015).

$$OLR = \frac{S_o}{HRT} = S_o * \frac{Q}{V} \quad (2.5)$$

Where S_o = Influent substrate concentration, OLR = Organic loading rate, Q = flow rate (L/d), and V = anaerobic digester volume (L), and HRT = Hydraulic retention time (d).

The organic loading rate depends on the chemical properties of the kitchen food waste and municipal solid waste. Kitchen food waste mostly comprises proteins, carbohydrates, lipids, and some trace amounts of inorganic compounds. The composition varies due to the type of waste/ feedstock used and its constituents. According to (Jiang et al., 2018) biogas generation rises from 0.17 - 4.03 L/(L.d) when the organic loading rate rises from 0.75- 9.00 g VS/(L.d) for municipal solid waste digestion. Nevertheless, the biogas yield dropped to 3.8 L/ (L.d) when the organic loading rate increased up to 11 g VS/(L.d). It is because overfeeding of the bio-digester causes the accumulation of volatile fatty acid and makes the environment less favorable for the microbial to survive due to the drop in pH level. The organic loading rate is an important parameter as it affects the anaerobic digestion process and the stability of the biogas production in general and the optimal organic loading rate is needed to maximize biogas production if not yield will be low. Most kitchen wastes are readily degradable, have high solubility, low pH, and moisture content, and have high-energy content per dry matter.

2.14.4 Hydraulic retention time (HRT)

The hydraulic retention time is one of the most crucial parameters that affect the performance and efficiency of any anaerobic process. The retention time differs depending on various process variables, including total solids concentration, process temperature, mixing intensity, and waste composition. Both short and long retention times have an impact on the AD; too short time leads to the generation of low gas yield because the organic matter was not fully biodegraded while the longer retention time necessitates a large digester capacity and raises capital costs with a high amount of biogas generation. **Table 2.2** displays the recommended retention time at each temperature. It is recommended to reduce the hydraulic retention time of the feedstock inside the digester to increase methane production and the efficiency of the anaerobic process. In addition to that, the process of changing the hydraulic retention time can affect the microbial community structure that results in low or negligible biogas yield. Improper hydraulic retention resulted in an imbalance between slow-growing methanogens and fast-growing microorganisms (acidogenic and hydrolytic bacteria) that led to insufficient usage of hydrolysis-acidogenesis products. The acidogenic methanogens are mostly sensitive to environmental change as compared to hydrogen trophic methanogens in the bio-digester.

According to Tripathi, et al. (2021), the optimum HRT for mesophilic digestion bacteria ranges from 10–40 days, as that of thermophilic process is 14 days. On the other hand, another study was done on food waste co-digested with cattle manure on the effect of hydraulic retention time 4, 5, 7, 10, 15, 20, and 25 days where the highest methane yield was obtained at 1.48 L/L/d with a hydraulic retention time of 5 days. The highest methane production was achieved at 1.48 L/L/d with an HRT of 5 days. The maximum methane generation of 236–257 mL/g-VS was obtained at a hydraulic retention time

≥ 15 days and started to decrease from 10-5 days leading to low methane yields and failure of the process at a hydraulic retention time of 4 days, because of the accumulation of volatile fatty acid in the digester. The anaerobic digestion power plant has a short Hydraulic Retention Time (HRT), and a high Organic Loading Rate indicating that the digestate still contains a significant amount of undigested food substrate to be slowly digested during landfill or storage. Under this circumstance, if the digestate is left uncovered on the ground a significant amount of methane will be released into the atmosphere and hence contribute to global warming. On the other hand, when the anaerobic digestion power plant has a very low organic loading rate and a high hydraulic retention time, then it can be noted that the methane yield is negligible.

A study done by Wandera et al., (2019) on biogas production from sewage sludge using syntrophic acetate coupled with hydrogen trophic methanogens under mesophilic conditions shows that biogas yield increases at low hydraulic retention time. Therefore, there is a need to understand the relationship between microbial community function and their structure with the operation conditions like hydraulic retention time for an efficient and effective anaerobic digestion performance.

Table 2.2: Recommended design retention times for anaerobic digestion (Wandera et al., 2019).

Operating Temperature (°C)	Minimum RT (Day)	Maximum RT (Day)
18	11	28
24	8	20
30	6	14
35	4	10
40	4	10

2.14.5 Temperature

To operate at the optimal temperature it is important to consider the type of bacteria present in the biogas plant and their condition for survival. These microorganisms are

normally classified according to the temperature range in which they grow. Temperature classification of microorganisms is mesophilic, psychrophilic, and thermophilic (Ndiweni et al., 2017). Psychrophilic optimal operating temperature is $<20^{\circ}\text{C}$, mesophilic works better between $20\text{--}45^{\circ}\text{C}$ but its optimal temperature are about 40°C and thermophilic bacteria works under temperature $>50^{\circ}\text{C}$ although the optimal temperature is 55°C **Table 2.3**. Different studies have suggested that there is a relationship between biogas produced during the anaerobic process and a range of temperature settings (Mutegoa et al., 2020). Thus, the preferable environment for anaerobic bacteria in the biogas digester is thermophilic and mesophilic. The thermophilic environment is faster and the best than the remaining two conditions but the main disadvantage of the thermophilic environment is that it requires a higher amount of energy to heat the bio-digester system. The time for the feedstock to ferment inside the biogas digester depends on the temperature maintained. The optimal temperature controls the intracellular microbial activity of the enzyme which will affect the metabolic activity and the fermentation process in the digester. The microorganism breaks down the complex biopolymer molecules in the organic feedstock during the anaerobic digestion process to release biogas. The mutual interactions act as the basis for all four stages of AD and are needed for the complete degradation of the feedstock into soluble and gaseous products that affect the anaerobic digestion process. A decrease in temperature due to seasonal differences will lower fatty acid accumulation and chemical oxygen demand. Chemical Oxygen Demand is the amount of oxygen necessary to oxidize insoluble and soluble organic matter present in the bio-digester. The addition of flocculants and coagulants inside the bio-digester is one of the best methods of controlling lower saluted chemical oxygen demand.

Although high temperature influences the rapid degradation of substrates it is not recommended because it is less effective in terms of biogas production, operational complications, large energy input, and therefore not economical. However, many researchers show that at high temperatures the formation of hydrogen-by-hydrogen trophic methanogens is less favored. Under the thermophilic condition, the degradation of organic acid is faster compared to mesophilic conditions. Despite all these advantages most of the biogas plants work under mesophilic conditions to avoid the risk brought by thermophilic. Under thermophilic conditions, biodegradation during co-digestion of sewage and sugar beet pulp was much limited due to high volatile fatty acid (HVFA) accumulation while complete biodegradable was reached under mesophilic conditions (Xie et al., 2016).

Table 2.3: Temperature ranges and corresponding retention time for AD

Classification	Temperature (°C)	Retention Time (days)
Mesophilic	<20	11-28
Psychrophilic	20 – 45	6-30
Thermophilic	≥50	4-14

2.14.6 Operating pH

The pH is a crucial factor that affects the growth of microbes during the fermentation of the feedstock in the bio-digester. The required pH range of the digester should be between 6.5 and 7.4 (Vijayakumar et al., 2022). The rate of methane generation normally decreases for values outside the specified range. Therefore, at low pH, biogas production is low while at high pH levels outside the range low yield can be observed and sometimes inhibition of the production. There are some situations when the pH level needs to be raised using a basic solution like sodium hydroxide or sodium carbonate or lowered using an acidic solution such as dil HCl. Mixing food substrates

from different sources is normally highly complex as they contain various compounds that result in either successful optimization of the process or unprofitably production of biogas if not controlled properly. The pH of the bio-digester is affected by carbon dioxide and the accumulation of volatile fatty acids to progress with the anaerobic fermentation process, the volatile fatty acid and acetic acid concentration range should be under 2000 mg/L (Sreekrishnan et al., 2004). The higher pH value has an effect on ammonia-ammonium balance and a rise in cation concentration will affect the anaerobic digestion process. Therefore, acid production and its concentration in the digester will lead to the decline of biogas production. A study done (Dasgupta & Chandel, 2020) on the neutralization of slurry using sodium hydroxide on adjusting pH value to 7.0 ± 0.2 before the anaerobic digestion process found that neutralization is an essential step after alkaline pretreatment of the feedstock material for biogas production. This process was done to ensure optimal pH for the microbial activities during anaerobic process, prevent the reactor from corrosion in case of excessive addition of an alkaline agent.

2.14.7 Particle size

The lignocellulosic nature of crop residue poses recalcitrance to its complete decomposition through an anaerobic digestion process. Pretreatment of feedstock substrate for biogas production is an important step to break the resistant layer of lignin material found in the feedstock, by reducing the crystallinity of cellulose and increasing the availability of starch material. Physical pretreatment of biomass requires size reduction using grinding, a ball mill, mechanical extrusion irradiation, and chipping. The biomass size can be reduced up to 5–30 mm by chipping however, with the assistance of milling and grinding the particle size can be reduced to 0.2 mm. Mechanical grinding can be done using a knife, colloid mill hammer, and ball milling.

Particle size can affect the rate of anaerobic digestion as it affects the availability of surface area to hydrolyze enzymes.

The kitchen remains and municipal waste as fibers degradation and methane yield increase with the decrease in substrate particle size from 100 mm to 2 mm (Mshandete et al., 2006). The smaller particle sizes increase the surface area to volume ratio available for microbial activity that results in food available for bacteria, thus anaerobic biodegradability increases. The particle size has some impact on biogas yield as the larger size of feedstock resulted in the clogging of the bio-digester meanwhile when the particle size of the feedstock is smaller, leads to an increase in microbial activity, which increases biogas generation. The physical pretreatment reduces the particle size and thus increases the surface area of biomass for enzyme accessibility. The effect of mechanical pretreatment of lignocellulosic feedstock varies as suggested by different researchers depending on the pretreatment method used (chipping, cutting, grinding, milling) structure of substrates, and particle size reduction methods. A study done by Mshandete et al. (2006) found that biogas yield increased by 22% as sisal fiber particle size reduced from 10 cm to 2 mm. Meanwhile, another researcher found that the mechanical pretreatment of wheat straw and barley resulted in an increase of methane potential by 54% and 83.5% as particle size reduced from 0.5 cm to 0.2 cm respectively. Literature reported that the size of the feedstock was grounded to 0.088 mm the biogas yield was higher compared to other larger particle sizes while at 25 μm the biogas production was much higher. Thus, the size of the feedstock is directly linked to the difference in the total surface area of exposed microbes.

Various methods of pre-treatment are used in literature the physical pre-treatment of feedstock is the most important method which helps to increase the surface area therefore making it easy for digestibility of these substrates through an anaerobic

digestion process in the digester. The physical pre-treatment ways include; liquid hot water, steam explosion microwave irradiation although they are expensive methods and therefore cannot be affordable by low-income households families. All pre-treatment methods aimed at improving the enzymatic hydrolysis process and increasing the surface area of the lignocellulosic feedstock. The alkali pre-treatment is one of the significant techniques used to reduce the crystallinity of the cellulose materials, and finally, the removal of lignin that can be most useful for biogas generation.

2.14.8 Carbon to nitrogen ratio (CN)

Biogas yield from power plants mainly depends on the feedstock chosen and the carbon-to-nitrogen ratio and the value of pH depends on the feedstock's carbon-nitrogen ratio. The high amount of carbon dioxide and carbon nutrients in the feedstock simulates the lower pH value in the digester while high nitrogen content and ammonia gas production stimulate a higher pH value. The carbon-to-nitrogen ratio is a fundamental framework used to characterize the fermentation feedstock materials; it is an effective and vital variable for assessing the stability and achievement of the anaerobic digestion process. CN ratio is a very important parameter in anaerobic digestion because when it is more than the optimal it creates an acidic condition in the reactor hence lowering the pH while when it is less than required it causes alkalinity in the system and raises the pH as the results affect microorganism that lead into digester failure. The carbon-to-nitrogen ratio plays an essential role in the anaerobic digestion process. To know the maximum slurry recirculation it is necessary to balance the carbon-to-nitrogen ratio and to get the optimal methane yield it is vital to perform an anaerobic digestion experiment using different mixtures of the feedstock with different mixing ratios. Many studies indicated that the optimal CN ratio ranges from 20-30; the exhaustion of nitrogen and carbon could be affected by a different operating condition such as temperature, and pH that results in

the occurrence of inhibitory effects. Temperature increase from mesophilic to thermophilic leads to ammonia inhibition. Nevertheless, this type of inhibition can be escaped via an increase of the CN ratio of the mixed food substrate to a certain appropriate level of the mixture. Improving methane yield and its efficiency has been a long-standing goal for the biogas industry and among the methods proposed include co-digestion of the feedstock because of its convenience and effectiveness as researchers have shown its advantages in balancing the carbon to nitrogen ratio in biogas digesters. The study done by Rughoonundun et al. (2012) shows that the maximum yield was 0.36 g acid/g V and was achieved by mixing S₃₀, S₄₀ and S₆₀ while CN ratio ranges from 13.2 to 24.5 g CN (Rughoonundun et al., 2012), however, increasing the CN ratio from 25-31.8 causes a reduction of yield by 16%. The above results confirm that microbial metabolism is significantly influenced by nutrient ratio. Literature shows that the feed at a CN ratio of 30:1 results in optimum methane yield (Matheri et al., 2017). When the level of the CN ratio is higher then there is a fast depletion of nitrogen used by bacteria to produce methane to satisfy their protein needs, therefore, lowering the production of methane. To operate the biogas plant at an optimum CN ratio, biodegradable materials with a high CN ratio should be blended with materials with a low CN ratio. However, these mixing ratios are not satisfactory for different kinds of organic wastes, as the amount of nutrient differ considerably.

2.14.9 Presence of heavy metals in the feedstock for biogas production

Heavy metals are necessary elements in the anaerobic process that include Nickel, Cadmium, zinc, and Copper that promote biogas yield (Cai et al., 2017). However, uncontrolled heavy metals inhibit the microbial activity in the digester as they act as toxic compounds and therefore limit biogas production. Copper metal interacts with the cellulose materials and affects the hydrolysis process. The effect of heavy metals in

biogas production can be observed in larger-scale livestock keepers where some additive substances contain heavy metals like Cu^{2+} in domesticated bird feedstock. Some amount of copper iron added in poultry food cannot be adsorbed in the digestive system and therefore poultry manure contains a higher amount of Cu^{2+} . The rate of limiting step for anaerobic digestion containing lignocellulose is a hydrolysis process and is characterized by cellulase. A study done by using a feedstock containing copper ions with a concentration of 150 mg/kg Cu^{2+} shows a cellulase of 16.3%, which is a higher value, compared with a control experiment. The trace amount of copper, Iron, and Nickel may be necessary for anaerobic microbial activities, which act as a cofactor. When the concentration of Cu^{2+} was 300 mg/kg, the enzymic activity was 5.86% which is lower than the control experiment and the microbial activities were completely hesitant. The presence of Cu^{2+} can affect the production of volatile fatty acids. It should be noted that VFA is an important intermediate product during the anaerobic process. However, a high amount of volatile Fatty acid can lead to a decrease in pH and eventually inhibit acetogenesis and hydrolysis. Studies showed that 100 mg/L copper ion accelerates the degradation of volatile fatty acids. Meanwhile, Cu^{2+} greater than 100mg/L limit acidification processes results in to low biogas yield (Hao et al., 2017).

The presence of Cu^{2+} affects the growth and activity of methanogenic bacteria as it is the final and the most important stage of the anaerobic process, and the methanogens require a trace amount of heavy metals like copper to maintain their microbial activities. The presence of Cu^{2+} at a low concentration of about 5 mg/L accelerated the activity of methanogens, while at higher amount a from 300 mg/kg Cu^{2+} causes total inhibition of the methanogenic actives and therefore lows the biogas production (Jiang et al., 2018). The optimum amount of Cu^{2+} is in a range of 5–30 mg/ L, in which methane and biogas productions are optimized. The small concentration of Cu^{2+} accelerates the production

of volatile fatty acid and the activity of enzymes in the digester, while a high amount of Cu^{2+} limits the growth of bacteria and the activity of enzymes. On the other hand, the optimum amount of Ni^{2+} concentrations for biogas and methane yield ranges from 0.8 mg/L-4 mg/L. The content of Fe^{2+} greater than 8000 mg/L hinders the production of biogas (Andriamanohiarisoamanana et al., 2018), when the amount of Fe^{2+} found to be less than 12000 mg/L, the yield of biogas is not significantly affected but at a concentration of 20000 mg/L Fe^{2+} content, the production of biogas is significantly inhibited.

On the other hand, the concentration of cadmium and zinc ions affects the growth and activity of methanogenic bacteria, when the amount of Cd^{2+} is between 3.0 and 20 mg/L, it limits the methanogenic activity. In the anaerobic process, when the biogas digester contained 0, 2.5, and 5 ppm of Cd^{2+} , the total amount of biogas yield was 2360, 5960, and 5040 mL, respectively (Kumar et al., 2006), while Zn ions promote the methanogenic activity at a concentration of 5 mg/L and inhibitory for biogas production at a concentration 50 mg/L.

2.15 Effect of Design of a Digester on Biogas Production

Regularly the lower retention time and organic loading rate are the necessary elements for the design of a bio-digester. It can be operated at different phases like multiphase units, dual-stage systems, and single-stage. The disadvantages and advantages can be used to decide the operating system. The single-phase and dual digesters have something in common in nature although dual digesters system has some potential advantages in terms of energy recovery as compared to single-stage digesters. The capital, operation, maintenance, and cost for multiphase digester is much higher and therefore it is more recommended for industrial purposes than for commercial applications. The optimum condition for microorganisms and the operational

parameters could be much more difficult in multistage systems, but the stability of the digester will be enhanced. The feedstock flow in different stages in a multiphase digester is highly homogenous in terms of quantity and quality. The quality of biogas from the digester can be improved by the removal of volatile fatty acids from the system. The multistage anaerobic reactor has a higher removal efficiency of volatile matter when compared to other single-stage digesters (De Gioannis et al., 2017). The selection of a suitable and potential feedstock normally is the starting point in the anaerobic digestion process and determines the amount of biogas generation **Figure 2.3**.

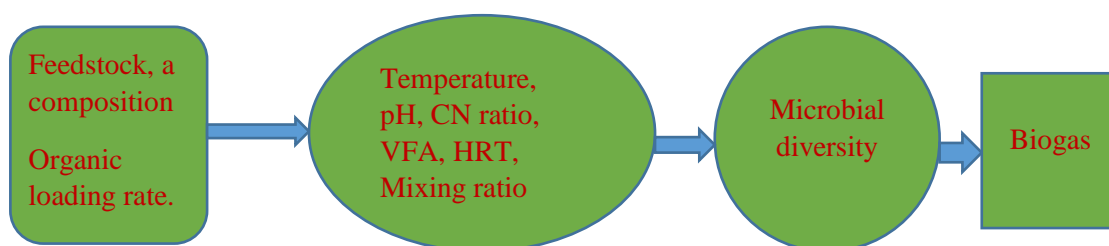


Figure 2.3: Operational parameters for the biogas power plants.

2.16 Inoculum

Inoculum is a substance supplied to a digester to provide a live source of microorganisms for the start-up and operation of biogas processes. It aids in the anaerobic digestion process by giving the required bacteria for biodegradation (Madondo, 2017). It helps in the anaerobic digestion process by providing the initially required bacteria for the biodegradation of complex molecules. An inoculum must be added since it will increase the yield of biogas, and the amount of methane it contains, speed up the process, and improve stability. To decrease the anaerobic digestion period and digester volume, utilization of active inoculum from animal manure is always preferable. Cow manure that has been digested from a functioning biogas plant, well-rotted manure pit material, cow dung slurry, and sewage sludge can be used as

inoculum. Because it contains an activated microbial consortium, the bio-digested slurry was employed as an inoculum.

2.17 Mathematical Modeling and Simulation in Adsorption

A mathematical model is a description of a system using mathematical concepts and language. Biogas adsorption can be explained better using models; the models vary according to the requirement. The batch adsorption takes place in a closed system that contains a required amount of sorbent that can contact a certain volume of sorbate but in solution form (Inchauspe, 2021). While fixed-bed adsorption occurs in an open space system, whereby adsorbate solution passes through a column that is packed with sorbent (Xu et al., 2013). The behavior of a fixed bed column can be explained in terms of the breakthrough curve and the effluent. The shape of the equilibrium isotherm and the individual transport processes in the column and adsorbent determine the shape of the curve.

2.17.1 Adsorption modeling

There are widely used models to predict breakthrough curves as Bohart-Adam's model, the Clark model, the general rate model, the wave propagation theory model, the Wang model, the Yoon-Nelson model, and the Thomas model (Xu et al., 2013). Among the models, mentioned literature shows that Bohart-Adam's, Yoon-Nelson's and Thomas's models are essentially the same, both use logistic equations with minor differences in the definition of the parameters while the mathematical used is the same (Chu, 2020).

2.17.1.1 Adams-Bohart model

Literature shows that this model performed poorly during data fitting as compared to other models (Ghosh et al., 2014; Yan et al., 2017; Zhang et al., 2018) otherwise, it can only fit the initial portions of the breakthrough curves (Karimi et al., 2012). The

deficiency of this model identified by some researchers has been troubling as it has been and remains a cornerstone of fixed bed adsorber analysis and design. The B-A model, along with its variant the bed depth-service time (BDST) equations which is the rearranged form of the Bohart-Adams model can be found in every wastewater treatment textbook (Cooney, 1999). The model predicts the linear relationship between the depth of the bed and the time taken for the breakthrough R^2 (Chu, 2020). The linear relationship of this model simplifies the tasks of adsorber design and analysis and provides a straightforward approach to running pilot tests. In some papers that provide evidence of unsatisfactory results using this model, the model **equation 2.6** without an exception takes this form

$$\ln\left(\frac{C_o}{C}\right) = \frac{k_{BA}N_oL}{U} - k_{BA}C_o t \quad (2.6)$$

Where C is the column exit concentration at time t , C_o is the initial adsorbate concentration, k_{BA} is the B-A rate coefficient, L is the bed depth, N_o is the adsorption capacity of the adsorbent per unit volume of the bed, and u is the superficial velocity. The values of N_o (maximum adsorption capacity) and K_{AB} (Adams-Bohart constant) will be obtained from intercept and slope at the different flow rates, bed height, and concentration.

2.17.1.2 Thomas model

The model presumes the plug flow behavior within the bed reactor. In general, it is a popular model used to explain the performance theory of the sorption mechanism in any fixed bed column (Chen et al., 2012). The linear form of this model is as per **equation 2.7**. The model assumes that the axial dispersion is negligible, and it is based on second-order kinetics and therefore does not limit adsorption by chemical reaction hence its limitation, it is controlled by a mass transfer mechanism (Bharathi & Ramesh, 2013).

$$\ln\left(\frac{C_o}{C_t} - 1\right) = \left(\frac{k_{Th}q_{Th}m}{Q}\right) - k_{Th}C_o t \quad (2.7)$$

Where q_o is the adsorption capacity (mg/g), t stands for total flow time (min), k_{Th} is the Thomas model constant (mL/min mg), Q_o is the equilibrium Malachite green uptake per g of the adsorbent (mg/ g).

The values of q_o and k_{Th} can be determined from the plot of $\ln [(C_o/C_t)-1]$ against t . The coefficients and relative constants can be obtained using linear regression analysis.

2.17.1.3 Yoon-Nelson model

Yoon-Nelson model deduces the possibility of adsorption of adsorbate and the breakthrough curves. It does not require comprehensive information about the characteristics of adsorbate adsorbent and the physical properties of the bed, and therefore it is easier to implement than the rest of the model. The model is normally expressed in the following as per **equation 2.8**.

$$\ln\left(\frac{C_t}{C_o - C_t}\right) = K_{YN}t - \tau K_{YN} \quad (2.8)$$

Where τ is the time required for 50% breakthrough and k_{YN} is the Yoon-Nelson rate coefficient, q_{OYN} can be estimated from the slope and intercept of the Yoon-Nelson plot at different concentrations, bed height, and flow rates. The summary of the three models is indicated in **Table 2.4**.

Table 2.4: Fixed bed column model used in the current study

Models	Nonlinear	Linear	Plot made	Reference
Adams-Bohart	$T = \left[\frac{N_{OZ}}{C_{ov}} \right] - \ln \frac{\left(\frac{C_o}{C_t} - 1 \right)}{C_o k_{AB}}$	$\ln \left(\frac{C_t}{C_o} \right) = \frac{k_{BA} N_{OL}}{U} - k_{BA} C_o t$	$\ln \left(\frac{C_t}{C_o} \right) Vs t$	(Hanbali et al., 2014)
Thomas	$\frac{C_t}{C_o} = \frac{1}{[1 + \exp(k_{Th} q_{Th} m)] - k_{Th} C_o t}$	$\ln \left(\frac{C_t}{C_o} - 1 \right) = \left(\frac{k_{Th} q_{Th} m}{Q} \right) - k_{Th} C_o t$	$\ln \left(\frac{C_o}{C_t} - 1 \right) Vs t$	(Chen et al., 2012)
Yoon-Nelson	$\frac{C_t}{C_o} = \frac{1}{1 + e^{K_{YN}(t-T)}}$	$\ln \left(\frac{C_t}{C_o - C_t} \right) = K_{YN} t - \tau K_{YN}$	$\ln \left(\frac{C_t}{C_o - C_t} \right) Vs t$	(Chen et al., 2012)

2.17.2 Adsorption Isotherms

Adsorption isotherms are widely used to remove impurities from gas phase or aqueous solutions. Adsorption is a process whereby gaseous, liquid, or solid substances attach to the surface of another material which is the sorbent. In this situation, the bonds such as metallic, covalent, or ionic occur in between the adsorbent's constituent atoms and adsorbent materials (Saravanan et al., 2021). On the other hand, atoms on the surface of the adsorbent are not surrounded by various other adsorbent atoms and can assemble some more adsorbate. It is very important to study adsorption equilibrium before the prediction of the optimal sorption process, and therefore adsorption is cost-effective and very easy among separation methods. An adsorption phenomenon exists in most biological, natural, as well as chemical systems and it has wide applications in industries, treatment plants, and water purification processes. Physicochemical characteristics of the adsorbent, porous nature, surface area, and mechanical and chemical strength of the sorbents play a vital role in the separation process. However, commercial sorbent for biogas purification is expensive and to overcome this researchers have studied the locally available sorbent such as the activated carbon from

many naturally available carbonaceous components such as bagasse, sawdust, bamboo bamboo-based plants.

A thermodynamic understanding of the adsorption process is crucial for the proper utilization of adsorbent materials. The adsorption equilibrium gives the maximum limit to which an adsorbent-adsorbate exists in equilibrium. Following experimental data, the adsorption capacities for biogas purification can be presented using the adsorption equilibrium of different isotherms as Langmuir, Freundlich models, and Jovanovich isotherm models. Among these isotherms, the Langmuir isotherm is the most widely used and it simulates the monolayer adsorption of the adsorbate onto a homogenous adsorbent surface.

2.17.2.1 The Langmuir isotherm

The Langmuir adsorption isotherms imitate the monolayer adsorption of the adsorbate onto a homogenous adsorbent surface. Initially, it was developed for gas-to-solid interaction but is also used for various adsorbent materials. It is an empirical isotherm that is based on kinetic fundamentals; that is, the surface rates of adsorption and desorption are equal with zero accumulation at equilibrium conditions. The parameters of Langmuir isotherm have a great meaning that describes the maximum adsorption capacity and the properties of adsorbent material. The Langmuir model reports that at maximum adsorption, only a monolayer is formed, and adsorbate molecules do not deposit on other, already adsorbed molecules of adsorbate, only on the free surface of the adsorbent (Hami et al., 2020; Nadimi et al., 2021). If it happened an adsorbed molecule enters an adsorption site, then there occurs no further adsorption. To approximate the parameters in Langmuir, the non-linear Langmuir is normally transformed into a linear form of Langmuir, and this process can allow calculations of Langmuir parameters using the linear regression method, which is more superficial,

appropriate, and easily to be performed by the use of originPro software (Guo & Wang, 2019). The monolayer assumption requires identical adsorption sites and only one molecule can be adsorbed at each site. There is no more adsorption in a site once a surfactant molecule has occupied it. The Langmuir basic assumptions for the adsorption of gases on the adsorbent material can be summarized as the surface of the sorbent is homogeneous. The adsorption energy is constant throughout the adsorption sites; the adsorption on surface of the sorbent is localized; the adsorption site of the sorbent can accommodate only one molecule or atom of the sorbate (Chilev et al., 2022).

Literature shows that the linearized Langmuir isotherm plots can be expressed in four different ways as C_e/q_e Vs C_e , $1/q_e$ Vs $1/C_e$, q_e/C_e Vs q_e , and q_e Vs q_e/C_e where the necessary parameters can be drawn from the plots. Kumar and Sivanesan found that Langmuir-1 was written as C_e/q_e Vs C_e and Langmuir-2 written as $1/q_e$ Vs $1/C_e$, could estimate accurately the Langmuir parameters for the adsorption of safranin onto rice husk. Parimal et al. (2010) observed that the Langmuir -1 which is written as a plot of C_e/q_e Vs C_e can best explain the adsorption of lead, copper, and zinc onto pyrophyllite. Therefore, getting into an equilibrium quality and the saturated monolayer isotherm curve be expressed in equation 5 which was essential for the monolayer adsorption process, the linear structure of the Langmuir isotherm equation is written as per **equations 2.9** (Parimal et al., 2010).

$$\frac{C_{eq}}{q_e} = \left(\frac{1}{q_{max}} \right) C_{eq} + \frac{1}{K_L q_{max}} \quad (2.9)$$

Where, q_e is the equilibrium adsorption capacity, q_{max} (mg/g) is the maximum adsorption capacity, K_L (L/mg) Langmuir constant; C_e is the equilibrium adsorbate concentration, C_{eq} (mg/L) is the concentration at equilibrium, q_{max} (mg/g) is the maximum adsorption capacity, R_L (L/mg) is the Langmuir equilibrium constant.

The adsorption capacity can be calculated using **equation 2.10** as illustrated by (Guo & Wang, 2019)

$$qe = \left(\frac{C_0 - C_e}{w}\right) * v \quad (2.10)$$

Where V is the solution volume (L), q_e is the equilibrium adsorbate concentration in the solid phase (mg/g), m is the adsorbent mass (g), and C_e and C_0 are the equilibrium adsorbate concentrations and initial in the gas phase (mg/L), respectively.

The Langmuir model/ isotherm can be expressed in nonlinear form as per **equation 2.11**

$$qe = \frac{q_{max} K_L C_e}{1 + K_L C_e} \quad (2.11)$$

Where q_m is the maximum adsorption capacity (mg/g), K_L is the affinity constant (L/mg), q_e is the amount of adsorbate concentration in the solid phase equilibrium (mg/g), and C_e is the amount of adsorbate concentration in the gas phase at equilibrium (mg/L).

The essential properties of the Langmuir model/ isotherm can be expressed by a dimensionless constant that is referred to separation factor as per **equation 2.12** that is used to affinity between the adsorbate molecules and adsorbent materials.

$$RL = \frac{1}{1 + K_L C_0} \quad (2.12)$$

In general, $RL < 1$ shows that adsorption is favorable; $RL = 1$ indicates that the adsorption isotherm is linear and does not depend on the concentration, $RL \sim 0$ indicates that adsorption is irreversible because the adsorbate cannot diffuse (usually occurs in chemisorption), and $RL > 1$ corresponds to unfavorable adsorption because desorption occurs.

2.17.2.2 The Freundlich isotherm

Unlike the Langmuir model, this empirical isotherm can be used for multilayer adsorption on heterogeneous sites. It assumes that the affinities toward the heterogeneous surface and the adsorption heat distribution are non-uniform. Freundlich isotherm describes adsorption as a mechanism that happens through heterogeneous surfaces with a mechanism of multilayer adsorption. It explains the multilayer heterogeneous adsorption process where isotherm assumes that the adsorption process occurs on the heterogeneous surface of the adsorbent. The mathematical expression model for the Freundlich isotherm is as shown in equation 9. The linear form of the Freundlich isotherm model is expressed as per **equations 2.13** and **2.14** which was deduced from Equation 9. The Freundlich parameters can be calculated via the plot of $\log q_e$ versus $\log C_e$ after regression for analyzing the applicability of the Freundlich sorption isotherm. The summary of all parameters used in Freundlich isotherms is as per **Table 2.5**.

$$q_e = K_F C_e^{1/n} \quad (2.13)$$

Where $1/n$ is the adsorption intensity or surface heterogeneity and b is the adsorption capacity in L/mg. Unfavorable adsorption occurs when $1/n > 1$, irreversible at $1/n = 1$. While $0 < 1/n < 1$, adsorption is considered favorable with the chemisorption process.

$$\text{Log } q_e = \frac{1}{n} \log C_e + \log K_f \quad (2.14)$$

Where n is the adsorption intensity constant, K_f (L/g) is the Freundlich adsorption constant and $1/n$ is the measure of adsorption intensity ranges between 0 and 1 and C_e (mg/L) is the concentration at equilibrium. However, equation (13) is further deduced to equation (14) for quantification of parameters.

From the Linearized Freundlich **equation, 2.14**, a plot of $\log q_e$ versus $\log C_e$ gives a straight line with a slope = $1/n$ and intercept = $\ln b$ where all the parameters can be easily calculated. The linearized form is an uncomplicated and straightforward kind of isotherm, although it can generate propagation errors that have some effects in erroneously predicting Freundlich parameters. Thus, the use of a non-Linear Freundlich isotherm acts as a mitigating measure to solve the problem associated with the linear form of Freundlich isotherm. The Freundlich model explains multilayer adsorption and assumes exponential decay in the energy distribution of adsorbed sites. Nevertheless, it is not valid for a large range of adsorption data. The determination of R^2 and the comparison between the experimental and the approximated q_e are the most used standards to validate the fitting of the experimental data (González-López et al., 2022).

Table 2.5: The meaning of $1/n$ and n parameters as used in Freundlich isotherm.

Condition	Explanations
$n = 1$	There is a linear adsorption process with a concentration-independent partition between two phases of the equilibrium
$n < 1$	Characteristic of the adsorption process showing a chemisorption process
$n > 1$	Characteristic of the adsorption process with the physisorption process
$1/n < 1$	Characteristic of the normal adsorption process
$1 < 1/n < 0$	Characteristic of a favorable process adsorption because there is no desorption process
$0 < 1/n < 1$	Adsorption on heterogeneous surfaces with lateral interaction (a $1/n$ value close to 0 indicates that the adsorbent surface is increasingly heterogeneous).

2.17.2.3 The Jovanovich isotherm

The Jovanovich model considered the assumptions as in the Langmuir classic isotherm/model and remains successful in the existence of lateral interplay among the adsorbed molecule species. However, the possibility of mechanical contact between the adsorbate and adsorbent is mostly taken into consideration in the Jovanovich isotherm models

model (Al Jaberi et al., 2020; Dai et al., 2011). It is appropriate for both mobile and localized adsorptions. The parameter n takes into account the lateral interaction between the adsorbed molecules. The Jovanovich isotherm reaches the saturation point at a very high pressure. Kiseler reported the use of the Jovanovich isotherm model when determining adsorption isotherms for L-Lysine imprinted polymer and found that the best prediction of retention capacity was obtained by using the Jovanovich isotherm model (Panahi et al., 2008). The equation of this isotherm reaches the limit of saturation when the concentration of the sorbate is high, while at low concentration it is reduced to Henry's law. When making a comparison to the Langmuir equation, the Jovanovich equation has a slower approach toward saturation (Al-Ghouti & Da'ana, 2020).

The linear Jovanovich equation is written as per **equation 2.15** (Mutegoa et al., 2021).

$$\ln q_e = \ln q_{max} - K_j C_e \quad (2.15)$$

Where q_e (mg/g) is the concentration of impurities adsorbed at equilibrium, q_{max} (mg/g) is the maximum adsorption capacity, K_j (l/g) is the Jovanovich constant, and C_e (mg/L) is the concentration at equilibrium.

2.17.3 Adsorption kinetics

The kinetics of biogas purification is explained by four kinetic models pseudo-first order, pseudo-second order, intra-particle diffusion, and Elovich models. The equations for adsorption kinetics were presented in **Table 2.6** and linear plots were done using originPro. According to Dermirbas et al. (2004), Lagergren introduced the pseudo-first-order model (PFO) in the late 19th century (Demirbas et al., 2004). The model explained that there is a direct relationship between the surface of adsorption capacity and the adsorption rate. This model is expressed in linear form as shown in **equation 2.16**.

The Pseudo second order model (PSO) was first applied in 1984 (Sari et al., 2019), it describes the linear relationship between the adsorption rate and surface of adsorption capacity. The model can be expressed in linear form as per **equation 2.17**. Tompkins and Aharonic developed the Elovich adsorption model in 1970 (Sari et al., 2019). It relates the chemisorption essence of adsorption and the interaction of biogas molecules with the heterogeneous surface of the adsorbent **equation 2.18**. Weber and Morris developed the Intra particle diffusion model in 1963, which is an older model. It describes the controlled mechanism of diffusion and it is expressed in linear form as per **equation 2.19**.

Whereas k_1 is the pseudo-first-order rate constant, (min^{-1}), q_t is the adsorption capacity at a particular time, K_2 is a pseudo-second-order rate constant (g/mg.min), t is time, α is the initial adsorption rate (mg/g.min), K_{id} is intra-particle diffusion rate $\text{mg/g.min}^{0.5}$, C is constant and β is the desorption constant (mg/g).

Table 2.6: Four types of adsorption kinetic models in non-linear form.

Adsorption kinetics model	Linear	Equation
Pseudo first-order model	$\ln\left(\frac{C_i}{C_t}\right) = k_1 t$	2.16
Pseudo second order model	$\frac{t}{q_t} = \frac{1}{k q_e^2} + t/q_e$	2.17
Elovich model	$q_t = \frac{1}{\alpha} \ln(\alpha \beta) + \frac{1}{\alpha} \ln t$	2.8
Intra-particles diffusion models	$q_t = k_{id} t^{0.5} + C$	2.19

2.18 Presence of Impurities in Biogas

Biogas produced through anaerobic digestion of biodegradable substances normally contains hydrogen sulfide, carbon dioxide, water, and ammonia impurities (Syed et al., 2006). It is produced from the degradation of carbohydrates and some sulfur-containing compounds within the biogas plant. Hydrogen sulfide can cause degradation of the engine, corrosion of metal parts, and form poisonous sulfur dioxide, which can irritate

the mucous membrane dizziness, headache, and sudden death. Depending on the feedstock material, it was observed that anaerobic digestion of biomass could contain ammonia up to 450 ppm (Yellezuome et al., 2022). Ammonia is an essential component for bacterial growth but also in high concentration, it inhibits anaerobic digestion. In case biogas used in the gas engine is unpurified, it may increase environmental polluting NO_x emission and decrease fuel lifetime. The percentage of carbon dioxide in biogas varies with water contents, the maturity of the feedstock, temperature, bacterial action, and the loading rate of the feedstock. The presence of carbon dioxide in the biogas reduces the burning velocity which will directly affect the performance of the engine (Gupta & Mittal, 2019).

2.19 Methods for Purification

Biogas upgrading technologies obtained from gas-purified industry, technologies use and sorption and separation approaches have advantages of the physical, biological, and chemical properties of gas constituents. Biogas can be utilized directly for household purposes as well as the generation of thermal energy that is used in industries. The particular mixture of biogas can be transformed into highly valuable intermediate products such as syngas through a process known as dry reforming. It is better to upgrade and purify biogas before using them to avoid the aforementioned effects. Upgraded biogas has high methane content that can be compressed into bio-compressed natural gas (Bio-CNG). Compressed natural gas is directly used as a vehicle fuel although this process requires high pressure. Thus; methods for biogas purification include physical method, biological method, pressure swelling, and chemical.

2.19.1 Chemical methods

Chemical and physical methods are rapid and efficient although they are expensive and produce secondary pollutants (Atelge et al., 2021). There are several processes

explained by different researchers concerning biogas purification especially the removal of hydrogen sulfide, water contents, and carbon dioxide from biogas. Generally, chemical methods are known to be effective in the adsorption of hydrogen sulfide at room temperature and high temperature. Hydrogen sulfide in humans at a concentration of 1000-3000ppm may cause an instantaneous death as it reacts with enzymes in the blood and inhibits cellular respiration which leads to pulmonary paralysis, sudden collapse, and death (Khoshnevisan et al., 2017). A sulfur compound in combustible fuels such as biogas is subject to progressively stringent constraints for environmental issues.

Watanabe (2021) analyzed natural gas desulfurization technology as fixed-bed columns, liquid absorption, and slurry reactors. For the sour gasses, alkyl amine (Comite et al., 2016) is mostly preferred and it is adopted in large industrial areas (Comite et al., 2017) they are economically demanding for high operation costs. A study done by (Andriani et al., 2020) compared the concentration of hydrogen sulfide produced from landfill anaerobic digestion (LAD) with digester anaerobic digestion (DAD) and found that H₂S concentration in AD biogas is 40 times more than (LAD). Depending on the use of biogas, some important treatment measures are required; in some application that requires the biogas to have high energy content such as grid injection, and vehicle fuel (Pettersson & Wellinger, 2009) where the concentration of H₂S ranges from 0.5-10 ppm (Weinlaender et al., 2017). High concentration of H₂S in biogas triggers rapid electrode deterioration and therefore dramatic loss of performance (Costa et al., 2020). A fixed bed reactor with a solid sorbent for H₂S capture may operate according to two main principles chemisorption and physisorption. Chemisorption is the formation of chemical bonds between the sorbent and the substrate (Georgiadis et al., 2020) while physisorption is a surface-based exothermic process where there is a transfer of

molecules from the adsorbate to the adsorbent (Rouquerol et al., 2013). Physical adsorption is mostly dominated by electrostatic interaction and weak Van der Waals forces while chemical adsorption is by strong chemical bonds like a covalent bond between the adsorbate and the adsorbent.

Moreover, amine-functionalized magnesium oxide (MgO), calcium oxide (CaO), and sodium carbonate (NaCO₃) can be used to remove hydrogen sulfide and carbon dioxide from biogas. However, these processes have some disadvantages like high equipment corrosion rate, high-energy consumption for solvent regeneration, solvent degradation, and fouling of the process equipment. A study on the removal of hydrogen sulfide from biogas by impregnated carbon with sodium carbonate has been done and it shows that the sorption capacity on the impregnated carbons is much greater than that of the unmodified carbon hence H₂S is no longer removed mainly by physical adsorption but chemical reaction (Yan et al., 2017). When the molecules of H₂S contact with the impregnating compound sodium carbonate (Na₂CO₃), they react instantaneously; similarly, Na₂CO₃ can react with moisture content in biogas and carbon dioxide as per **equation 2.20**.



The presence of a high amount of carbon dioxide increases the break-specific fuel, which decreases the temperature hence resulting in incomplete combustion. It reduces the laminar speed delays ignition and contributes to global warming therefore upgrading is required for the safe application of biogas. The production of biomethane from biogas through anaerobic digestion motivates environmentalists and researchers in general. The purified and upgraded biogas composition depends on the country's policy and its application. It can be injected into the natural gas unit, power generation in the

combined heat and power pipelines, and fuel for vehicles. Upgraded biogas can be converted into bio-compressed natural gas (bio-CNG) easily stored and distributed through gas pipelines (Xu et al., 2015). It is estimated that bio-compressed natural gas used in vehicles worldwide will increase from 2% in 2021 to 27% in 2050 (Khan et al., 2021). In recent years, different techniques have been applied for removing contaminants from biogas and expanding their application. The techniques available in biogas upgrading are mainly water scrubbing, pressure swing adsorption, membrane separation, and physical scrubbing (Dębowski et al., 2021). Due to its versatility and efficiency, sorption is mostly used technology, and meets the economic requirement; innovative renewable and low-cost sorption materials are needed.

Eggshells are the wastes from chicken eggs that contain a high amount of calcium and carbonate and are mainly disposed of in landfills in most countries. They contain about 1% magnesium carbonate, 90–95% calcium carbonate in the form of calcite, 1% calcium phosphate, and some organic compounds (Baláž, 2018). Most of these materials are discarded although it has multidisciplinary application (Pliya & Cree, 2015) as a dehalogenation process (Davie et al., 2008) composite of filter (Toro et al., 2007) and purification of biogas (Baláž, 2018). One of the methods for capturing carbon dioxide before its exposure to the atmosphere is by adsorbing it using calcium-based sorbent like CaO (Bilton et al., 2012) **Figure 2.4.**

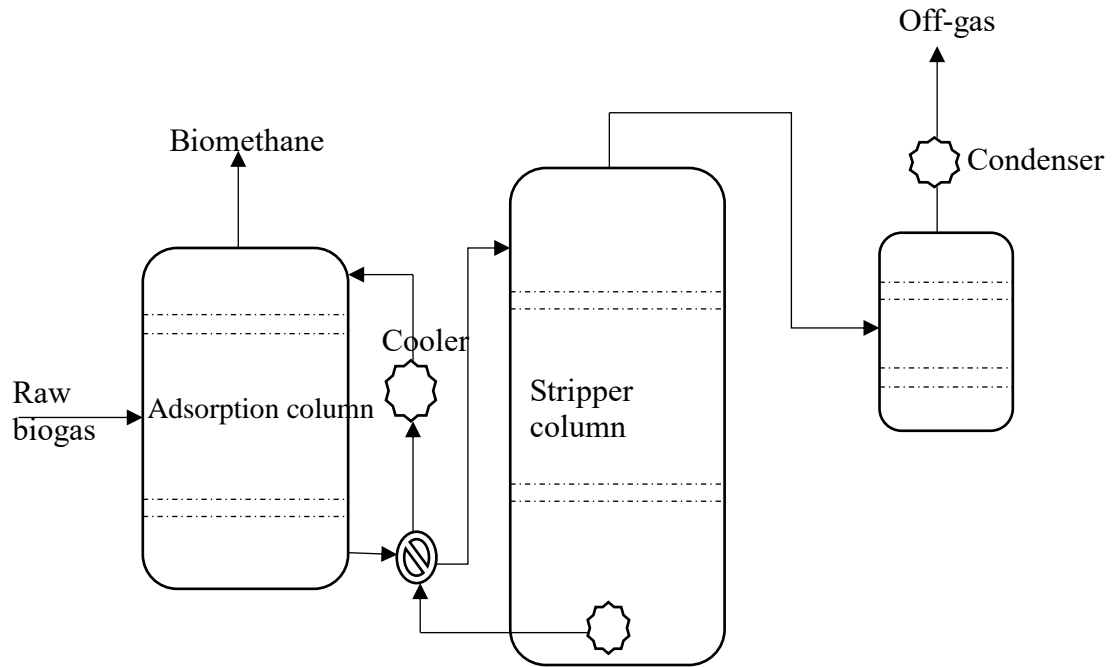


Figure 2.4: Chemical scrubbing method using amine scrubber. Adapted from Bauer et al. (2013).

2.19.2 Physical methods

This involves methods like the use of activated carbon that contains a large porous internal surface area. They are prepared by burning partial materials like coconut shells, sweet potato leaves, and grain pinewood. The coconut shell-activated carbon was applied as an adsorbent for hydrogen sulfide removal from biogas (Choo et al., 2013b). According to this researcher, three basic KOH, K_2CO_3 , and NaOH, while varying the ratios impregnated activated carbon and it was observed that KOH-impregnated activated carbons were able to adsorb hydrogen sulfide at a meager impregnation ratio while increasing in K_2CO_3 impregnation ratio results in adsorbing more hydrogen sulfide. The drawback of this activated carbon is that it is mostly limited by moisture content found in biogas and therefore blockage of mesoporous sites that limits its application and efficiency. Literature shows that physisorption methods that encompass the use of zinc oxide, iron oxides, magnesium oxide, water scrubbing materials, and

alkaline solution are the most traditional techniques and are still in use to date and have shown an excellent in the removal of hydrogen sulfide from biogas.

2.19.3 Water scrubbing methods method

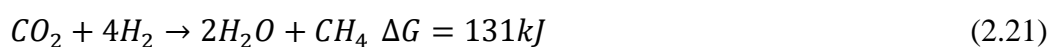
Water scrubbing technologies uses the advantage of different degrees of solubility in various composition/ component of biogas in water to extract and separate methane from other components of biogas like hydrogen sulfide, carbon dioxide ammonia, and siloxane compounds. The most popular technique for the removal of hydrogen sulfide and carbon dioxide from biogas is adsorption via the use of a water scrubbing technique. Literature shows that scrubbing using water techniques is mostly used in the world as compared to other techniques; it reaches about 41% of all biogas upgrading power plants. The solubility of carbon dioxide and hydrogen sulfide is much more as compared to methane. Carbon dioxide at 26°C has almost 26-fold solubility in water is greater than the solubility of methane in water, and performed under 6–10 bars. Mass transfer between water and biogas can be enhanced via packing of the sorbent in a fixed bed column by designating the coefficient of more mass transfer. The biogas from the digester passes uphill in a counter-current way to water hydrogen sulfide and carbon dioxide and is miscible in water. From the top of the adsorption column, the purified biogas can exit while water carries up hydrogen sulfide and carbon dioxide, and some amount of methane exits via the bottom of the adsorption column. For biomethane to be collected the flash tank pressure should be decreased to 3–4 bars. During the water scrubbing method, a large quantity of methane can be lost because of the high-pressure difference between the desorption and absorption columns. Some other parameters that had an impact on bio-methane loss using water scrubbing techniques include biogas concentration, pressure, and the rate of water flowing in the scrubbing unit (Upadhyay

et al., 2022). On the other hand, when using this technique is necessary to know the solubility of the major component of biogas in water.

The process is uncounated by frequent clogging and foaming formation due to the growth of bacteria which depends on the pressure which is almost 4 bars. Water scrubbing has less methane loss <2% while its efficiency is high (>97% CH₄). This method can work well in a place having adequate water supply, and therefore it is not appropriate in some environments. The water in this process needs to be replaced continuously to avoid the accumulation of carbon dioxide and the decrease in pH that will cause the oxidation of hydrogen sulfide. The main disadvantage of this is that it is less efficient than other processes in terms of energy. The purified methane needs to be dried after leaving the scrubber, which makes this method more costly and calls upon a modified low-cost material for upgrading.

2.19.4 Biological Method or Chemoautotrophic

The biological method includes bio-tricking, bio-filter, and bio-scrubber (Barbusiński & Kalemba, 2016) which directly metabolizes hydrogen sulfide into sulfate, which is efficient and not expensive. This involves the transformation of carbon dioxide and hydrogen sulfide to methane by hydrogenotrophic methanogenic bacteria that act as a primary postulation of chemoautotrophic biogas upgrade as per **equation 2.21**. Besides the use of microbes, there are some limitations example bacteria are very sensitive to temperature; therefore, time-consuming for them to be stable hence as a result this method is very slow.



During the upgrading of raw biogas, using the chemoautotrophic technique hydrogen gas is very important in the whole process and it is fed into the anaerobic digester that

can react with the carbon dioxide present in the biogas reactor and form methane via hydrogenotrophic methanogenic bacteria. This technique is employed using microbes that are capable of transforming carbon dioxide into methane, and syngas produced by coal biomass gasification may be transformed into methane and it can be used as a biofuel. Some examples of methanogens are *Methanococcus* sp., *Methanospirillum* sp., *Methanosarcina* sp., *Methanothermobacter* sp., *Methanoculleus* sp., and *Methanobacterium* sp. In recent years, it has been much more possible to transform CO₂ into CH₄ via methanogenic bacteria either by direct injection of hydrogen into the bioreactor or in a separate bioreactor. The main problem of adding hydrogen to the bioreactor is that it raises the digester pH that can lead to failure of the process that can be done as ex-situ, in-situ, and hybrid processes. This technique can recover about 97% methane.

2.19.5 Cryogenic upgrading method

Cryogenic separation is based on different boiling points of different gasses for the separation of methane and carbon dioxide. The biogas is compressed and cooled to a temperature where the CO₂ condenses -78.2°C vs -161.5°C (Kadam & Panwar, 2017) which is lower than methane and can be separated as a liquid, while the gas phase is concentrated with methane. The operational condition to achieve this must be 80 bar of pressure and -170°C of temperature (Andriani et al., 2014) and to avoid freezing, water is then removed before entering into the cryogenic unit (Petersson & Wellinger, 2009), cryogenic separation is as seen in **Figure 2.5**. Since carbon dioxide is in a mixture of gasses in biogas, high pressure, and/or low temperature is needed to get the sublime CO₂ (Margareta Persson, 2003) as it sublimates at 194,6 K (Baena-Moreno et al., 2019). It is highly recommended to remove other impurities in biogas to avoid logging as other techniques (Sun et al., 2015). The new technology to obtain liquefied biogas (LBG) is

needed in the world of renewable and sustainable energy. In this way, cryogenic technology is a promising method for upgrading biogas (Baena-Moreno et al., 2021). There are almost three methods of separating carbon dioxide and methane under cryogenic technology namely, liquefaction combined with desublimation technology, distillation system, and liquefaction system (Tan et al., 2017). Through the use of this method, a range of 95 and 99% methane concentration can be obtained after upgrading (Baena-Moreno et al., 2019). This technology is characterized by having high-energy demand, high investment, and operational costs as a result they make it less competitive as compared to other technologies (Langè et al., 2015). However, the technology may not remove all the contaminants (Mulu, et al., 2021). Cryogenic technology requires the use of more equipment and instruments, such as distillation columns, compressors, heat exchangers, and turbines (M Persson, 2003) and therefore, it needs high capital and operating costs **Figure 2.5**.

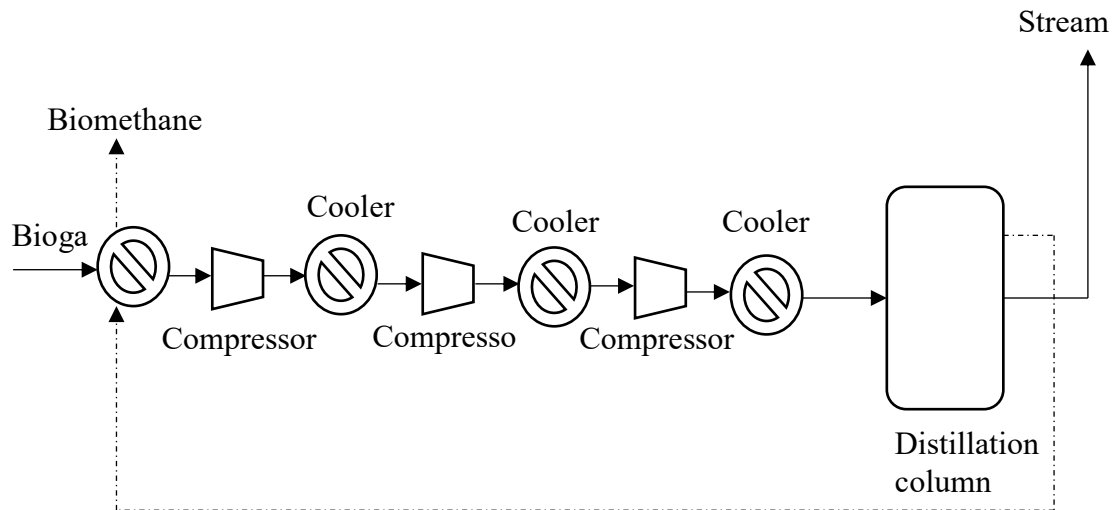


Figure 2.5: Cryogenic separation diagram. Adapted from (Persson 2003).

2.19.6 Pressure swing adsorption (PSA)

This is a technique used to separate unwanted gases from a mixture of different gasses; it is done under high pressure according to the species' molecular weight/characteristics

and affinity to adsorbent material. High-pressure gasses tend to be trapped on a solid surface. This technology has the following advantages low capital cost, compactness of the equipment, safety, and simplicity in operation although its drawbacks are high energy requirement and low and low methane recovery. It produces an off-gas stream with a high amount of methane content that will require some treatment to avoid the emission of methane into the atmosphere. The advantages it has over others make the process suitable even for small installations (Baena-Moreno et al., 2019). According to the research, it shows that pressure PSA has been proposed for upgrading biogas to more than 98% purity and has been simulated using some models. The technology of pressure swing adsorption is mostly used mostly in Austria and Sweden (Niesner et al., 2013). The choice of the adsorbent is critical to the effective operation of a PSA unit

Figure 2.6. The best adsorbent in pressure swing adsorption for biogas upgrading was silicalite, zeolite, silica gel, alumina, and activated carbon PSA for better performance should be conducted under 6 bars for the pressurization and feed step, and a minimum of 1 bar for the purge step and blow down (Siqueira et al., 2017).

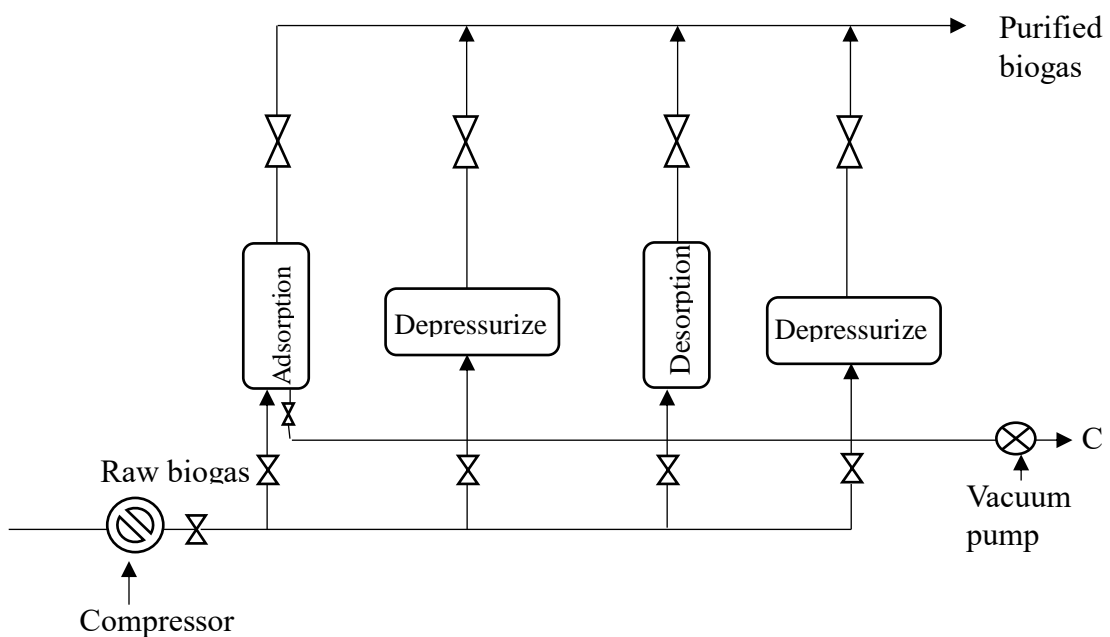


Figure 2.6: PSA unit. Adapted from Kadam and Panwar (2017).

2.19.7 Membrane upgrading method

It is used to separate carbon dioxide and hydrogen sulfide from methane in biogas by using gas permeation membranes and membrane contactors. The first uses conventional gas separation processes to purify biogas at a natural gas level although it does not use any addictive substance. It is a multistep operation technique, which makes it more expensive to be used in literature and it can separate carbon dioxide from biogas 13 folds higher than methane. Literature shows that membrane separation can purify biogas and archive 98% CH₄ concentration. Membrane contractors as upgrading technology can be improved by additional alkaline solutions like sodium hydroxide. The flow chart for biogas separation by membrane technique is seen in **Figure 2.7**. This method works on the principles of the pressure difference between the two sides of the gases. The membranes, which are available for separation, can be grouped into a two-separation group such as low-pressure and high-pressure membrane separation. The high-pressure membrane separation process is usually operated at a pressure < than 20 bars while in some systems it is operated around 8–10 bars where methane enrichment is more than 96% (Kadam & Panwar, 2017). In a multistage membrane separation, the recycling of the waste gases from the first stage is important to enrich more methane concentration. The pressure membranes work at the pressure close to the atmosphere. To achieve a better carbon dioxide and hydrogen sulfide separation the membrane must be selective to methane and carbon dioxide (Kadam & Panwar, 2017). The membrane used must be a hollow fiber module type to achieve the highest surface area for the absorption process. The hollow fibers are made from polymers, which have a greater permeability of about 20 to 60 times higher for CO₂ and H₂S than for methane while hydrogen sulfide must be removed from the biogas before it passes through the membrane to avoid corrosion. Separation by using this method may use high pressure of about 20-40 bars.

The energy consumption for a specific application relies on different parameters like the methane losses, the methane purity of the biomethane produced, the pressure applied to the membrane, and the installed membrane area while **Figure 2.8** shows a pathway for biogas utilization.

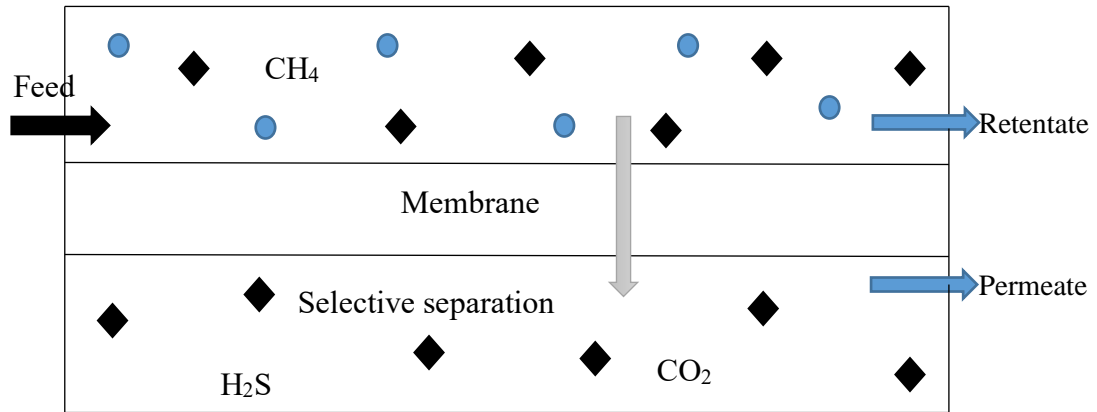


Figure 2.7: Biogas upgrading process using a membrane. Adapted from Khan et al. (2017).

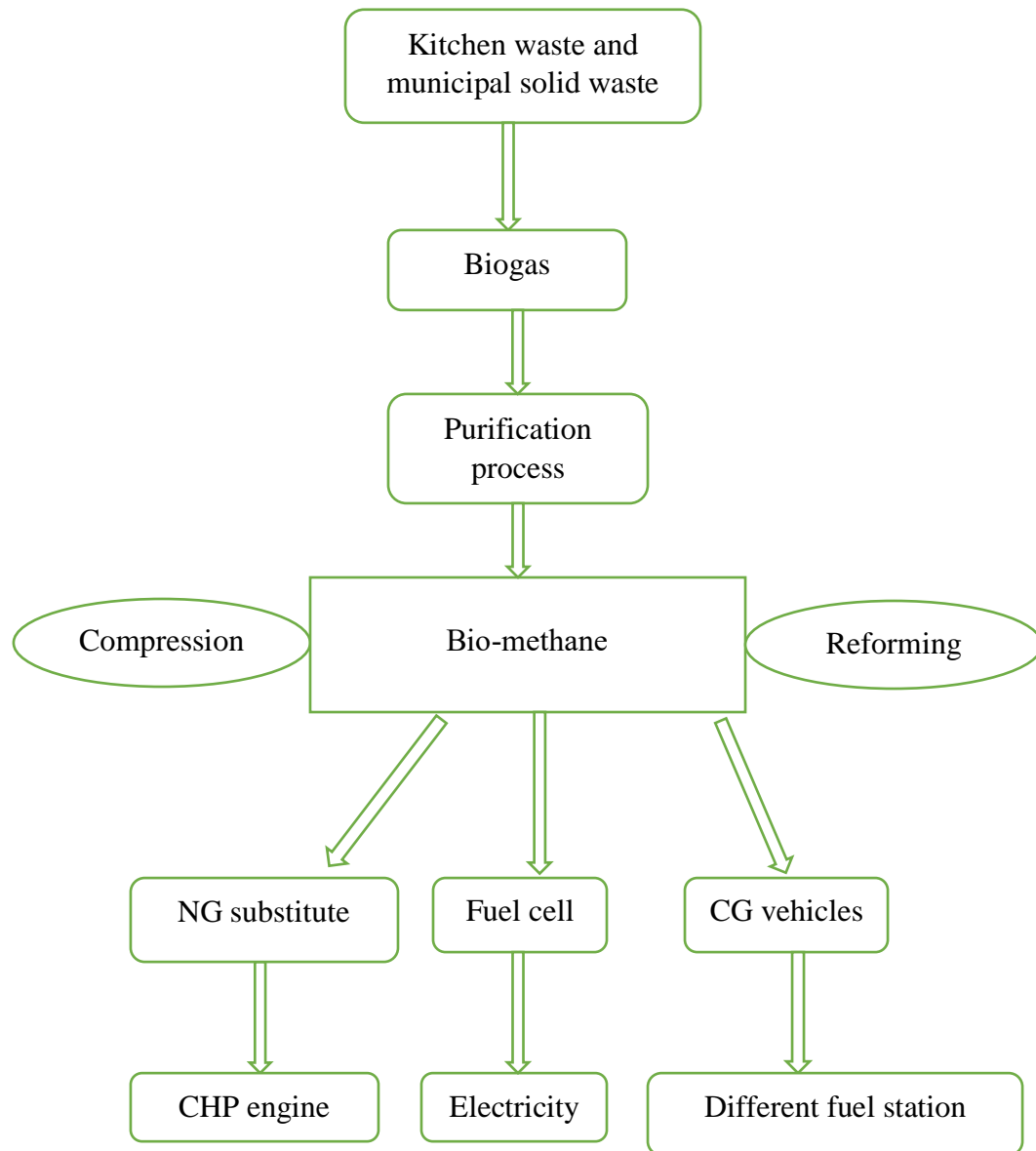


Figure 2.8: A pathway showing ways of biogas utilization

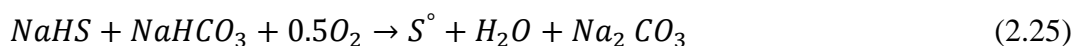
2.20 Regeneration of the Spent Sorbent

For the sorbent to be viable and cost-effective it should be regenerated and reused at least five times. The calcium oxide adsorbs carbon dioxide from biogas to produce calcium carbonate (CaCO_3) which is a reversible process, and when it reaches the saturation point thermal regeneration can be done by heating the sorbent (CaCO_3) under

750°C to reform CaO (Bilton et al., 2012) as per **equation 2.22** decomposition reaction while **equation 2.23** re-use sorption reaction.



The regeneration and re-use of soda ash after the adsorption of hydrogen sulfide from biogas can be done by exposing the spent sorbent to the atmosphere hence losing the adsorbed sulfide and returning to the bed reactor for the adsorption process as per **equations 2.24 & 2.25**.



Generally, biogas generation can be produced from either a single-stage or two-stage anaerobic digestion process the recommended single-stage anaerobic digestion as the two-stage requires high operation and investment cost, and thus for small-scale domestic digesters a two-stage process is neither advantageous nor practical. There are various factors affecting biogas generation, therefore monitoring of those factors is an important issue for the enhancement of the yield. The presence of a contaminant in biogas lowers its energy value and flammability rate and thus purification using various techniques is required. In this chapter different materials for upgrading and desulfurization have been discussed and their regeneration process. The experimental data can be fitted to different models to test the validity of the results.

The chapter entails the utilization of kitchen and municipal solid waste for biogas production as a way of reducing environmental pollution due to undesirable waste disposal techniques, as well as climate change, which is now an agenda worldwide. Before the biogas production process, it is necessary to explore the physical-chemical

characteristics of the feedstock and further the nutrients available in the respective feedstock material. Different pretreatment methods for size reduction have been explored, however physical method was explored in this study due to its simplicity and affordable. The presence of impurities in biogas has forced researchers to look at locally available sorbents to save the purpose. The literature suggests that soda ash and calcined eggshell waste are promising absorbents for gasses. However, it is crucial to critically assess the effectiveness of these absorbents in removing specific impurities in biogas.

CHAPTER THREE

MATERIALS AND METHODS

3.1 Material Used

During characterization of the feedstock, the following kitchen wastes (KW) were used cooked rice (CR), ugali (UG), cooked banana (CBN), cooked beans (CB), and cooked Irish potatoes (CIP). The nine selected municipal solid wastes with varying weights were pineapple peels (PNP), banana peels (Fruit waste (FrW)), Irish potato peel (Tuber waste (TW)), kale (Sww), spinach (SW), cabbage (CBG), carrot peels (CP), rotten tomatoes (TW₂) and remains from black nightshade vegetables (AFNT).

During mono-digestion the following substrates were used five varieties of kitchen waste were collected from the Moi University cafeteria. These were ugali, cooked rice, cooked Irish potatoes, cooked beans, and cooked banana. Municipal solid wastes obtained from the Moi University market included Irish potato peel, banana peels, kale, cabbage leftover, and spinach leftover. The choice of the feedstock was made by considering their availability throughout the year and the equipment was selected based on methods used as per literature. Furthermore, during co-digestion, different feedstock were co-digested to enhance production and balance nutrients as all food waste was co-digested, all vegetable waste, food waste co-digested with tuber waste, fruit waste and vegetable waste, food waste and fruit waste and tuber waste and fruit waste and inoculum used as a catalyst.

On the purification part, soda ash was collected from Lake Natron in Tanzania; eggshells were collected around the international student residential area in Moi University, sand used as pore-forming material was obtained around Moi University, a plastic bottle 13 cm in height and 4 cm in width, and cotton wool and biogas.

3.2 Equipment

The following types of equipment were used to determine the moisture content and total solids: crucibles, electronic precision balance (model HZT –A200), and laboratory oven (model LDO-150), while for total volatile solid and ash content muffle furnace (model ELF11/14B 220-240V 1PH+N) was used. The determination of electrical conductivity and total dissolved solids (TDS) was done using a multipara meter (model HQ40d); while nitrates were determined using a spectrophotometer (model DR-900). The spectrophotometer (model DR-900) was used for chemical oxygen demand while the BOD₅ incubator (model WTW™ 208432) was used to determine the biological oxygen demand (Iordache et al., 2020).

During mono-digestion and co-digestion the following equipment was used a plastic biogas digester, a water bath from Krishna scientific suppliers double-walled model SS 304, the pH was measured using a digital pH meter (Tecnal, Brazil), the digital thermometer model XHF 2001 was for temperature measurements. During the purification and regeneration part, the following equipment was used the clear tube (1/16), a grinder model HK-820, sieves, masking tape 12mm×50m, aluminum foil, flow meter model JBD2-5-SA and biogas analyzer model Geotech 5000.

3.3 Methods

3.3.1 Determination of moisture content

Moisture content is the weight of the water contained in a substrate usually expressed as a percentage by weight. The following procedures were followed in finding out the amount of moisture content after evaporation has taken place. The crucible was properly washed and dried in a laboratory oven at 105°C for about half an hour and left in an oven for cooling. The empty dried crucible was weighed before use and the weight as (W_1). The wet sample was added to the crucible and diligently placed in the laboratory

oven model LDO-150 at a temperature of 105°C for about 2-3 hours until a constant weight was attained and named (W_2). The crucible and the substrate were allowed to cool in the oven to balance the temperature. The crucible plus substrate residue was weighed using the electronic precision balance model HZT –A200 named (W_3), and **equation 3.1** as observed in (Bradley, 2010) was applied in calculating moisture content. The rationale behind choosing specific temperatures and time durations as stated for various steps was relay on literature (Orhorhoro et al., 2017), and the data were taken as an average value for minimization of biases.

$$MC = \frac{(W_2 - W_1) - (W_3 - W_1)}{(W_2 - W_1)} \times 100\% \quad (3.1)$$

The %MC is a percentage of moisture content; W_1 = Weight of dried empty crucible, W_2 is the weight of the sample before the drying process and W_3 is the weight of the sample after the drying process.

3.3.2 Determination of total solid (TS)

Total solid is the amount of solid present in the sample after the loss of water molecules present in it or is the amount of organic matter left in the crucible after the evaporation process. The drying process was done in an oven under 105°C as illustrated in (Orhorhoro et al., 2017), **equation 3.2** was applied in calculating the percentage of total solids;

$$TS = \frac{W_3 - W_1}{W_2 - W_1} \times 100\% \quad (3.2)$$

3.3.3 Determination of total volatile solid (TVS)

The volatile solid is the solid remaining after evaporation of all volatile organic matter after being ignited at 550°C. The following procedures were used in the determination of the total volatile solid of all substrates used in this research. The residues obtained

during the determination of TS were ignited at 550°C in a muffle furnace for 1 hour until grayish-white ash was obtained. The ignited sample and the crucible were allowed to cool in the furnace for six hours. The sample was weighed when the temperature was balanced with the atmospheric temperature and recorded weight as W_4 , **equation 3.3** was used in calculating TVS. The procedures were carried out in MIT Lab at Moi University as per **Figure 3.1**. To minimize potential sources of error or bias during the experimental section the data were taken as an average value.

$$\text{TVS} = \frac{W_3 - W_4}{W_3 - W_1} \times 100\% \quad (3.3)$$

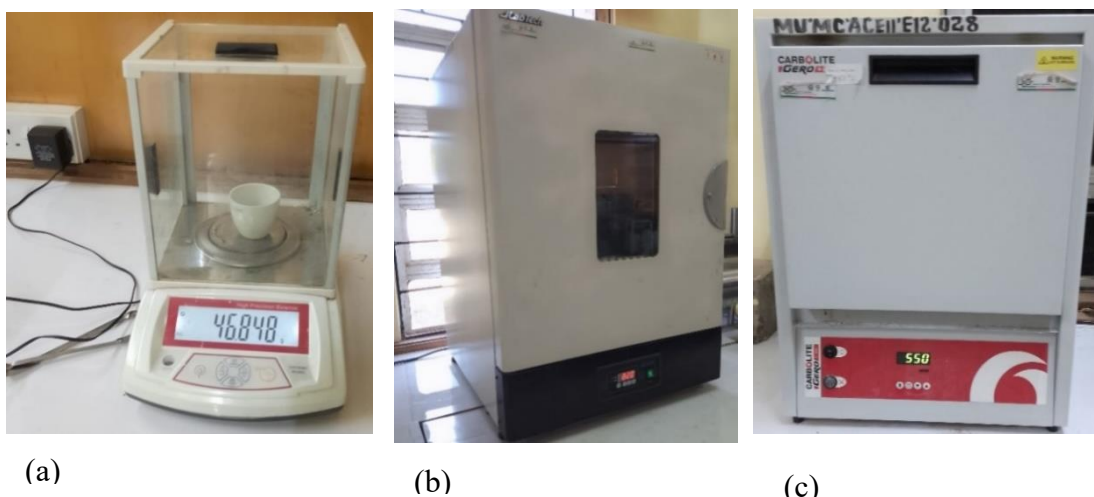


Figure 3.11: (a) Weighing balance, (b) oven, and (c) muffle furnace used in the characterization of KW and MSW samples.

3.4 Experimental Setup for Mono-Digestion

The feedstock was blended uniformly using an electrical blender for size reduction and to enlarge the surface area to volume ratio for microbial activity. Anaerobic digestion was conducted in plastic bottle reactors (working volume of 1.5 L) with an organic loading rate of 80gVs/L under batch conditions in duplicate **Figure 3.2**. The active microbial inoculum used was collected from an active biogas plant around Eldoret town in Kenya and about 25mL was added in each bio-digester. The nature sludge used was watery in form while the amount of the total mixture in each digester was 1200g. The

biogas plant was working at mesophilic temperature using cow dung as feedstock with the existence of a large array of the highly active methanogenic community for the AD process. After feeding the reactor with the substrate it was closed tightly to avoid air entering, and the biogas generated was measured through the water displacement method, (Huang et al., 2016; Pavi et al., 2017).

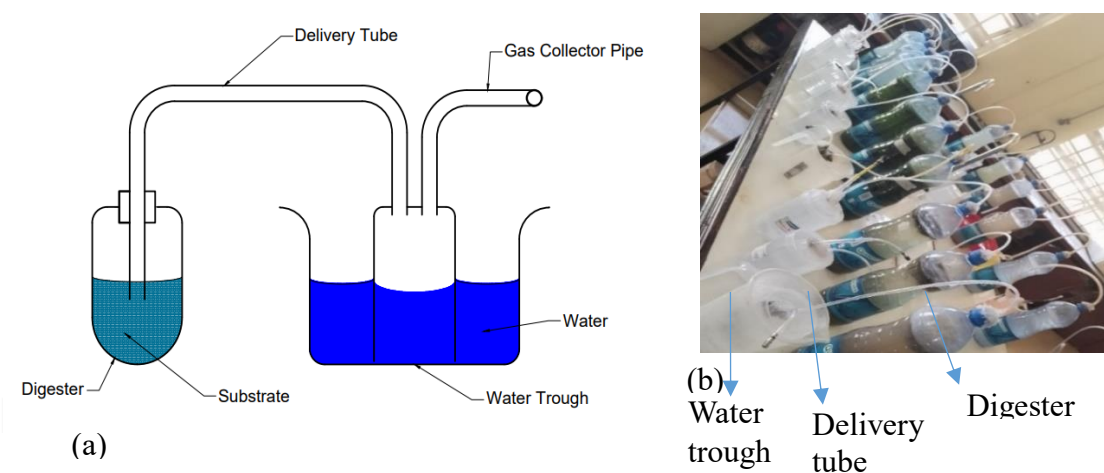


Figure 3.2: (a) Schematic diagram (b) Lab-scale setup for mono-digestion for 10 substrates in duplicate

3.5 Experimental Setup for Co-digestion

Experiments were done in a batch system to evaluate biogas production on a laboratory scale. Anaerobic co-digestion experiments were conducted using plastic bottle reactors with a working volume of 1.5L while the organic loading rate was 80gVs/L, and about 25mL of inoculum was added in each bio-digester. Different food wastes (FW) and some selected municipal solid wastes (MSW) were co-digested in separate reactors. The nature sludge used was watery in form while the total mixture in each digester was 1200g, this was applied for both digesters during the co-digestion process. The co-digested feedstock that gives the highest yield was tested for other parameters. The effect of substrate mixing ratio, temperature, and pH was studied. Typically, four different ratios of co-digested substrate were tested, 1:1 (TW: FrW_{1&2}), 1:2 (TW:

FrW_{1&2}), 1:3 (TW: FrW_{1&2}), and 1:4 (TW: FrW_{1&2}), a range of temperature 20 - 40°C with an incremental of 5°C, and pH of 6.5, 6.9, and 7.3 were investigated in this study. Substrates were fed into airtight digesters under anaerobic conditions and biogas was measured by the water displacement method, production started within the first 8 hours **Figure 3.3**, while research runs design as per **Table 3.1**. One end of the plastic pipe was connected to the digester while the other end was connected to the inverted cup-like apparatus, which was immersed in a container, and contained water. The displaced water was measured and was equal to the amount of biogas produced. The biogas was collected in a sampling gasbag for analysis. The HRT for this experiment was 15 days, thereafter the production stopped.

Table 3.1: Research run design for co-digestion

Variables	Range of values
Mixing ratio (Irish potato peels and banana peels)	1:1, 1:2, 1:3 and 1:4
Temperature	20, 25, 30, 35, and 40°C
pH	6.5, 6.9 and 7.4

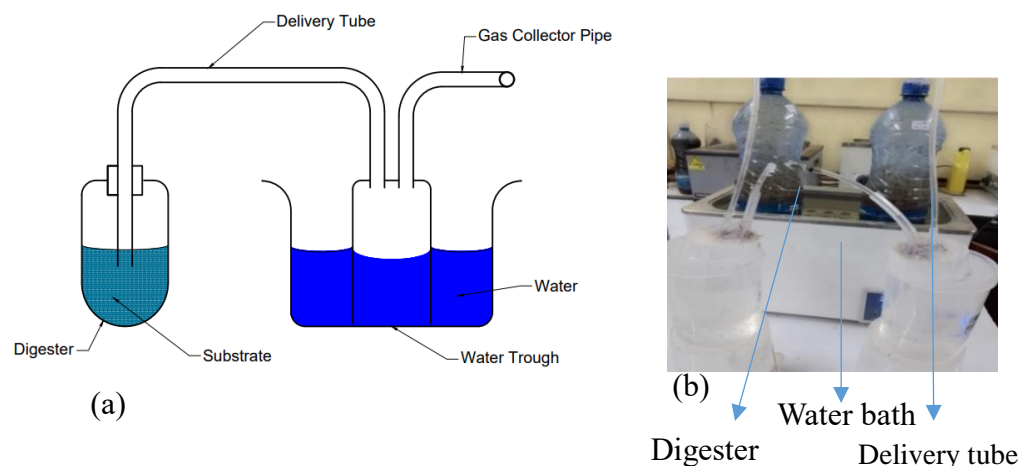


Figure 3.32: (a) schematic diagram (b) Lab-scale setup for co-digestion of Irish potato peels and banana peels in duplicate

3.5.1 Experimental setup for co-digestion on the effect of mixing ratio

Co-digestion of tuber waste and fruit waste was done 1:1 (TW:FrW1&2), 1:2 (TW:FrW1&2), 1:3 (TW:FrW1&2), and 1:4 (TW:FrW1&2) **Figure 3.4**; where 1:1 shows high production compared to the rest setup. The highest production in 1:1 may be contributed by several factors like the balance of CN ratio, NO_3 , SO_4 , BOD, and COD. The optimum CN ratio for anaerobic co-digestion to obtain the highest biogas yield depends upon the co-substrate used in balancing the CN ratio (Haider et al., 2015).



Figure 3.4: Lab-scale setup for co-digestion for different ratios for the 15 days

3.5.2 Experimental setup for co-digestion on the effect of temperature

Anaerobic co-digestion experiments were conducted in the plastic bottle reactors in a duplicate form with a working volume of 1.5 L. Co-digestion of Irish potato peels and banana peels on the effect of temperature was done **in Figure 3.5**. The organic loading rate (OLR) in the form of a total solid of 80 g was used for both reactors. After feeding the digester with the substrate and close tightly to avoid air entering which will automatically interfere with the microbe's activity, biogas was measured through the water displacement method, and reactors were maintained at different temperatures as 20, 25, 30, 35, and 40 °C using a water bath, high production was observed at 40°C.



Figure 3.53: Lab-scale setup for co-digestion of TW: FrW on the effect of temperature

3.5.3 Experimental setup for co-digestion on the effect of pH

The effect of pH variation was investigated in the study whereby pH of 6.5, 6.9, and 7.3 was used where the highest yield was observed in the digester with a pH of 7.3. The experiment was conducted at 40 °C **Figure 3.6**, which was a temperature that provides the highest yield during variation of temperature on biogas yield. To raise the pH of the substrate from 6.9 to 7.3 a drop of 0.25M NaOH was used in this study and was maintained until the end of production while lowering the pH from 6.9 to 6.5 two drops of lemon juice were used. The biogas was collected in a biogas sampling bag for analysis.

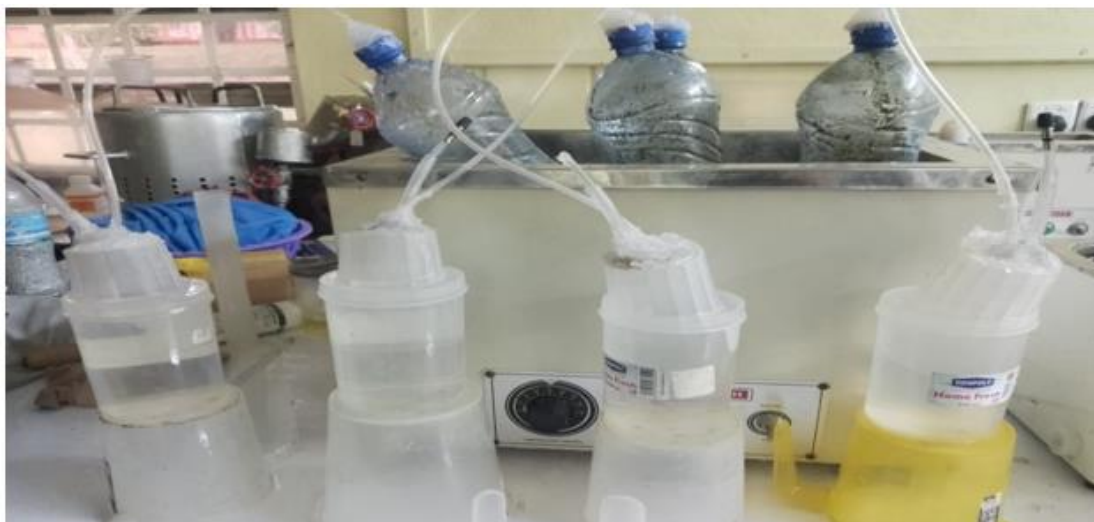


Figure 3.64: Lab-scale setup for co-digestion of TW: FrW on the effect of pH variation

3.6 The Quantification of Lab-Scale Biogas

Biogas obtained during the mono-digestion and co-digestion process was analyzed using the biogas analyzer model SKY200-M4-WH, the biogas was collected in a biogas sampling bag for analysis. **Figure 3.7** shows the biogas analyzer and sampling bag used.

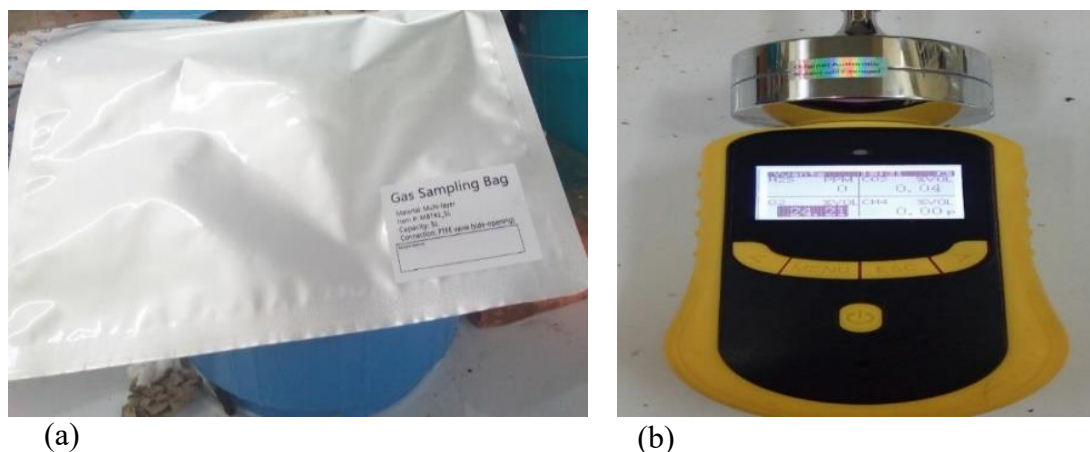


Figure 3.7: Lab scale biogas sampling equipment (a) sampling bag (b) biogas analyzer

3.7 Sorbent Preparation for Biogas Purification

3.7.1 Eggshells collection and calcination

Eggshells were collected around the international student residential area at Moi University and some from the local cafeteria in Makumira Arusha for about four

months. They were washed thoroughly with tap water and dried in the sun for two days and then tightly in a bag collector. It was then ground with a grinder, and sieved into 280 and 400 μm , **Figure 3.8**. The sample was then calcined under 800, 850, and 900 $^{\circ}\text{C}$ (Bilton et al., 2012) to convert the calcium carbonate compound present in eggshells into calcium oxide. The presence of CaO in calcined eggshell waste will facilitate the whole process of adsorption.



Figure 3.8: Eggshells preparation for adsorption experiment: (a) raw eggshells (b) grinder (c) sieving machines (d) working particle size 280 μm

3.7.2 Soda ash collection and preparation

Soda ash was collected from Lake Natron in Tanzania, ground, and then sieved into 280 and 400 μm , and the material was packed ready for the adsorption process. **Figure 3.9** summarizes the process.



Figure 3.95: Soda ash preparation for adsorption experiment: (a) Large particle size (b) grinder (c) working particle size (d) packed column bed reactor

3.8 Material Characterization

The textural characteristics of the sorbent materials were examined for three samples of soda ash for hydrogen sulfide removal as raw sample (S_1), spent (S_2), and regenerated samples (S_3) and for eggshells sorbent for carbon dioxide removal, three samples were investigated for E_1 , E_2 , and E_3 . The Brunauer-Emmett-Teller (BET) method was used to determine the specific surface area for both samples (S_1 - S_3 , and E_1 - E_3), while Barrett-Joyner-Halenda (BJH) method was used for pore size distribution evaluation. The Quantachrome NOVA 4200 (Win©1994-2013, v11.03) was used to assess the nitrogen adsorption-desorption isotherms under 77K at the University of Dar es Salaam, Tanzania. Before nitrogen adsorption-desorption studies, samples were degassed at 120 °C for 3 hours. The pore volume, pore diameter, and BET surface area for both samples were analyzed for the raw sample, spent sample, and regenerated sorbent for soda ash while for eggshells waste were calcined unspent sample (E_1), calcined spent sample (E_2), and regenerated samples (E_3). The composition of the sorbent was determined by an energy-dispersive X-ray fluorescence spectrometer (XRF), model MiniPal4 (Pw4030)-Rh manufactured by PAN Analytical, using the software provided with the instrument at Tanzania Atomic Energy Commission (TAEC, Tanzania. The Zeiss Ultra Plus Field Emission Scanning Electron Microscopy (FE-SEM) was used for surface morphology and was done at the Indian Institute of Science and Technology Bengaluru, India using model MiniPal4 (Pw4030)-Rh manufactured by PAN Analytical.

3.9 Purification Experiments

The scrubbing system consists of two sorbents where one sorbent was placed in a unit until the inlet concentration was the same as the outlet concentration. In the purification process, calcined eggshells and soda ash were used **Figure 3.10**. The soda ash sorbent (Na_2CO_3) reacted with hydrogen sulfide while calcium oxide (CaO) from the calcined

eggshell to remove carbon dioxide from biogas. The experiment was conducted by allowing the raw biogas to flow through the sorbent while varying the biogas flow rate, mass of sorbent, and sorbent particle size. The biogas leaving the scrubbing unit has increased the methane concentration while the sorbent in the scrubbing unit contained a high quantity of hydrogen sulfide and carbon dioxide depending on the sorbent used in the scrubbing unit, which is in line with (Mrosso et al.,2023a).

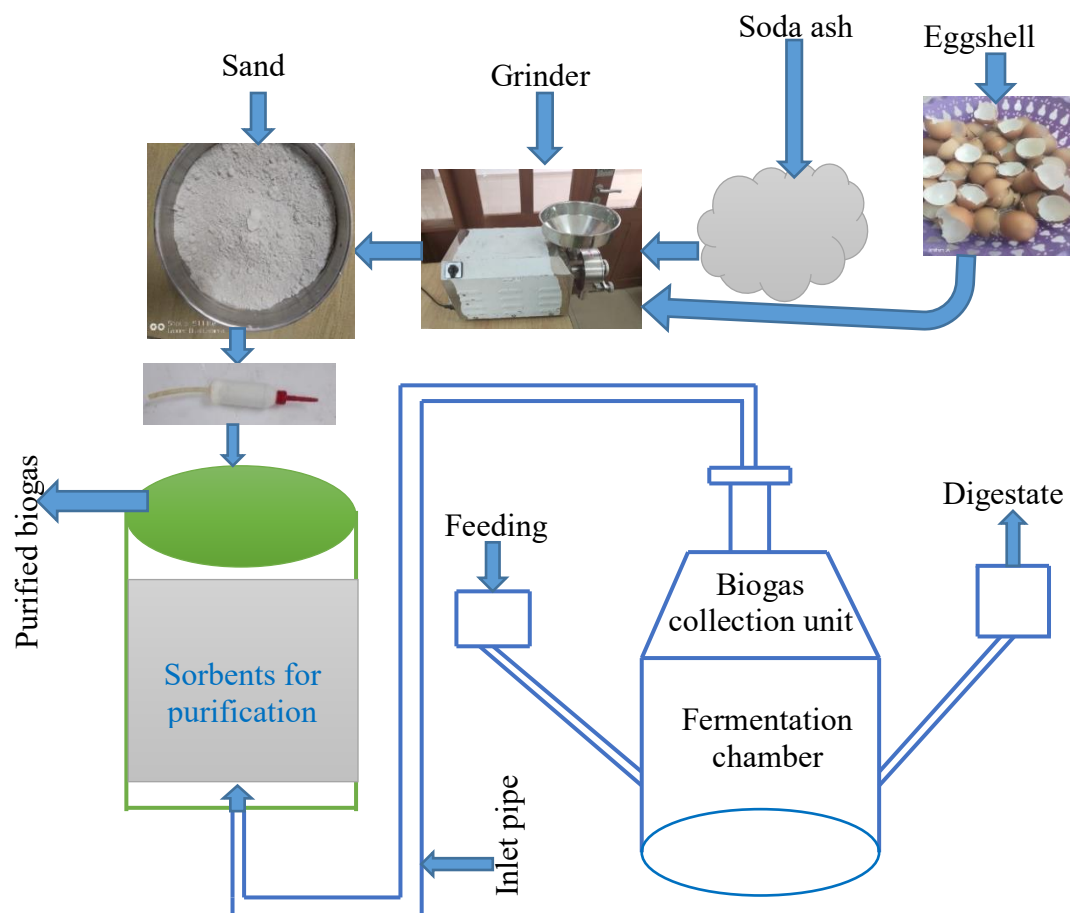


Figure 3.106: Schematic diagram for both hydrogen sulfide and carbon dioxide purification unit

3.9.1 Adsorption and performance evaluation using soda ash from Lake Natron

A bed reactor of plastic material height of 13 cm and 4 cm in diameter was filled up with cotton wool, in the absence of the adsorbent, the biogas was passed in at an ambient temperature to confirm if cotton wool adsorbs hydrogen sulfide from biogas or not. It

was noted that cotton wool does not react with hydrogen sulfide from biogas, as the inlet concentration was equal to the outlet concentration. The removal efficiency and sorption capacity of the two sorbents were calculated using **equations 3.4 & 3.5** respectively. The inert material that was sand was mixed with the adsorbent material to avoid overlapping and blockage of adsorbent sites, it was then packed in a fixed bed column in the reactor where both ends were held up with cotton wool, and biogas was allowed to pass through. The quantity of hydrogen sulfide was noted once before the starting of the adsorption process and monitored every 15 minutes after the filter. A schematic diagram and photo for the on-site experiment are shown in **Figure 3.11**.

$$RE = \frac{C_{in} - C_{out}}{C_{in}} \times 100\% \quad (3.4)$$

$$SC = WHSV \times \left[\frac{M}{V_{mol}} \times \int_0^t (C_{in} - C_{out}) dt \right] \quad (3.5)$$

where M is the atomic weight of H₂S (34 g/mol), WHSV is the weight hourly space velocity in mLh⁻¹g⁻¹, V_{mol} is the molar volume of the gas at STP in 22.4 Lmol⁻¹, and C_{in} and C_{out} are the amounts of H₂S prior and after adsorption, respectively, in ppm, and t is operating time (Garces et al., 2012).

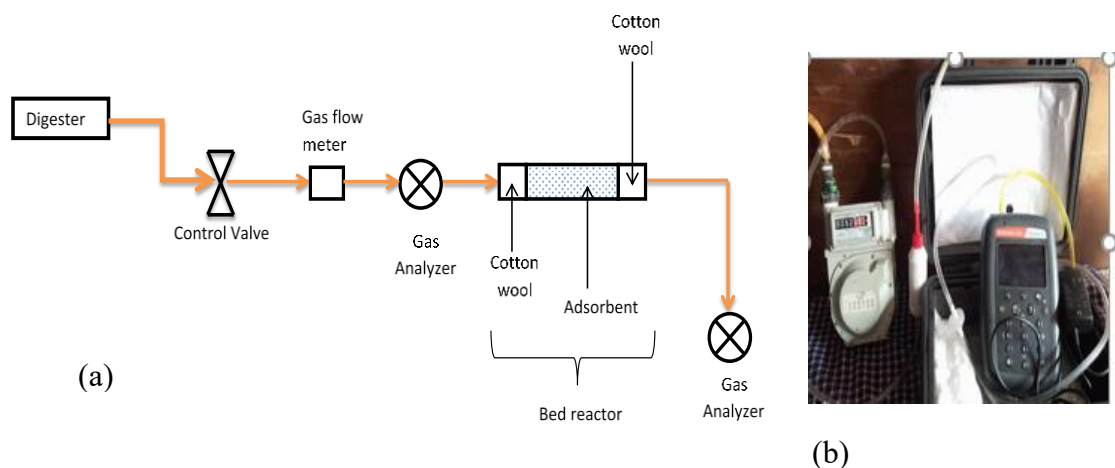


Figure 3.117: On-site experiment purification: (a) schematic diagram (b) photo

3.9.2 Adsorption of carbon dioxide and performance evaluation using eggshell waste

Sorption experiments were conducted in a domestic household, biogas was produced in two digesters and the feedstock was biomass, human waste, and kitchen waste. The carbon dioxide adsorption was carried out in a plastic fixed bed column 4 cm in width, and 13 cm in height. The sorbent was packed with the addition of sand for porosity purposes and both ends were filled with cotton wool. The concentration of carbon dioxide was measured once before the adsorption process and monitored every 15 min after the filter. A schematic diagram and photo for the experimental setup are shown in **Figure 3.11** above. Flow meter model JBD2-5-SA and biogas analyzer model Geotech 5000 were used to control the flow rate and measure the composition of biogas respectively. The performance of the adsorbent was expressed as percentage removal (RE) which was calculated using the **equations 3.6 and 3.7** respectively.

$$RE = \frac{C_{in} - C_{out}}{C_{in}} \times 100\% \quad (3.6)$$

$$SC = WHSV \times \left[\frac{M}{V_{mol}} \times \int_0^t (C_{in} - C_{out}) dt \right] \quad (3.7)$$

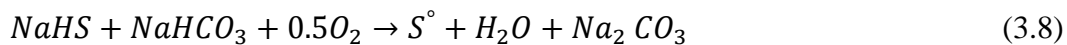
where M is the atomic weight of CO₂ (44 g/mol), WHSV is the weight hourly space velocity in mLh⁻¹g⁻¹, V_{mol} is the molar volume of the gas at STP in 22.4 Lmol⁻¹, and C_{in} and C_{out} are the amounts of CO₂ prior and after adsorption, respectively, in %, and t is operating time (Garces et al., 2012).

3.10 Regeneration Process

3.10.1 Regeneration of spent soda ash

The regeneration of spent soda ash after adsorption of hydrogen sulfide from biogas was done by selecting the sorbent that performed better than others and spreading it on a sheet for 1, 5, and 7 days. The sample was then mixed with sand particle size 400 μm

which acts as a pore-forming material as the soda ash is powdery in form and hence will block the passage of biogas and returned to the bed reactor for purification purposes **equations 3.8 & 3.9** respectively.



3.10.2 Regeneration of spent eggshells waste

After the adsorption of carbon dioxide from biogas by CaO from calcinated eggshell, the spent sorbent that performed better than others was removed from the bed reactor and re-calcinated under temperature beyond its calcination temperature (750°C) using a muffle furnace (model ELF11/14B 220-240V 1PH+N) to reform CaO (Lee et al., 2006) (Bajracharya et al., 2009; Bilton et al., 2012). The re-calcined spent sample was then mixed with a pore-forming material with particle size 400 µm, as the calcined eggshell is powdery in a form that will block the biogas passage and return to the bed reactor. The presence of CaO will facilitate the whole process of adsorption as observed in **equations 3.10 & 3.11** respectively.



3.11 Adsorption Isotherms

3.11.1 Langmuir Isotherm

The equilibrium behavior of hydrogen sulfide and carbon dioxide exchange with the adsorbents in different ratios was characterized by fitting the model equations to the data obtained during on-site experiments. The Langmuir model is expressed in nonlinear form as per **equation 3.12a**.

$$q_e = \frac{q_{max} K_L C_e}{1 + K_L C_e} \quad (3.12a)$$

Where, q_e is the equilibrium adsorption capacity, q_{max} (mg/g) is the maximum adsorption capacity, K_L (L/mg) Langmuir constant; C_e is the equilibrium adsorbate concentration. The linear Langmuir equation is written as per **equations 3.12(b-e)**. A plot of C_e/q_e versus C_e will create a straight line with a slope of $1/q_0$ and an intercept equal to $1/K_L q_0$ where all other parameters were obtained using equations 18, 19, and 20.

$$\frac{C_{eq}}{q_e} = \left(\frac{1}{q_{max}} \right) C_{eq} + \frac{1}{K_L q_{max}} \quad (3.12b)$$

Where q_e (mg/g) is the amount of H_2S and CO_2 adsorbed per gram of sorbent at equilibrium, C_{eq} (mg/L) is the concentration at equilibrium, q_{max} (mg/g) is the maximum adsorption capacity, K_L (L/mg) is the Langmuir equilibrium constant.

$$q_{max} = \frac{1}{intercept} \quad (3.12c)$$

$$RL = \frac{1}{1 + K_L C_0} \quad (3.12d)$$

$$KL = \frac{1}{slope * q_{max}} \quad (3.12e)$$

3.11.2 Freundlich isotherm

Freundlich isotherm describes the multilayer adsorption/ heterogeneous adsorption process where isotherm assumes that the adsorption process occurs on the heterogeneous surface of the adsorbent **equations 3.13(a-d)**. The isotherm shows clearly a relative distribution of energy and the heterogeneity site of the adsorbate. Freundlich isotherm explains the interaction between carbon dioxide and hydrogen sulfide on the porous adsorbent, which are calcined eggshell waste and soda ash collected from Lake Natron respectively. The Freundlich isotherm constant ($1/n$) value

will be used to calculate the intensity of the reaction, the adsorption capacity, and the favorability of the adsorption process. The value of $1/n$ recommends the type of sorption process using calcined eggshell waste and soda ash for carbon dioxide and hydrogen sulfide adsorption from biogas respectively. The adsorption process can be either favorable ($0 < 1/n < 1$), irreversible ($1/n = 0$), or unfavorable ($1/n > 1$). The adsorption isotherms at very low solute concentrations are often linear indicating that the value of R^2 is much higher. All the required parameters can be obtained directly from the plot of $\text{Log } q_e$ vs $\text{log } C_e$.

$$\text{Log } q_e = \frac{1}{n} \text{log } C_e + \text{log } K_f \quad (3.13a)$$

$$n = \frac{1}{\text{slope}} \quad (3.13b)$$

$$\text{Intercept} = \text{log } k_f \quad (3.13c)$$

$$k_f = \text{ant log results of intercept value} \quad (3.13d)$$

Where n is the adsorption intensity constant, K_f (L/g) is the Freundlich adsorption constant and $1/n$ is the measure of adsorption intensity ranges between 0 and 1 and C_e (mg/L) is the concentration at equilibrium.

3.11.3 Jovanovich

The linear Jovanovich equation used in fitting the on-site experimental data can be written as per **equations 3.14(a-c)**. A linear plot of Jovanovich isotherm obtained via $\text{In } q_e$ Vs C_e can be used to deduce the parameters that are maximum adsorption capacity and Jovanovich constant as per equations (20b) and (20c).

$$\text{In } q_e = \text{In } q_{\text{max}} - K_j C_e \quad (3.14a)$$

Where q_e (mg/g) is the concentration of impurities adsorbed at equilibrium, q_{max} (mg/g) is the maximum adsorption capacity, K_j (l/g) is the Jovanovich constant, and C_e (mg/L) is the concentration at equilibrium.

$$K_j = \text{Slope} \quad (3.14b)$$

$$\ln q_{max} = \text{Intercept} \quad (3.14c)$$

3.12 Adsorption Modeling

Three models were employed in this study Adams-Bohart, Thomas, and Yoon-Nelson models, which were developed to describe and possibly to predict the dynamic characteristics of the bed in column performance. Different parameters were derived from each model, which described the performance of the adsorption processes. The fixed bed models are admired as their model equation can be linearized authorizing their unknown parameters to be evaluated using linear regression analysis. In this study, the three fixed models were used to fit the data obtained from on-site experiments, and they were compared using the coefficient of determination R^2 (Chu, 2020).

3.12.1 Adams-Bohart model

The model predicts the linear relationship between the depth of the bed and the time taken for the breakthrough R^2 . The linear relationship of this model simplifies the tasks of absorber design and analysis and provides a straightforward approach to running pilot tests as per equations 3.15(a-d).

$$\ln\left(\frac{C_o}{C}\right) = \frac{k_{BA}N_oL}{U} - k_{BA}C_o t \quad (3.15a)$$

Where C is the column exit concentration at time t , C_o is the initial adsorbate concentration, k_{BA} is the B-A rate coefficient, L is the bed depth, N_o is the adsorption capacity of the adsorbent per unit volume of the bed, and u is the superficial velocity.

The necessary parameters such as k_{AB} and N_o were obtained from the plot $\ln(C_t/C_o)$ against time as per equations below; where N_o is maximum adsorption capacity (L/mg min) while k_{AB} is Bohart –Adams constant.

$$\text{Slope} = k_{AB} * C_o \quad (3.15b)$$

$$k_{AB} = \frac{\text{Slope}}{C_o} \quad (3.15c)$$

$$\text{Intrecept} = -k * N_o * \left(\frac{z}{U_o}\right) \quad (3.15d)$$

3.12.2 Thomas model

The model presumes the plug flow behavior within the bed reactor. In general, it is a popular model used to explain the performance theory of the sorption mechanism in any fixed bed column (Chen et al., 2012). The linear form of this model is as per **equations 3.16(a-c)**. The model assumes that the axial dispersion is negligible, and it is based on second-order kinetics and therefore does not limit adsorption by chemical reaction hence its limitation, it is controlled by a mass transfer mechanism (Bharathi & Ramesh, 2013).

$$\ln\left(\frac{C_o}{C_t} - 1\right) = \left(\frac{k_{Th}q_{Th}m}{Q}\right) - k_{Th}C_o t \quad (3.16a)$$

Where q_o is the adsorption capacity (mg/g), t stands for total flow time (min), k_{Th} is the Thomas model constant (mL/min mg), Q_o is the equilibrium Malachite green uptake per g of the adsorbent (mg/ g).

The values of q_o and k_{Th} can be determined from the plot of $\ln [(C_o/C_t)-1]$ against t , where k_{Th} is Thomas's constant (mL/ min mg), and q_o is the adsorption capacity (mL/min mg). The coefficients and relative constants can be obtained using linear

regression analysis according to **equation 3.16a**. The parameters were obtained using **equations 3.16b** and **3.16c**.

$$k_{Th} = -\left(\frac{Slope}{C_o}\right) \quad (3.16b)$$

$$q_o = \frac{Intercept}{k_{Th}} \quad (3.16c)$$

3.12.3 Yoon-Nelson

The model is normally expressed in the as per the **equations 3.17(a-c)**.

$$\ln\left(\frac{C_t}{C_o - C_t}\right) = K_{YN}t - \tau K_{YN} \quad (3.17a)$$

Where τ is the time required for 50% breakthrough expressed in (min), and k_{YN} is the Yoon-Nelson rate coefficient (min^{-1}), both parameters k_{YN} and τ can be estimated from the slope and intercept of the Yoon-Nelson plot respectively at different concentrations, bed height, and flow rates as per **equations 3.17b** and **3.17c**.

$$k_{YN} = Slope \quad (3.17b)$$

$$\tau_{kY} = Intercept \quad (3.17c)$$

3.13 Adsorption Kinetics

The kinetics of hydrogen sulfide and carbon dioxide removal from biogas using soda ash and calcined eggshell waste was investigated at room temperature. The experimental data were fitted into four kinetic models: pseudo-first order, pseudo-second order, intra-particle diffusion, and Elovich models. The equations for adsorption kinetics were presented in **Table 3.2** and linear plots were done using originPro.

3.13.1 Pseudo-first-order kinetics (PFO)

According to Dermirbas et al. (2004), Lagergren introduced the pseudo-first-order model (PFO) in the late 19th century (Demirbas et al., 2004). The model explained that there is a direct relationship between the surface of adsorption capacity and the

adsorption rate. The model is expressed in linear form and a plot was obtained as shown in **equations 3.18(a-b)**. The necessary parameter that was k_1 (the pseudo-first-order rate constant, min^{-1}), was obtained from the plot of $\ln(q_e - q_t)$ against time in min where slope was used to determine the value of k_1 .

$$q_t = q_e(1 - e^{-k_1 t}) \quad (3.18a)$$

$$k_1 = \text{Slope} \quad (3.18b)$$

Where k_1 is the constant of pseudo-first order (min^{-1}), q_e adsorption capacity at equilibrium, and q_t is the adsorption capacity at a particular time t that is expressed in milligram of adsorbent per g (mg/ g);

3.13.2 Pseudo-sec-order kinetics (PSO)

The Pseudo second order model (PSO) was first applied in 1984 (Sari et al., 2019), it describes the linear relationship between the adsorption rate and surface of adsorption capacity. The model can be expressed in linear form as per **equation 3.19a** while the necessary parameters that are k_2 and q_e can be obtained from the plot t/q_t against time in min as per **equations 3.19(b-c)**.

$$q_t = \frac{1}{\frac{1}{(k_2 q_e^2) + t/q_e}} \quad (3.19a)$$

$$k_2 = \frac{1}{\text{Intercept} * q_e^2} \quad (3.19b)$$

$$q_e = \frac{1}{\text{Slope}} \quad (3.19c)$$

Where k_2 is the second-order adsorption constant ($\text{g}^{-1} \text{min}^{-1}$). This constant is obtained from the graph of t/q_t vs t). Similarly, q_e is the adsorption capacity at equilibrium, and q_t is the adsorption capacity at time t .

3.13.3 Elovich adsorption kinetics

Tompkins and Aharonic developed the Elovich adsorption model in 1970 (Sari et al., 2019). It relates the chemisorption essence of adsorption and the interaction of biogas molecules with the heterogeneous surface of the adsorbent **equation 3.20(a-c)**. The necessary parameters such as α and β were obtained using a linear plot qt Vs $\ln t$

$$q_t = 1/\beta \ln(\alpha\beta t) \quad (3.20a)$$

$$\alpha = \frac{1}{\text{Slope}} \quad (3.20b)$$

$$\text{Intercept} = 1/\alpha \ln(\alpha\beta) \quad (3.20c)$$

Where β is the constant associated with surface coverage and the activation energy in the chemisorption process (g/mg), while α is the initial adsorption rate of the model (mg/g*min).

3.13.4 Intra particles diffusion

Weber and Morris developed the intra-particle diffusion model in 1963, which is an older model. It describes the controlled mechanism of diffusion and it is expressed in linear form as per **equation 3.21a** where the necessary parameters such as c and k_{id} can be obtained from the linear plot qt (mg/g) against $t^{0.5}$ as per **equations 3.21(b-c)**. **Table 3.2** shows the linear form of all the kinetic models used in the current study.

$$qt = k_{id}t^{0.5} + C \quad (3.21a)$$

$$C = \text{Intercept} \quad (3.21b)$$

$$k_{id} = \text{Slope} \quad (3.21c)$$

Where K_{id} is intra-particle diffusion rate $\text{mg/g}\cdot\text{min}^{0.5}$, C is constant associated with intercept for any experiment and qt is the gas phase concentration at time t .

Table 3.2: A summary of the four types of adsorption kinetic models in linear form.

Adsorption kinetics model	Linear	Equation
Pseudo first-order model	$\ln\left(\frac{C_i}{C_t}\right) = k_1 t$	3.18
Pseudo second order model	$\frac{t}{q_t} = \frac{1}{k q_e^2} + t/q_e$	3.19
Elovich model	$q_t = \frac{1}{\alpha} \ln(\alpha \beta) + \frac{1}{\alpha} \ln t$	3.20
Intra-particles diffusion models	$q_t = k_{id} t^{0.5} + C$	3.21

CHAPTER FOUR

RESULTS AND DISCUSSIONS

4.1 Characterization of Kitchen Waste and Municipal Solid Waste for Biogas Production

The data obtained from the experiment during the characterization of feedstock on the moisture content, total solid, volatile solid, and ash content of the kitchen waste (KW) and some of the municipal solid waste (MSW) used in this study for each substrate are presented in **Table 4.1-4.14**. The significance of these analyses on biogas production is that they can give a clue on the quality and quantity of biogas generation, although other factors like C/N ratio, temperature, pH, and presence of heavy metal play a role as well.

Table 4.1: Moisture content, total solid, volatile solid, and ash content of pineapple peels

No.	Characteristics	Present work (%)	Other studies (%)	References
1.	Moisture content	82.00	79.97 86.81	(Chulalaksananukul et al., 2012) (Kodagoda & Marapana, 2017)
2.	Total solid	18.00	13.19 15.89	(Kodagoda & Marapana, 2017) (Suhartini et al., 2021)
3.	Total volatile solid	95.50	96.12	(Rani & Nand, 2004)
4.	Ash content	4.50	3.88	(Rani & Nand, 2004)

Table 4.2: Moisture content, total solid, volatile solid, and ash content of banana peels

No.	Characteristics	Present work (%)	Other studies %	References
1.	Moisture content	78.33	60 83.30 81.00	(Kalemelawa et al., 2012) (Gumisiriza et al., 2019) (Deressa et al., 2015)
2.	Total solid	21.67	16.70 19.00	(Gumisiriza et al., 2019) (Deressa et al., 2015)
3.	Volatile solid	94.00	86.78 86.44 92.6	(Gumisiriza et al., 2019) (Achak et al., 2009) (Deressa et al., 2015)
4.	Ash content	06.00	13.22 7.40	(Gumisiriza et al., 2019) (Deressa et al., 2015)

Table 4.3: Moisture content, total solid, volatile solid, and ash content of Irish potato peels

No.	Characteristics	Present work (%)	Other studies (%)	References
1	Moisture content	72.00	78.00 77.10 88.0	(Hossain et al., 2015). (Muhondwa et al., 2015). (Lucas, 2014)
2.	Total solid	28.00	22.90 9.20	(Muhondwa et al., 2015). (Liang & McDonald, 2015).
3.	Volatile solid	92.00	93.40 82.00	Lucas, 2014) (Liang & McDonald, 2015)
4.	Ash content	8.00	6.60 6.34	Lucas, 2014) (Pathak et al., 2018)

Table 4.4: Moisture content, total solid, volatile solid, and ash content of cooked rice

No.	Characteristics	Present work (%)	Other studies (%)	References
1.	Moisture content	69.00	67.95 69.72	(Deressa et al., 2015) (Glivin & Sekhar, 2019)
2.	Total solid	31.00	68.00 30.28	(Gashaw et al., 2014) (Glivin & Sekhar, 2019)
3.	Volatile solid	83.00	31.38 90.11	(Gashaw et al., 2014) (Glivin & Sekhar, 2019)
4.	Ash content	17.00	90.10 9.00 9.90	(Gashaw et al., 2014) (Glivin & Sekhar, 2019) (Gashaw et al., 2014)

Table 4.5: Moisture content, total solid, volatile solid, and ash content of ugali

No.	Characteristics	Present work (%)	Other studies (%)	Reference
1.	Moisture content	67.21	71.00	(Carlsson et al., 1999)
			67.80	(Mwaniki et al., 2016)
2.	Total solid	32.79	32.20	(Mwaniki et al., 2016)
3.	Volatile solid	86.00	95.30	(Mwaniki et al., 2016)
4.	Ash content	14.00	-	

Table 4.6: Moisture content, total solid, volatile solid, and ash content of cooked beans

No.	Characteristics	Present work (%)	Other studies (%)	References
1.	Moisture content	66.73	72.00	(Abu-Ghannam, 1998)
2.	Total solid	33.27	28.00	(Abu-Ghannam, 1998)
			18.00	(Athukorala et al., 2021)
3.	Volatile solid	86.00	92.80	(Athukorala et al., 2021)
4.	Ash content	14.00	7.20	(Athukorala et al., 2021)

Table 4.7: Moisture content, total solid, volatile solid, and ash content of cooked banana

No.	Characteristics	Present work (%)	Other studies (%)	References
1.	Moisture content	76.00	78	(Dotto et al., 2019)
			87.2	(Athukorala et al., 2021)
2.	Total solid	24	12.8	(Athukorala et al., 2021)
3.	Volatile solid	94.87	94.3	(Athukorala et al., 2021)
4.	Ash content	5.13	5.70	(Athukorala et al., 2021)

Table 4.81: Moisture content, total solid, volatile solid, and ash content of cooked Irish potatoes

No.	Characteristics	Present work (%)	Other studies (%)	References
1.	Moisture contents	78.40	63-83	(Puttongsiri et al., 2012)
2.	Total solid	21.60	-	-
3.	Volatile solid	94.92	-	-
4.	Ash content	5.80	-	-

Table 4.92: Moisture content, total solid, volatile solid, and ash content of cabbage

No.	Characteristics	Present work (%)	Other studies (%)	References
1.	Moisture content	92.00	82-85 92	(Kim & Kafle, 2010) (Mariga et al., 2012)
2.	Total solid	08.00	81.20 15-18	(Kafle et al., 2014) (Kim & Kafle, 2010)
3.	Volatile solid	96.36	08.00 12.80	(Mariga et al., 2012) (Kafle et al., 2014)
4.	Ash content	3.64	10-13 08.00	(Kim & Kafle, 2010) (Kafle et al., 2014)
			87-90 92.00	(Kim & Kafle, 2010) (Kafle et al., 2014)

Table 4.10: Moisture content, total solid, volatile solid, and ash content of african nightshades

No.	Characteristics	Present work (%)	Other studies (%)	References
1.	Moisture content	90.32	87.71 82.11	(Traoré et al., 2017) (Dushimimana et al., 2018)
2.	Total solid	9.68	12.29 17.89	(Traoré et al., 2017) (Dushimimana et al., 2018)
3.	Volatile solid	81.58	89.43	(Traoré et al., 2017)
4.	Ash content	18.42	10.57	(Traoré et al., 2017)

Table 4.11: Moisture content, total solid, volatile solid, and ash content of spinach waste

No.	Characteristics	Present work (%)	Other studies (%)	References
1.	Moisture content	91.70	91.00 91.43	(Mariga et al., 2012) (Soeprijanto et al., 2021)
2.	Total solid	8.30	94.2 9.00	(Singh et al., 2001) (Mariga et al., 2012)
3.	Volatile solid	76.59	8.57 77.75	(Soeprijanto et al., 2021) (Soeprijanto et al., 2021)
4.	Ash content	23.41	22.25	(Soeprijanto et al., 2021)

Table 4.123: Moisture content, total solid, volatile solid, and ash content of kale waste

No.	Characteristics	Present work (%)	Other studies (%)	Reference
1.	Moisture contents	84.86	83.00	(Mariga <i>et al.</i> , 2012)
			90.77	(Dushimimana <i>et al.</i> , 2018)
2.	Total solid	15.14	17.00	(Mariga <i>et al.</i> , 2012)
3.	Volatile solid	84.56	-	-
4.	Ash content	15.44	-	-

Table 4.13: Moisture content, total solid, volatile solid, and ash content of tomato waste

No.	Characteristics	Present work (%)	Other studies (%)	Reference
1.	Moisture contents	93.43	93.89 - 94.10	(Mohammed & Kuhiyep, 2020)
			83.14	(Deressa <i>et al.</i> , 2015)
2.	Total solid	06.57	16.86	(Deressa <i>et al.</i> , 2015)
			5.90 - 6.11	Mohammed & Kuhiyep, 2020).
3.	Volatile solid	82.00	92.85	(Deressa <i>et al.</i> , 2015)
4.	Ash content	08.00	7.15	(Deressa <i>et al.</i> , 2015)

Table 4.14: Moisture content, total solid, volatile solid, and ash content of carrot peels

No.	Characteristics	Present work (%)	Other studies (%)	References
1.	Moisture content	85.00	84.23	(Shyamala & Jamuna, 2010)
			95.4	(Singh <i>et al.</i> , 2001)
2.	Total solid	15.00	15.77	(Shyamala & Jamuna, 2010)
3.	Volatile solid	88.62	88.00	(Babæe & Shayegan, 2011)
4.	Ash content	11.38	5.78	(Shyamala & Jamuna, 2010)

High moisture content in a feedstock favors the biochemical conversion process that proceeds without the addition of water hence reducing the cost contributed to water (Gumisiriza *et al.*, 2019). Moisture content within the substrate affects microbial

activity, composite temperature, and the rate of decomposition as well as facilitates the transportation of nutrients. The moisture content of the feedstock in this study ranged from 66.73 - 93.43% (**Table 4.1-4.14**) and was comparable with the literature. Tomato waste and cabbage showed the highest MC (93.43 and 92% respectively) which is favorable for high biogas yield. Cooked beans and ugali showed the lowest MC (66.73% and 67.21% respectively).

The total solid content of the substrates/feedstock used in the current study ranged from 06 - 33.27% (**Table 4.1-4.14**). From the table, it is evident that tomatoes had a minimum total solid of 06.57% while cooked beans had a maximum TS value of 33.27%. (Deressa et al., 2015) reported the TS for cooked rice waste to be 32.05 % which is comparable with the values presented in this study. Therefore, the results obtained from this work for each waste are equivalent to values reported in the literature.

The volatile solid for all samples ranged from 76.59 – 96.36%, which is related to the values reported in the literature. Reference to (**Table 4.9 & 4.11**) indicated that cabbage had the highest TVS of 96.36% while spinach had the lowest TVS of 76.59%. (Kafle et al., 2014) reported the highest TVS for cabbage leftover was 92.00% which is following the present work. On the other hand, the value for total volatile solids for cooked rice waste obtained from the current study was 83%. The values reported in the literature (Glivin & Sekhar, 2019) showed that TVS for rice waste was 90.11%, while (Deressa et al., 2015) reported 93.2% shows some variation with the current work which may be contributed by the kind of the rice used and the climatic condition for their growth.

4.2 Physical-chemical Analysis

The physical-chemical analysis was performed for the three substrates having high volatile solid (cabbage), high CN ratio (cooked rice waste), and high total solid (ugali) and the results are as per **Table 4.15**.

Table 4.154: Physical-chemical analysis of selected substrates

Substrates	Parameters					
	TDS (mg/L)	NO ₃ (mg/L)	EC (mS/cm)	COD (mg/L)	BOD (mg/L)	Biodegradability index
Ugali	328.00	81.00	678.00	1618.00	460	0.28
Rice	805.00	54.00	16.28	1323.00	720	0.54
Cabbage	323.00	99.25	664.00	1200.50	820	0.68

Determination of the general composition of the substrate is necessary to calculate the quality and quantity of biogas generated. The feedstock with BOD: COD: (BI values) which varies from zero to unity (Saravanathamizhan & Perarasu, 2021; Tchobanoglous et al., 2003). The biodegradability index (BI) value must be above 0.3 for the complete degradation of the feedstock this is in line with the present study whereby cooked rice waste and cabbage leftovers were in the range of 0.54 and 0.68 respectively while the ugali was observed to be 0.28. Therefore, it is easy for methanogenic bacteria to degrade rice waste and cabbage rather than ugali, and was noted that cabbage forms volatile fatty acids easily thus production ceased in a few days. A high level of nitrate in the feedstock leads to the formation of acidic compounds that lower the pH value and therefore, methanogenic bacteria cannot sustain resulting in low yield. The increase in CO₂ concentration and decrease in methane yield resulting from the high concentration of NO₃-N can be attributed to the inhibition effects due to the intermediate compounds due to the denitrification process and by increasing ox-red potential with the increase in nitrate concentration. Therefore, an increase in nitrate concentration resulted in the inhibition of the yield. Total dissolved solids (TDS) of the substrates showed that

cooked rice waste had the highest TDS, which may probably contribute to the highest biogas yield as compared to the rest of the substrates used in this study.

4.3 Mono-digestion of Kitchen Waste and Municipal Solid Waste Substrates

To make the feedstock attainable to extracellular microorganisms that are released by fermentative and hydrolytic bacteria in the biodigester during the first stage of anaerobic digestion, the anatomy of kitchen waste and some selected municipal solid waste has to be disrupted via pretreatment technology. Some studies have explored various ways of decreasing the lignocellulose structure such as physical, chemical, mechanical thermal, and biological pretreatments either in combination or alone. The current study uses mechanical pretreatment such as grinding using a blender for size reduction and therefore increases the surface area to volume ratio for methanogenic bacteria. Anaerobic digestion of kitchen and municipal solid wastes was conducted at room temperature assessing the effect of different parameters such as total solids, and volatile solids among others as discussed in the above sections, and the results are shown in **Figure 4.1**. Biogas production is directly proportional to the rate of biological breakdown of organic waste. Other factors may also play an important role during the anaerobic digestion process; they include TVS, TS, COD: BOD, temperature, and pH. The physical characteristics of kitchen waste and municipal solid waste used in the current study are tabulated in the previous section.

4.3.1 Biogas yield from different substrates

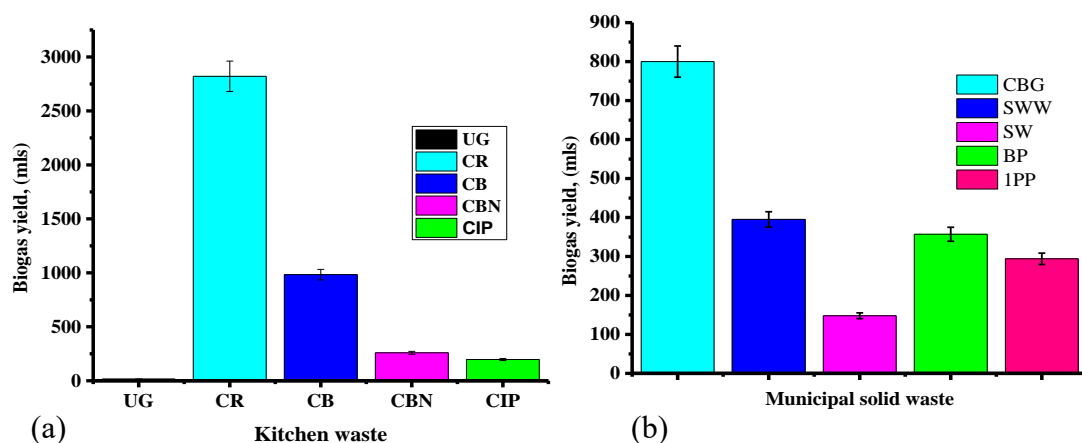


Figure 4.1: A graph of biogas yield against (a) kitchen waste and (b) municipal solid waste substrates

Figure 4.1 (a, b) indicates the biogas yield against feedstock, KW, and MSW respectively where biogas production was observed to begin within the first 8 hours in cooked bananas, cooked Irish potatoes, cabbage, spinach, Irish potato peels, and banana peels; which is following (Koch et al., 2015) and it is because of the existence of more degradable compounds in those feedstocks. On the other hand, no gas was observed in cooked rice waste, cooked beans waste, ugali, and kale for the first 8 hours due to the presence of hard degradable compounds in the feedstock (Koch et al., 2015). The experiment was conducted only for 10 days, production of biogas was measured daily and then was observed to cease thereafter except for cooked beans and rice whereby production in cooked beans ceased after 11 days but cooked rice continued until 28 days when production stopped. During anaerobic digestion (AD) of cooked rice waste and cooked beans waste, the hydrolysis and acidogenesis process occur which leads to the accumulation of intermediate products (Koch et al., 2015) as the growth rate of acidogenic is higher in comparison to methanogens. The acid-consuming microbes are more sensitive and inhibited by an accumulation of acid and therefore decrease pH than

the acid-producing microbes. This resulted in a decrease in biogas yield until the acid-consuming microbe's activity was recovered. This was observed in cooked rice waste whereby production within the first 8 days was very low and increased with the increase in time. The highest biogas yield in kitchen waste was observed in cooked rice ($2821 \pm 31.03 \text{ mL}$) followed by cooked beans ($983 \pm 10.81 \text{ mL}$) and the lowest was in ugali ($15 \pm 0.17 \text{ mL}$) **Figure 4.1a**. Based on characterization data and literature information the current study revealed that not necessary for the feedstock to have a high total volatile solid to have a high biogas yield rather it reveals that biogas generation can be contributed by many other factors apart from total volatile solid. Food waste remained wealthy in protein and lipid and yet indicated the highest biogas generation in cooked rice and cooked beans in comparison to municipal solid waste. This may be attributed to the fact that the lipids available in food waste used in this study especially cooked rice and cooked beans can be metabolized via enzymic, degraded to hydrogen and acetate through β -oxidation by microbe's community, and syntrophic with acetoclastic and hydrogenotrophic methanogens (Amha et al., 2018).

Figure 4.1b, shows biogas generation from some selected municipal solid waste where cabbage produces the highest amount of biogas followed by kale. A major problem of the anaerobic digestion process (AD) of vegetable waste and fruit waste is the rapid acid formation because of low pH and high levels of Fatty acid formation that hinder methanogenic activities. The low yield that was observed in some feedstocks such as spinach, banana peels, Irish potato peels, cooked Irish potato peels, and cooked banana may be attributed to the presence of lignin component hence microbes find it difficult to decompose. Literature indicated that high CN greater or lower than the recommended 20-30:1 CN ratio and low biodegradability of substrates may act as a major constraint of anaerobic digestion (AD) which leads to process hindrance due to

the accumulation of VFA (Jabeen et al., 2015). To solve this problem of the mono-digestion process co-digestion is recommended. The inoculum used had great potential in improving the anaerobic digestion and balancing of the CN ratio. Meanwhile, Nitrogen is tremendously necessary for microbes to grow, the accumulation of large amounts of nitrogen leads to the formation of free ammonia that hinders the anaerobic digestion process. The pH values for both digesters were recorded at the beginning of the experiment and the end of the anaerobic digestion process. Using mono-digestion substrate, high biogas yield was obtained in the digester having cooked rice waste and therefore it is recommended to be used as mono-digested feedstock rather than co-digestion, and therefore a viable alternative for biogas generation. The mono-digestion experiment was considered completed when the rate of methane production was unnoticeable or less than 1% of the total production for three days. Literature shows that the production of biogas using animal waste, some kitchen waste, and municipal solid waste as mono-digestion feedstock generates a small amount of biogas with low methane concentration which could not be economically viable (Piñas et al., 2018). The current study evaluated the possibility of using mono-digestion feedstock and proved that only cooked rice waste among the feedstock used can be utilized as a mono-digestion feedstock, which is in line with the literature. Nevertheless, results obtained from the current study strengthen the economic and technical viability of cooked rice waste as a mono-digestion feedstock for biogas generation.

4.3.2 Effect of total solid content on biogas yield

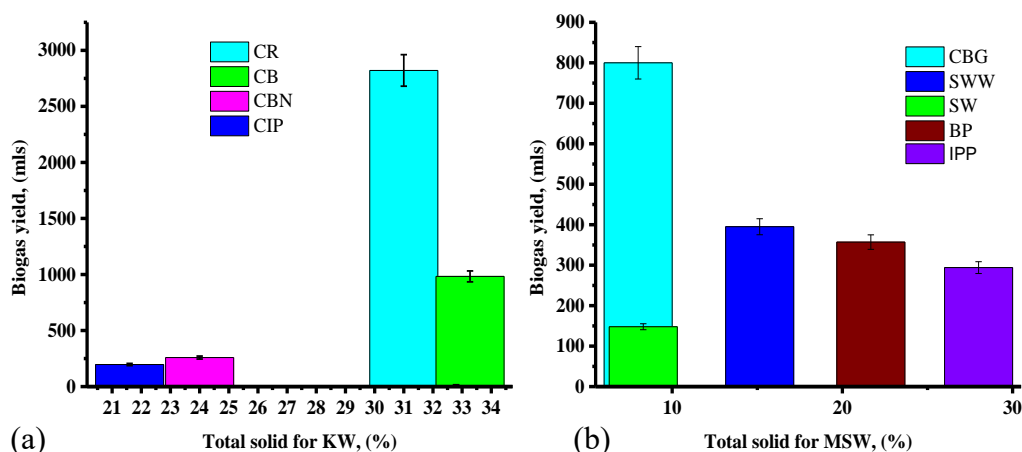


Figure 4.2: Biogas yield against TS for (a) KW and (b) MSW

Figure 4.2(a, b) indicates the effect of total solid on biogas yield of different KW and MSW, the study indicates that the highest biogas production was attained in cooked rice waste having TS of 31.00% which generated 2.821 L/(g VS) for 28 days. (Maamri & Amrani, 2014) study the effect of total solid concentration on the quantity and quality of biogas generated where the results showed that biogas yield rate and biogas yield potential increased with the increase in total solid concentration. From the above literature, (Maamri & Amrani, 2014) the total solid concentration was 12.02, 17.58, 23.28, 26.75, 35.2 g/L were 0.186, 0.189, 0.93, 0.213, and 0.231 L/(g VS), respectively. (Sathish et al., 2019) observed that the quantity of biogas yield varies according to the TS used as 10% TS, 20% TS, and 30% TS was 1.130, 1.250, and 1.030 L/ (g VS), respectively. Song et al., (2010) studied the effect of total solid and temperature and reported that biogas yield does not depend on total solid concentration this is in line with the current study. Therefore, based on these findings, biogas yield depends on the total solids as well as other factors include BI, NO₃, EC, among others.

4.3.3 Effect of total volatile solids on biogas yield

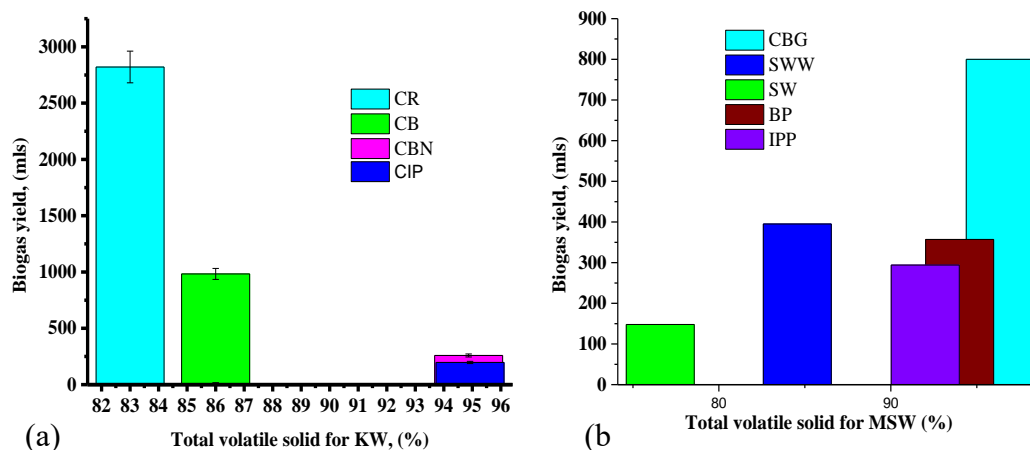


Figure 4.3: Biogas yield against TVS for different feedstock (a) KW and (b) MSW

Figure 4.3(a, b) shows biogas yield against total volatile solids of KW and MSW substrates. Volatile solids are among the factors that contribute to the amount of biogas production, although other factors play a role as well. It depends on many factors not only VS, for instance, a study whereby reduction of VS showed the highest biogas yield (Hill & Bolte, 2000). Regarding the current study, cabbage is the substrate that has a high TVS of 96.36% and yet did not produce the highest amount of biogas as compared to cooked rice and beans as its CN ratio of 13.9 is lower than the minimum recommended value for the methanogenic bacterial. The pH for cabbage was 6.2, which leads to easy accumulation of VFA (Kafle et al., 2014; Ranjitha & Vijayalakshmi, 2014). Hydrolysis and alcoholic formation of vegetable and fruit waste occur at a higher speed as compared to other organic food waste substrates (Di Maria et al., 2014) which leads to low production of biogas in cabbage. Food wastes and vegetable wastes as mono-digestion substrates had the smallest duration of producing biogas except for CR with a total solid of 31%, which produced the highest yield for 28 days. Food waste substrates are highly useful for AD due to their high biodegradability and methane yield as well as the influence of pretreatment (Deepanraj et al., 2017) regardless of other

factors like C/N ratio, pH, nitrates, conductivity, and alkalinity which automatically contribute to high methane yield in cooked rice. Therefore, to enhance biogas yield from vegetable waste co-digestion with the substrate with a higher CN ratio and pH is required. Biogas composition obtained from mono-digestion of cooked rice waste was found to be 62.8% methane, 36.30% carbon dioxide, 0.1% oxygen, ammonia 75 ppm, and hydrogen sulfide 681 ppm.

4.4 Co-digestion of Different Substrates

To raise the nutritive and biological environment for methanogenic bacteria in the digester and increase the production of biogas production an appropriate feedstock for co-digestion should be selected. After characterization of the feedstock, the current study co-digests different feedstock depending on its availability throughout the year to find an appropriate substrate for the anaerobic co-digestion process and the results are shown in **Figure 4.4**.

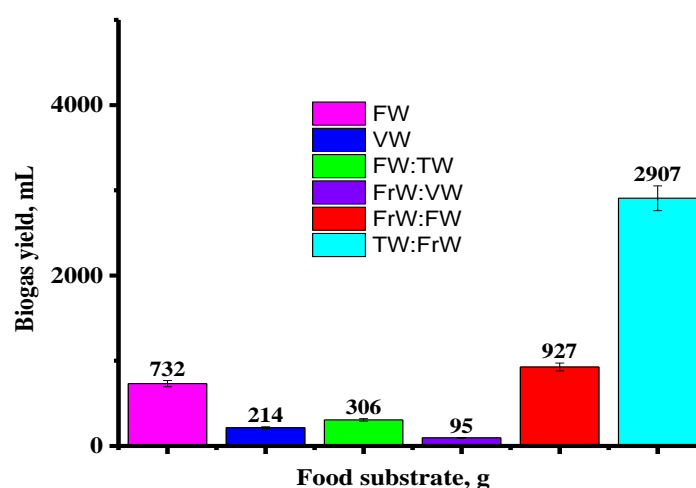


Figure 4.4: Biogas yield versus co-digestion of different feedstock

Figure 4.4 indicates the biogas production from the co-digestion of different feedstock. The co-digestion of vegetable waste (VW) and fruit waste (FrW) produced the lowest yield (95 ± 1.1 mL) which may have been caused by the decomposition of easily

digestible materials that lead to the production of more volatile fatty acids that hinder the methanogenesis process (Brown & Li, 2013). The highest yield (2907 ± 32 mL) was observed in the digester composed of tuber waste (TW) and fruit waste (FrW) due to the high biodegradability index (BI) of banana peels and tuber waste (Tchobanoglous et al., 2003). The CN ratio of banana peels was observed to be 28:1 while that for Irish potato peels was 18:1 which is in line with (El Barnossi et al., 2022) and (Muhondwa et al., 2015) respectively. The CN ratio in Irish potato peels was found to be less than the recommended 20-30:1 (Okonkwo et al., 2018) which implies that it is the nitrogen-rich substrate and therefore co-digestion with the carbon-rich compound is required. The commutative methane yield during the co-digestion experiment follows the order TW: FrW > FrW:FW > FW > FW:TW > VW > FrW:VW. A low amount of methane yield was observed in Fruit waste co-digested with vegetable waste, as it is easier for vegetable and fruit waste to accumulate volatile fatty acid and therefore leads to failure of methanogenic bacteria as the digester's pH was affected. Fruit and vegetable waste are mostly produced in different households and industrial sectors and high amounts. FrW and VW are highly decomposable feedstock with a high amount of water content; thus a potential feedstock for biogas production (Ganesh et al., 2014) but its high moisture content and CN ratio resulted into digester instability.

Digestion of fruit waste and vegetable waste had a short period of producing biogas which resembles (Elsayed et al., 2021) who reported that the production ceased within 13 days. A reasonable and high amount of biogas yield via fruit and vegetable waste could be co-digested with other waste such as agricultural waste, food waste, etc. (Vats et al., 2019). This is done to improve the digestibility and balances the nutrient in the digester, which is in line with the current study. The highest amount of biogas was observed in tuber waste co-digested with fruit waste, and therefore the rest of the study

on the co-digestion process was only considered tuber waster and fruit waste while vary other parameters such as mixing ratio, temperature and pH. The corresponding high methane yield obtained from this part might have resulted due to the balancing of carbon and nitrogen ration in the digester.

4.4.1 Effect of substrate mixing ratios

To study the effect of co-digestion of tuber waste and fruit waste at the lab scale level, the experiments were carried out with different mixing ratios using inoculum from an active biogas power plant with a constant concentration in each biodigester. The quality and quantity of inoculums are crucial to the duration, efficiency, and stability of methanogenic bacteria. The Irish potato peels and banana peels were mixed in four ratios 1:1, 1:2, 1:3, and 1:4 **Figure 4.5**.

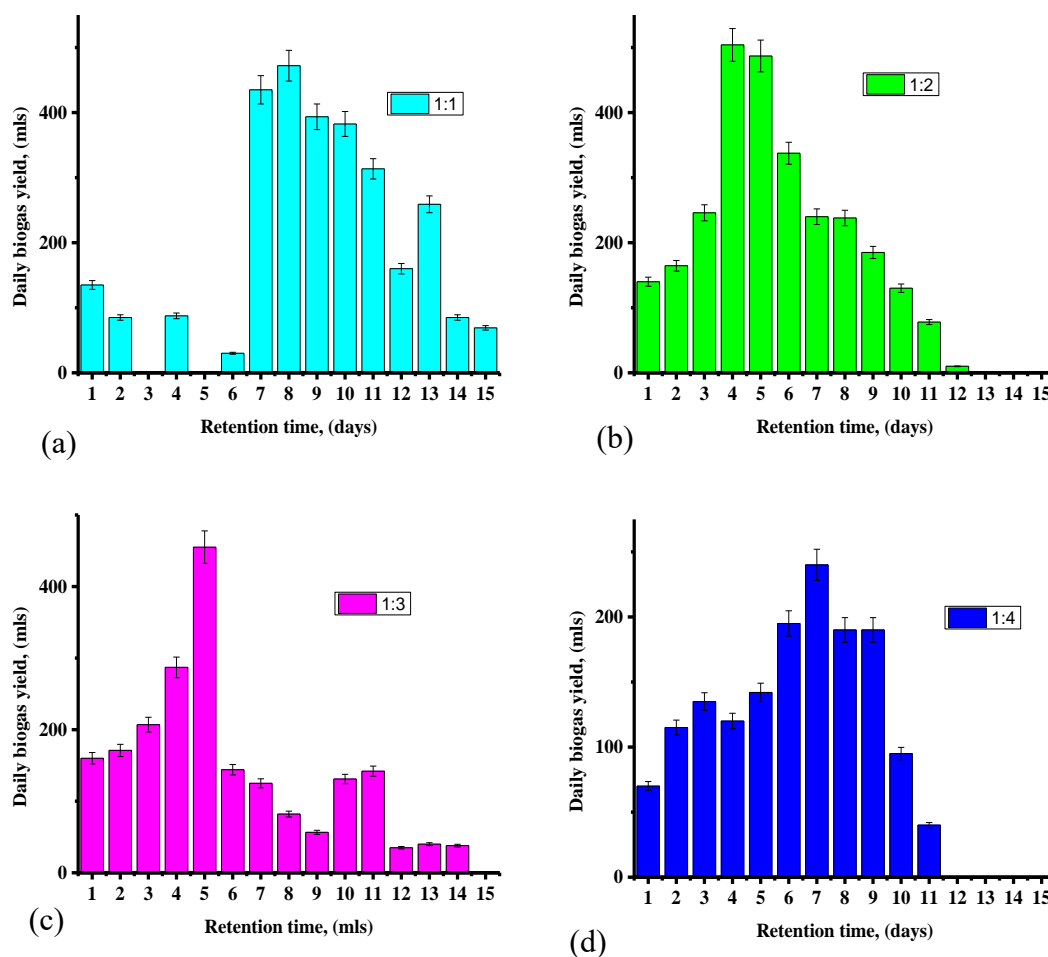


Figure 4.5: Daily biogas yield against retention time in various ratios for TW: FrW

Figure 4.5 It was noticed that co-digestion of tuber waste and fruit was in the ratio of 1:1 giving the highest quantity of biogas generation in comparison to the rest of the ratios (2907±32mL). The time for the hydrolysis process was reduced as compared to mono-digestion where other feedstock took almost a month. Hydrolysis time depends on the biodegradation of feedstock available. The phase of hydrolysis in the co-digestion process seems to be reduced due to the balancing of the CN ratio; therefore, the microbes can easily decompose the feedstock resulting in bio-digester stability and thus; early biogas production. The commutative methane generation took a trend of 1:1 (TW: FrW)>1:2(TW: FrW)>1:3(TW: FrW) and >1:4(TW: FrW).

The mixing ratio acts as synergism to expand the existence of an adaptable and dynamic microbial community and balance the nutrients whereby pH for both reactors was decreased as the production proceeded. Co-digestion of banana peels and Irish potato peels is very crucial as it balances the nutrients, maintains the reactor equilibrium, accelerates the hydrolysis process, and improves the yield. Physical pretreatment was done for both substrates, biogas production commences within the first 8hrs after setup for all the mixing ratios. On the 15th day, the pH of the reactors decreased from 6.8 to 6.2 and this was due to the accumulation of VFA, which led to the cessation of the product after 15 days. The volatile fatty acid accumulation resulted from banana peels as shown in the literature (Barua et al., 2019) compared to Irish potato peels. **Figure 4.5(a-d)** shows the daily biogas production for different mixing ratios. The cumulative biogas yield increased progressively throughout the process.

Production decreases with the increase in mixing ratio as it can be observed that the mixing ratio of 1:1 displays the highest yield of 472 ± 5.2 mL on day 8, and 1:2 the highest yield on day 4 (504 ± 5.5 mL). On the other hand, a mixing ratio of 1:3 produced the highest yield on day 5 (455 ± 5.0 mL), and the 1:4 reactor displayed the highest yield (240 ± 2.64 mL) on day 7. A cumulative biogas yield of 2907 ± 32 mL was observed in the digester with 1:1 (TW: FrW) by the end of 15 days which is nearly twice a mixing ratio of 1:4 which experienced a low biogas yield of 1532 ± 17 mL. This could have been due to an increase in nutrients (C: N) than the maximum as a result the reactor could not be maintained at equilibrium therefore decelerating the hydrolysis process. Syaichurrozi, (2018) reported the maximum biogas production of 114 mL on day 18 from co-digestion of rice straw and banana peels in the ratio of 2:3 while (Barua et al., 2019) recorded the highest biogas yield of 170 mL during the 16th day. (Tasnim et al., 2017) reported methane at 65%, and carbon dioxide at 14%, while other gases were reported to be 21%

during co-digestion of cow dung, sewage sludge, and water hyacinth. Co-digestion of banana peels and water hyacinth reported the highest methane yield with a methane content of 65.65%, carbon dioxide 25%, and hydrogen 8.67% (Barua et al., 2019). This was comparable with the current study, as the composition of biogas produced in this study was methane 58.7%, carbon dioxide 41.0%, oxygen 0.2%, and hydrogen sulfide 903 ppm.

4.4.2 Effect of temperature on biogas yield

The temperature has a great effect on the microbe's community and the performance of the anaerobic digestion process. Several studies indicated that there is a direct relationship between the amount of biogas produced and the operational temperature of the digester. Three main temperature ranges for anaerobic digestion are classified as psychrophilic where temperatures less than 20°C mesophilic (20–45°C), and thermophilic (45–60 °C). Thermophilic anaerobic digestion (AD) has proven to have a high quantity of biogas generation and better quality of digestate and was noted that this kind of AD faced a problem of digester instability (Rahman et al., 2021). The instability can be due to a high amount of ammonia and VFA accumulation because of the low growth rate of acetoclastic methanogens and slow metabolism. Meanwhile, thermophilic anaerobic digestion is not much economically viable option because of a high-energy requirement to heat the digestion system, (Rahman et al., 2021) which is in line with the current study. By considering the stability of the process and the economic feasibility, the current study considers about five different temperatures and was noted that biogas production increases continuously with an increase in temperature to the optimal range under mesophilic conditions **Figure 4.6(a, b)**.

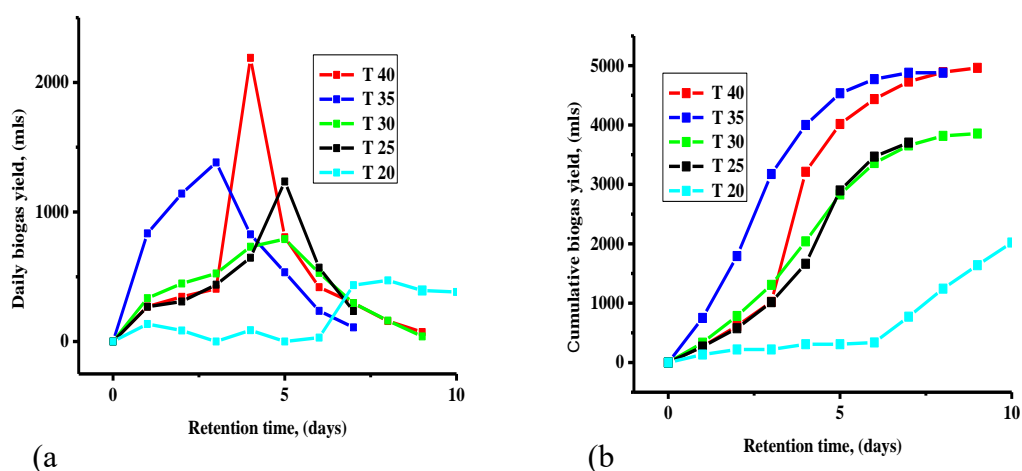


Figure 4.6: Biogas yield per retention time on the effect of temperature (a) daily (b) cumulative

Five different working temperatures were considered and the cumulative biogas yield obtained from the reactor at 20, 25, 30, 35, and 40 °C were 2907, 3703, 3856, 4881, and 4963mL respectively. The room temperature at the time when the current experiment was conducted was about 20°C. From the results obtained, it was noted that yield increases with the temperature rise. The amount of biogas obtained at a lower temperature of 20°C was a much lower yield of 2907±32mL as compared to 40°C producing the highest yield of 4963±55mL, nearly twice that of 20°C **Figure 4.6(a, b)**. The cumulative biogas yield was higher at 40°C and was observed to increase with the increase in temperature. The cumulative biogas yield from the digester with a temperature of 40 °C is a 70.7% increase as compared to the yield in the digester at 20°C. A related trend was noticed by (Deepanraj et al., 2015; Kim et al., 2006) who studied the effect of temperature on biogas yield from the AD of food wastes. The results revealed that the microbe's activity in this work depends on the operating temperature. Temperature is considered one of the major limitations that affect methanogenic bacteria, and therefore low yield is obtained at low temperatures. It was likely due to less COD being degraded at an operation temperature of 20°C.

Furthermore, the methane yield was noticed at a low temperature of 20°C and continues to decrease due to the lower biogas production and lower methane.

Therefore, the results disclose that at low operation temperatures, there is a low biodegradation process.

4.4.3 Effect of pH on biogas yield

The pH is one of the most crucial parameters in digestion systems. Different metabolic activities occurred due to the growth of the microbial community and changes in microbial population when environmental and operational conditions varied, thereby resulting in different fermentation types. Under the alkaline and acidic conditions, three different levels of pH (pH 6.5, 6.9, and 7.3) were investigated. The effect of pH on daily and cumulative biogas production is shown in **Figure 4.7(a, b)**.

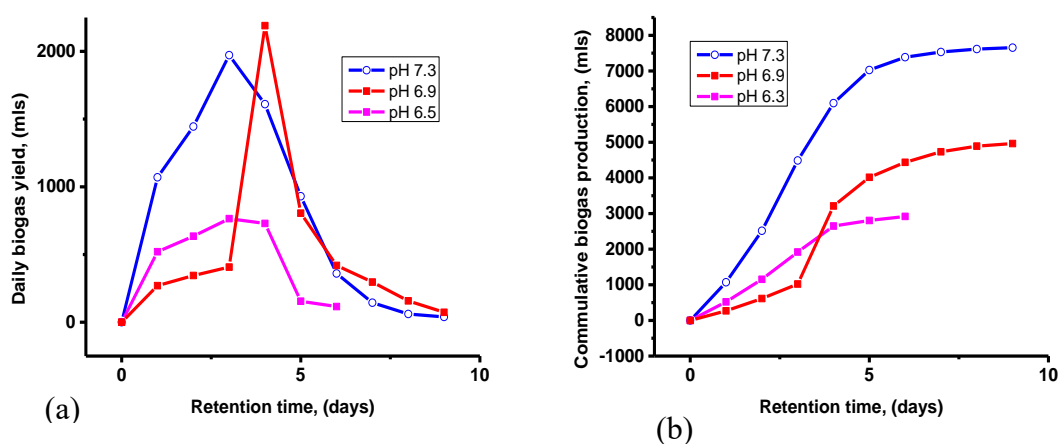


Figure 4.7: Biogas yield per retention time on the effect of pH (a) daily (b) cumulative. The daily and cumulative biogas production versus retention time for all the digesters are shown in **Figure 4.7(a, b)**. The experiment was conducted for 7 days at a pH of 6.5 while for a pH of 6.9 and 7.3, it took 10 days for the production to cease. The anaerobic digestion performance differs from one feedstock to another due to the characteristics of the respective feedstock, the presence of inhibitors, operation parameters, and the

presence of inhibitors in the feedstock (Czubaszek et al., 2022). Thus, some feedstocks took 7 days and others 10 days for production to cease which is in line with the literature. The highest production ($7810\pm 86\text{mL}$) was achieved at a pH of 7.3 at 40°C , which is a 178.1% increase while $2808\pm 31\text{mL}$ was attained at a pH of 6.5. As observed in **Figure 4.7a**, the daily biogas production in the digester having pH of 6.9 was significantly increased especially on the 1st -3rd days, while on day 4th there was an instantly raised and started to decrease from the 5th-9th day, which may be contributed by the accumulation of VFA and decrease of food for microbes. The cumulative biogas production was higher at a pH of 7.3 and it was observed that production increases, as there is an increase in pH to the optimal.

The production of biogas in the digester pH 7.3 was instantly raised from day 1st -3rd and started to decrease from day 4 while stopped on day 9. The optimal pH for biogas production ranges from 6.5-7.5 (Liu et al., 2008). A study by (Abudi et al., 2020) on the effects of an alkali pre-treatment of mango leaves for biogas production by variation of pH from 6.5-8.0 shows that high production was obtained at the optimal range of pH 7.5. The addition of lemon juice causes the pH to drop from 6.9-6.5 because lemon, being highly acidic is the reason for this decrease in pH hence inhibiting the methanogenic activities and thus lowering biogas production in the digester as compared to the yield with a pH of 7.3. The results revealed that the activity of methanogenic microbes used in this study depends on the operating pH. In addition, a constant pH of 7.3 was conveniently beneficial for enabling acidogenic fermentation, although a drop of lemon juice was used to adjust pH to study the effect of different pH on biogas production.

The biogas produced contained methane 58.7%, carbon dioxide 41.0%, oxygen 0.1%, and hydrogen sulfide 903 ppm. A similar trend to the current study was observed in a

study done by (Ali et al., 2019) where the maximum methane production (CH₄ 94%) was noticed in a digester having a pH of 7.0 while other digesters with a low pH value the methane content was lower as compared to this digester.

4.5 Synergy Effect of Anaerobic co-digestion

The methane produced from mono-digestion of tuber waste and fruit waste was 294 and 357 mL, respectively. The synergy index (SI) value was obtained under the same conditions (temperature 20°C). **Table 4.16** indicates the synergy index values for the co-digestion of tuber and fruit waste.

Table 54.16: SI for co-digestion of tuber waste (Irish potato peels) and fruit waste (banana peels).

Feedstock	Biogas yield, mL	SI
Mono-digestion (TW)	294	-
Mon-digestion (FrW)	357	-
Co- digestion (TW: FrW)	2907	4.5

It was observed that co-digestion has visibly positive synergistic results (SI greater than 1) on AD for methane yield from the two substrates (tuber waste and fruit waste). Kim et al., (2017) observed that co-digestion of toilet paper, human excrete, and FW had no significant synergistic effect as the synergy index values vary from 0.939 - 1.05. (Ebner et al., 2016) obtained a synergy index of 0.68 for the co-digestion of dairy manure and FW which shows a significant antagonistic effect. In contrast, to this study, the two feedstock used had significant synergistic results. The current study found that co-digestion of tuber waste and fruit waste can give a successful approach to generating energy by using the available biomass wastes. The SI results may be related to the mixture proportions and characteristics of the feedstock, which could increase the corresponding buffer capacity, stimulate microbial synergism, balance the nutrients, and dilute the toxic compounds during digestion. According to (Wang et al., 2018), the

synergistic effect is due to some additional beneficial nutrients which can enhance biodegradability and increase microbes' metabolism rate in the digester.

4.6 Biogas Composition from Onsite Digesters

To assess the stability of the anaerobic digestion system, it is important to evaluate the content of the biogas produced in terms of methane (CH₄), carbon dioxide (CO₂), and other minor impurities. The composition of raw biogas from the two digesters was determined using the biogas analyzer model Geotech 5000, the results are shown in **Table 4.17**, and the site for the experiment was allocated around Kesses, Eldoret in a household premises.

Table 4.17: Biogas composition from the two working digesters

Component	Digester 1	Digester 2
CH ₄ %	67-69.1	69-70.1
CO ₂ %	29.7-30.1	30.1-30.8
O ₂ %	0.1-0.2	0.1-0.2
NH ₃ ppm	331-421	331-530
H ₂ S ppm	530-606	748-1480

Biogas composition in the two digesters differs, as the feedstock was different day after day. The feedstock was generated from kitchen waste, biomass (plant leaves), and human waste, and an on-site experiment for determining the adsorption ability of soda ash from Lake Natron and eggshell waste was carried out at domestic household premises. The substrate used had an impact on biogas production; within the two digesters, it was noted that sometimes when biogas production was low there was an addition of some additive substrates for enhancing and balancing the nutrient in the biogas power plant.

4.7 Characterization of the sorbents

4.7.1 Textural properties of the soda ash adsorbent

The study of the porous structure/arrangement of the sorbent material (total pore volume, cm^3/g , specific surface area S_{BET} , m^2/g , mesoporous volume, V_{me} , cm^3/g , and V_{miso} cm^3/g was carried out at the University of Dar es Salaam using the Quantachrome NOVA 4200 (Win©1994-2013, v11.03). The textural characteristics of the sorbent material were analyzed for three samples, raw sample (S_1), spent (S_2), and regenerated sample (S_3) as observed in Table 4.18.

Table 4.186: Multipoint BET data for unspent sample (S_1), spent sample (S_2), and regenerated sample (S_3) with $280\mu\text{m}$ particle size.

Sample	$S_{\text{(BET)}}$ (m^2/g)	Pore radius (A°)	$V(\text{total})$ (cm^3/g)
S_1	409	17.685	0.742
S_2	264	17.539	0.311
S_3	103	17.377	0.143

The multipoint BET analysis is shown in Table 4.18 for the three sorbents: as it is observed, the BET surface area of the unspent sorbent S_1 is greater in contrast to the spent and regenerated sorbents. Finally, it decreases in the S_2 that undergoes adsorption because the mesoporous site had been occupied by hydrogen sulfide as adsorbate. The evaluation of pore size for all samples shows they are mesoporous rather than macroporous and micropores as the pore size ranges from 2-50 nm Figure 4.8(a, b). The current study is supported by literature (Shadjou & Hasanzadeh, 2015a, 2015b).

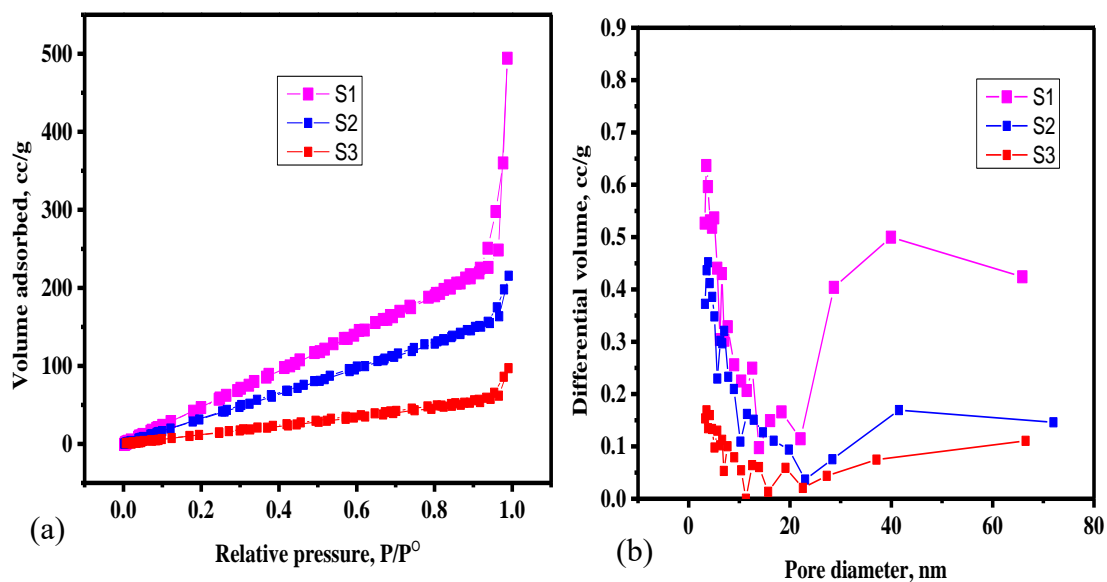


Figure 4.8: (a) Nitrogen adsorption/desorption isotherms. (b) Pore size distribution was calculated from desorption isotherm using the BJH method.

Nitrogen adsorption/desorption isotherms are displayed in Figure 4.8(a), while Figure 4.8(b) displays pore size distribution, calculated through the BJH method. By considering Figure 4.8(a), the unspent sorbent S₁ adsorbs more N₂ in contrast to the rest as it has the highest BET surface area Table 4.18. In Figure 4.8(b), it can be noticed, that as sample S₁ owns a large BET surface area and pore radius; hence, it has a high differential volume when compared to other samples, which is due to the high surface area of the respective sorbent. The higher the surface area the greater number of adsorption sites for H₂S removal (He et al., 2011).

4.7.2 Sorbent morphology/Soda ash morphological structure

SEM/EDS analysis was performed on the sorbent samples S₁-S₃ to observe the morphological and surface structure of the materials. **Figure 4.9-4.11** indicates the SEM image for the unspent sorbent (S₁), spent sorbent (S₂), and regenerated (S₃) respectively.

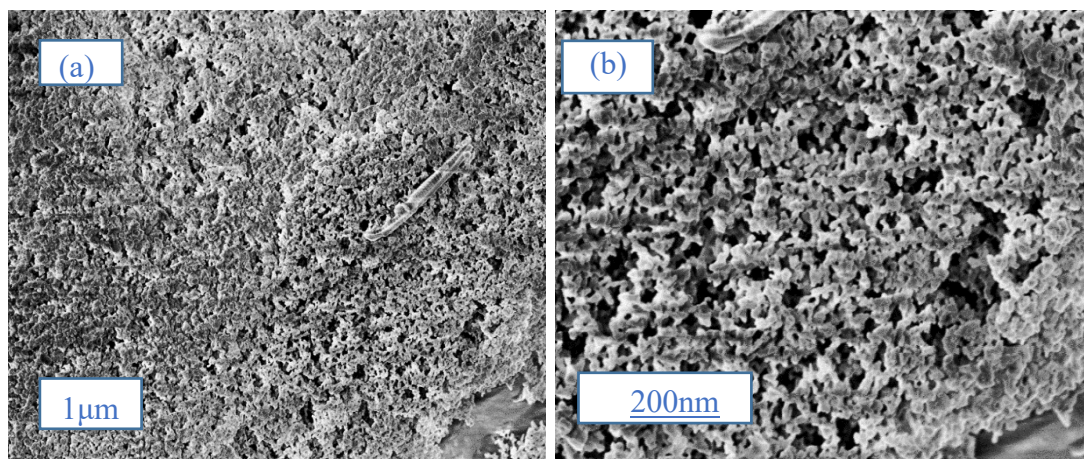


Figure 4.9 (a): SEM micrograph images of the adsorbent S₁ (a) 10 KX (b) 25 KX

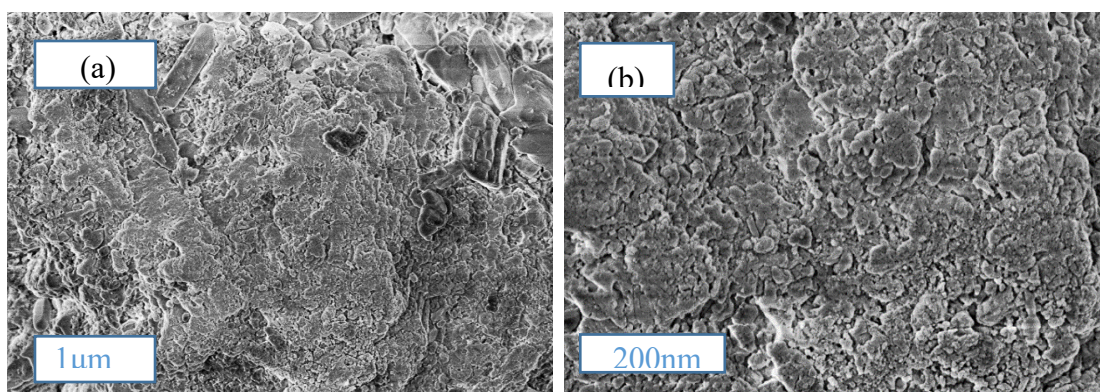


Figure 4.10: SEM micrograph images of the adsorbent S₂ (a) 10 KX (b) 25 KX

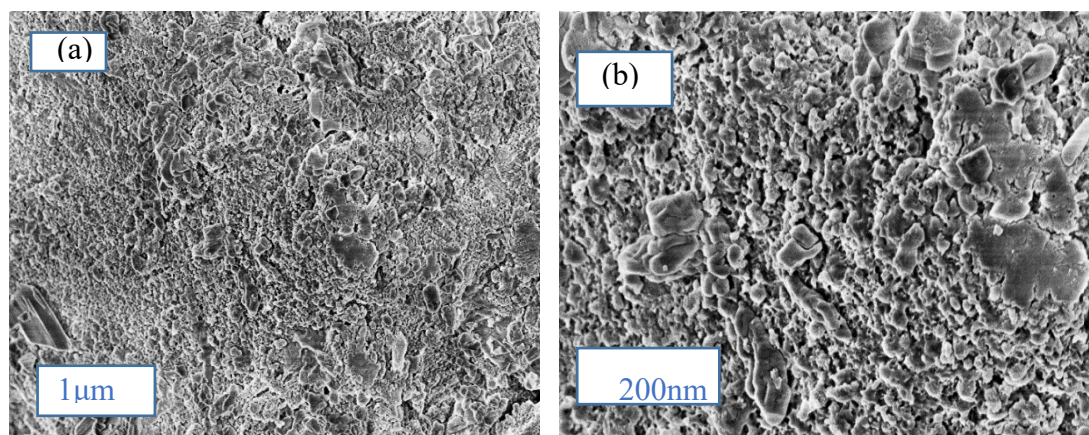


Figure 4.11: SEM micrograph images of the adsorbent S₃ (a) 10 KX (b) 25 KX

Figure 4.9 shows the external surface area of unspent sorbent (S_1) appears relatively rough, having extremely hollow pores, irregular crystal structure, and therefore porosity, which facilitate the whole process of H_2S removal. **Figure 4.10** illustrates the smooth surface of the sorbent (S_2) and the quantity of masses attached to the surface which fills up the hollow pores and hence reduces the porosity of the sorbent that indicates the attachment of hydrogen sulfide from the biogas, which is in line with (Thanakunpaisit et al., 2017). **Figure 4.11** indicates a regenerated sample with masses attached to the hollows of the micrograph indicating the attachment of H_2S .

4.8 Mineral composition and pH of soda ash sorbent

The elemental composition of soda ash sorbent is displayed in **Table 4.19**; where XRF analysis shows that sodium carbonate, Iron, Chlorine, Potassium, Calcium, and Zirconium are the most abundant elements present in the sorbent.

Table 4.19: Composition of soda ash from XRF analysis

Element	Na	Si	Cl	K	Ca	Fe	Zr
Composition (mg/L)	211407.7	965.68	10484.8	1061.08	735.1	247.6	191.86

The pH value for the soda ash sorbent is alkaline (12), which favors the adsorption of hydrogen sulfide (Coppola & Papurello, 2018). The presence of a high amount of sodium carbonate in the sorbent in contrast to other elements facilitates the adsorption of hydrogen sulfide removal from biogas. The relationship between hydrogen sulfide adsorption capacities and removal efficiency with the soda ash surface chemical composition was investigated via results from XRF analysis. Hydrogen sulfide is acidic gas, thus after the adsorption of hydrogen sulfide from biogas the pH of the sorbent material dropped.

4.9 Adsorption Ability of Soda Ash

The development of biogas upgrading techniques is an important issue in the recovery of bio-vehicle methane. Nowadays, low-cost materials for biogas purification and upgrading techniques have been investigated. The use of locally available sorbents such as soda ash will add value in the world of biogas upgrading technologies. The adsorption ability of soda ash was studied at varying particle sizes, gas flow rates, and adsorbent masses to assess the potentiality of the material in removing H_2S from biogas. The sorbent does not react with the CH_4 component of biogas. Soda ash reacts with hydrogen sulfide from biogas and forms reaction products which are sodium hydrogen sulfide and sodium bicarbonate, as the sorbent pores are occupied by contaminant gas and saturated at a specific time (Kulkarni & Ghanegaonkar, 2019). The adsorption ability of this soda ash was consistent with its physical and chemical characteristics as it shows a high content of sodium carbonate, a large BET surface area, and good alkalinity properties.

4.9.1 Effect of adsorbent mass

The percentage removal and sorption capacity of hydrogen sulfide from biogas was obtained by varying the adsorbent mass while, maintaining the constant volume, particle size, and concentration of H_2S as observed in **Figure 4.12(a, b)**. The removal efficiency and sorption capacity of the sorbent were taken at each 15 min of the experiment and not a commutative value and thus q_t was observed to decrease with the increase in time.

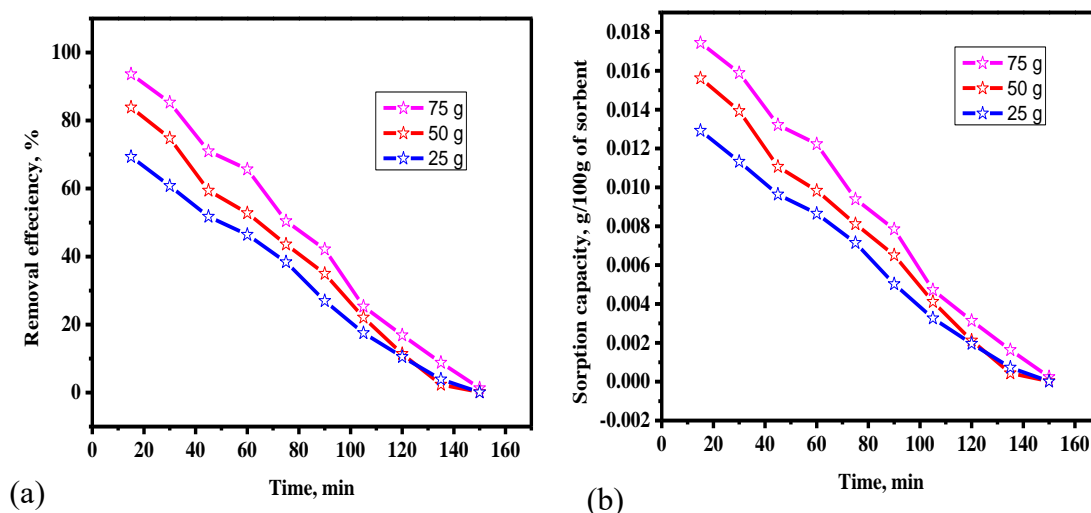


Figure 4.12: Effect of adsorbent mass on the performance of soda ash (a) Removal efficiency (b) Sorption capacity. Test condition: Flow rate =0.03m³/h, particle size 280 μ m and Co=1227ppm

The %removal of hydrogen sulfide defines the total amount of hydrogen sulfide taken from biogas while H₂S uptake explains the maximum H₂S adsorbate per gram of adsorbent. An increase in the mass of adsorbent resulted in an increase in removal efficiency, sorption capacity, and delay of breakthrough (Sigot et al., 2014). The removal efficiency and sorption ability of soda ash were observed to increase as the mass of the sorbent increased. As the material saturate the less the removal efficiency and sorption capacity was observed. Additionally, the longer the saturation time the better the material or sorbent is and it can authorize more time for use before the regeneration process. The adsorption and removal plots show that the more the saturation time of 150 minutes was noticed for 75 g in comparison to 50 and 25 g. Choo et al., (2013a) and (Mulu, et al., 2021), observed similar findings. Increasing the adsorbent mass increases the free sites for adsorption. This is due to the increase in interfacial external area for biogas to contact the soda ash sorbent that resulted in the increase in saturation time, removal efficiency, and sorption capacity.

On that account, for the sorbent to last longer before regeneration, a long bed column that can accommodate a large mass of sorbent is required. A study done on hydrogen sulfide removal using sweet potato leaves on 1g of sorbent gives a removal efficiency of 96% with an SC 3.7g/100g (Juma et al., 2020), while using 0.6g with a RE 95% and SC of 0.37 g/100 g of sorbent (Mrosso et al., 2020) which is in line with the current study. The effective use of soda ash from Lake Natron in the removal of hydrogen sulfide from raw biogas was done and was observed that hydrogen sulfide molecules had more chance to contact with the adsorption site for soda ash having a mass of 75g as compared to a mass of 50 g and 25 g. Therefore, a mass of 75 g provides the best results for both removal efficiency and adsorption capacity of the material. The 50 and 25 g of sorbent were recorded with a removal efficiency of 69, 83%, and sorption capacity of 0.013 and 0.015 g/100g of sorbent respectively. Thus, the sorbent efficiency can be classified due to the increase in masses from $75 > 50 > 25$ g. The higher removal efficiency and sorption capacity of 75 g of soda ash can be described by the presence of more adsorption sites.

4.9.2 Effect of particle size

To increase the sorbent's adsorption ability, the particle size of the material is an important aspect of the adsorption process and kinetics and hence should be considered as the rate of the process depends inversely on particle size (Cherosky & Li, 2013). The uptake and percentage removal efficiency of hydrogen sulfide from biogas is influenced by particle size, the removal efficiency increases with the decrease in particle size

Figure 4.13.

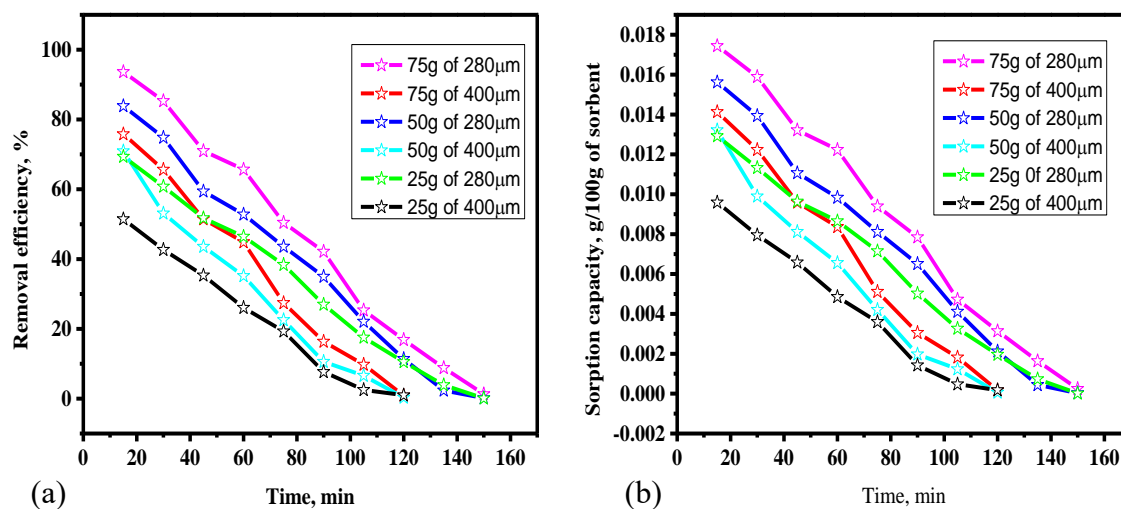


Figure 4.13: Effect of particle size on the performance of soda ash (a) Removal efficiency, (b) Sorption capacity. Test condition: Flow rate $0.03\text{m}^3/\text{h}$ and $C_0 = 1228\text{ ppm}$. The intake capacity of adsorbent is increased at high initial concentrations due to the enhancement of mass transfer (Dawodu & Akpomie, 2014). Particles with small diameters have higher adsorption ability than larger particle sizes. This is probably attributed to the large surface area to volume ratio, **Figure 4.13(a, b)**. Witoon 2011, and (Wang, 2013) reported that the smaller particle size of the sorbent provides more exposure to the surface for the adsorption process and therefore high removal efficiency and sorption capacity. A study done by (Kalsum & Hasan, 2022) reported that the methane concentration in purified biogas increases from 87.5 to 90% as the particle size decreases. This is in the same trend as this study, the small particle size of 280 μm provides a large surface area for adsorption compared to the larger surface area of 400 μm, and as a result, the high removal efficiency of 94% and SC 0.02g/100g of sorbent were obtained using a particle size of 280 μm during the first 15min.

Moreover, the effect of adsorbent particle size on the removal efficiency of hydrogen sulfide from biogas has a related tendency with other adsorbent materials used in literature. Mrosso et al., (2020) explored the removal efficiency of red rock sorbent at different particle sizes from 0.32 - 250 μm, 250 - 500 μm, 500 - 750 μm, 750 μm- 1 mm,

and 1 - 1.5 mm. The researchers established that the sample that was calcinated at a temperature of 1000 °C and sieved at 0.32–250 μm expressed a removal efficiency of 95% while its sorption ability was 3.7 mg/g. Meanwhile, (Juntarachat & Onthong, 2022) investigated the effect of pellet size of biochar with various sizes as 0.50, 1.0, and 1.50 cm on H_2S removal from biogas and found that sample sieved at 0.50 cm showed high removal efficiency and sorption capacity of 7.65mg/g. Similarly, Thanakunpaisit et al. studied the adsorption of H_2S from biogas using soybean-based ink wastes from some printing industry at different particle size as from 0.25, 0.50, 1.00, and 1.50 cm found that the material of 0.25 cm had the highest adsorption efficiency as compared to the large particle size. Thus, the smaller the particle size of the adsorbent, the larger the surface area and the greater the adsorption capacity that is in line with the current study.

4.9.3 Effect of biogas flow rate

The biogas flow rate influences the adsorption ability of the sorbent. The ability of soda ash to uptake hydrogen sulfide from biogas is reduced as the biogas flow rate rises. When the flow rate is low, the percentage of hydrogen sulfide removal and sorption capacity increase with the residence time **Figure 4.14(a, b)**.

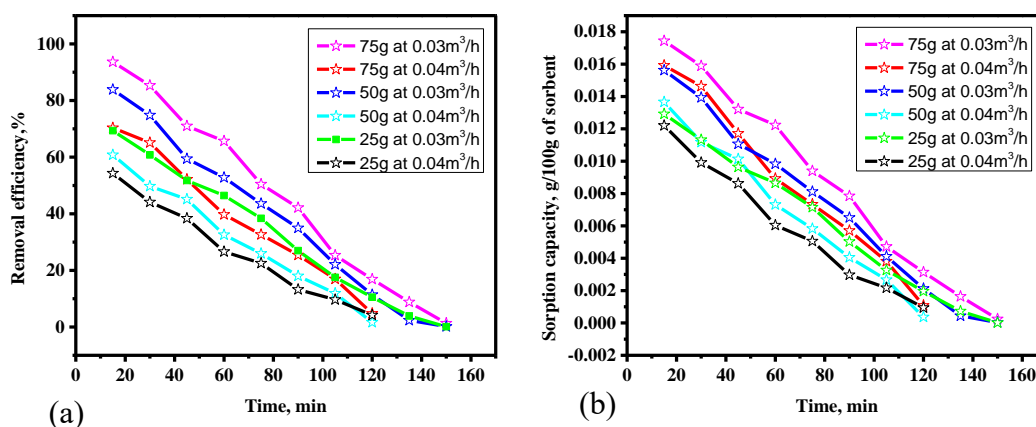


Figure 4.14: Effect of flow rate on the performance of soda ash (a) Removal efficiency, (b) Sorption capacity. Test condition: Particle size 280 μm and $C_0 = 1480\text{ppm}$

A high flow rate decreases the contact time between the sorbent and the adsorbate (Thuy & Chi, 2016), and therefore hydrogen sulfide passes through the adsorbent without being adsorbed which leads to low removal efficiency and sorption capacity as compared to a low flow rate. **Figure 4.14(a, b)** shows the removal efficiency of hydrogen sulfide from biogas at two different flow rates of $0.03\text{m}^3/\text{h}$ and $0.04\text{m}^3/\text{h}$, whereby the flow rate of $0.03\text{m}^3/\text{h}$ shows high removal efficiency and sorption capacity of 94% and $0.02\text{ g}/100\text{g}$ of sorbent. The results obtained from this study are consistent with those reported in (Sidabutar & Iriany, 2018) which disclose that when the flow rate is low, the exposure time between the adsorbent and the adsorbate in the adsorption bed column becomes prolonged. Thus, the removal efficiency and sorption capacity increase because the contact time is sufficient for the gas molecules to disperse into the adsorbent mesoporous. Contrarily, the removal efficiency and sorption capacity decreased with the increase in flow rate as the residence time of adsorbate in the bed column became shorter. Therefore, from the results on the removal of hydrogen sulfide from biogas it was observed that more H_2S was adsorbed at low biogas flow rate.

4.10 A comparison of soda ash with other sorbent materials used in literature

Soda ash sorbent was compared with other sorbents from the literature on the removal efficiency and uptake of hydrogen sulfide from biogas **Table 4.20**. Soda ash demonstrated comparatively high performance and thus is a suitable material for biogas desulfurization.

Table 4.207: A comparison between soda ash sorbent with the literature studies

Adsorbent	Flow rate (m ³ /h)	Contact time (h)	Re (%)	References
Red Rock	0.006	2.5	95	(Mrosso et al., 2020)
Oldonyo Lengai ashes	0.120	1.5	96	(Kandola et al., 2018)
WHAC-1:1-650	0.024	2.0	93	(Makauki et al., 2017a)
Fe/EDTA	0.016	0.8	84.5	(Frare et al., 2010)
Red mud soil	0.003	1.5	-	(Sahu et al., 2011)
Sweet potatoes leaves	0.020	1.2	95	(Juma et al., 2020)
Soda ash	0.030	2.5	94	Present work

4.11 Textural properties of the eggshell waste

The data analysis indicated that an increase in calcination temperature for calcined eggshells leads to an increase in pore size, number, and volume as it was approved by the removal efficiency and sorption capacity of calcined eggshells at 850°C.

Nitrogen adsorption-desorption isotherms plots of the three samples calcined unspent sample (E₁), calcined spent sample (E₂), and regenerated samples (E₃) are shown in **Figure 4.15(a, b)**. The pore size distribution for the three sorbents was calculated from the Nitrogen desorption data with BJH methods. **Figure 4.15(b)** shows the pore size distribution of the three samples as calcined unspent sample (E₁), calcined spent sample (E₂), and regenerated samples (E₃).

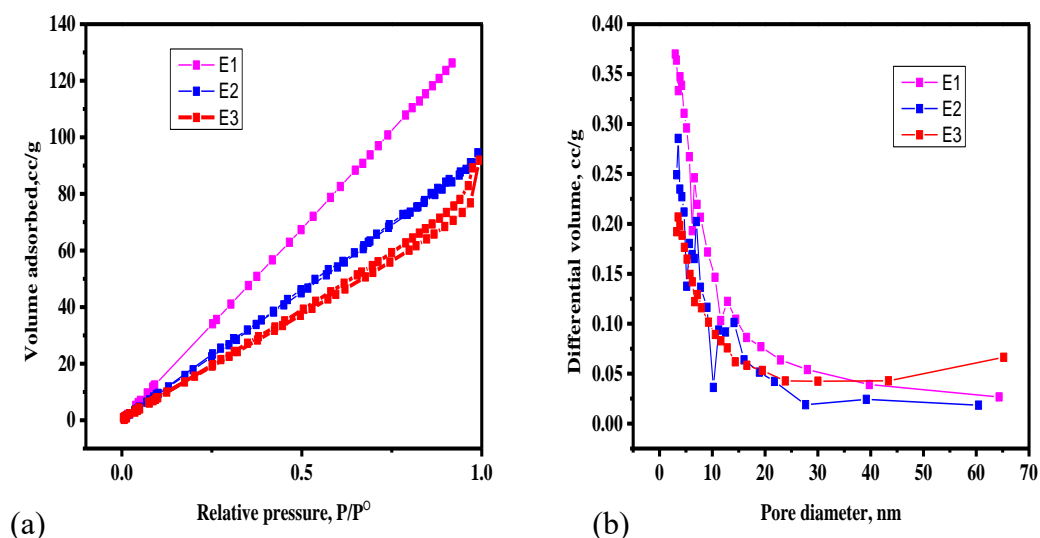


Figure 4.15: (a) Nitrogen adsorption/desorption isotherms. (b) Pore size distribution was calculated from desorption isotherm using the BJH method.

From **Figure 4.15(b)**, it can be observed that E₁ possesses more differential volume as compared to E₂ and E₃, indicating that E₁ has more pores as compared to the rest. However, when the sorbent was used in the adsorption process the differential volume decreased which suggests that the pores were occupied by the adsorbate. The regenerated sorbent shows much less differential volume as compared to the rest, which indicates that the pores collapsed. The E₁, E₂, and E₃ have high differential pore volumes at a pore size ranging from 2.0-20.0 nm as shown in **Fig 4.15(b)** which indicates that the calcined eggshells possess mesoporous as classified by IUPAC. The availability of mesoporous in the calcined eggshell sample is paramount as it facilitates the whole process of adsorption. As the sorbent adsorbs the carbon dioxide from biogas the amount of Nitrogen adsorbed decreases indicating that there is a decrease in pore volume and surface area. The regenerated sorbent shows much less on the adsorbed Nitrogen as compared to the spent and unspent sample indicating that the sorbent starts to lose its ability in the adsorption process as pores lose their ability to adsorb which

leads to easy saturation it is evident that calcination temperature has different effects on the surface and pore structure of eggshells as observed in (W Ahmad et al., 2021).

The multipoint BET surface areas for the three samples are tabulated in **Table 4.21**.

Table 4.21: Multipoint BET summary for calcined unspent sample (E₁), calcined spent sample (E₂), and regenerated sample (E₃) with 280 μ m particle size.

Sample	Particle size (μ m)	S _(BET) (m ² /g)	Pore radius (Å)	V(total) (cc/g)	References
E1	280	227.6	17.6	0.2	This study
E2	280	152.3	16.2	0.1	This study
E3	280	127.3	14.9	0.1	This study
CEW	149-420	19.32	18.2	0.1	(Köse & Kıvanç, 2011)

It was observed that the adsorbed volume increased extremely from (E₃-E₁) which revealed the increase in pore volume and specific surface area. The E₁ shows the highest N₂ adsorption capacity with S_(BET) of 227.608 m²/g as observed in **Table 4.21** due to calcination temperature. Finally, it decreases in the E₂ that undergoes adsorption because the mesoporous generated during calcination had been occupied by adsorbate. The BET surface area and the pore radius decrease from E₁-E₃, due to the adsorption. The BET surface area of the calcined sample E₁ is greater while it decreases in the E₂ that undergoes adsorption because the mesoporous generated during calcination had been occupied by carbon dioxide as adsorbate, and further decreased in regenerated sorbent (E₃) which may be due to sintering effect. Waseem et al. (2021, reported that high calcination temperature decreases the surface area of the eggshells. An increase in the specific surface area represents an increase in the number of adsorption sites that favor the adsorption of carbon dioxide from biogas. The BET surface area of calcinated eggshells obtained in the present study is larger than those reported by (Waseem et al., (2021). The evaluation of pore size for all samples used in this study shows they are mesoporous rather than macroporous and microspores as their pore diameter ranges

from 2.0-50.0 nm which is in line with (Alothman, 2012). The low BET surface area of CEW can be due to the presence of impurities, indicating poor eggshell preparation.

4.12 The Surface Morphological Studies of Calcined Eggshell Waste

The morphology of the calcined unspent sample (E_1), calcined spent sample (E_2), and regenerated sample (E_3) are as observed in the SEM image in **Figure 4.16-4.18** where it was examined with Field Emission Scanning Electron Microscope (FESEM)

instrument

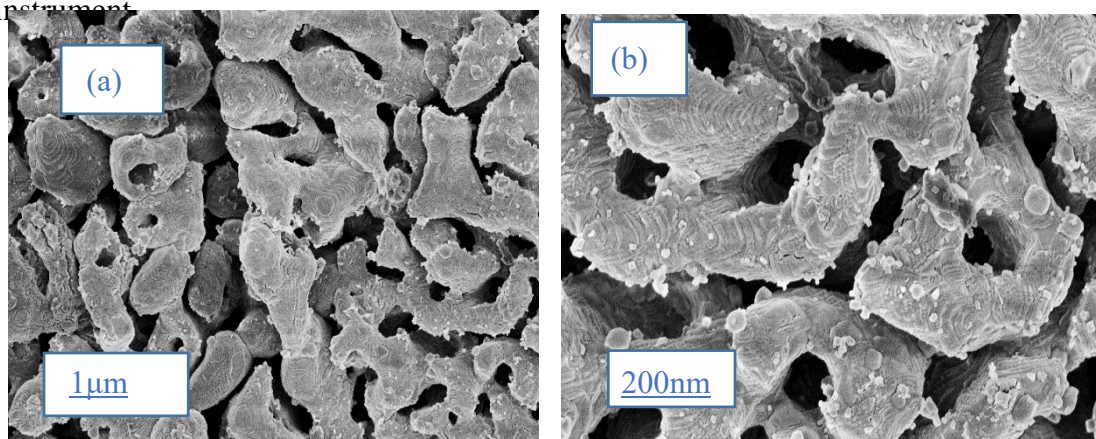


Figure 4.16: SEM micrograph images of the adsorbent E_1 (a) 10 KX (b) 25 KX

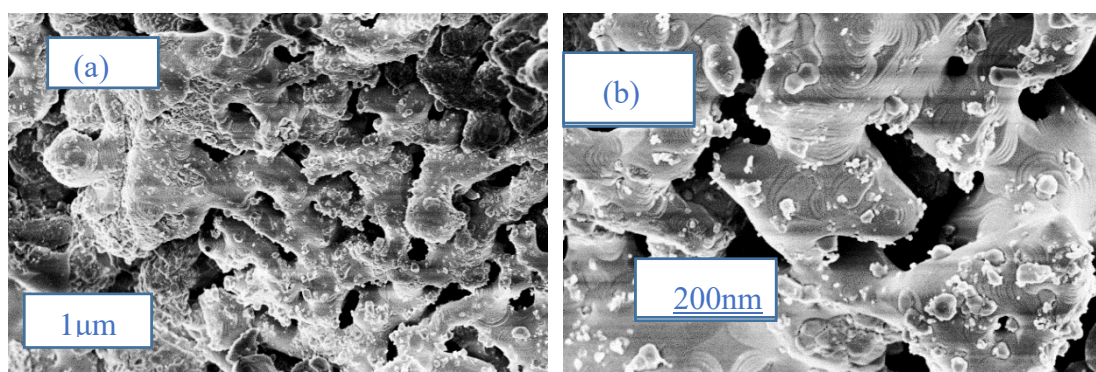


Figure 4.17: SEM micrograph images of the adsorbent E_2 (a) 10 KX (b) 25 KX

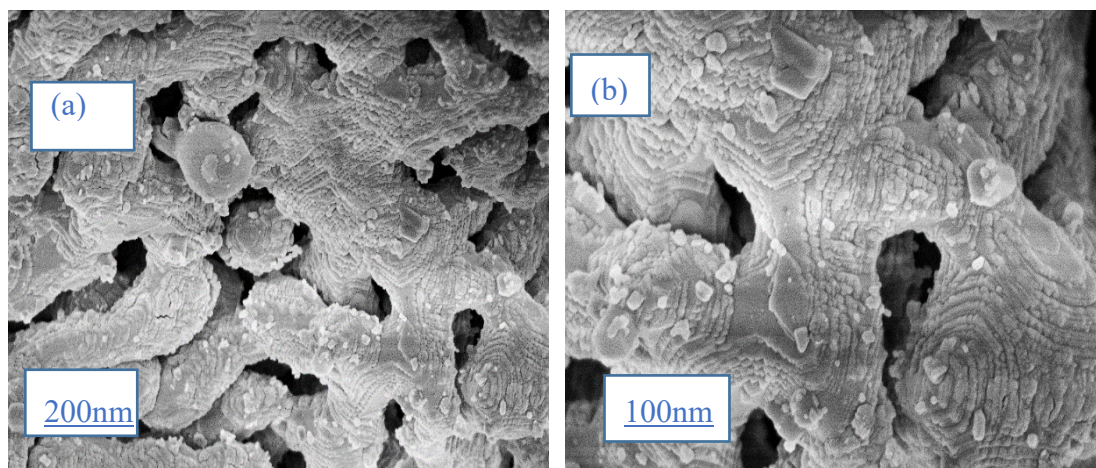


Figure 4.18: SEM micrograph images of the adsorbent E3 (a) 25 KX (b) 50 KX

The calcined unspent sorbent indicates that there was extremely irregular pore size with the smooth surface because of the calcination process under 850°C, **Figure 4.16** which is mostly preferred for adsorption and therefore surface area increased which is reflected in **Table 4.21**. The spent sorbent image (E₂) shows some pores collapsed with the formation of many white aggregate spots which indicates there is an attachment of carbon dioxide from biogas, which is a good sign that the eggshell waste is a promising sorbent for carbon dioxide adsorption **Figure 4.17**. The regenerated sorbent shows even more collapse of the pore, which might be due to attachment of CO₂ and hence start losing its ability in the upgrading process **Figure 4.18**, the morphology of the eggshell sorbent is very similar to (Machunda & Pogrebnaya, 2020; Sahu et al., 2011).

4.13 Mineral Composition and Eggshell Sorbent

The elemental composition of calcined eggshells is displayed in **Table 4.22**. The XRF analysis indicated that Mg, Si, P, Ca, Sr, Cl, Al, and Pb are the elements present in the sample.

Table 4.228: XRF analysis for calcined eggshells showing the chemical composition

Element	Mg	Si	P	Ca	Fe	Sr	Cl	Al	Pb
Composition	2286.1	1322.08	2137.48	371512.06	217.12	651.16	1062.72	95.4	23.62

The pH value for the eggshell sorbent falls under basic (11), and calcium oxide was observed in high amount as compared to other elements which facilitate the whole process of adsorption of carbon dioxide from biogas using calcined eggshell, this is observed in (Coppola & Papurello, 2018).

4.14 Adsorption Ability of Calcined Eggshells Sorbent

The onsite experiments were carried out to assess the sorption ability of the chosen sorbent. Biogas upgrading techniques are an important issue in the recovery of bio-vehicle methane especially the use of locally available and waste sorbent material. Currently, low-cost materials for biogas purification and upgrading techniques have been investigated. The use of locally available sorbent such as eggshell waste will add value to the world of biogas purification. The calcium oxide from calcined eggshell waste reacts with carbon dioxide from biogas and forms products that are calcium carbonate. Thus, the adsorption ability of calcium oxide derived from eggshells was studied in terms of particle size, flow rate, and mass of adsorbent on the removal and sorption capacity of carbon dioxide from biogas. The performance of the sorbent material was observed to rely on the operational conditions and was observed that the material did not react with the methane content of biogas.

4.14.1 Effect of particle size

To enhance the adsorption ability of the sorbent; the particle size of the material is a significant aspect to be considered (Cherosky & Li, 2013). The particle size of the material has a crucial role to play in improving the overall performance of the system. The overall increase in pore size improves the adsorption ability of the calcined eggshell for the removal of CO₂ from biogas. The calcined eggshell waste with a small diameter has a high specific surface area thus high removal efficiency and sorption capacity of the material **Figure 4.19(a, b)**.

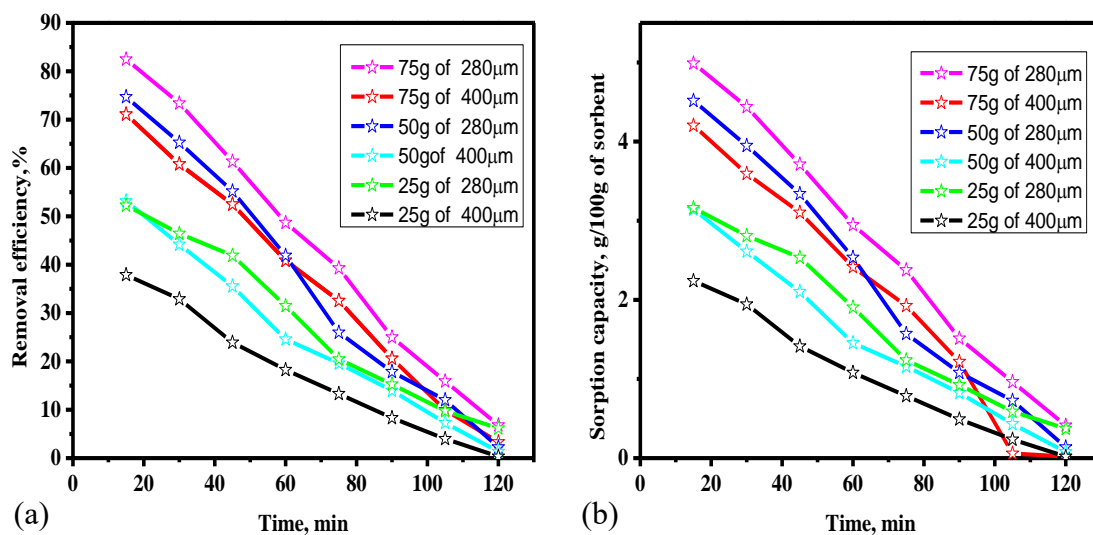


Figure 4.19: Effect of particle size on the performance of CaO derived from eggshells (a) Removal efficiency (b) Sorption capacity. Test condition: Flow rate =0.03m³/h, temperature 850°C and Co=30.8%.

Two different particle sizes were considered in this experiment 280 and 400 μm, and therefore particle size range 280μm shows high removal efficiency and adsorption ability of 82.5% and 5.0 g/100g of sorbent respectively as compared to the large particle size of 400μm due to the large surface area to volume ratio. Particle size with a small diameter has a higher adsorption ability than the larger particle size. This is probably attributed to the large surface area to volume ratio of the sorbent material. It was observed that the adsorption ability was high at the beginning of the adsorption process but decreased at the end of the process for each setup. It was mainly caused by the saturation of the sorbent as more carbon dioxide is adsorbed by the adsorbent, especially within the first 15 minutes of the experiment. Moreover, the effect of adsorbent particle size on the removal efficiency of carbon dioxide from biogas has a related tendency with other adsorbent materials used in literature.

4.14.2 Effect of mass of CaO derived from eggshells on the adsorption ability

The sorption capacity and removal efficiency of calcium oxide derived from eggshells were observed to increase as the mass of the sorbent increased while decreasing with the decrease in mass **Figure 4.20(a, b)** which was also observed in (Choo et al., 2013a).

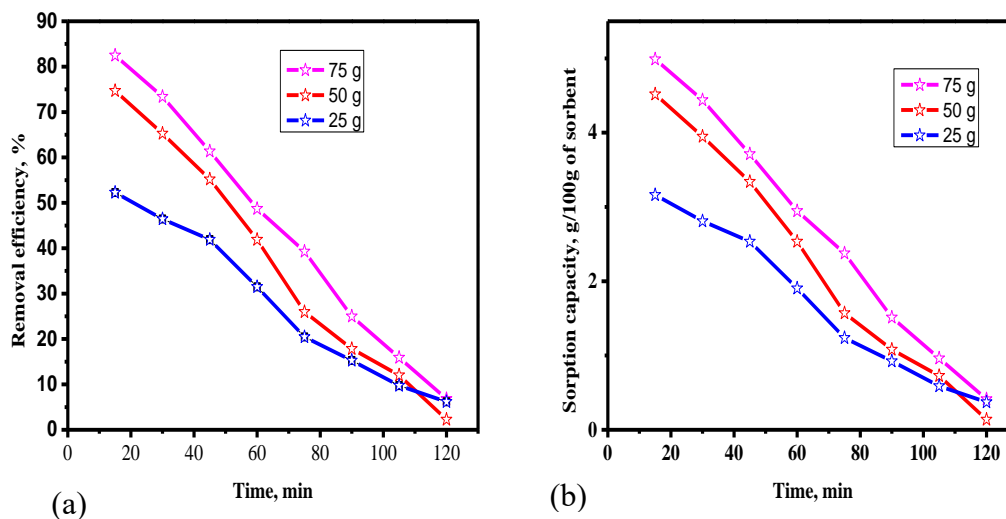


Figure 4.208: Effect of adsorbent mass on the performance of CaO derived from eggshells (a) Removal efficiency (b) Sorption capacity. Test condition: Flow rate = 0.03, particle size 280 μm , 850°C and $C_0 = 30.8\%$.

This is because of the increase in external interfacial area for biogas to contact the calcium oxide sorbent. The molecules of carbon dioxide had more chance to contact with the adsorption site for calcium oxide having a mass of 75 g as compared to a mass of 50 g and 25 g, and therefore highest removal efficiency and sorption capacity were observed when the mass of 75 g was used **Figure 4.20(a, b)**. The results can be influenced by more CaO obtained from calcined eggshell waste, which will enhance more contact area for CO_2 to be held within the adsorbent pores and thus higher sorption capacity and removal efficiency.

4.14.3 Effect of biogas flow rate on the adsorption process

Flow rate influences the adsorption ability of the sorbent. The ability of calcium oxide derived from eggshells to adsorb carbon dioxide from biogas decreases as the biogas

flow rate increases. A high flow rate ($0.04 \text{ m}^3/\text{h}$) decreases the contact time between the sorbent and the impurities which are in line with (Thuy & Chi, 2016). The current study revealed that the increase in biogas flow rate decreases the residence time of biogas in the sorbent which has a negative implication to the carbon dioxide adsorption. Literature divulges that a high biogas flow rate does not give more time for carbon dioxide impurities from biogas to contact with the sorbent material. Therefore, CO_2 passes the adsorbent without being adsorbed which leads to low removal efficiency and sorption capacity as compared to a low flow rate ($0.03 \text{ m}^3/\text{h}$) **Figure 4.21(a, b)**. Thus, the rate of methane (CH_4) recovering from biogas decreases with the rise in biogas flow rate.

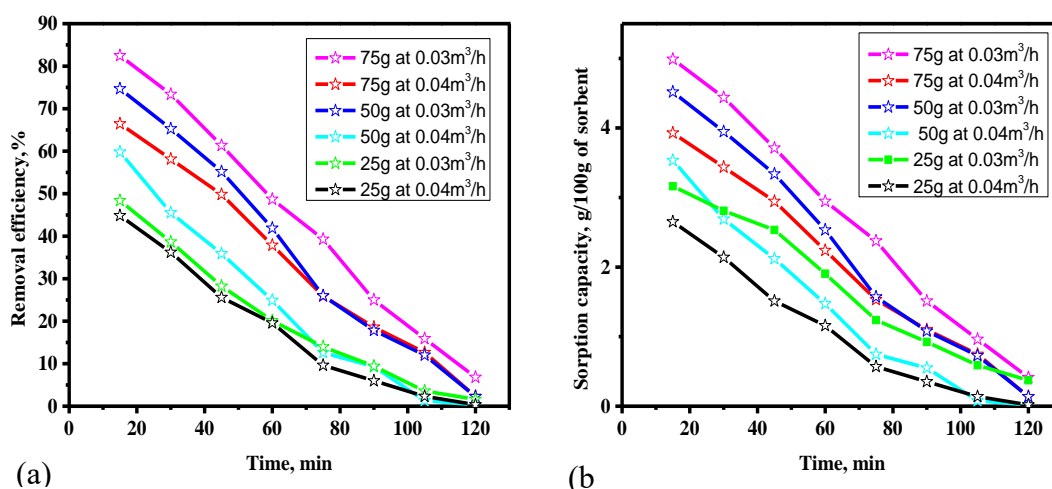


Figure 4.21: Effect of flow rate on the performance of CaO derived from eggshells (a) Removal efficiency (b) Sorption capacity. Test condition: Flow rate = 0.03 & $0.04 \text{ m}^3/\text{h}$, particle size $280 \text{ }\mu\text{m}$, 850°C and $\text{Co}=30.8\%$.

Based on the research data obtained on the purification experiment it was observed that when using the same mass of sorbent but differing in a biogas flow rate of 75 g at $0.04 \text{ m}^3/\text{h}$ and 75 g at $0.03 \text{ m}^3/\text{h}$ the removal efficiency obtained was 66% and 82% respectively, which is almost 24.24% increase. The sorption capacity of the sorbent was observed to be $3.9 \text{ g}/100 \text{ g}$ of the sorbent at 75 g at $0.04 \text{ m}^3/\text{h}$ while at $5.0 \text{ g}/100 \text{ g}$ of the sorbent at the mass of 75 g at $0.03 \text{ m}^3/\text{h}$, which is 28.21% increase **Figure 4.21(a, b)**.

(Mulu, M'Arimi, Ramkat, et al., 2021) reported a value of 0.23g/100g using modified natural clay for carbon dioxide absorption which is much lower than the value obtained in this study and may be attributed to the method used in the activation process. The results are consistent with those studied by (Sidabutar & Iriany, 2018) who explored the removal efficiency of the sorbent at different flow rates as 200, 400, and 600 ml/min for 30 minutes with a particle size of 140 mesh, 400 °C for 4 hours and found that 200 ml/min showed a removal efficiency of 92.5%. Therefore, the small flow rate allows the carbon dioxide to have a long period of contact with the sorbent which is in line with the present study.

This shows that carbon dioxide uptake capacity using CaO derived from eggshells can be similar to that of commercial adsorbents for CO₂ uptake from biogas and it's due to the presence of high content of CaO compound as observed in XRF analysis. The results and plots it was observed that a low biogas flow rate, ensures more carbon dioxide adsorption. The results show that CaO derived from eggshell waste is a promising adsorbent for carbon dioxide uptake from biogas and it is due to the presence of a high amount of calcium oxide (CaO) compound as observed in XRF analysis. It will not only solve the issue of clean energy technologies but also waste management.

4.14.4. Effect of calcination temperature on the adsorption process

The eggshell samples were calcined at various temperatures (800°C, 850°C, and 900°C). The calcination temperature influenced the sorption ability of the eggshell waste sorbent. The sample calcined at a temperature of 850°C performed better during the adsorption process in comparison to other temperatures, and therefore maximum adsorption capacity (5.0g/100 g of sorbent) and removal efficiency of (82.5%) was noted in Figure 4.22.

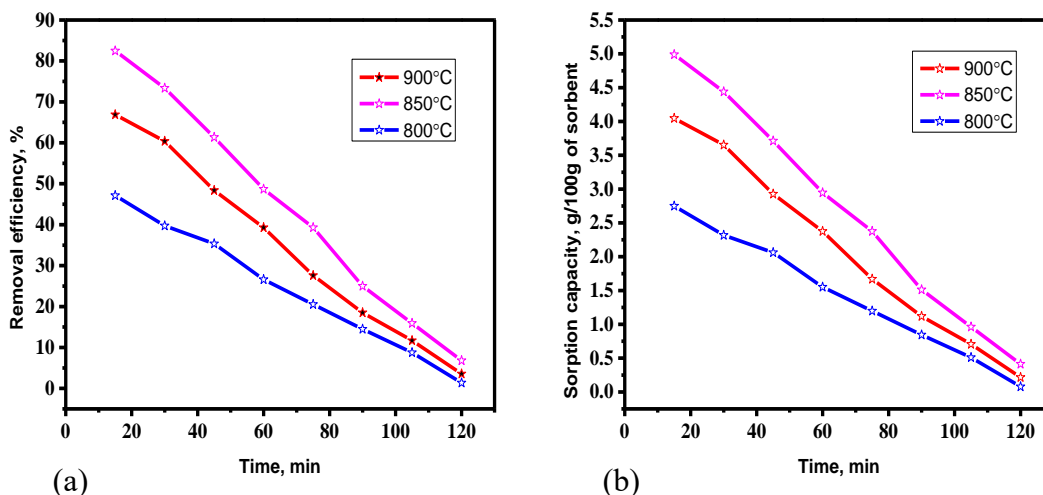


Figure 4.22: Effect of temperature on the achievement of CaO derived from eggshells (a) RE (b) SC. Condition for testing: Flow rate (FR) = 0.03, size 280 μ m, 850 $^{\circ}$ C, sorbent mass 75g, and Co=30.8%.

The removal efficiency and adsorption capacity of the eggshell sorbent are influenced by the exhibition of agglomeration that was supported by the surface area obtained from the Brunauer-Emmett-Teller technique. The surface area obtained under 850 $^{\circ}$ C (227.6 m²/g) has proven advantageous for carbon dioxide capture from biogas using eggshell waste which is in line with the literature (Bilton et al., 2012).

Fig 4.22(a, b) displays the effect of calcination temperature on the performance of calcium oxide derived from eggshell waste. Before the calcination of eggshell waste, the sorbent contains about 95% CaCO₃ as a major inorganic compound in it. The results obtained after the calcination proved that the main constituent from eggshell was CaO while the minor includes MgO, Al₂O₃, FeO, and C, previous studies reported the same (Park et al., 2007; Tsai et al., 2008). Based on the results obtained, it revealed that temperature 850 $^{\circ}$ C had noteworthy results due to significant attraction between the adsorbate and adsorbent. The chemisorption process facilitated the process and was noted that the performance increased with the increase in temperature to 850 $^{\circ}$ C. Temperature above 850 $^{\circ}$ C the performance starts to decline that may be caused by the

destruction of the adsorption site, therefore low performance of the sorbent calcined at 900°C.

4.15 A Comparison of Eggshell Waste with Other Sorbent used in Literature

Eggshell waste was compared with other sorbents from the literature on the uptake and removal efficiency of carbon dioxide from biogas as observed in **Table 4.23**. Soda ash demonstrated comparatively high performance and thus is a suitable material for biogas upgrading.

Table 4.23: A comparison of eggshell wastes with the previous adsorbent on CO₂ removal

Material	Flow rate (ml/min)	RE (%)	References
Natural zeolite	200	92.5	(Sidabutar & Iriany, 2018)
Modified natural clay	45	93.8%	(Mulu et al., 2021)
Calcined eggshell	500	82.5	This work

4.16 Sorbent Regeneration

4.16.1 Regeneration of soda ash sorbent for hydrogen sulfide removal

Saturated sorbent recovers its selectivity and activity after regeneration. The regeneration ability of the sorbent is a crucial issue to be considered before the selection of any absorbent for the biogas purification process. Among the factors that influenced the regenerative ability of the sorbent material, include the number of exposure days and the number of regenerative cycles. The regeneration of spent sorbent was done for 1, 5, and 7 days of exposure to the atmosphere, and a comparison between the removal efficiency and sorption ability of the original and the regenerated sorbent was made, it was observed that the original sorbent performs better than the regenerated one. The contact time was higher in the original sample, which took almost 150 minutes as compared to the regenerated sample **Figure 4.23(a, b)**.

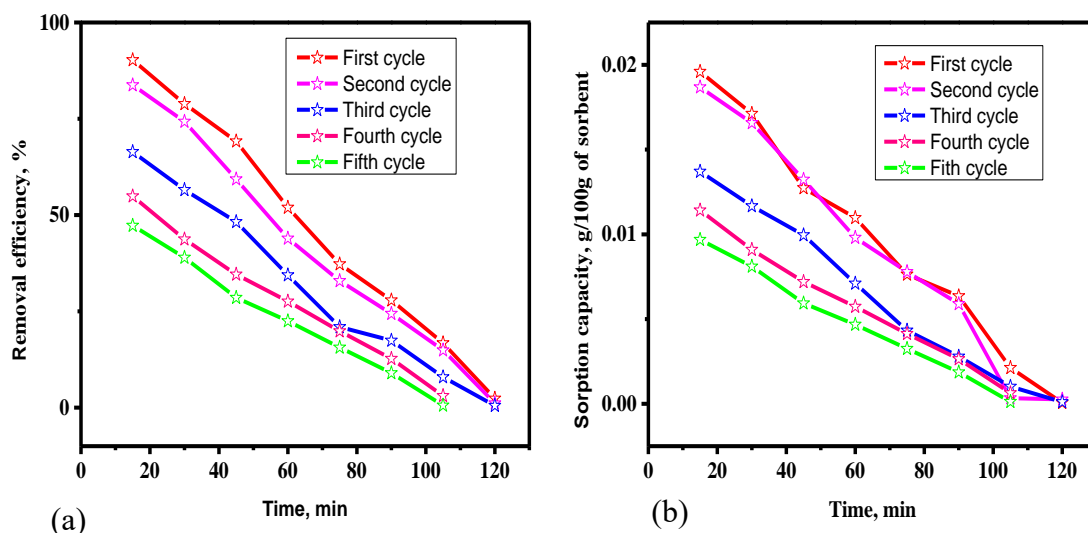


Figure 4.23: Removal efficiency and adsorption capacity of regenerated soda ash: Particle size 280 μm , Flow rate 0.03m³/h, exposure days 7.

The 7-day regenerated sorbent for the 1st-3rd cycles took 120 minutes to saturate while the 4th-5th cycle saturated around 105 min. The contact time between the sorbent and the contaminant for the last two cycles decreased as the soda ash pores lost their ability to adsorb H₂S, which leads to easy saturation, and therefore not all the mesoporous sites could be recovered. During the first 15min of the first cycle, the removal efficiency was about 90% with an SC of 0.016/100g while at 60 min was 52% with an SC of 0.01 g/100g of sorbent. Therefore, the trend within the 7-day exposure indicates that as you move from the first cycle to the fifth cycle, adsorption capacity decreases largely. Thus, crystallinity loss leads to the decrease of mesoporous, microporous, and hence total surface area.

During the 5-day exposure experiment, the first cycle took 120 minutes to reach saturation point while the 2nd-4th cycle took 105 minutes **Figure 4.24(a, b)**. During the first 15 minutes of the first cycle, the removal efficiency was 78% while at 60 minutes was 48%. There is a sudden decrease in the adsorption of the regenerated samples especially the day 1 and 5 exposure, which may be attributed to the inability to recover the entire adsorption site (Ania et al., 2005). The first 15 min for both cycles gives the

removal efficiency of more than 50%, which is a good indication that the sorbent can be regenerated and provides good results hence recommended for hydrogen sulfide removal from biogas.

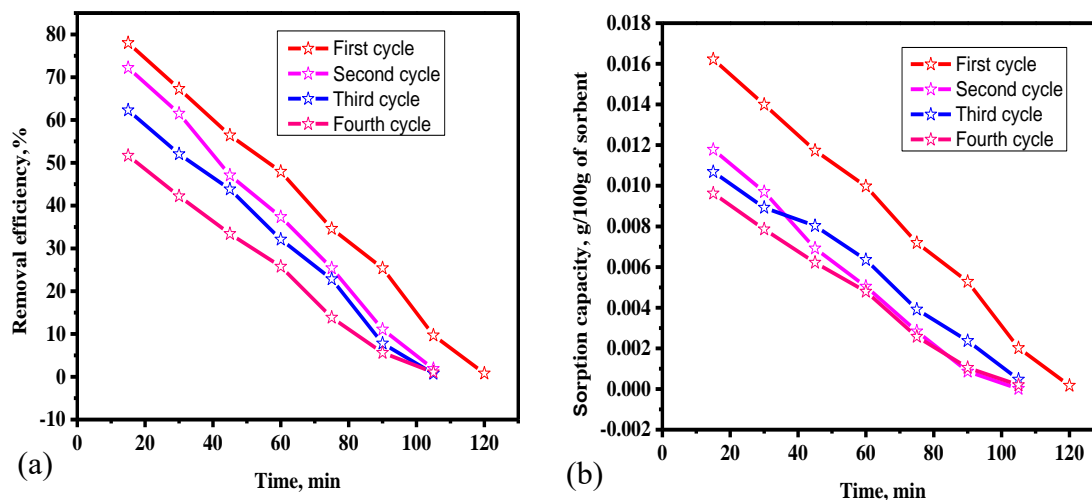


Figure 4.24: Removal efficiency and adsorption capacity of regenerated soda ash: Particle size 280 μm , Flow rate 0.03 m^3/h , exposure days 5.

The 1-day exposure showed less contact time between the absorbent and hydrogen sulfide and resulted in low adsorption ability, as we were not able to recover the entire adsorption site (Meng et al., 2019). The results demonstrated that a greater number of days of exposure of the spent sorbent to the atmosphere rather than a few days achieves high bio-methane. The removal efficiency and sorption capacity of the regenerated sorbent for 1 day are as in **Figure 4.25(a, b)**. During the absorption process, as the sorbent uptakes the hydrogen sulfide for a while, it loses its ability, as the removal efficiency of the original sample was 94% while regenerated for 7 days in the first cycle during the first 15min was 90%. The sorption capacity and removal efficiency of the regenerated samples for both day 1, 5, and 7 exposures were lower as compared to the original sample. Therefore, the sorbent spread in the atmosphere for 7 days showed a high performance as compared to 5 days and 1 day of exposure.

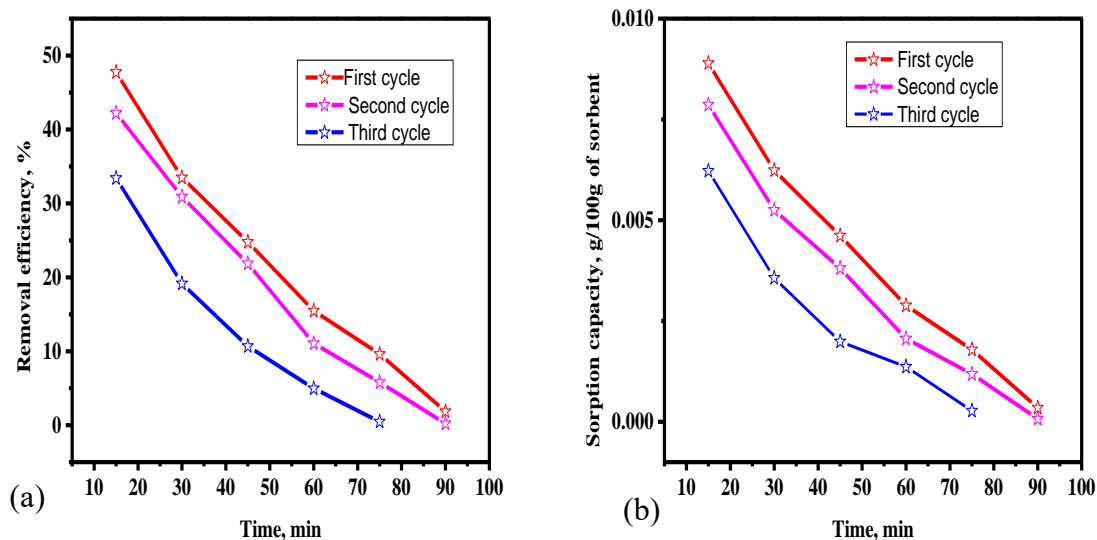


Figure 4.25: Removal efficiency and adsorption capacity of regenerated soda ash: Particle size 280 μm , Flow rate 0.03m³/h, exposure days 1.

4.16.2 Regeneration of eggshell waste sorbent for carbon dioxide removal

An eggshell was successfully regenerated several times and a comparison between the removal efficiency and sorption ability of the original and the regenerated sample was made. It was noticed that the original sorbent performed nearly similarly to the regenerated sample, especially for the first cycle and the contact time between the original and regenerated sample was more in the original sample than the regenerated sample **Figure 4.26(a, b)**.

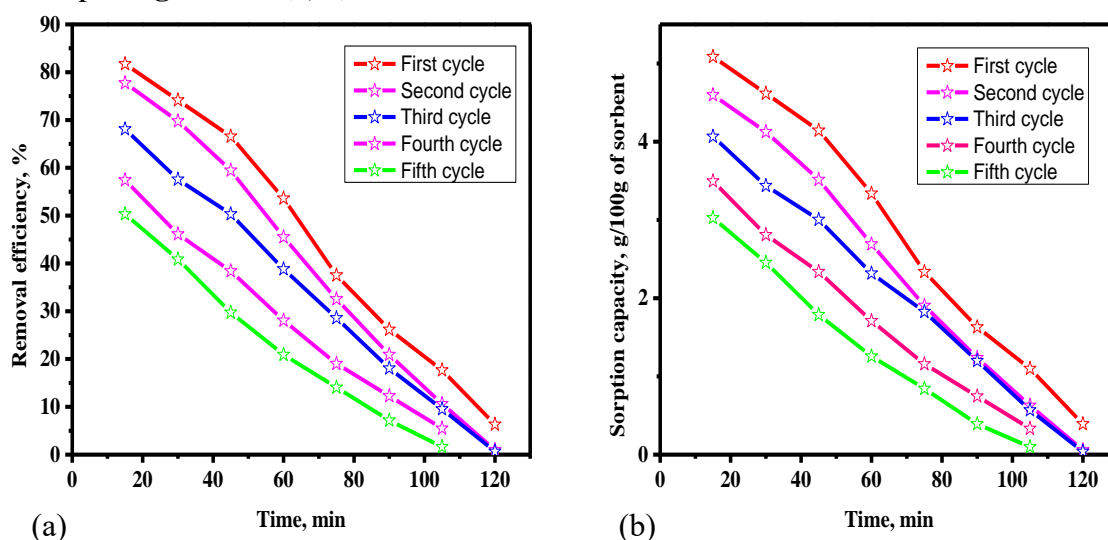


Figure 4.26: A comparison between removal efficiency of original and regenerated eggshells: Particle size 280 μm , Flow rate 0.03m³/h, temperature 850°C.

Moreover, an unexpected characteristic was noticed for a bed reactor with 75g of calcined eggshell as it not only recovered its activity but rather its sorption ability was improved remarkably especially for the first cycle. The removal efficiency and sorption capacity of the original and regenerated sorbent are as in **Figure 4.26 (a, b)** using the same mass of 75 g for the original and regenerated sorbent. The results show that as the sorbent adsorbs carbon dioxide it loses its ability, as the removal efficiency of the original sample was 82.5% while regenerated was 79.8%. The sorption capacity of the regenerated sample seems to be nearly the same as the original sample with a value of 4.97g/100g at the first 15 min while that of the original was 5.0g/100g as the maximum value for the first 15 min. The sorbents were successfully regenerated five times and the performance decreased with increasing generation cycle. There is not much difference found in carbon dioxide adsorption ability between the first and second cycles.

4.17 Equilibrium Adsorption Isotherms

The equilibrium isotherms were examined using Freundlich, Langmuir, and Jovanovich's isotherms models to investigate the interaction behavior between active mesoporous sites of soda and calcined eggshells as surfaces and the adsorbate particles. These isotherm models give the correlation between the equilibrium amounts of hydrogen sulfide and carbon dioxide adsorbed, and that are in the adsorbent phase.

4.17.1 The Langmuir isotherm

The Langmuir isotherm parameters summarized in **Table 4.24** were computed by using equations (16) and (17) to give the plots shown in **Figure 4.27(a, b)**. The intercept and slope of linearized Langmuir plots of C_e/q_e against C_e were used to obtain the value for K_L , R_L , q_m , and R^2 . The usefulness of adsorption was worked out by the separation factor value R_L **equation (38b-d)**. Scientifically if $R_L=1$ there is a linear adsorption, 0

$< RL < 1$ is a favorable adsorption, $RL > 1$ is considered as unfavorable adsorption while $RL = 0$ is an irreversible (Baskaralingam et al., 2006). Based on the values of R^2 obtained from hydrogen sulfide and carbon dioxide adsorption mechanism in **Table 4.24** it shows that Langmuir isotherms fit well on carbon dioxide removal rather than hydrogen sulfide removal with RL value of 0.00216 while its R^2 was 0.97384. This indicates that the adsorption of carbon dioxide from biogas is favorable via Langmuir isotherm.

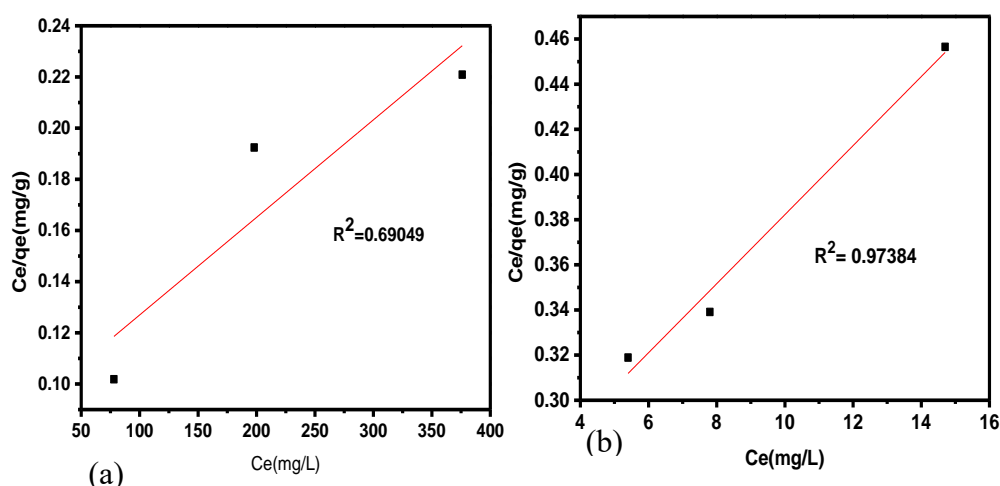


Figure 4.27: Langmuir isotherm plots for (a) H_2S and (b) CO_2 removal.

4.17.2 The Freundlich adsorption isotherm

Freundlich adsorption model described the uptake of hydrogen sulfide and carbon dioxide for multilayer adsorption processes occurring due to heterogeneous surfaces [5]. This model fails at high pressure, and therefore more studies are needed not only to determine the up taking of biogas impurities but also to determine the suitability of the model in the adsorption process. According to Freundlich, The surface of adsorbent material has heterogeneous energy levels indicating that can be homogenous and others can be heterogeneous. The homogenous parts behave as Langmuir. The linearized plots for $\log q_e$ Vs $\log C_e$ shown in **Figure 4.28(a, b)** were used to determine the value of parameters n and K_f in **Table 4.24** which provides awareness of heterogeneity and the

degree of adsorption. Using this model the process is favorable if $1 < n < 10$ or $0 < 1/n < 1$. On the other hand, when $n < 1$ indicates the sorption process is slow while $n = 1$ there is a linear adsorption process. The $1/n$ value obtained in this study was 0.4 for H_2S and 0.6 for CO_2 removal with the R^2 of 0.87 and 0.97 respectively. The obtained results indicate that the uptake of both hydrogen sulfide and carbon dioxide fits well to this isotherm as both had a correlation coefficient near 1 and the values for $1/n$ were in a range of $0 < 1/n < 1$ which is in line with literature [6]. It is now concluded that the Freundlich adsorption isotherm was able to predict the adsorption of the biogas impurities within the current study.

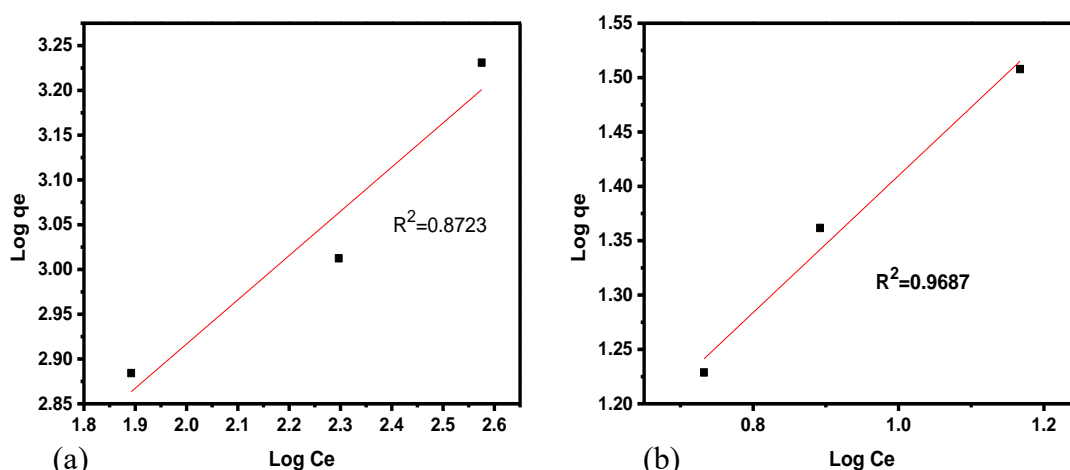


Figure 4.28: Freundlich adsorption isotherm plots for (a) H_2S and (b) CO_2 removal.

4.17.3 The Jovanovich adsorption isotherm

The Jovanovich adsorption isotherm was tested and the results are summarized in **Table 4.24**. Plots of $\ln q_e$ Vs C_e **Figure 4.29(a, b)** were applied to obtain the isotherm parameters using the experimental data. The experimental data from hydrogen sulfide removal fits well in the Jovanovich adsorption model since K_j was in a favorable range of $0 < K_j < 1$ with a correlation coefficient of 0.997 which is in line with Khan et al. (Khan et al., 2015). The fitness of the model was possible because there was a mechanical contact between the adsorbate and the adsorbent. The phenomenon is

possible due to the presence of sodium carbonate in the sorbents for the removal of hydrogen sulfide from biogas. The regression coefficients (R^2) of the Jovanovich model were very close to unity for H_2S 0.997 which was higher compared to the regression coefficients obtained from the Langmuir and Freundlich isotherms in hydrogen sulfide removal. It is apparent from our findings that the maximum adsorption capacities (q_m , (mg/g)) for the Jovanovich model (**Table 4.24**) are lower than those obtained from Langmuir isotherms regardless of a correlation coefficient. This can be a point for consideration for further research on the effect of biogas pressure on the adsorption process. Based on the results obtained from a plot of Jovanovich isotherm the adsorbent capacity is 6.42 mg/g for hydrogen sulfide removal and 2.54 mg/g for carbon dioxide removal (**Table 4.24**). The less q_{max} value indicates that the adsorbent has a weak adsorption capacity (Ragadhita & Nandiyanto, 2021).

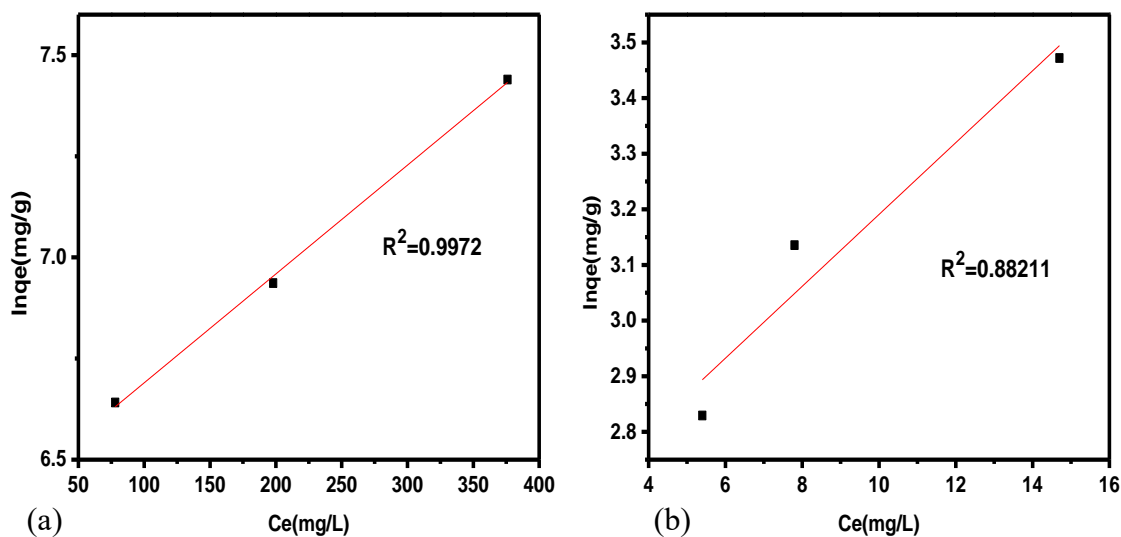


Figure 4.299: Jovanovich adsorption isotherm plots for (a) H_2S and (b) CO_2 removal.

Table 4.24: Summarized isotherm parameters for the adsorption of hydrogen sulfide and carbon dioxide from biogas during on-site experiments.

Model Parameters	Langmuir isotherm				Freundlich isotherm		
	q _{max} (mg/g)	K _L (L/mg)	R _L	R ²	k _f	n	R ²
H ₂ S	11.25	233.8	3.45×10 ⁻⁶	0.69	84.9	0.4	0.87
CO ₂	4.36	15	2.16×10 ⁻³	0.97	6.02	0.6	0.97

Model Parameters	Jovanovich isotherm		
	q _{max} (mg/g)	K _j (L/g)	R ²
H ₂ S	6.42	0.003	0.997
CO ₂	2.54	0.003	0.882

4.18 Adsorption Modeling

Three models were employed in this study Adams-Bohart, Thomas, and Yoon-Nelson models, which were developed to describe and possibly to predict the dynamic characteristics of the bed in column performance. Different parameters were derived from each model, which described the performance of the adsorption column. The fixed bed models are admired as their model equation can be linearized authorizing their unknown parameters to be evaluated using linear regression analysis. In this study, the three fixed models were used to fit the data obtained from on-site experiments, and they were compared using the coefficient of determination R² (Chu, 2020).

4.18.1 Adams–Bohart model for the removal of carbon dioxide from biogas

To prove the adsorption capacity of the adsorbent material the continuous column adsorption experiment was carried out at different initial concentrations of the sorbents with different bed heights 75 g (10 cm), 50 g (7 cm), and 25 g (4 cm). **Table 4.25** and **Figure 4.30(a-c)** show the column adsorption capacity and the breakthrough curves for calcined eggshells for the removal of carbon dioxide from biogas. The values of K_{AB} (coefficient of mass transfer) and N_o (maximum adsorption capacity) were determined from the intercept and slope of the Adams-Bohart plot at different bed heights, and concentrations as shown in **Table 4.25**. The values of k_{AB} were found to increase with

the increase in concentration and bed height along with the correlation coefficients (R^2). Generally, it indicates the system kinetics was influenced by external mass transfer (Ahmad & Hameed, 2010) while its value decreased with an increase in bed height **Table 4.25** for calcined eggshells sorbent which is in line with (Omitola et al., 2022). The Adams–Bohart model provides a comprehensive and simple approach to evaluating and conducting the sorption-column experiment. However, its validity is restricted to the various conditions used (Han et al., 2009; Ahmad & Hameed, 2010).

Adam-Bohart breakthrough curves for carbon dioxide removal from biogas at different bed heights.

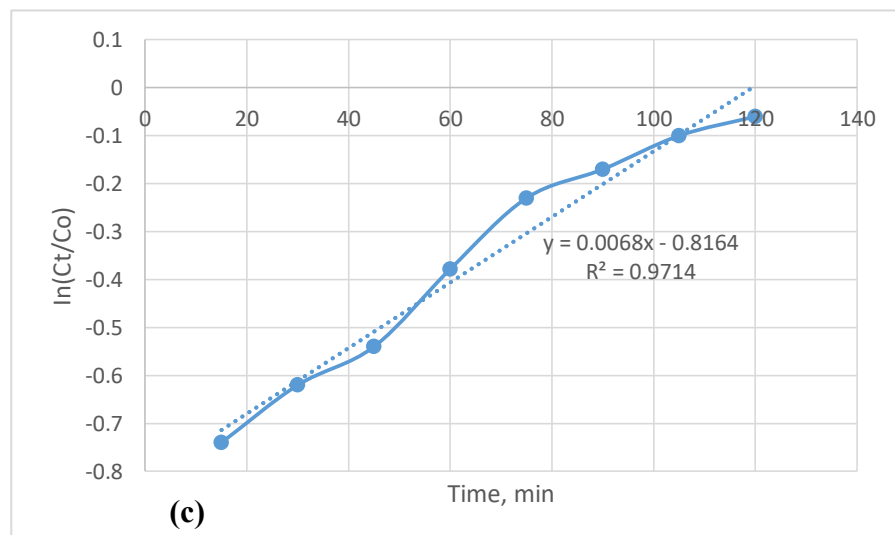
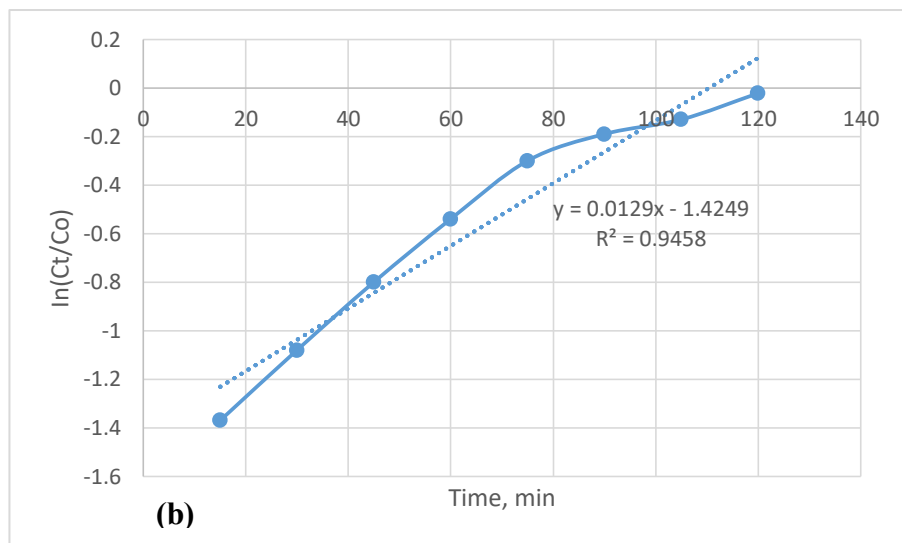
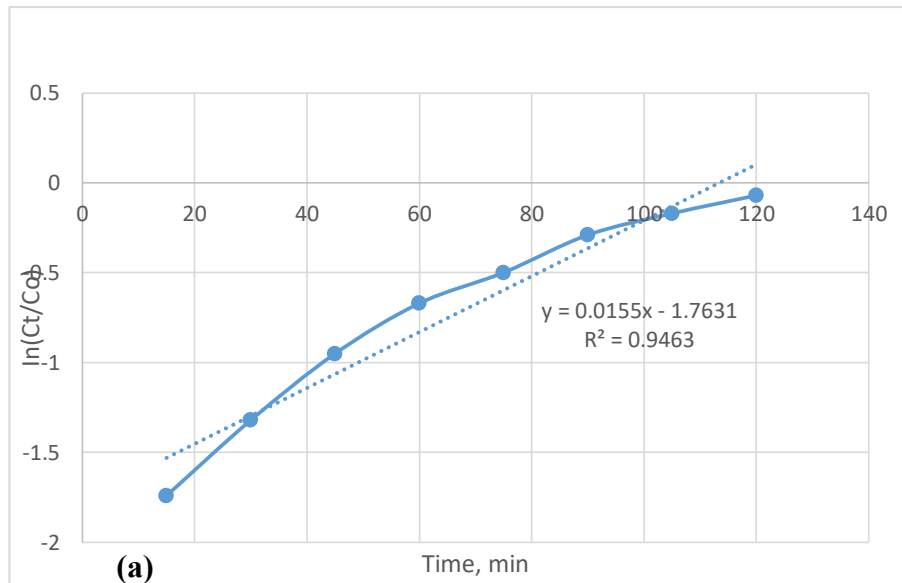


Figure 4.30: Breakthrough curve for carbon dioxide removal (a) 10, (b) 7, and, (c) 4cm

4.18.2 Adams–Bohart model for the removal of hydrogen sulfide from biogas

The adsorption capacity of the soda ash adsorbent material in the continuous column adsorption experiment was carried out at different bed heights in addition to inert material that was used as a pore-forming material to avoid biogas blockage. The bed height during the on-site experiment for hydrogen sulfide removal from biogas was 10, 7, and 4 cm. **Table 4.25** and **Figure 4.31(a-c)** show the column adsorption capacity and the breakthrough curves for soda ash collected from Lake Natron, Tanzania for the removal of hydrogen sulfide from biogas. The values of K_{AB} (coefficient of mass transfer) and N_0 (maximum adsorption capacity) were determined from the intercept and slope of the Adams-Bohart plot at different bed heights, and concentrations as shown in **Table 4.25**. The values of k_{AB} were found to increase with the increase in concentration and bed height along with the correlation coefficients (R^2). Substantially, this indicates that the system kinetics was influenced by external mass transfer (Ahmad & Hameed, 2010) while its value decreased with an increase in bed height (**Table 4.25**) for soda ash sorbent which is in line with (Omitola et al., 2022). The Adams–Bohart model provides a simple and comprehensive approach to assess and conducting the sorption-column experiment by fitting the on-site experimental data to the model. However, its validity is restricted to the various conditions used (Han et al., 2009) (Ahmad & Hameed, 2010).

Adam-Bohart breakthrough curves for carbon dioxide removal from biogas at different bed heights.

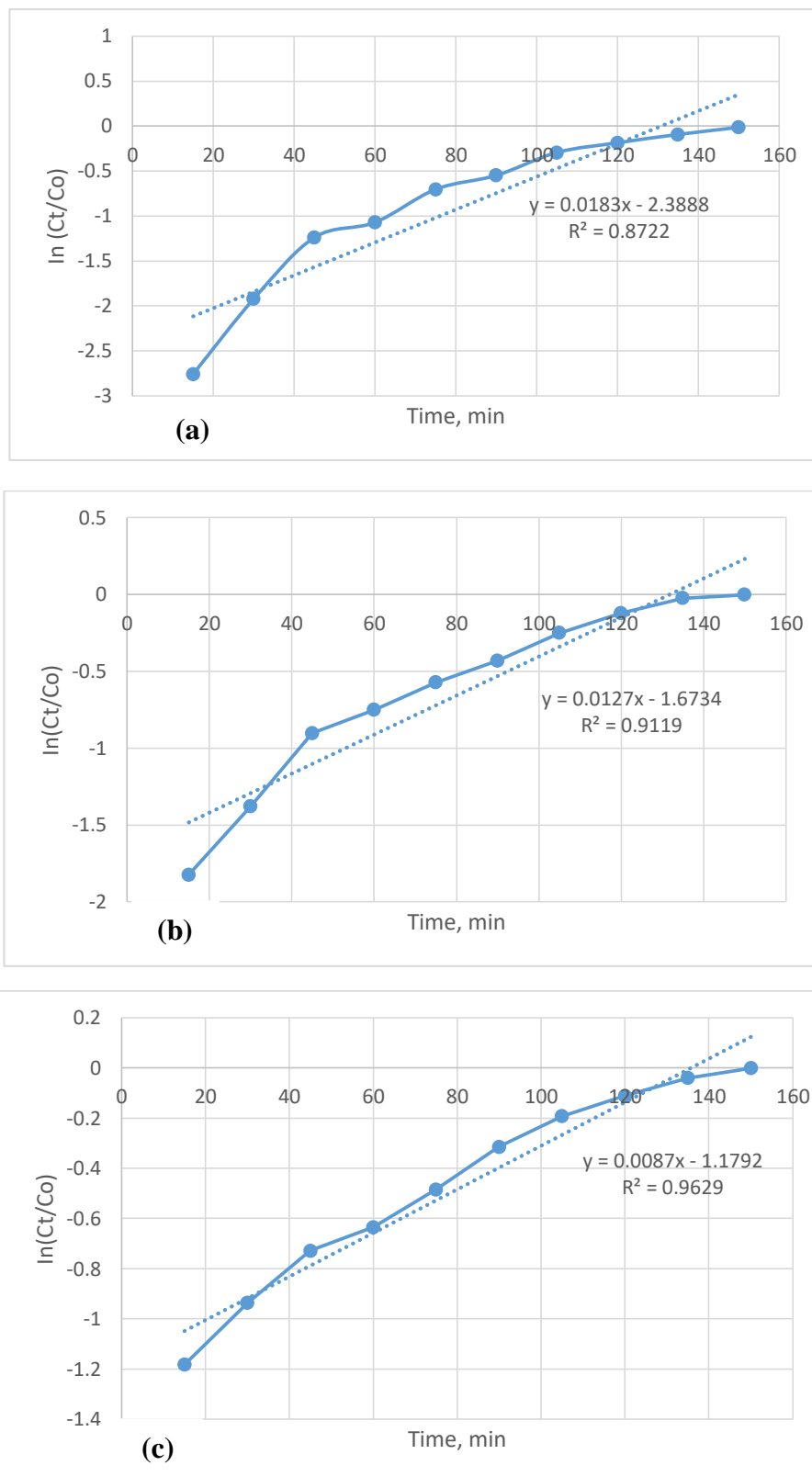


Figure 4.3110: Breakthrough curve for hydrogen sulfide from biogas (a) 10, (b) 7, and, (c) 4cms

Table 4.25: Parameters of the Adams–Bohart model under different conditions using linear regression analysis

Adams–Bohart Model - CO ₂ adsorption					Adams-Bohart model – H ₂ S adsorption				
Co (%)	Z (cm)	kAB*10-4 (L/mg min)	N _o (mg/L)	R ²	Co (ppm)	Z (cm)	kAB (L/mg min)	N _o (mg/L)	R ²
30.8	4	2.2	28.15	0.9463	1227	4	7.09*10 ⁻⁶	1248	0.9629
30.8	7	4.0	15.00	0.9458	1227	7	1.04*10 ⁻⁵	693	0.9119
30.8	10	5.0	10.56	0.9714	1227	10	1.49*10 ⁻⁵	480	0.8722

4.18.3 Thomas model for carbon dioxide removal from biogas

Thomas model was applied in fitting the on-site experiment data, coefficients and relative constants were obtained using linear regression analysis following **equation 4.26** and the results were presented in **Table 4.26**, which were obtained using **Figures 4.32(a-c)**. It was observed that the Thomas mode R² ranged from 0.9481- 0.989 for carbon dioxide removal while 0.7768-0.9559 for hydrogen sulfide removal. From **Table 4.26** it can be noticed that the k_{Th} values decreased with the increase in the bed depth while an increase in flow rate and concentration leads to an increase in both q_o and k_{TH}. Based on the experimental data, as bed height increased from 4, 7, and 10 the values of q_o and k_{TH} decreased, which is supported by literature (Omitola et al., 2022). It was accredited as the driving force for adsorption due to concentration difference. Thus, the higher bed depth, higher influent concentration, and lower flow rate would increase the adsorption of carbon dioxide from biogas on the fixed bed adsorption column. The experimental data for carbon dioxide removal were found to be well-fitted with the Thomas model with correlation coefficients in the range from 0.95-0.98.

Thomas model breakthrough curves for carbon dioxide removal from biogas at different bed heights.

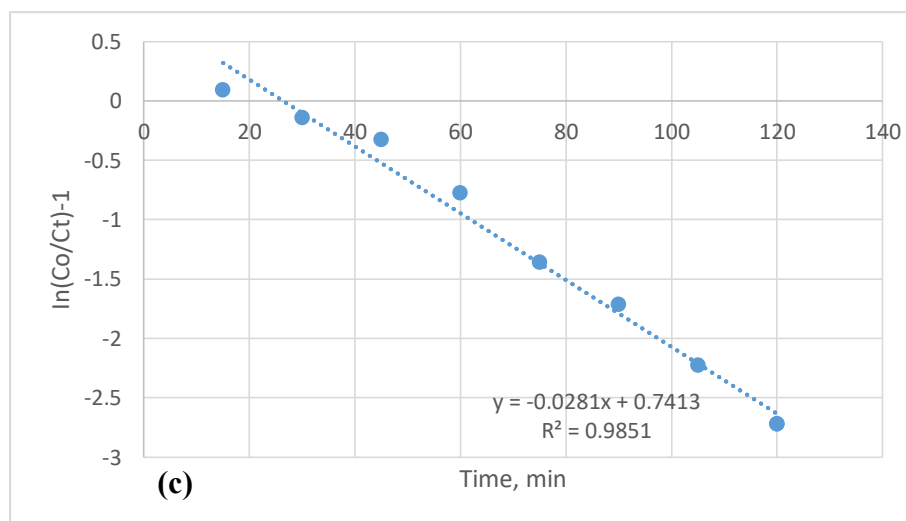
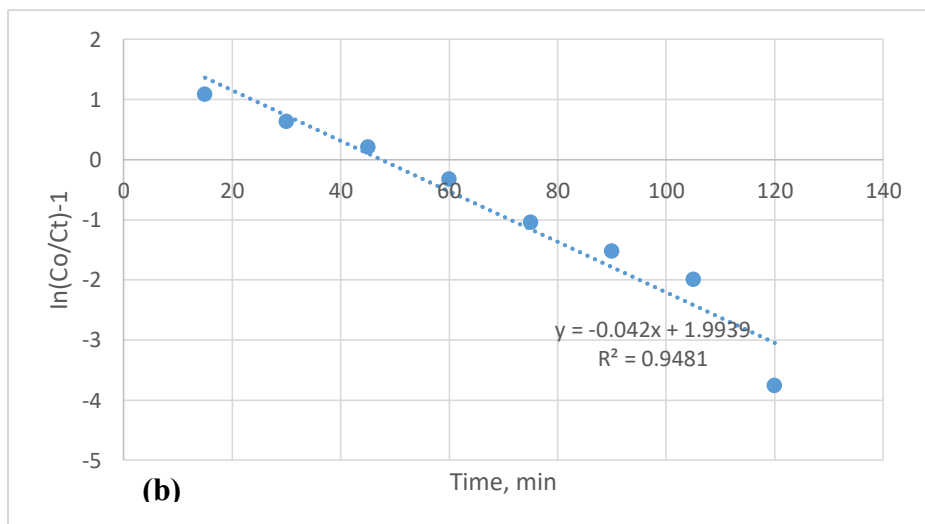
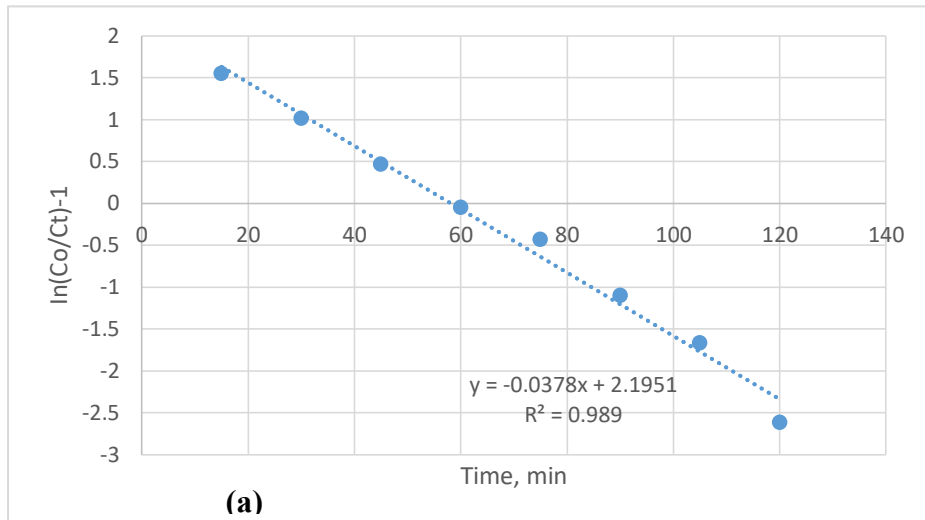


Figure 4.3211: Breakthrough curve for CO₂ from biogas (a) 10, (b) 7, and, (c) 4cm

4.18.4 Thomas model for hydrogen sulfide removal from biogas

The model was applied in fitting the on-site experiment data, coefficients and relative constants were obtained using linear regression analysis following **equation 22** and the results were presented in **Table 4.26**, which were obtained using **Figures 4.33(a-c)**. It was observed that the Thomas mode R^2 ranged from 0.7768-0.9559 for hydrogen sulfide removal. From **Table 4.26** it can be noticed that the k_{TH} values decreased with the increase in the bed depth while an increase in flow rate and concentration leads to an increase in both q_0 and k_{TH} . It was accredited as the driving force for adsorption due to concentration difference. Thus, the higher bed depth, higher influent concentration, and lower flow rate would increase the adsorption of carbon dioxide from biogas on the fixed bed adsorption column. The experimental data for hydrogen sulfide removal were not well-fitted with the Thomas model.

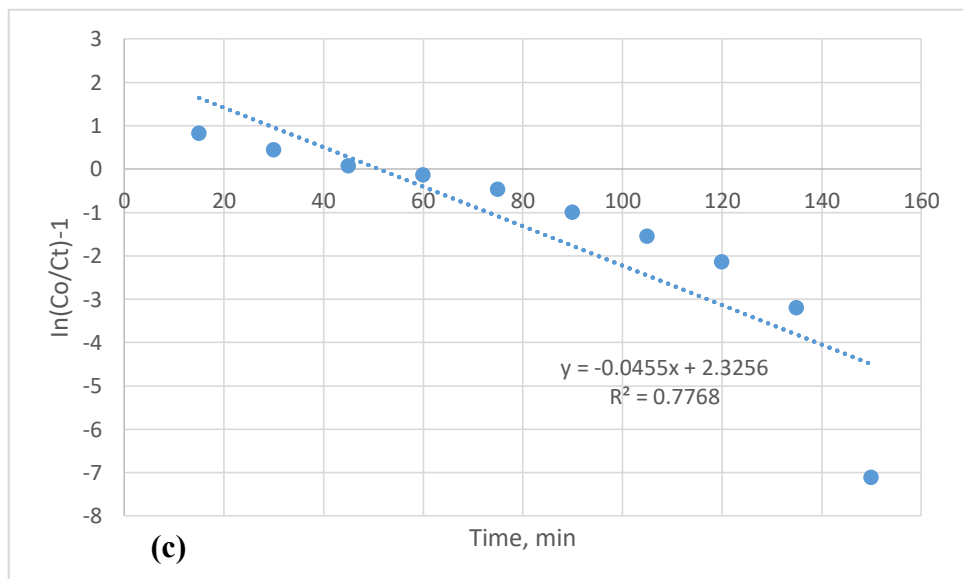
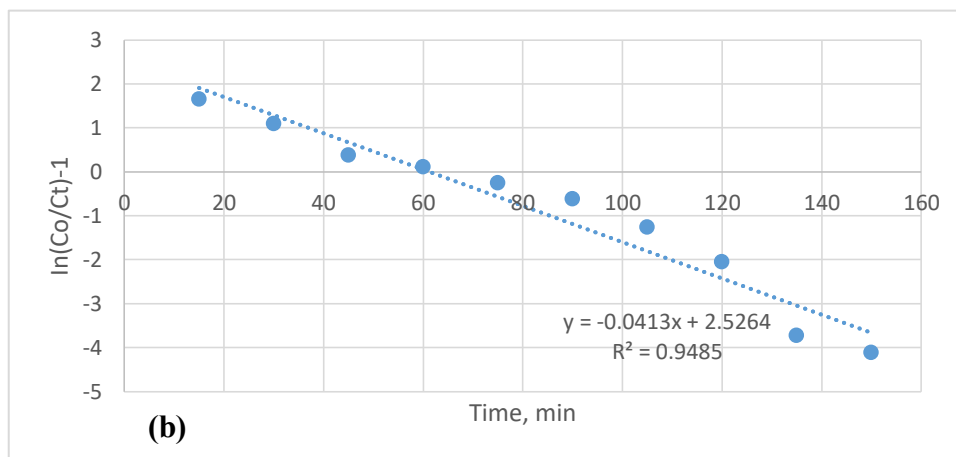
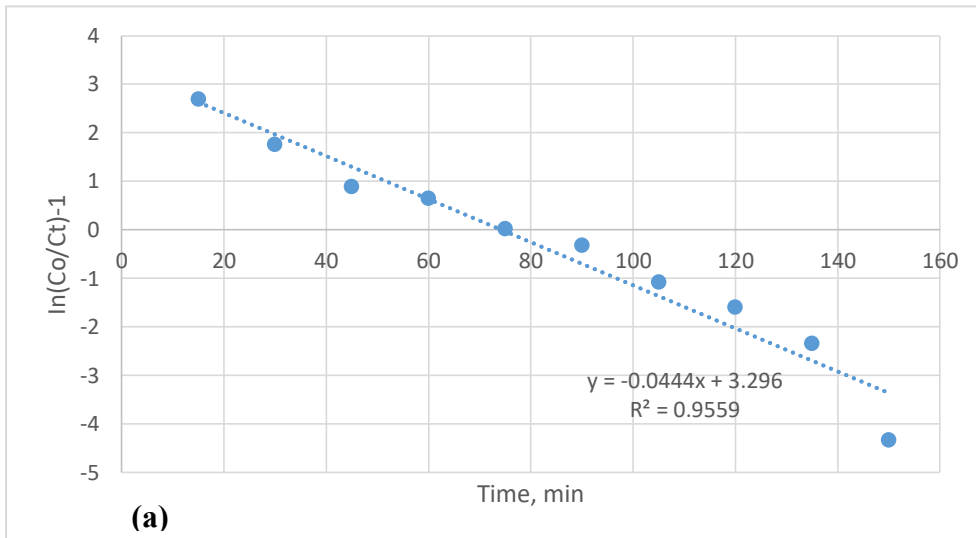


Figure 4.33: Breakthrough curve for hydrogen sulfide removal from biogas (a) 10, (b) 7, and, (c) 4cm

Table 4.269: Parameters of Thomas model under different conditions using linear regression analysis.

Thomas Model - CO ₂ adsorption					Thomas model – H ₂ S adsorption				
Co (%)	Z (cm)	k _{Th} * (mL/min mg)	q _o (mL/min mg)	R ²	Co (ppm)	Z (cm)	k _{Th} (mL/min mg)*10 ⁻⁵	q _o (mL/m in mg)	R ²
30.8	4	9.12*10 ⁻⁶	16257	0.9851	1227	4	3.62	1254	0.9559
30.8	7	1.36*10 ⁻⁶	14661	0.9481	1227	7	3.37	750	0.9485
30.8	10	1.23*10 ⁻⁶	11924	0.989	1227	10	3.17	607	0.7768

4.18.5 Yoon Nelson model for carbon dioxide removal from biogas

The k_{YN} (rate constant), and τ (time required for 50% carbon dioxide breakthrough) values were estimated from plot **equation 4.27** using the slope and intercept as shown in **Table 4.27**, obtained from **Figure 4.34 (a-c)**. The k_{YN} values increase with the decrease in bed height and flow rate while values of τ decrease with the increase in bed height and concentration. An increase in τ as the flow rate increases indicates that as the flow rate increases, the rate at which the adsorbent bed is consumed is slower which is desirable for the adsorption process. The value of τ represents the time at which 50% of the adsorbent in the column would reach a breakthrough point, as the value becomes higher, the better the performance of the bed column, similar information was reported by (Yagub et al., 2014; Omitola et al., 2022). Yoon- Nelson breakthrough curves for carbon dioxide removal from biogas at different bed heights.

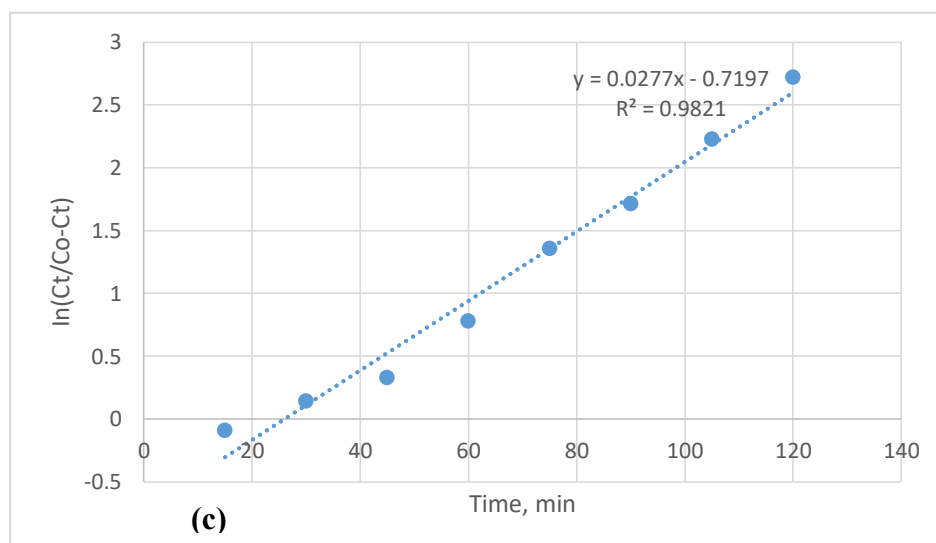
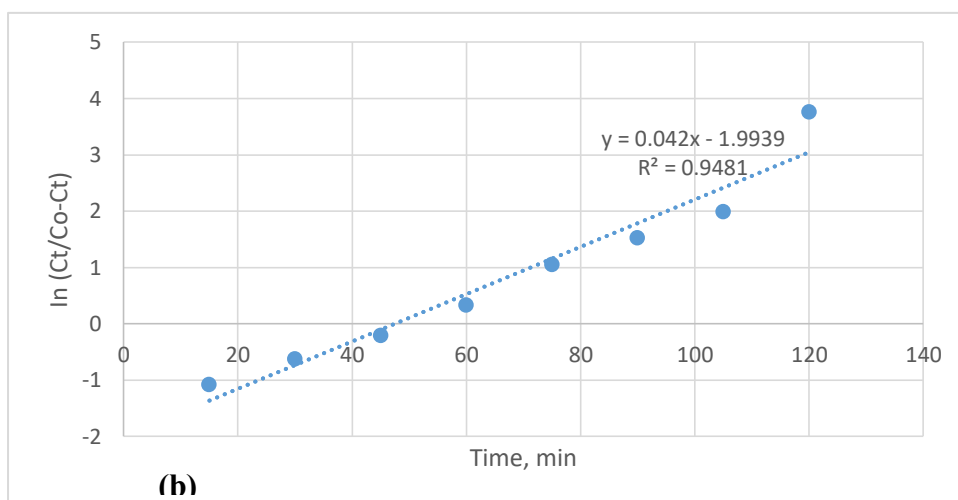
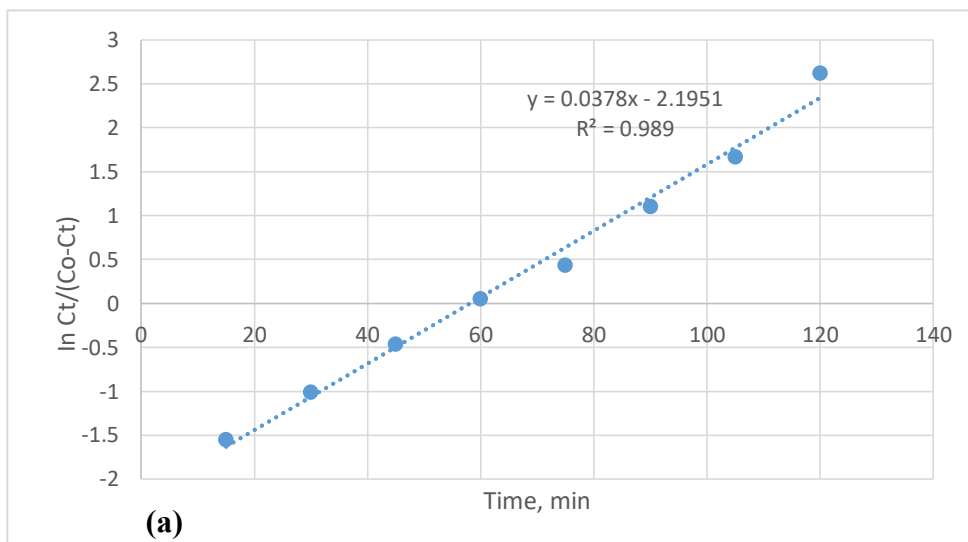


Figure 4.3412: Breakthrough curve for CO₂ removal from biogas (a) 10, (b) 7, and, (c) 4cm

4.18.6 Yoon Nelson model for hydrogen sulfide removal from biogas

The onsite experimental data obtained were carefully substituted in the Yoon Nelson model equation and theoretically predicted the values of t_{YN} and k_{YN} . The optimal on-site experimental conditions used in this study were 10 cm bed height, 0.03m³/h while the initial concentration was 1227 ppm. From the Table, it can be deduced that R² values 0.9536-0.9559 were higher than those obtained using the Adam-Bohart and Thomas model. The t_{YN} and k_{YN} seem to decrease with the increase in bed height. As the adsorbent bed height increases the time to reach saturation of the column increases which depends on the area of adsorption. A comparison of the breakthrough obtained at different conditions using the Yoon –Nelson model and the experimental breakthrough curves for the adsorption of hydrogen sulfide is shown in **Figure 4.35(a, b)**. The interpretation of **Table 4.27 and Figure 4.35(a, b)** together shows that the Yoon-Nelson model is successful in modeling the removal of hydrogen sulfide from biogas in the fixed column.

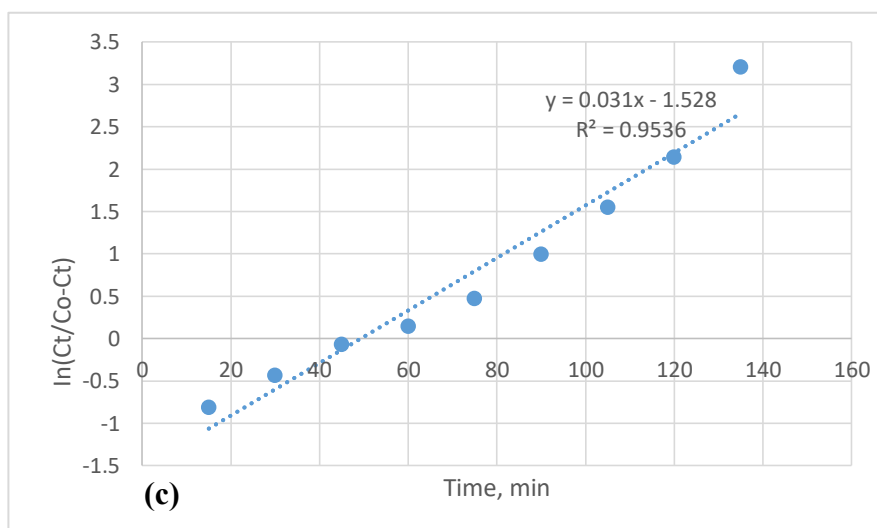
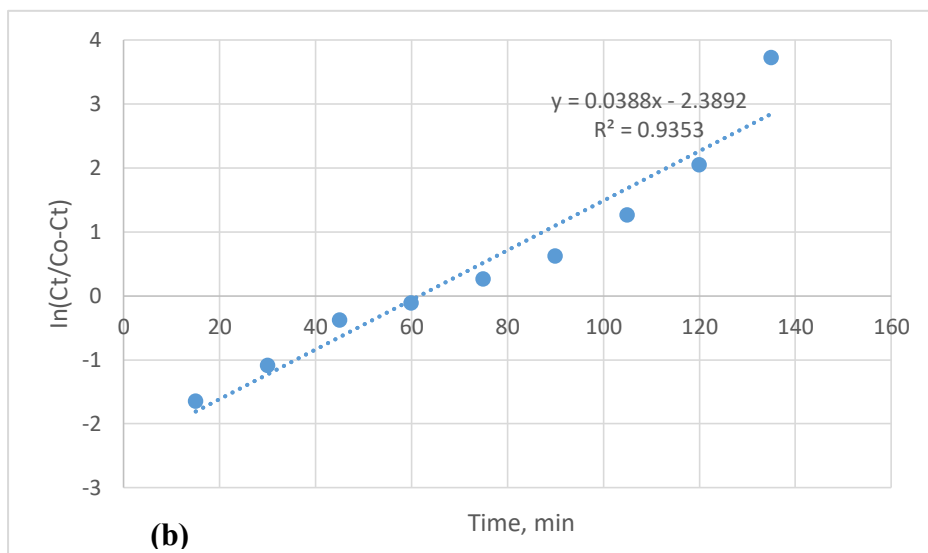
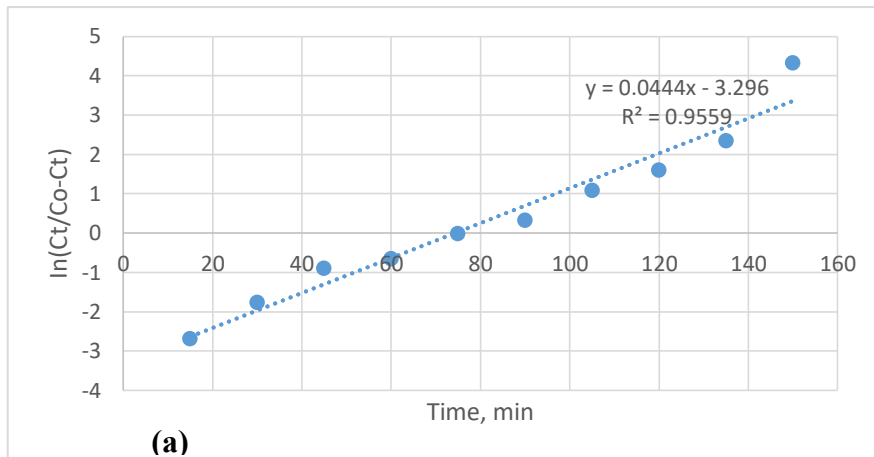


Figure 4.3513: Breakthrough curve for hydrogen sulfide removal from biogas (a) 10, (b) 7, and, (c) 4cm

Table 4.27: Yoon Nelson Model for the removal of CO₂ and H₂S from biogas

Yoon Nelson Model - CO ₂ adsorption					Yoon Nelson model – H ₂ S adsorption				
Co (%)	Z (cm)	k _{YN} *10 ⁻² (min ⁻¹)	Γ (min)	R ²	Co (ppm)	Z (cm)	k _{YN} *10 ⁻² (min ⁻¹)	Γ (min)	R ²
30.8	4	4.2	58	0.989	1227	4	4.4	74	0.9559
30.8	7	3.8	47	0.9481	1227	7	3.9	62	0.9353
30.8	10	2.8	25	0.9821	1227	10	3.1	50	0.9536

4.19 Effect of adsorbent mass on the removal of both carbon dioxide and hydrogen sulfide from biogas using the Adam-Bohart model.

The effects of adsorbent mass were studied using masses 75 and 25 g, it was found that in Adam –the Bohart model the increase in mass of both calcined eggshells and soda ash sorbent leads to the increase of K_{AB} while a decrease in N_o. In the Thomas-Bohart, model increase in mass leads to a decrease in both K_{TH} and q_o. In Yoon Nelson, an increase in the mass of both sorbents leads to the decrease of K_{YN} and τ, the parameters for both models were deduced from **Figure 4.36-4.41** and **Table 4.28-4.30**.

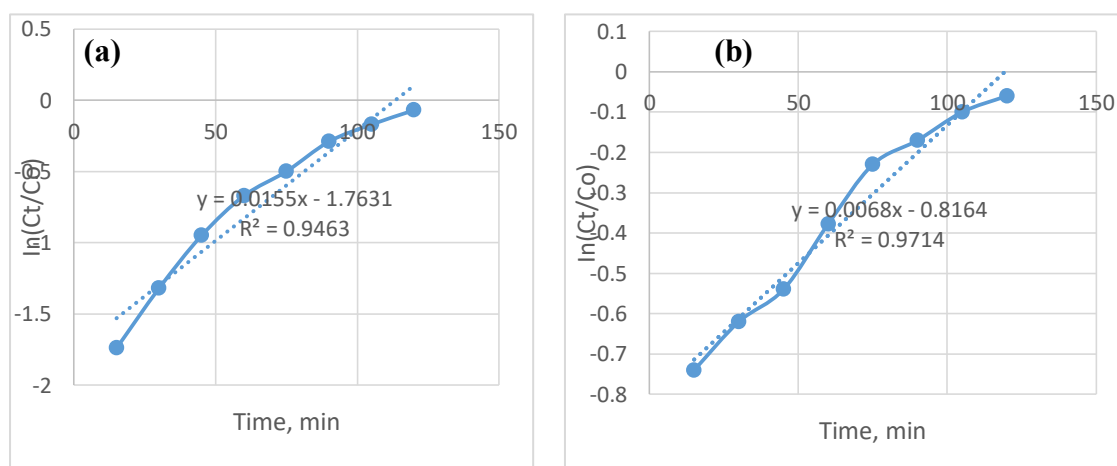


Figure 4.36: Effect of adsorbent mass on the removal of carbon dioxide from biogas a) 75 g (b) 25 g.

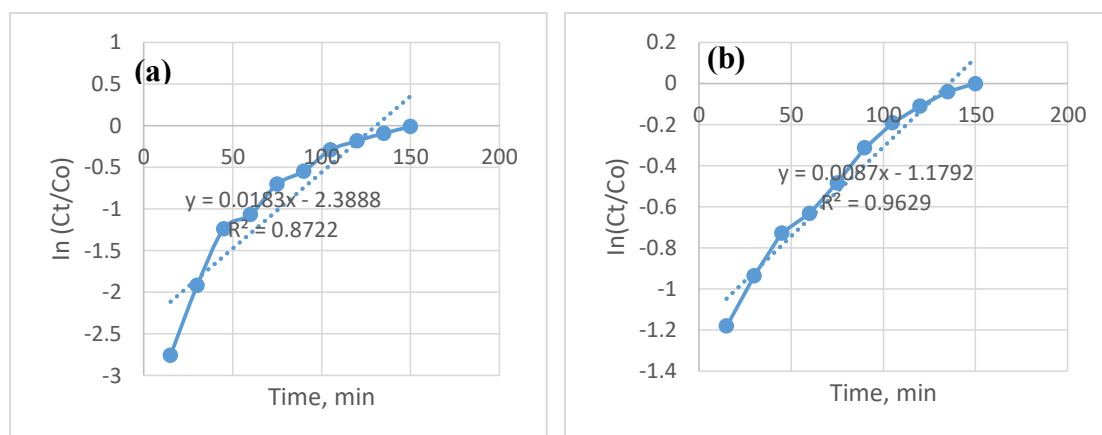


Figure 4.37: Effect of adsorbent mass on the removal of hydrogen sulfide from biogas.

Table 4.28: Effect of mass on the removal of CO₂ and H₂S from the biogas Adam-Bohart model

Adam-Bohart model - CO ₂ removal				Adam-Bohart model - H ₂ S removal		
Mass of sorbent (g)	$k_{AB} \cdot 10^{-4}$ (L/mg min)	N_0	R^2	$k_{AB} \cdot 10^{-5}$ (L/mg min)	N_0	R^2
25	2.2	10.56	0.9714	7.09	1248	0.9629
75	5.0	28.15	0.9463	1.49	480	0.8722

4.20 Effect of Adsorbent Mass on the Removal of Both Carbon Dioxide and Hydrogen Sulfide from Biogas using the Thomas Model

Table 4.29: Effect of mass on the removal of CO₂ and H₂S from biogas - Thomas model

Thomas model - CO ₂ removal				Thomas model - H ₂ S removal		
Mass of sorbent (g)	K_{TH} (L/mg min)	q_0	R^2	$k_{AB} \cdot 10^{-5}$ (L/mg min)	q_0	R^2
25	$9.12 \cdot 10^{-7}$	16257	0.9851	3.62	1254	0.9559
75	$1.23 \cdot 10^{-6}$	11924	0.989	3.17	607	0.7768

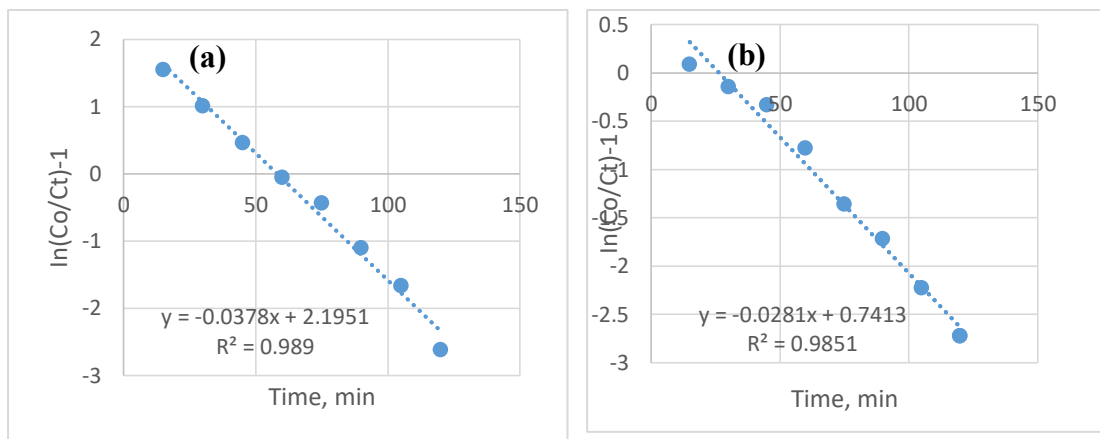


Figure 4.38: Effect of adsorbent mass on the removal of CO₂ from biogas.

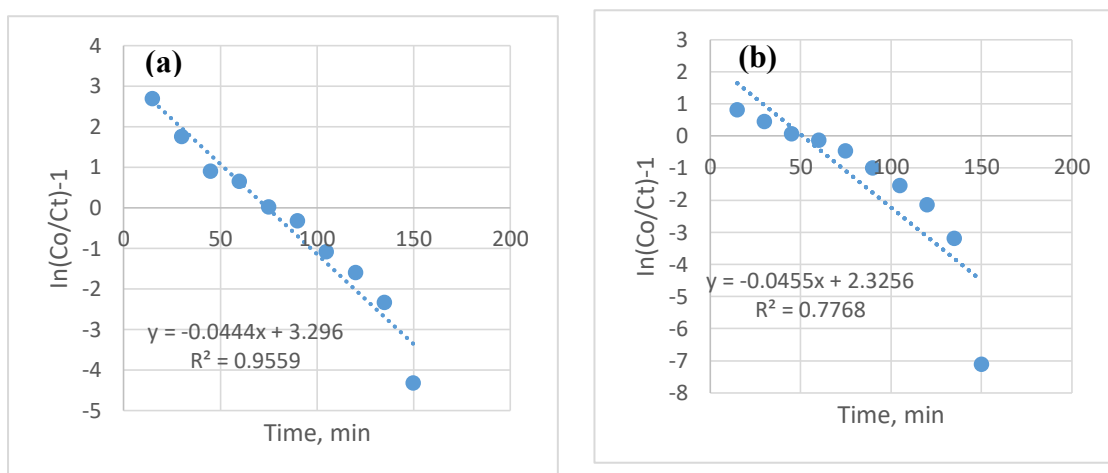


Figure 4.3914: Effect of adsorbent mass on the removal of H₂S from biogas

4.21 Effect of Adsorbent Mass on the Removal of Both Carbon Dioxide and Hydrogen Sulfide from Biogas using the Yoon -Nelson model

Table 4.30: Effect of adsorbent mass on the removal of CO₂ and H₂S from biogas Yoon model

Mass of sorbent (g)	Yoon Nelson model-CO ₂ removal			Yoon Nelson model		
	$k_{YN} * 10^{-2}(\text{min}^{-1})$	τ (min)	R^2	$k_{YN} * 10^{-2}(\text{min}^{-1})$	τ (min)	R^2
25	4.2	58	0.989	4.4	74	0.9559
75	2.8	25	0.9821	3.1	50	0.9536

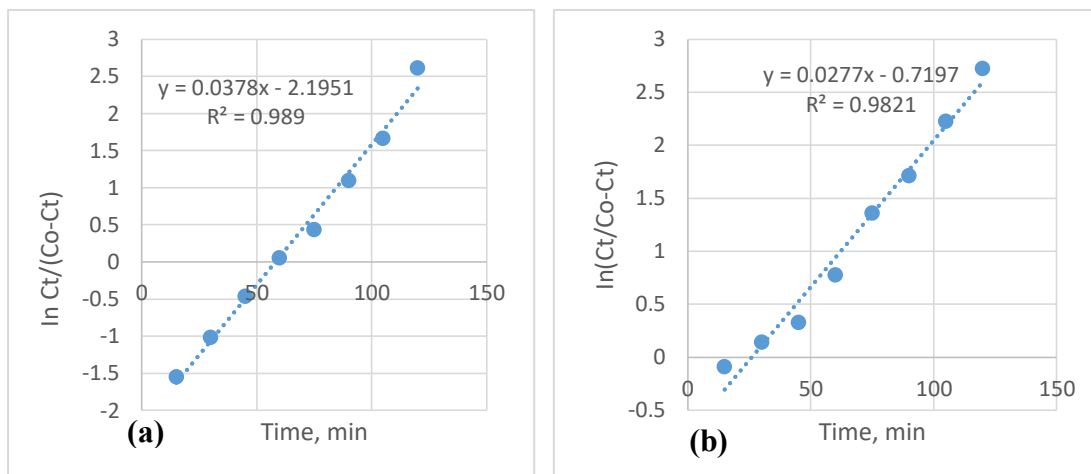


Figure 4.40: Effect of adsorbent mass on the removal of CO₂ from biogas.

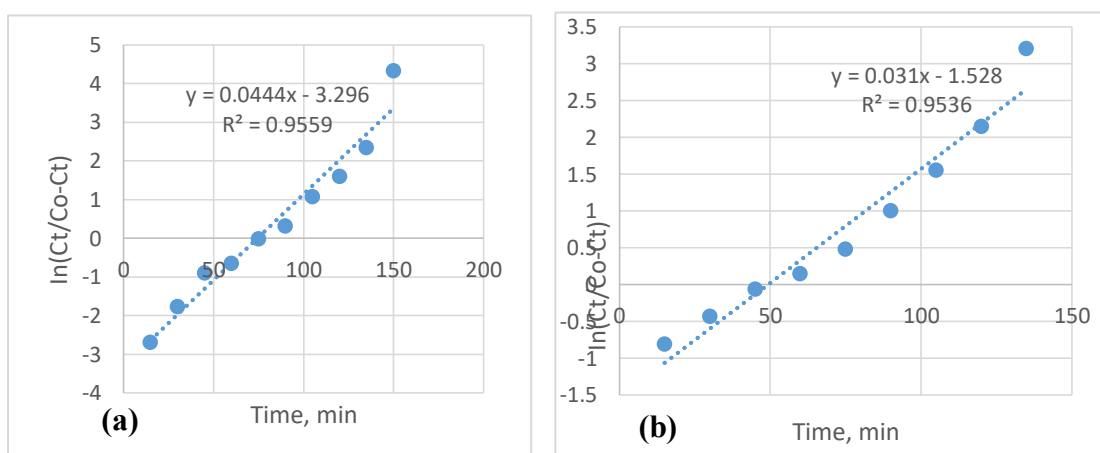


Figure 4.41: Effect of adsorbent mass on the removal of H₂S from biogas.

The three models were used to fit the on-site experimental data, and it was found that for the Adam-Bohart model, the values of k_{AB} were found to increase with an increase in concentration and flow rate while its value decreased with an increase in bed height for both calcined eggshells and soda ash sorbents. The N_o value decreases with the increase in the bed height. Thomas's model increase in bed height led to a decrease in both q_o and k_{TH} . The k_{YN} values increase with the decrease in bed height and flow rate while values of τ decrease with the increase in bed height and concentration while values of τ decrease with the increase in bed height and concentration. The experimental data for carbon dioxide removal were best fitted to the Thomas model while hydrogen

sulfide fitted best with the Yoon Nelson model. The significance of the study indicates that calcined eggshell waste and soda ash are efficient adsorbents for biogas purification.

4.22 Adsorption Kinetics

The kinetics of hydrogen sulfide and carbon dioxide removal from biogas using soda ash and calcined eggshell waste was investigated at room temperature. The experimental data were fitted into four kinetic models: pseudo-first order, pseudo-second order, intra-particle diffusion, and Elovich models. The equations for adsorption kinetics were presented in the literature and linear plots were done using originPro. The corresponding mathematical equation was transformed into linear forms, for which regressions with the experimental data were calculated. Finally, the correlation coefficient R^2 was used to evaluate the correlation of the on-site experiment data with the kinetics model.

4.22.1 Pseudo-first order for carbon dioxide and hydrogen sulfide removal from biogas

The Lagergren introduced the pseudo-first-order model (PFO) in the late 19th century, which is also known as pseudo-first-order kinetics. The model describes adsorption in a heterogeneous system and is the oldest adsorption model. The model is valid only when the adsorption kinetics are controlled by surface reaction and there is low adsorbate concentration or excess adsorbent mass (Vareda, 2023), and suggests occupancy of only one active surface site by the adsorbate which is hydrogen sulfide and carbon dioxide molecules from biogas. The first-order kinetics model is related to the adsorption process being only dependent on the amount of adsorbate, a diffusion-controlled process. Linear PFO model needs a preliminary knowledge of q_e to obtain/estimate the other necessary parameters using an equation. On the other hand, q_e

can be approximated by deducing the onsite experiment data to $t=\infty$. All these can be possible by making an assumption of an initial value of q_e and performing a linear fitting to look for k_1 and a new value of q_e . The values of q_e , k_1 as well and R obtained using pseudo-first-order kinetics for both hydrogen sulfide and carbon dioxide removal from biogas are as indicated in **Table 4.31-4.32**, and can be the model is expressed in linear form in **Figure 4.42**.

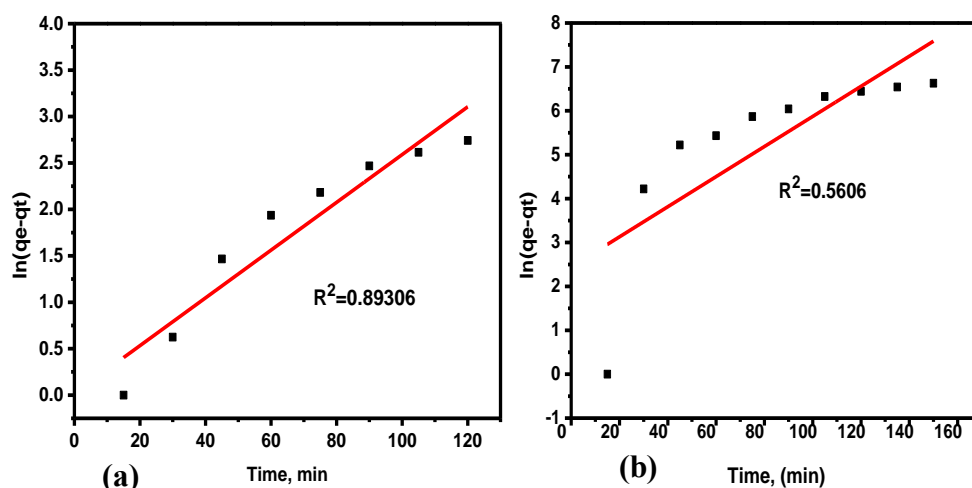


Figure 4.42: First-order adsorption kinetics model for biogas purification (a) CO_2 (b) H_2S removal

The model explained that there is a direct relationship between the surface of adsorption capacity and the adsorption rate. The fitness of the model can be obtained when the value of q_e (mg/g) calculated approaches the experimental q_e (mg/g). The calculated q_e for both carbon dioxide and hydrogen sulfide did not match with the experimental q_e , and thus the model did not fit the experimental data.

4.22.2 Pseudo-second order for carbon dioxide and hydrogen sulfide removal from biogas

The Pseudo second order model (PSO) was first applied in 1984 (Sari et al., 2019), it describes the linear relationship between the adsorption rate and surface of adsorption capacity. The model can be expressed in linear form and the necessary parameters can

be obtained as indicated in **Table 4.31-4.32**. The on-site experimental data were used to plot **Figure 4.43** and the parameters were deduced from the figure. The adsorption kinetics studies of hydrogen sulfide and carbon dioxide removal from biogas using pseudo-second order were made in batch adsorption systems under room temperature. It can be observed that the adsorption of carbon dioxide from biogas increased rapidly in the first 50 minutes **Figure 4.43**

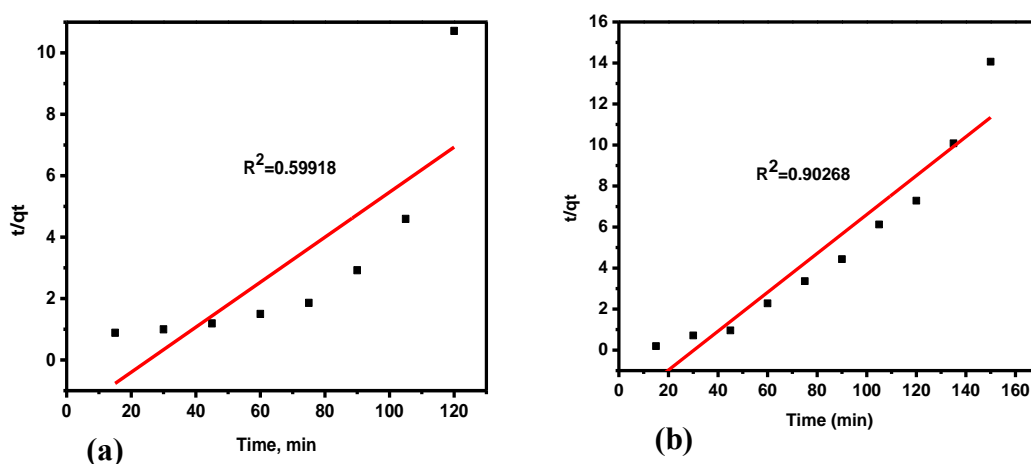


Figure 4.43: Pseudo sec-order adsorption kinetics model for biogas purification (a) CO_2 (b) H_2S removal.

The adsorption kinetic parameters, determined from the second-order kinetics equation, are presented in **Table 4.31-4.32** and are compared for each case with those that are obtained from the slopes and the intercepts of linear equations of the previous model. The values of the linear plots (R^2) for carbon dioxide uptake using the PSO model were 0.599 for carbon dioxide uptake and 0.903 for hydrogen sulfide uptake respectively. The obtained values of R^2 , k , and q_e show that the pseudo-second-order did not fit the experimental data. However, the pseudo-second-order can be more applicable for carbon dioxide removal at a time less than 50 min while for hydrogen sulfide at less than 30 minutes, which is in line with (Moussout et al., 2018). Generally, the calculated q_e and R^2 for both hydrogen sulfide and carbon dioxide proved that the model did not fit the experimental data.

4.22.3 Elovich model for carbon dioxide and hydrogen sulfide removal from biogas

Tompkins and Aharonic developed the Elovich adsorption model in 1970 (Sari et al., 2019). It relates the chemisorption essence of adsorption and the interaction of biogas molecules with the heterogeneous surface of the adsorbent. The summary of the parameters obtained in this model for carbon dioxide and hydrogen sulfide removal is in **Table 4.31-4.32** and **Figure 4.44**.

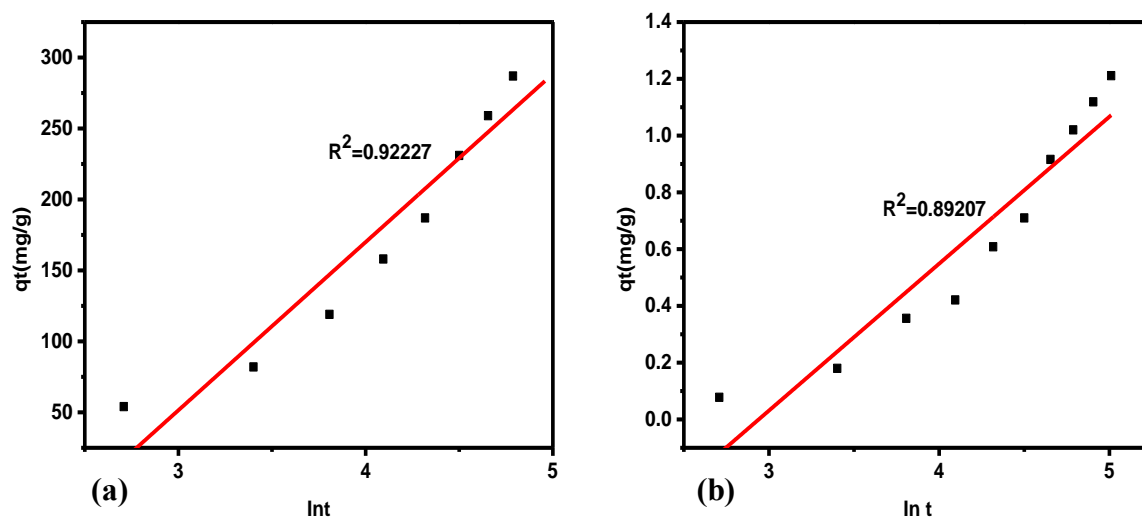


Figure 4.44: Elovich adsorption kinetics model for biogas purification (a) CO₂ removal (b) H₂S removal

The values of the linear regression plots for carbon dioxide uptake using the Elovich model were 0.92227 for carbon dioxide uptake and 0.89204 for hydrogen sulfide uptake respectively. The Elovich model makes the assumption the sites for adsorption rise exponentially with a multilayer adsorption process through the kinetics principles. The model assumes that the rate of adsorption decreases exponentially with the increase in the number of calcined eggshell waste and soda ash sorbent molecules following the mechanism of chemisorption. The kinetics of this model is described by α , β , and R^2 where the necessary parameters can be obtained from the linear plots of both carbon dioxide and hydrogen sulfide removal. It was noted that the obtained value of R^2 for

both carbon dioxide and hydrogen sulfide removal is closer to unity compared to PFO and PSO. This showed that there is a good chemisorption interaction between carbon dioxide and hydrogen sulfide with the sorbent material. The values of α and β were calculated from the plot of q_t vs $\ln t$ **Figure 4.44**. The corresponding parameter values are tabulated in **Table 4.31-4.32** which indicates that the Elovich kinetics model provides a moderate fit to the on-site adsorption data based on the R^2 values were less than 0.95.

It can be observed that there is minimal adsorption between the initial adsorption rate of carbon dioxide using the calcinated eggshells (0.008mg/g min) and hydrogen sulfide using soda ash from Lake Natron (1.9 mg/g min). On the other hand, the desorption rate (β) of carbon dioxide using calcined eggshell waste seems to be higher in CO_2 than hydrogen sulfide using soda ash. This suggested that the rate of desorption of carbon dioxide using calcined eggshells is higher while the rate of desorption of hydrogen sulfide using soda ash was slow which is in line with (Yakub et al., 2020).

4.22.4 Intra-particle diffusion model for carbon dioxide and hydrogen sulfide removal from biogas

Weber and Morris developed the intra-particle diffusion model in 1963, which is an older model. It describes the controlled mechanism of diffusion and it is expressed in linear form. The model was involved to investigate whether there is a mass transfer process involved in any adsorption process. The model equation demonstrates a linear regression relationship between adsorption capacity and the square root of time **Figure 4.45**.

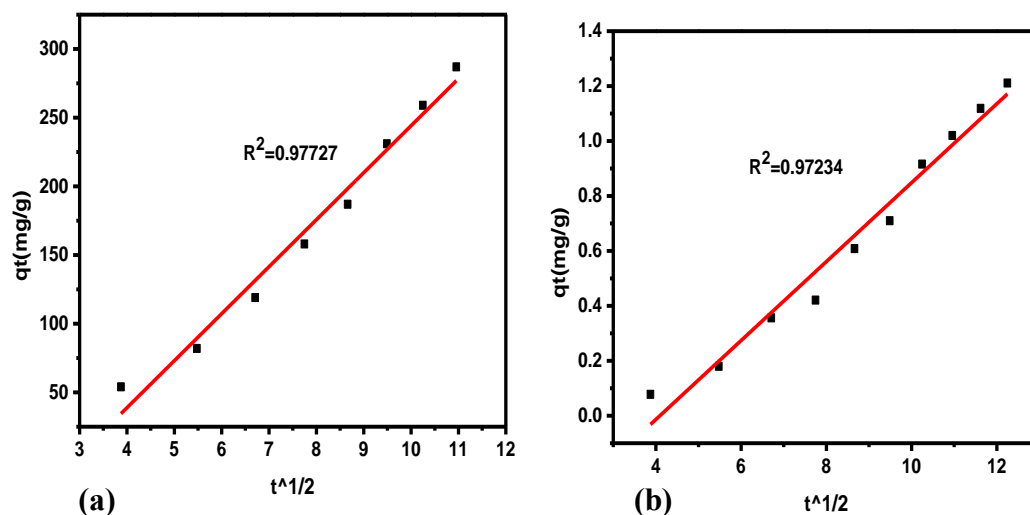


Figure 4.45: Intra-particle diffusion kinetics model for biogas purification (a) CO₂ removal (b) H₂S removal

Figure 4.45(a, b) shows a plot of qt vs $t^{1/2}$ for carbon dioxide and hydrogen sulfide adsorption in calcined eggshell waste and soda ash sorbents respectively. The plot therefore suggests that the adsorption process takes place via surface adsorption and intra-particle. The parameters k_{id} and c can be determined from the slope of the plot and intercept of qt versus $t^{1/2}$. If a linear regression fitting is observed in the plot of qt vs $t^{1/2}$ and passes through the origin point it is possible to confirm that there were a mass transfer process was taking place in the adsorption process (Vinh et al., 2017). The parameters obtained from the plots are tabulated in **Table 4.31-4.32**. The values of R^2 for both carbon dioxide and hydrogen sulfide removal from biogas are closer to unity compared to other models and thus suggested the mechanism for the diffusion of carbon dioxide and hydrogen sulfide in both calcined eggshell waste and soda ash sorbents. The values of k_{id} obtained and c (mg/g) depict the thickness of the boundary and therefore suggest that both sorbents can be applied for the chemisorption process. Thus, the model fits well the experimental data in comparison to other models.

Table 4.31: Adsorption kinetics model parameters for the four models on CO₂ removal

Pseudo-First order			Pseudo-second order			Elovich model		
k ₁	R ²	q _e (m g/g)	k ₂	q _e (mg/g)	R ²	α	β	R ²
2.14*10 ⁻⁴	0.893	1.01	3.2E-06	13.64	0.599	0.008	9.1	0.922

Intra-particle			
Parameters	k _{id}	c	R ²
Value	34	98	0.977

Table 4.3210: Adsorption kinetics model parameters for the four models on H₂S removal

Pseudo-First order			Pseudo-second order			Elovich model		
k ₁	R ²	q _e (m g/g)	k ₂	q _e (m g/g)	R ²	α	β	R ²
2.3*10 ⁻⁴	0.561	11.5	3.2E-06	10.5	0.903	1.9	0.03	0.892

Intra-particle			
Parameters	k _{id}	c	R ²
Value	0.14	0.59	0.972

Whereas k₁ is the pseudo-first-order rate constant, (min⁻¹), q_t is the adsorption capacity at a particular time, k₂ is a pseudo-second-order rate constant (g/mg.min), t is time, α is the initial adsorption rate (mg/g.min), K_{id} is intra-particle diffusion rate mg/g.min^{0.5}, C is constant and β is the desorption constant (mg/g).

Four different models were used to fit the on-site experiment data and was found that the kinetics of adsorption of carbon dioxide and hydrogen sulfide uptake from biogas was found to follow the intra-particle diffusion model compared to other models.

CHAPTER FIVE

CONCLUSIONS AND RECOMMENDATIONS

5.1 Conclusion

Feedstock characteristics have a major role in biogas yield. About 5 kitchen wastes and 9 municipal solid wastes were characterized for moisture content, total solid, volatile solid, and ash content before the anaerobic digestion process. The moisture contents of the feedstock used in the current study range from 66.73-93.43% while the total solid content of the substrates/feedstock used in the current study differs from 06-33.27%. Meanwhile, the volatile solid for all samples ranges from 76.59–96.36%, which matches the values found in the literature. The results indicated that cooked Irish potato showed a high volatile solid of $94.92 \pm 1.71\%$, cooked rice had a volatile solid of 83.00 ± 1.49 while municipal solid waste cabbage showed a high volatile solid of $96.36 \pm 1.73\%$. On the other hand, cooked rice was $31.00 \pm 0.56\%$ total solid while, cabbage showed a total solid of $08.00 \pm 0.14\%$. Meanwhile, the evaluation on moisture content indicated that cooked rice had a moisture content of $69.00 \pm 1.04\%$ while cabbage was $92.00 \pm 1.38\%$.

Ten of this feedstock was selected for mono-digestion in a batch reactor but depended on its availability throughout the year. Biogas production indicated that cabbage with a $96.36 \pm 1.73\%$ volatile solid gives a biogas yield of $800 \pm 8.8\text{mL}$ within 10 days, while cooked rice having $83.00 \pm 1.49\%$ volatile solid, generated a biogas yield of $2821 \pm 31.03\text{mL}$ within 28 days. Relying on the literature cabbage was expected to have the highest biogas generation rather than cooked rice, instead cooked rice showed the highest yield as compared to cabbage. This could be accompanied by the fact that the CN ratio for cabbage was low about 13.9, which is lower than the minimum recommended value of 20:1 and cooked rice waste was 30.9. Their pH values were 6.2

for cabbage which is lower than the recommended value of 6.5-7.4 and 7.2 for cooked rice. Based on these psychical chemical characterizations it was easy for cabbage to form volatile fatty acids as cabbage falls on vegetable waste. On the other hand, cooked rice waste had a biodegradability index of 0.54, cabbage leftovers were in the range of and 0.68. Therefore, it is easier for methanogenic bacteria to degrade rice waste and cabbage as their BI is in the required range for methanogens to degrade the organic matter through cabbage form volatile fatty acid easily thus its production ceased within a few days of production. The BI for ugali was below the range and thus not easy for bacteria to work on it for biogas generation. The physical-chemical analysis of cooked rice waste, ugali, and cabbage showed that there is a direct relationship between CN ratio, biodegradability index, electrical conductivity, nitrates, and total dissolved solids with biogas yield. Objective one of the current study recommends that cooked rice waste can be utilized alone as feedstock for biogas generation while other substrates studied require co-digestion to achieve the required CN ratios that will accelerate degradation and hence high methane yield. Among these substrates, biogas production from cooked rice lasted longer and this could be an important factor in commercial large-scale production of biogas.

The results obtained from the co-digestion of different food wastes and some selected municipal solid waste show that the co-digestion of TW and FrW produces more yield as compared to the rest of the reactors. On the effect of the mixing ratio, it was observed that a high yield ($2907 \pm 32 \text{ mL}$) was observed when the mixing ratio was 1:1 which is nearly twice the yield observed at 1:4 ($1532 \pm 17 \text{ mL}$). On the other hand, the effect of temperature was noted that high yield was observed at the temperature of 40°C ($4963 \pm 55 \text{ mL}$), nearly twice the yield obtained at 20°C while low yield at 20°C ($2907 \pm 32 \text{ mL}$). Furthermore, the effect of pH was observed that at pH of 6.5 and 7.3,

yields were 2808 ± 31 and 7810 ± 86 mL respectively, which is a 178.1% increase. The synergy effect of co-digestion of tuber waste and fruit waste shows a positive result of about 4.5, which was not obtained in any co-digestion before the current study. Therefore, production increases with the increase in temperature and pH to the optimal while decreasing with the increase in mixing ratio. Irish potato peels and banana peels produced the highest biogas yield and are recommended for use as co-digested feedstock.

Purification of H_2S from biogas using soda ash adsorbent at ambient conditions indicated that the chemical composition of soda ash obtained from XRF analysis shows the presence of sodium as a major element facilitates the whole process of hydrogen sulfide removal. On-site experiments were carried on to test the performance of soda ash where particle size $280 \mu\text{m}$, mass 75 g, and flow rate of $0.03 \text{m}^3/\text{h}$ showed a high RE of 94% and sorption capacity of 0.02g/100g of sorbent during the first 15 min. This was brought by the high surface area of the sorbent as observed in the BET multipoint summary; the pores are mesoporous as observed in the pore size distribution curve calculated from the BJH method. Zeiss Ultra Plus Field Emission Scanning Electron Microscopy was used to characterize surface morphology. The use of soda ash as a desulfurization sorbent ensures the health and safety of the end users.

On the other hand, spent soda ash was successfully regenerated with the regeneration done for 7 days of exposure showing a removal efficiency of 90% while the sorption capacity was 0.01g/100g of the sorbent. Meanwhile, safety disposal methods should be observed to ensure better health of the organisms. These findings indicate that soda ash from Lake Natron in Tanzania has great potential to be used as an adsorbent for the removal of hydrogen sulfide from biogas and can be regenerated and reused five times.

The decrease in removal efficiency and adsorption capacity can be due to the sintering effect.

Purification of carbon dioxide from biogas using calcium oxide derived from calcined eggshell adsorbent was successfully done at an ordinary temperature and well discussed. Experiments were performed on-site in testing the ability of CaO derived from eggshells; mass 75 g, size 280 μm , and flow rate of $0.03\text{m}^3/\text{h}$ exhibit high removal efficiency of 82.5% and up taking ability of 5.0g/100 g of sorbent. This was contributed by the large surface area of the sorbent due to calcination temperature at 850°C ; the presence of CaO from XRF analysis facilitates the sorption process of purification. The BET results indicate that the pores are mesoporous as perceived in the pore distribution plot obtained from the BJH method. Scanning Electron Microscopy was used to characterize the morphological structure of the calcined eggshell.

The sorbent was successfully regenerated five times with the highest RE of 79.8% and SC of 4.97g/100g of sorbent. The decrease in adsorption capacity and removal efficiency of calcined eggshell waste can be due to the sintering effect. The results indicate that CaO derived from chicken eggshells is a promising sorbent for the removal of carbon dioxide from biogas.

In the modeling part, the data obtained from on-site experiments for the removal of hydrogen sulfide and carbon dioxide from biogas was studied using three different isotherms such as Langmuir, Freundlich, and Jovanovich models. It was observed that the experimental data for both H_2S and CO_2 removal fitted well to the Freundlich for with a range of $0 < 1/n < 1$ whereas H_2S removal fits to Jovanovich model with a range of $0 < K_j < 1$. On the other hand, the three models were used to fit the on-site experimental data, and it was found that for the Adam-Bohart model, the values of k_{AB}

were found to increase with an increase in concentration and flow rate while its value decreased with an increase in bed height for both calcined eggshells and soda ash sorbents. The N_0 value decreases with the increase in the bed height. Thomas's model increase in bed height led to a decrease in both q_0 and k_{TH} . The k_{YN} values increase with the decrease in bed height and flow rate while values of τ decrease with the increase in bed height and concentration while values of τ decrease with the increase in bed height and concentration. The experimental data for carbon dioxide removal were best fitted to the Thomas model with the values R^2 0.94-0.99 while hydrogen sulfide fitted best with the Yoon Nelson model with R^2 0.93-0.98. On adsorption kinetics, four different models as Pseudo-First order, Pseudo-second order, Elovich model, and Intra-particle were used to fit the on-site experiment data, and was found that the kinetics of adsorption of carbon dioxide and hydrogen sulfide uptake from biogas was found to follow the intra-particle diffusion model compared to other models. Thus, the significance of the study indicates that calcined eggshell waste and soda ash are efficient and promising adsorbents for biogas purification.

5.2 The Environmental Benefits of Biogas Purification

Biogas is a profitable renewable energy source that also acts as a safe waste management solution that has a net positive impact on the environment in comparison to non-renewable energy resources (Werkneh, 2022). The presence of a high concentration of hydrogen sulfide and carbon dioxide in the biogas reduces the calorific value thus making the biogas not economically viable for transportation and compression during offsite utilization. The biogas impurities can be detrimental to the downstream utilization processes, where hydrogen sulfide is corrosive to the compressors, co-generators, pipelines, and storage facilities. However, the increasing emission of carbon dioxide into the atmosphere is the main contributor to environmental

crises. Impurities in biogas have several health implications as well as environmental consequences. Biogas production, upgrading, and desulfurization lead to the reduction of environmental pollution due to undesirable waste disposal techniques, as well as climate change, due to emissions from both biogas and poor waste disposal which is now an agenda worldwide.

5.3 Recommendations for Further Research Work

On the mono-digestion part, the study recommends that cooked rice waste can be utilized alone as feedstock for biogas generation while other substrates studied require co-digestion to achieve the required CN ratios that will accelerate degradation and hence high methane yield. The study recommends this because the yield obtained using cooked rice waste was higher and lasted longer in comparison to other feedstocks used in the current study.

On the co-digestion part, the study focused on the co-digestion of Irish potato peels and banana peels as representative of MSW and KW. More studies can be done using other components of MSW and KW under various process conditions. This will enable the researchers to make a comparison between the yield obtained with the current study and advise biogas users and policymakers accordingly.

In the purification part, the study recommends the use of small particle size in pellet form and low flow rate in comparison to this study for clear future perspectives. Sorbent materials from different sources may vary in composition and pH. Studies should be done to assess their performance and suitability and critically assess their performance in comparison to the current study

During the regeneration of soda ash, the study recommends that the sorbent be exposed to the atmosphere for more than 7 days and observe how it perform in term of RE and

Sc. On this, the researcher can be able to advise the biogas users according to the regeneration of the soda ash sorbent effectively.

In the modeling part, the study recommends that more isotherms, adsorption kinetics, and models should be applied to test the validity and feasibility of the models.

REFERENCES

- Abdalla, K. Z., & Hammam, G. (2014). Correlation between biochemical oxygen demand and chemical oxygen demand for various wastewater treatment plants in Egypt to obtain the biodegradability indices. *International Journal of Sciences: Basic and Applied Research*, 13(1), 42-48.
- Abu-Ghannam, N. (1998). Modelling textural changes during the hydration process of red beans. *Journal of Food Engineering*, 38(3), 341-352. [doi: 10.1016/S0260-8774\(98\)00127-7](https://doi.org/10.1016/S0260-8774(98)00127-7)
- Abudi, Z. N., Hu, Z., Abood, A. R., Liu, D., & Gao, A. (2020). Effects of alkali pretreatment, total solid content, substrate to inoculum ratio, and pH on biogas production from anaerobic digestion of mango leaves. *Waste and biomass valorization*, 11(3), 887-897. [doi:10.1007/s12649-018-0437-0](https://doi.org/10.1007/s12649-018-0437-0)
- Achak, M., Hafidi, A., Ouazzani, N., Sayadi, S., & Mandi, L. (2009). Low cost biosorbent “banana peel” for the removal of phenolic compounds from olive mill wastewater: Kinetic and equilibrium studies. *Journal of Hazardous Materials*, 166(1), 117-125. [doi: 10.1016/j.jhazmat.2008.11.036](https://doi.org/10.1016/j.jhazmat.2008.11.036)
- Ahmad, A., & Hameed, B., (2010). Fixed-bed adsorption of reactive azo dye onto granular activated carbon prepared from waste. *Journal of Hazardous Materials*, 175(1-3), 298-303. [doi:10.1016/j.jhazmat.2009.10.003](https://doi.org/10.1016/j.jhazmat.2009.10.003)
- Ahmad, W., Sethupathi, S., Munusamy, Y., & Kanthasamy, R. (2021). Valorization of raw and calcined chicken eggshell for sulfur dioxide and hydrogen sulfide removal at low temperature. *Catalysts*, 11(2), 295. [doi:10.3390/catal11020295](https://doi.org/10.3390/catal11020295)
- Ahmad, W., Sethupathi, S., Munusamy, Y., & Kanthasamy, R. (2021). Valorization of Raw and Calcined Eggshell for Sulfur Dioxide and Hydrogen Sulfide Removal at Low Temperature. 2021, 11, 295: s Note: MDPI stays neutral with regard to jurisdictional claims in
- Al-Ghouthi, M. A., & Da'ana, D. A. (2020). Guidelines for the use and interpretation of adsorption isotherm models: A review. *Journal of Hazardous Materials*, 393, 122383. [doi:10.1016/j.jhazmat.2020.122383](https://doi.org/10.1016/j.jhazmat.2020.122383)
- Al Jaber, F., Jabbar, S., & Jabbar, N. (2020). Modeling of adsorption isotherms of oil content through the electrocoagulation treatment of real oily wastewater. Paper presented at the AIP Conference Proceedings.
- Ali, S., Hua, B., Huang, J. J., Droste, R. L., Zhou, Q., Zhao, W., & Chen, L. (2019). Effect of different initial low pH conditions on biogas production, composition, and shift in the acetoclastic methanogenic population. *Bioresource technology*, 289, 121579. [doi:10.1016/j.biortech.2019.121579](https://doi.org/10.1016/j.biortech.2019.121579)
- Allothman, Z. A. (2012). A review: fundamental aspects of silicate mesoporous materials. *Materials*, 5(12), 2874-2902. [doi:10.3390/ma5122874](https://doi.org/10.3390/ma5122874)
- Amha, Y. M., Anwar, M. Z., Brower, A., Jacobsen, C. S., Stadler, L. B., Webster, T. M., & Smith, A. L., (2018). Inhibition of anaerobic digestion processes: applications of molecular tools. *Bioresource technology*, 247, 999-1014. [doi:10.1016/j.biortech.2017.08.210](https://doi.org/10.1016/j.biortech.2017.08.210)

- Andriamanohiarisoamanana, F. J., Shirai, T., Yamashiro, T., Yasui, S., Iwasaki, M., Ihara, I., . . . , & Umetsu, K. (2018). Valorizing waste iron powder in biogas production: Hydrogen sulfide control and process performances. *Journal of environmental management*, 208, 134-141. [doi:10.1016/j.jenvman.2017.12.012](https://doi.org/10.1016/j.jenvman.2017.12.012)
- Andriani, D., Rajani, A., Santosa, A., Saepudin, A., Wresta, A., & Atmaja, T. (2020). A review on biogas purification through hydrogen sulphide removal. Paper presented at the IOP Conference Series: Earth and Environmental Science.
- Andriani, D., Wresta, A., Atmaja, T. D., & Saepudin, A. (2014). A review on optimization production and upgrading biogas through CO₂ removal using various techniques. *Applied biochemistry and biotechnology*, 172(4), 1909-1928. [doi:10.1007/s12010-013-0652-x](https://doi.org/10.1007/s12010-013-0652-x)
- Angelidaki, I., Treu, L., Tsapekos, P., Luo, G., Campanaro, S., Wenzel, H., & Kougias, P. G. (2018). Biogas upgrading and utilization: Current status and perspectives. *Biotechnology advances*, 36(2), 452-466. [doi:10.1016/j.biotechadv.2018.01.011](https://doi.org/10.1016/j.biotechadv.2018.01.011)
- Ania, C., Parra, J., Menéndez, J., & Pis, J. (2005). Effect of microwave and conventional regeneration on the microporous and mesoporous network and on the adsorptive capacity of activated carbons. *Microporous and Mesoporous Materials*, 85(1-2), 7-15. [doi:10.1016/j.micromeso.2005.06.013](https://doi.org/10.1016/j.micromeso.2005.06.013)
- Aslanzadeh, S. (2014). *Pretreatment of cellulosic waste and high rate biogas production*. University of Borås, School of Engineering.
- Atelge, M. R., Senol, H., Djaafri, M., Hansu, T. A., Krisa, D., Atabani, A., . . . , & Kalloum, S. (2021). A Critical overview of the state-of-the-art methods for biogas purification and utilization processes. *Sustainability*, 13(20), 11515. [doi:10.3390/su132011515](https://doi.org/10.3390/su132011515)
- Athukorala, S., Bandara, R., & De Soyza, M. (2021). *Analysis of the Potential Use of the Anaerobic Digester to Treat the Food Waste at KDU Cadets' Mess*. Retrieved from <https://scholar.google.com/scholar?hl>
- Babæ, A., & Shayegan, J. (2011). Effect of organic loading rates (OLR) on production of methane from anaerobic digestion of vegetables waste. Paper presented at the World Renewable Energy Congress-Sweden; 8-13 May; 2011; Linköping; Sweden.
- Baena-Moreno, F. M., Gallego, L. M., Vega, F., & Navarrete, B. (2021). Cryogenic techniques: an innovative approach for biogas upgrading *Emerging Technologies and Biological Systems for Biogas Upgrading* (pp. 159-186): Elsevier.
- Baena-Moreno, F. M., Rodríguez-Galán, M., Vega, F., Vilches, L. F., & Navarrete, B. (2019). Recent advances in biogas purifying technologies. *International Journal of Green Energy*, 16(5), 401-412. [doi:10.1080/15435075.2019.1572610](https://doi.org/10.1080/15435075.2019.1572610)
- Baena-Moreno, F. M., Rodríguez-Galán, M., Vega, F., Vilches, L. F., Navarrete, B., & Zhang, Z., (2019). Biogas upgrading by cryogenic techniques. *Environmental Chemistry Letters*, 17(3), 1251-1261. [doi: 10.1007/s10311-019-00872-2](https://doi.org/10.1007/s10311-019-00872-2)

- Bajracharya, T. R., Dhungana, A., Thapaliya, N., & Hamal, G. (2009). Purification and compression of biogas: A research experience. *Journal of the Institute of Engineering*, 7(1), 90-98. [doi:10.3126/jie.v7i1.2066](https://doi.org/10.3126/jie.v7i1.2066)
- Baláž, M. (2018). Ball milling of eggshell waste as a green and sustainable approach: a review. *Advances in colloid and interface science*, 256, 256-275. [doi:10.1016/j.cis.2018.04.001](https://doi.org/10.1016/j.cis.2018.04.001)
- Barbusiński, K., & Kalembe, J. (2016). Use of biological methods for removal of H₂S from biogas in wastewater treatment plants—a review. *Architecture Civil Engineering Environment*, 9(1), 103-112.
- Barua, V. B., Rathore, V., & Kalamdhad, A. S. (2019). Anaerobic co-digestion of water hyacinth and banana peels with and without thermal pretreatment. *Renewable Energy*, 134, 103-112. [doi:10.1016/j.renene.2018.11.018](https://doi.org/10.1016/j.renene.2018.11.018)
- Baskaralingam, P., Pulikesi, M., Elango, D., Ramamurthi, V., & Sivanesan, S. (2006). Adsorption of acid dye onto organobentonite. *Journal of Hazardous Materials*, 128(2-3), 138-144. [doi:10.1016/j.jhazmat.2005.07.049](https://doi.org/10.1016/j.jhazmat.2005.07.049)
- Bharathi, K. S., & Ramesh, S. P. T. (2013). Fixed-bed column studies on biosorption of crystal violet from aqueous solution by *Citrullus lanatus* rind and *Cyperus rotundus*. *Applied Water Science*, 3, 673-687. [doi:10.1007/s13201-013-0103-4](https://doi.org/10.1007/s13201-013-0103-4)
- Bhatt, A. H., & Tao, L. (2020). Economic perspectives of biogas production via anaerobic digestion. *Bioengineering*, 7(3), 74. [doi:10.3390/bioengineering7030074](https://doi.org/10.3390/bioengineering7030074)
- Bilton, M., Brown, A., & Milne, S. (2012). Investigating the optimum conditions for the formation of calcium oxide, used for CO₂ sequestration, by thermal decomposition of calcium acetate. Paper presented at the Journal of Physics: Conference Series.
- Boe, K., & Angelidaki, I. (2012). Pilot-scale application of an online VFA sensor for monitoring and control of a manure digester. *Water Science and Technology*, 66(11), 2496-2503. [doi:10.2166/wst.2012.498](https://doi.org/10.2166/wst.2012.498)
- Bradley, R. L. (2010). Moisture and total solids analysis *Food analysis* (pp. 85-104): Springer.
- Brown, D., & Li, Y. (2013). Solid state anaerobic co-digestion of yard waste and food waste for biogas production. *Bioresource technology*, 127, 275-280. [doi:10.1016/j.biortech.2012.09.081](https://doi.org/10.1016/j.biortech.2012.09.081)
- Budiyono, B., Syaichurrozi, I., & Sumardiono, S. (2013). Biogas production from bioethanol waste: the effect of pH and urea addition to biogas production rate. *Waste Technology*, 1(1), 1-5. [doi:10.14710/1.1.1-5](https://doi.org/10.14710/1.1.1-5)
- Cai, Y., Hua, B., Gao, L., Hu, Y., Yuan, X., Cui, Z., . . . & Wang, X. (2017). Effects of adding trace elements on rice straw anaerobic mono-digestion: Focus on changes in microbial communities using high-throughput sequencing. *Bioresource technology*, 239, 454-463. [doi:10.1016/j.biortech.2017.04.071](https://doi.org/10.1016/j.biortech.2017.04.071)
- Carlsson, L., Mlingi, N., Juma, A., Ronquist, G., & Rosling, H. (1999). Metabolic fates in humans of linamarin in cassava flour ingested as stiff porridge. *Food and chemical toxicology*, 37(4), 307-312. [doi:10.1016/S0278-6915\(99\)00015-0](https://doi.org/10.1016/S0278-6915(99)00015-0)

- Chen, S., Yue, Q., Gao, B., Li, Q., Xu, X., & Fu, K. (2012). Adsorption of hexavalent chromium from aqueous solution by modified corn stalk: a fixed-bed column study. *Bioresource technology*, *113*, 114-120. [doi:10.1016/j.biortech.2011.11.110](https://doi.org/10.1016/j.biortech.2011.11.110)
- Cheong, W. L., Chan, Y. J., Tiong, T. J., Chong, W. C., Kiatkittipong, W., Kiatkittipong, K., . . . & Sari, M. M. (2022). Anaerobic Co-digestion of food waste with sewage sludge: simulation and optimization for maximum biogas production. *Water*, *14*(7), 1075. [doi:10.3390/w14071075](https://doi.org/10.3390/w14071075)
- Cherosky, P., & Li, Y. (2013). Hydrogen sulfide removal from biogas by bio-based iron sponge. *Biosystems engineering*, *114*(1), 55-59. [doi:10.1016/j.biosystemeng.2012.10.010](https://doi.org/10.1016/j.biosystemeng.2012.10.010)
- Chilev, C., Dicko, M., Langlois, P., & Lamari, F. (2022). Modelling of single-gas adsorption isotherms. *Metals*, *12*(10), 1698. [doi:10.3390/met12101698](https://doi.org/10.3390/met12101698)
- Choo, H. S., Lau, L. C., Mohamed, A. R., & Lee, K. T. (2013a). Hydrogen sulfide adsorption by alkaline impregnated coconut shell activated carbon. *Journal of Engineering Science and Technology*, *8*(6), 741-753.
- Choo, H. S., Lau, L. C., Mohamed, A. R., & Lee, K. T. (2013b). Hydrogen sulfide adsorption by alkaline impregnated coconut shell activated carbon. *J. Eng. Sci. Technol*, *8*(6), 741-753.
- Chu, K. H., (2020). Breakthrough curve analysis by simplistic models of fixed bed adsorption: In defense of the century-old Bohart-Adams model. *Chemical Engineering Journal*, *380*, 122513. [doi:10.1016/j.cej.2019.122513](https://doi.org/10.1016/j.cej.2019.122513)
- Chulalaksananukul, S., Sinbuathong, N., & Chulalaksananukul, W. (2012). Bioconversion of pineapple solid waste under anaerobic condition through biogas production. *Asia-Pacific Journal of Science and Technology*, *17*(5), 734-742.
- Comite, A., Costa, C., Demartini, M., Di Felice, R., & Oliva, M. (2017). Exploring CO₂ capture from pressurized industrial gaseous effluents in membrane contactor-based pilot plant. *International Journal of Greenhouse Gas Control*, *67*, 60-70. [doi:10.1016/j.ijggc.2017.10.014](https://doi.org/10.1016/j.ijggc.2017.10.014)
- Comite, A., Costa, C., Demartini, M., Di Felice, R., & Rotondi, M. (2016). Rate of CO₂ transfer to loaded MEA solutions using a membrane contactor device. *International Journal of Greenhouse Gas Control*, *52*, 378-386. [doi:10.1016/j.ijggc.2016.07.029](https://doi.org/10.1016/j.ijggc.2016.07.029)
- Cooney, D. (1999). Adsorption design for wastewater treatment, CRC Pres. INC., Boca Raton, Florida, USA.
- Coppola, G., & Papurello, D. (2018). Biogas cleaning: activated carbon regeneration for H₂S removal. *Clean Technologies*, *1*(1), 40-57. [doi:10.3390/cleantechnol1010004](https://doi.org/10.3390/cleantechnol1010004)
- Costa, C., Cornacchia, M., Pagliero, M., Fabiano, B., Vocciant, M., & Reverberi, A. P. (2020). Hydrogen sulfide adsorption by iron oxides and their polymer composites: a case-study application to biogas purification. *Materials*, *13*(21), 4725. [doi:10.3390/ma13214725](https://doi.org/10.3390/ma13214725)

- Czubaszek, R., Wysocka-Czubaszek, A., & Banaszuk, P. (2022). Importance of Feedstock in a Small-Scale Agricultural Biogas Plant. *Energies*, 15(20), 7749. [doi:10.3390/en15207749](https://doi.org/10.3390/en15207749)
- Dai, Y., Niu, J., Yin, L., Xu, J., & Xi, Y. (2011). Sorption of polycyclic aromatic hydrocarbons on electrospun nanofibrous membranes: sorption kinetics and mechanism. *Journal of Hazardous Materials*, 192(3), 1409-1417. [doi:10.1016/j.jhazmat.2011.06.055](https://doi.org/10.1016/j.jhazmat.2011.06.055)
- Dasgupta, A., & Chandel, M. K. (2020). Enhancement of biogas production from organic fraction of municipal solid waste using alkali pretreatment. *Journal of material cycles and waste management*, 22, 757-767. [doi:10.1007/s10163-020-00970-2](https://doi.org/10.1007/s10163-020-00970-2)
- Davie, M. G., Cheng, H., Hopkins, G. D., Lebron, C. A., & Reinhard, M. (2008). Implementing heterogeneous catalytic dechlorination technology for remediating TCE-contaminated groundwater. *Environmental science & technology*, 42(23), 8908-8915. [doi: 10.1021/es8014919](https://doi.org/10.1021/es8014919)
- Dawodu, F. A., & Akpomie, K. G. (2014). Simultaneous adsorption of Ni (II) and Mn (II) ions from aqueous solution unto a Nigerian kaolinite clay. *Journal of materials research and technology*, 3(2), 129-141. [doi:10.1016/j.jmrt.2014.03.00](https://doi.org/10.1016/j.jmrt.2014.03.00)
- De Gioannis, G., Muntoni, A., Poletini, A., Pomi, R., & Spiga, D. (2017). Energy recovery from one-and two-stage anaerobic digestion of food waste. *Waste management*, 68, 595-602. [doi: 10.1016/j.wasman.2017.06.013](https://doi.org/10.1016/j.wasman.2017.06.013)
- Dębowski, M., Krzemieniewski, M., Zieliński, M., & Kazimierowicz, J. (2021). Immobilized microalgae-based photobioreactor for CO₂ capture (IMC-CO₂PBR): Efficiency estimation, technological parameters, and prototype concept. *Atmosphere*, 12(8), 1031. [doi:10.3390/atmos12081031](https://doi.org/10.3390/atmos12081031)
- Deepanraj, B., Senthilkumar, N., & Ranjitha, J. (2021). Effect of solid concentration on biogas production through anaerobic digestion of rapeseed oil cake. *Energy Sources, Part A: Recovery, Utilization, and Environmental Effects*, 43(11), 1329-1336. [10.1080/15567036.2019.1636902](https://doi.org/10.1080/15567036.2019.1636902)
- Deepanraj, B., Sivasubramanian, V., & Jayaraj, S. (2017). Multi-response optimization of process parameters in biogas production from food waste using Taguchi–Grey relational analysis. *Energy conversion and management*, 141, 429-438. [doi:10.1016/j.enconman.2016.12.013](https://doi.org/10.1016/j.enconman.2016.12.013)
- Deepanraj, B., Sivasubramanian, V., & Jayaraj, S. (2015). Kinetic study on the effect of temperature on biogas production using a lab scale batch reactor. *Ecotoxicology and Environmental Safety*, 121, 100-104. [doi:10.1016/j.ecoenv.2015.04.051](https://doi.org/10.1016/j.ecoenv.2015.04.051)
- Demirbas, E., Kobya, M., Senturk, E., & Ozkan, T. (2004). Adsorption kinetics for the removal of chromium (VI) from aqueous solutions on the activated carbons prepared from agricultural wastes. *Water Sa*, 30(4), 533-539.

- Deressa, L., Libsu, S., Chavan, R., Manaye, D., & Dabassa, A. (2015). Production of biogas from fruit and vegetable wastes mixed with different wastes. *Environment and Ecology Research*, 3(3), 65-71. [doi:10.13189/eer.2015.030303](https://doi.org/10.13189/eer.2015.030303)
- Di Maria, F., Sordi, A., Cirulli, G., Gigliotti, G., Massaccesi, L., & Cucina, M. (2014). Co-treatment of fruit and vegetable waste in sludge digesters. An analysis of the relationship among bio-methane generation, process stability and digestate phytotoxicity. *Waste management*, 34(9), 1603-1608. [doi:10.1016/j.wasman.2014.05.017](https://doi.org/10.1016/j.wasman.2014.05.017)
- Dotto, J., Matem, A. O., & dakidemi, P. A. (2019). Nutrient composition and selected physicochemical properties of fifteen Mchare cooking bananas: A study conducted in northern Tanzania. *Scientific African*, 6, e00150. [doi:10.1016/j.sciaf.2019.e00150](https://doi.org/10.1016/j.sciaf.2019.e00150)
- Dushimimana, C., Nemerimana, M., Gatarira, P. C., Habineza, J. P. M., & Mungai, J. K. (2018). Nutritional content of certain indigenous vegetables for food insecurity and malnutrition reduction in Kiambu County, Kenya. *International Journal of Agronomy and Agricultural Research (IJAAR)*, 12(4).
- Ebner, J. H., Labatut, R. A., Lodge, J. S., Williamson, A. A., & Trabold, T. A. (2016). Anaerobic co-digestion of commercial food waste and dairy manure: Characterizing biochemical parameters and synergistic effects. *Waste management*, 52, 286-294. [doi:10.1016/j.wasman.2016.03.046](https://doi.org/10.1016/j.wasman.2016.03.046)
- Ebunilo, P., Aliu, S., & Orhorhoro, K. (2015). Comparative analysis of biogas yield from different composition of domestic wastes from Benin City, Nigeria. *Journal of Advanced & Applied Science (JAAS)*, 4(5), 169-177.
- El Barnossi, A., Moussaid, F. Z., Saghrouchni, H., Zoubi, B., & Iraqi Housseini, A. I. (2022). Tangerine, Pomegranate, and Banana Peels: A Promising Environmentally Friendly Bioorganic Fertilizers for Seed Germination and Cultivation of *Pisum sativum* L. *Waste and biomass valorization*, 1-17. [doi:10.1007/s12649-022-01743-8](https://doi.org/10.1007/s12649-022-01743-8)
- Elsayed, M., Diab, A., & Soliman, M. (2021). Methane production from anaerobic co-digestion of sludge with fruit and vegetable wastes: Effect of mixing ratio and inoculum type. *Biomass Conversion and Biorefinery*, 11(3), 989-998. [doi:10.1007/s13399-020-00785-z](https://doi.org/10.1007/s13399-020-00785-z)
- Ephantus, M., Robert, K., & Paul, N. (2021). An analysis of solid waste generation and characterization in thika municipality of Kiambu County, Kenya.
- Felix, M., & Gheewala, S. H. (2011). A review of biomass energy dependency in Tanzania. *Energy procedia*, 9, 338-343. [doi: 10.1016/j.egypro.2011.09.036](https://doi.org/10.1016/j.egypro.2011.09.036)
- Fezzani, B., & Cheikh, R. B. (2010). Two-phase anaerobic co-digestion of olive mill wastes in semi-continuous digesters at mesophilic temperature. *Bioresource technology*, 101(6), 1628-1634. [doi:10.1016/j.biortech.2009.09.067](https://doi.org/10.1016/j.biortech.2009.09.067)
- Frare, L. M., Vieira, M., Silva, M., Pereira, N., & Gimenes, M. (2010). Hydrogen sulfide removal from biogas using Fe/EDTA solution: gas/liquid contacting and sulfur formation. *Environmental Progress & Sustainable Energy*, 29(1), 34-41. <http://doi.org/10.1002/ep.10374>

- Ganesh, R., Torrijos, M., Sousbie, P., Lugardon, A., Steyer, J. P., & Delgenes, J. P. (2014). Single-phase and two-phase anaerobic digestion of fruit and vegetable waste: comparison of start-up, reactor stability and process performance. *Waste management*, 34(5), 875-885. [doi:10.1016/j.wasman.2014.02.023](https://doi.org/10.1016/j.wasman.2014.02.023)
- Garces, H. F., Espinal, A. E., & Suib, S. L. (2012). Tunable shape microwave synthesis of zinc oxide nanospheres and their desulfurization performance compared with nanorods and platelet-like morphologies for the removal of hydrogen sulfide. *The Journal of Physical Chemistry C*, 116(15), 8465-8474. [doi:10.1021/jp210755t](https://doi.org/10.1021/jp210755t)
- Gashaw, A., Libsu, S., & Chavan, R. (2014). Gashaw, Libsu & Chavan, 2014). *International Journal of Science and Research (IJSR)*, 3(5), 1122-1127.
- Georgiadis, A. G., Charisiou, N. D., & Goula, M. A. (2020). Removal of hydrogen sulfide from various industrial gases: A review of the most promising adsorbing materials. *Catalysts*, 10(5), 521. [doi:10.3390/catal10050521](https://doi.org/10.3390/catal10050521)
- Getahun, T., Gebrehiwot, M., Ambelu, A., Van Gerven, T., & Van der Bruggen, B. (2014). The potential of biogas production from municipal solid waste in a tropical climate. *Environmental monitoring and assessment*, 186(7), 4637-4646. [doi:10.1007/s10661-014-3727-4](https://doi.org/10.1007/s10661-014-3727-4)
- Ghosh, A., Chakrabarti, S., & Ghosh, U. C. (2014). Fixed-bed column performance of Mn-incorporated iron (III) oxide nanoparticle agglomerates on As (III) removal from the spiked groundwater in lab bench scale. *Chemical Engineering Journal*, 248, 18-26. [doi:10.1016/j.cej.2014.03.010](https://doi.org/10.1016/j.cej.2014.03.010)
- Glivin, G., & Sekhar, S. J. (2019). Studies on the feasibility of producing biogas from rice waste. *Rom Biotechnol. Lett*, 24, 728-735.
- González-Fernández, C., & García-Encina, P. A. (2009). Impact of substrate to inoculum ratio in anaerobic digestion of swine slurry. *Biomass and Bioenergy*, 33(8), 1065-1069. [doi:10.1016/j.biombioe.2009.03.008](https://doi.org/10.1016/j.biombioe.2009.03.008)
- González-López, M. E., Laureano-Anzaldo, C. M., Pérez-Fonseca, A. A., Arellano, M., & Robledo-Ortíz, J. R. (2022). A critical overview of adsorption models linearization: methodological and statistical inconsistencies. *Separation & Purification Reviews*, 51(3), 358-372. [doi:10.1080/15422119.2021.1951757](https://doi.org/10.1080/15422119.2021.1951757)
- Gumisiriza, R., Hawumba, J. F., Balyeidhusa, A. S. P., Okure, M., & Hensel, O. (2019). Processing of East African highland green bananas: Waste generation and characterization as a potential feedstock for biogas production in Uganda. *American Academic Scientific Research Journal for Engineering, Technology, and Sciences*, 53(1), 215-236.
- Gunaseelan, V. N. (2007). Regression models of ultimate methane yields of fruits and vegetable solid wastes, sorghum and napiergrass on chemical composition. *Bioresource technology*, 98(6), 1270-1277. [doi:10.1016/j.biortech.2006.05.014](https://doi.org/10.1016/j.biortech.2006.05.014)
- Guo, X., & Wang, J. (2019). Comparison of linearization methods for modeling the Langmuir adsorption isotherm. *Journal of Molecular Liquids*, 296, 111850. [doi:10.1016/j.molliq.2019.111850](https://doi.org/10.1016/j.molliq.2019.111850)

- Gupta, S. K., & Mittal, M. (2019). Effect of biogas composition variations on engine characteristics including operational limits of a spark-ignition engine. *Journal of Engineering for Gas Turbines and Power*, 141(10). doi:10.1115/1.4044195
- Hafner, J., Uckert, G., Graef, F., Hoffmann, H., Kimaro, A., Sererya, O., & Sieber, S. (2018). A quantitative performance assessment of improved cooking stoves and traditional three-stone-fire stoves using a two-pot test design in Chamwino, Dodoma, Tanzania. *Environmental Research Letters*, 13(2), 025002. doi:10.1088/1748-9326/999da3
- Hafner, J. M., Uckert, G., Hoffmann, H. K., Rosenstock, T. S., Sieber, S., & Kimaro, A. A. (2020). Efficiency of Three-Stone Fire and Improved Cooking Stoves using on-farm and off-farm fuels in semi-arid Tanzania. *Energy for Sustainable Development*, 59, 199-207. doi:10.1016/j.2020.10.012
- Haider, M. R., Yousaf, S., Malik, R. N., & Visvanathan, C. (2015). Effect of mixing ratio of food waste and rice husk co-digestion and substrate to inoculum ratio on biogas production. *Bioresource technology*, 190, 451-457. doi:10.1016/j.biortech.2015.02.105
- Hami, H. K., Abbas, R. F., Waheb, A. A., & Mahdi, N. I. (2020). Removal of Eriochrom Black T from aqueous solution using Al₂O₃ surface: linear and non-linear isotherm models, error analysis and thermodynamic studies. *Materials Today: Proceedings*, 20, 599-604. doi:10.1016/j.matpr.2019.09.196
- Han, R., Zou, L., Zhao, X., Xu, Y., Xu, F., Li, Y., & Wang, Y. (2009). Characterization and properties of iron oxide-coated zeolite as adsorbent for removal of copper (II) from solution in fixed bed column. *Chemical Engineering Journal*, 149(1-3), 123-131. doi:10.1016/j.cej.2008.10.015
- Hanbali, M., Holail, H., & Hammud, H. (2014). Remediation of lead by pretreated red algae: adsorption isotherm, kinetic, column modeling and simulation studies. *Green Chemistry Letters and Reviews*, 7(4), 342-358. doi:10.1080/17518253.2014.955062
- Hao, H., Tian, Y., Zhang, H., & Chai, Y. (2017). Copper stressed anaerobic fermentation: biogas properties, process stability, biodegradation and enzyme responses. *Biodegradation*, 28, 369-381. doi:10.1007/s10532-017-9802-0
- Harun, N., Hassan, Z., Zainol, N., Ibrahim, W. H. W., & Hashim, H. (2019). Anaerobic digestion process of food waste for biogas production: a simulation approach. *Chemical Engineering & Technology*, 42(9), 1834-1839. doi:10.1002/ceat.201800637
- He, R., Xia, F.-F., Wang, J., Pan, C.-L., & Fang, C.-R. (2011). Characterization of adsorption removal of hydrogen sulfide by waste biocover soil, an alternative landfill cover. *Journal of Hazardous Materials*, 186(1), 773-778. doi:10.1016/j.jhazmat.2010.11.062
- Hill, D., & Bolte, J. (2000). Methane production from low solid concentration liquid swine waste using conventional anaerobic fermentation. *Bioresource technology*, 74(3), 241-247. doi:10.1016/S0960-8524(00)00008-0
- Hoorweg, D., & Bhada-Tata, P. (2012). *What a waste: a global review of solid waste management*.

- Hossain, M. B., Aguiló-Aguayo, I., Lyng, J. G., Brunton, N. P., & Rai, D. K. (2015). Effect of pulsed electric field and pulsed light pre-treatment on the extraction of steroidal alkaloids from potato peels. *Innovative Food Science & Emerging Technologies*, 29, 9-14. [doi:10.1016/j.ifset.2014.10.014](https://doi.org/10.1016/j.ifset.2014.10.014)
- Huang, X., Yun, S., Zhu, J., Du, T., Zhang, C., & Li, X. (2016). Mesophilic anaerobic co-digestion of aloe peel waste with dairy manure in the batch digester: Focusing on mixing ratios and digestate stability. *Bioresource technology*, 218, 62-68. [doi:10.1016/j.biortech.2016.06.070](https://doi.org/10.1016/j.biortech.2016.06.070)
- Idris, A., Inanc, B., & Hassan, M. N. (2004). Overview of waste disposal and landfills/dumps in Asian countries. *Journal of material cycles and waste management*, 6(2), 104-110. [doi:10.1007/s10163-004-0117-y](https://doi.org/10.1007/s10163-004-0117-y)
- Inchauspe, M. E. (2021). *Simulation of fixed bed adsorption processes with simplified models. Application for CO₂ adsorption in biogas purification.*
- Iordache, O., Moga, I. C., Mitran, E. C., Sandulache, I., Memecica, M., Secareanu, L. O., . . . & Perdum, E. (2020). BOD & COD reduction from textile wastewater using bio-augmented HDPE carriers. Paper presented at the The 8th international conference on advanced materials and systems.
- Jabeen, M., Yousaf, S., Haider, M. R., & Malik, R. N. (2015). High-solids anaerobic co-digestion of food waste and rice husk at different organic loading rates. *International Biodeterioration & Biodegradation*, 102, 149-153. [doi:10.1016/j.ibiod.2015.03.023](https://doi.org/10.1016/j.ibiod.2015.03.023)
- Jansson, A. T., Patinvoh, R. J., Sárvári Horváth, I., & Taherzadeh, M. J. (2019). Dry anaerobic digestion of food and paper industry wastes at different solid contents. *Fermentation*, 5(2), 40. [doi:10.3390/fermentation5020040](https://doi.org/10.3390/fermentation5020040)
- Jiang, L., Hu, Z., Wang, Y., Ru, D., Li, J., & Fan, J. (2018). Effect of trace elements on the development of co-cultured nitrite-dependent anaerobic methane oxidation and methanogenic bacteria consortium. *Bioresource technology*, 268, 190-196. [doi:10.1016/j.biortech.2018.07.139](https://doi.org/10.1016/j.biortech.2018.07.139)
- Juma, G., Machunda, R., & Pogrebnaya, T. (2020). Performance of Sweet Potato's Leaf-Derived Activated Carbon for Hydrogen Sulphide Removal from Biogas. *Journal of Energy*, 2020. [doi: 10.1155/2020/9121085](https://doi.org/10.1155/2020/9121085)
- Juntarachat, N., & Onthong, U. (2022). Removal of hydrogen sulfide from biogas using banana peel and banana empty fruit bunch biochars as alternative adsorbents. *Biomass Conversion and Biorefinery*, 1-12. [doi:10.1007/s13399-022-03430-z](https://doi.org/10.1007/s13399-022-03430-z)
- Kadam, R., & Panwar, N. (2017). Recent advancement in biogas enrichment and its applications. *Renewable and Sustainable Energy Reviews*, 73, 892-903. [doi:10.1016/j.rser.2017.01.167](https://doi.org/10.1016/j.rser.2017.01.167)
- Kafle, G. K., Bhattarai, S., Kim, S. H., & Chen, L. (2014). Effect of feed to microbe ratios on anaerobic digestion of Chinese cabbage waste under mesophilic and thermophilic conditions: biogas potential and kinetic study. *Journal of environmental management*, 133, 293-301. [doi:10.1016/j.jenvman.2013.12.006](https://doi.org/10.1016/j.jenvman.2013.12.006)

- Kalemelawa, F., Nishihara, E., Endo, T., Ahmad, Z., Yeasmin, R., Tenywa, M. M., & Yamamoto, S. (2012). An evaluation of aerobic and anaerobic composting of banana peels treated with different inoculums for soil nutrient replenishment. *Bioresource technology*, 126, 375-382. doi:10.1016/j.biortech.2012.04.030
- Kalsum, L., & Hasan, A. (2022). The Effect of the Packing Flow Area and Biogas Flow Rate on Biogas Purification in Packed Bed Scrubber. *Journal of Ecological Engineering*, 23(11). doi:10.12911/22998993/153569
- Kameswari, K. S. B., Kalyanaraman, C., Porselvam, S., & Thanasekaran, K. (2012). Optimization of inoculum to substrate ratio for bio-energy generation in co-digestion of tannery solid wastes. *Clean Technologies and Environmental Policy*, 14(2), 241-250. doi:10.1007/s10098-011-0391-z
- Kandola, I., Pogrebnoi, A., & Pogrebnyaya, T. (2018). Oldoinyo Lengai Volcanic Ash for Removal of Hydrogen Sulfide and Ammonia from Biogas. *Journal of Materials Science and Chemical Engineering*, 6(04), 78. doi:10.4236/msce.2018.64010
- Karak, T., Bhagat, R., & Bhattacharyya, P. (2012). Municipal solid waste generation, composition, and management: the world scenario. *Critical Reviews in Environmental Science and Technology*, 42(15), 1509-1630. doi:10.1080/10643389.2011.569871
- Karienyee, D., & Kamiri, H. (2020). Trends of banana production among smallholders' farmers due to rainfall and temperature variations in Mount Kenya Region, Kenya. *Budapest International Research in Exact Sciences (BirEx-Journal) Vol*, 2(2), 213-227. doi:10.33258/birex.v2i2.878
- Karimi, M., Shojaei, A., Nematollahzadeh, A., & Abdekhodaie, M. J. (2012). Column study of Cr (VI) adsorption onto modified silica-polyacrylamide microspheres composite. *Chemical Engineering Journal*, 210, 280-288. doi:10.1016/j.cej.2012.08.046
- Karthikeyan, O. P., & Visvanathan, C. (2013). Bio-energy recovery from high-solid organic substrates by dry anaerobic bio-conversion processes: a review. *Reviews in Environmental Science and Bio/Technology*, 12(3), 257-284. doi:10.1007/s11157-012-9304-9
- Khan, M. U., Lee, J. T. E., Bashir, M. A., Dissanayake, P. D., Ok, Y. S., Tong, Y. W., . . . & Ahring, B. K. (2021). Current status of biogas upgrading for direct biomethane use: A review. *Renewable and Sustainable Energy Reviews*, 149, 111343. doi:10.1016/j.rser.2021.111343
- Khan, T. A., Chaudhry, S. A., & Ali, I. (2015). Equilibrium uptake, isotherm and kinetic studies of Cd (II) adsorption onto iron oxide activated red mud from aqueous solution. *Journal of Molecular Liquids*, 202, 165-175. doi:10.1016/j.molliq.2014.12.021
- Khoshnevisan, B., Tsapekos, P., Alfaro, N., Díaz, I., Fdz-Polanco, M., Rafiee, S., & Angelidaki, I. (2017). A review on prospects and challenges of biological H₂S removal from biogas with focus on biotrickling filtration and microaerobic desulfurization. *Biofuel research journal*, 4(4), 741-750. doi:10.18331/BRJ2017.4.4.6

- Kim, J., Baek, G., Kim, J., & Lee, C. (2019). Energy production from different organic wastes by anaerobic co-digestion: Maximizing methane yield versus maximizing synergistic effect. *Renewable Energy*, *136*, 683-690. [doi:10.1016/j.renene.2019.01.046](https://doi.org/10.1016/j.renene.2019.01.046)
- Kim, J., Kim, H., Baek, G., & Lee, C. (2017). Anaerobic co-digestion of spent coffee grounds with different waste feedstocks for biogas production. *Waste management*, *60*, 322-328. [doi:10.1016/j.wasman.2016.10.015](https://doi.org/10.1016/j.wasman.2016.10.015)
- Kim, J. K., Oh, B. R., Chun, Y. N., & Kim, S. W. (2006). Effects of temperature and hydraulic retention time on anaerobic digestion of food waste. *Journal of Bioscience and Bioengineering*, *102*(4), 328-332. [doi: 10.1263/jbb.102.328](https://doi.org/10.1263/jbb.102.328)
- Kim, S.-H., & Kafle, G. K. (2010). Effective treatment of swine manure with Chinese cabbage silage through two serial anaerobic digestion. *Journal of Biosystems Engineering*, *35*(1), 53-63. [doi: 10.5307/JBE.2010.35.1.053](https://doi.org/10.5307/JBE.2010.35.1.053)
- Koch, K., Helmreich, B., & Drewes, J. E. (2015). Co-digestion of food waste in municipal wastewater treatment plants: effect of different mixtures on methane yield and hydrolysis rate constant. *Applied Energy*, *137*, 250-255. [doi:10.1016/j.apenergy.2014.10.025](https://doi.org/10.1016/j.apenergy.2014.10.025)
- Kodagoda, K., & Marapana, R. (2017). Development of non-alcoholic wines from the wastes of mauritius pineapple variety and its physicochemical properties. *Journal of Pharmacognosy and Phytochemistry*.
- Koniuszewska, I., Korzeniewska, E., Harnisz, M., & Czatkowska, M. (2020). Intensification of biogas production using various technologies: A review. *International Journal of Energy Research*, *44*(8), 6240-6258. [doi:10.1002/er.5338](https://doi.org/10.1002/er.5338)
- Köse, T. E., & Kıvanç, B. (2011). Adsorption of phosphate from aqueous solutions using calcined waste eggshell. *Chemical Engineering Journal*, *178*, 34-39. [doi:10.1016/j.cej.2011.09.129](https://doi.org/10.1016/j.cej.2011.09.129)
- Kulkarni, M., & Ghanegaonkar, P. (2019). Hydrogen sulfide removal from biogas using chemical absorption technique in packed column reactors. *Global Journal of Environmental Science and Management*, *5*(2), 155-166. [doi:10.22034/gjesm.2019.02.02](https://doi.org/10.22034/gjesm.2019.02.02)
- Kumar, A., Miglani, P., Gupta, R., & Bhattacharya, T. (2006). Impact of Ni (II), Zn (II) and Cd (II) on biogassification of potato waste. *Journal of Environmental Biology*, *27*(1), 61-66.
- Kundu, S., & Sahoo, P. (2019). Estimation of hydrogen sulfide from crude petroleum: A unique invention using a simple chemosensor. *New Journal of Chemistry*, *43*(31), 12369-12374. [doi:10.1039/C9NJ02628B](https://doi.org/10.1039/C9NJ02628B)
- Kusekwa, M. A., Tzoneva, R., & Mohamed, A. K. (2007). *Evaluation of renewable energy as an alternative source for rural electrification in Tanzania*. Paper presented at the Proceedings of the IASTED International Conference on Energy and Power Systems.

- Labatut, R. A., & Pronto, J. L. (2018). Sustainable waste-to-energy technologies: Anaerobic digestion *Sustainable food waste-to-energy systems* (pp. 47-67): Elsevier.
- Langè, S., Pellegrini, L. A., Vergani, P., & Lo Savio, M. (2015). Energy and economic analysis of a new low-temperature distillation process for the upgrading of high-CO₂ content natural gas streams. *Industrial & engineering chemistry research*, *54*(40), 9770-9782. doi: [10.1021/acs.iecr.5b02211](https://doi.org/10.1021/acs.iecr.5b02211)
- Lee, S. C., Choi, B. Y., Lee, T. J., Ryu, C. K., Ahn, Y. S., & Kim, J. C. (2006). CO₂ absorption and regeneration of alkali metal-based solid sorbents. *Catalysis Today*, *111*(3-4), 385-390. doi: [10.1016/j.cattod.2005.10.051](https://doi.org/10.1016/j.cattod.2005.10.051)
- Li, Y., Chen, Y., & Wu, J. (2019). Enhancement of methane production in anaerobic digestion process: A review. *Applied Energy*, *240*, 120-137. doi: [10.1016/j.apenergy.2019.01.243](https://doi.org/10.1016/j.apenergy.2019.01.243)
- Liang, S., & McDonald, A. G. (2015). Anaerobic digestion of pre-fermented potato peel wastes for methane production. *Waste management*, *46*, 197-200. doi: [10.1016/j.wasman.2015.09.029](https://doi.org/10.1016/j.wasman.2015.09.029)
- Liu, C.-F., Yuan, X.-Z., Zeng, G.-M., Li, W.-W., & Li, J. (2008). Prediction of methane yield at optimum pH for anaerobic digestion of organic fraction of municipal solid waste. *Bioresource technology*, *99*(4), 882-888. doi: [10.1016/j.biortech.2007.01.013](https://doi.org/10.1016/j.biortech.2007.01.013)
- Liu, D., Liu, D., Zeng, R. J., & Angelidaki, I. (2006). Hydrogen and methane production from household solid waste in the two-stage fermentation process. *Water research*, *40*(11), 2230-2236. doi: [10.1016/j.watres.2006.03.029](https://doi.org/10.1016/j.watres.2006.03.029)
- López-Bellido, L., Wery, J., & López-Bellido, R. J. (2014). Energy crops: prospects in the context of sustainable agriculture. *European journal of agronomy*, *60*, 1-12. doi: [10.1016/j.eja.2014.07.001](https://doi.org/10.1016/j.eja.2014.07.001)
- Lu, J., & Gao, X. (2021). Biogas: Potential, challenges, and perspectives in a changing China. *Biomass and Bioenergy*, *150*, 106127. doi: [10.1016/j.biombioe.2021.106127](https://doi.org/10.1016/j.biombioe.2021.106127)
- Lucas, C. K. G. (2014). Biogas Production from Potato Peel Waste. (Thesis), Faculdade de Ciências e Tecnologia. Retrieved from URL [r?hl=en&as_sdt=0%2C5&q=](https://repositorio.fct.unesp.br/handle/en&as_sdt=0%2C5&q=)
- Luswaga, H., & Nuppenau, E.-A. (2020). Participatory forest management in West Usambara Tanzania: what is the community perception on success? *Sustainability*, *12*(3), 921. doi: [10.3390/su12030921](https://doi.org/10.3390/su12030921)
- Maamri, S., & Amrani, M. (2014). Biogas production from waste activated sludge using cattle dung inoculums: Effect of total solid contents and kinetics study. *Energy procedia*, *50*, 352-359. doi: [10.1016/j.egypro.2014.06.042](https://doi.org/10.1016/j.egypro.2014.06.042)
- Machunda, R., & Pogrebnaya, T. (2020). Removal of hydrogen sulfide from biogas using a red rock. *Journal of Energy*, *2020*. doi: [10.1155/2020/2309378](https://doi.org/10.1155/2020/2309378)
- Madondo, N. I. (2017). *Optimization of anaerobic co-digestion of sewage sludge using bio-chemical substrates*. Durban University of Technology.

- Makauki, E., King'onde, C. K., & Kibona, T. E. (2017a). Hydrogen sulfide and ammonia removal from biogas using water hyacinth-derived carbon nanomaterials. *African Journal of Environmental Science and Technology* 11(7), 375-383. [doi:10.5897/AJEST2016.2246](https://doi.org/10.5897/AJEST2016.2246)
- Makauki, E., King'onde, C. K., & Kibona, T. E. (2017b). Hydrogen sulfide and ammonia removal from biogas using water hyacinth-derived carbon nanomaterials. *African Journal of Environmental Science and Technology*, 11(7), 375-383. [doi:10.5897/AJEST2016.2246](https://doi.org/10.5897/AJEST2016.2246)
- Mariga, I., Mativha, L., & Maposa, D. (2012). Nutritional assessment of a traditional local vegetable (*Brassica oleracea* var. *acephala*). *Journal of Medicinal Plants Research*, 6(5), 784-789. [doi:10.5897/JMPR11.1426](https://doi.org/10.5897/JMPR11.1426)
- Matheri, A., Ndiweni, S., Belaid, M., Muzenda, E., & Hubert, R. (2017). Optimising biogas production from anaerobic co-digestion of chicken manure and organic fraction of municipal solid waste. *Renewable and Sustainable Energy Reviews*, 80, 756-764. [doi:10.1016/j.rser.2017.05.068](https://doi.org/10.1016/j.rser.2017.05.068)
- Mbaka, J., Mwangi, M., & Mwangi, M. (2008). Banana farming as a business: The role of tissue cultured planting materials in Kenya. *Journal of Applied Biosciences*, 9(1), 354-361.
- Mehariya, S., Patel, A. K., Obulisamy, P. K., Punniyakotti, E., & Wong, J. W. (2018). Co-digestion of food waste and sewage sludge for methane production: Current status and perspective. *Bioresource technology*, 265, 519-531. [doi:10.1016/j.biortech.2018.04.030](https://doi.org/10.1016/j.biortech.2018.04.030)
- Meng, Y., Jiang, J., Gao, Y., Aihemaiti, A., Ju, T., Xu, Y., & Liu, N. (2019). Biogas upgrading to methane: Application of a regenerable polyethyleneimine-impregnated polymeric resin (NKA-9) via CO₂ sorption. *Chemical Engineering Journal*, 361, 294-303. [doi:10.1016/j.cej.2018.12.091](https://doi.org/10.1016/j.cej.2018.12.091)
- Menind, A., & Normak, A. (2009). Study on grinding biomass as pre-treatment for biogasification. Paper presented at the International Scientific Conference.
- Mkoma, S. L., & Mabiki, F. P. (2012). *Jatropha* as energy potential biofuel in Tanzania. *Int. J. Environ. Sci*, 2(3), 1553-1564. [doi:10.6088/ijes.00202030040](https://doi.org/10.6088/ijes.00202030040)
- Mohammed, S., & Kuhiyep, C. (2020). Bacteria and fungi co-biodeterioration of selected fresh tomatoes sold within Ungwan Rimi, Kaduna. *Science World Journal*, 15(1), 48-55.
- Motte, J.-C., Escudie, R., Bernet, N., Delgenes, J.-P., Steyer, J.-P., & Dumas, C. (2013). Dynamic effect of total solid content, low substrate/inoculum ratio and particle size on solid-state anaerobic digestion. *Bioresource technology*, 144, 141-148. [doi:10.1016/j.biortech.2013.06.057](https://doi.org/10.1016/j.biortech.2013.06.057)
- Moussout, H., Ahlafi, H., Aazza, M., & Maghat, H. (2018). Critical of linear and nonlinear equations of pseudo-first order and pseudo-second order kinetic models. *Karbala International Journal of Modern Science*, 4(2), 244-254. [doi:10.1016/j.kijoms.2018.04.001](https://doi.org/10.1016/j.kijoms.2018.04.001)

- Mrosso, R, Kiplagat, J., & Mecha, A. C. (2023). Anaerobic Codigestion of Tuber Waste and Fruit Waste: Synergy and Enhanced Biogas Production. *International Journal of Chemical Engineering*, 2023. [doi:10.1155/2023/6637249](https://doi.org/10.1155/2023/6637249)
- Mrosso, R., Machunda, R., & Pogrebnaya, T. (2020). Removal of Hydrogen Sulfide from Biogas Using a Red Rock. *Journal of Energy*, 2020, 2309378. [doi:10.1155/2020/2309378](https://doi.org/10.1155/2020/2309378)
- Mrosso, R, Mecha, A. C., & Kiplagat, J. (2023). Biogas sweetening using new sorbent derived from soda ash from Lake Natron, Tanzania. *Cleaner Engineering and Technology*, 100646. [doi:10.1016/j.clet.2023.100646](https://doi.org/10.1016/j.clet.2023.100646)
- Mrosso, R, Mecha, A. C., & Kiplagat, J. (2023). Characterization of kitchen and municipal organic waste for biogas production: Effect of parameters. *Heliyon*. [doi:10.1016/j.heliyon.2023.e16360](https://doi.org/10.1016/j.heliyon.2023.e16360)
- Mshandete, A., Björnsson, L., Kivaisi, A. K., Rubindamayugi, M. S., & Mattiasson, B. (2006). Effect of particle size on biogas yield from sisal fibre waste. *Renewable Energy*, 31(14), 2385-2392. [doi:10.1016/j.renene.2005.10.015](https://doi.org/10.1016/j.renene.2005.10.015)
- Mshandete, A., Kivaisi, A., Rubindamayugi, M., & Mattiasson, B. (2004). Anaerobic batch co-digestion of sisal pulp and fish wastes. *Bioresource technology*, 95(1), 19-24. [doi:10.1016/j.biortech.2004.01.011](https://doi.org/10.1016/j.biortech.2004.01.011)
- Msuya, N., Masanya, E., & Temu, A. K. (2011). Environmental burden of charcoal production and use in Dar es Salaam, Tanzania.
- Muala, A., Rankin, G., Sehlstedt, M., Unosson, J., Bosson, J. A., Behndig, A., . . . & Bergvall, C. (2015). Acute exposure to wood smoke from incomplete combustion-indications of cytotoxicity. *Particle and fibre toxicology*, 12(1), 1-14. [doi:10.1186/s12989-015-0111-7](https://doi.org/10.1186/s12989-015-0111-7)
- Muhondwa, J. P., Martienssen, M., & Burkhardt, M. (2015). Feasibility of Anaerobic Digestion of Potato peels for Biogas as Mitigation of Greenhouse gases Emission Potential. *International Journal of Environmental Research*, 9(2).
- Mulu, E., M'Arimi, M., Ramkat, R., & Kiprop, A. (2021). Biogas upgrade using modified natural clay. *Energy Conversion and Management: X*, 12, 100134. [doi:10.1016/j.ecmx.2021.100134](https://doi.org/10.1016/j.ecmx.2021.100134)
- Mulu, E., M'Arimi, M. M., & Ramkat, R. C. (2021). A review of recent developments in application of low cost natural materials in purification and upgrade of biogas. *Renewable and Sustainable Energy Reviews*, 145, 111081. [doi:10.1016/j.rser.2021.111081](https://doi.org/10.1016/j.rser.2021.111081)
- Mulu, E., M'Arimi, M. M., Ramkat, R. C., & Mulu, E. (2022). Carbon dioxide removal from biogas through sorption processes using natural and activated zeolite adsorbents. *Indian Chemical Engineer*, 1-13. [doi:10.1080/00194506.2022.2144485](https://doi.org/10.1080/00194506.2022.2144485)
- Muniafu, M., & Otiato, E. (2010). Solid Waste Management in Nairobi, Kenya. A case for emerging economies. *Journal of Language, Technology & Entrepreneurship in Africa*, 2(1), 342-350. [doi:10.4314/jolte.v2i1.52009](https://doi.org/10.4314/jolte.v2i1.52009)

- Mutegoa, E., Hilonga, A., & Njau, K. N. (2020). Approaches to the mitigation of ammonia inhibition during anaerobic digestion—a review. *Water Practice & Technology*, 15(3), 551-570. [doi:10.2166/wpt.2020.047](https://doi.org/10.2166/wpt.2020.047)
- Mutegoa, E., Malima, N., Hilonga, A., & Njau, K. (2021). Effect of mixing ratios of natural inorganic additives in removing ammonia and sulfide in the liquid phase during anaerobic digestion of slaughterhouse waste. *Materials Today Chemistry*, 20, 100415. [doi:10.1016/j.mtchem.2020.100415](https://doi.org/10.1016/j.mtchem.2020.100415)
- Mwaniki, J. M., Mwazighe, F., & Masimba, D. M. (2016). Optimization of C/N ratio for Mesophilic anaerobic digestion from food wastes found in Nairobi a lab-scale case study. *Journal of Kenya Chemical Society*, 9(1).
- Nadimi, A., Yavary, M., & Ale Ebrahim, H. (2021). Investigation of adsorption coefficients of carbon dioxide and nitrogen on a coal-based activated carbon. *International Journal of Environmental Studies*, 78(4), 624-633. [doi:10.1080/00207233.2021.1886554](https://doi.org/10.1080/00207233.2021.1886554)
- Naik, L., Gebreegziabher, Z., Tumwesige, V., Balana, B. B., Mwirigi, J., & Austin, G. (2014). Factors determining the stability and productivity of small scale anaerobic digesters. *Biomass and Bioenergy*, 70, 51-57. [doi:10.1016/j.biombioe.2014.01.055](https://doi.org/10.1016/j.biombioe.2014.01.055)
- Nalinga, Y., & Legonda, I. (2016). The effect of particles size on biogas production.
- Ndiweni, S., Belaid, M., Muzenda, E., & Hubert, R. (2017). Optimising biogas production from anaerobic co-digestion of chicken manure and organic fraction of municipal solid waste. *Renewable and Sustainable Energy Reviews*, 80, 756-764. [doi:10.1016/j.rser.2017.05.068](https://doi.org/10.1016/j.rser.2017.05.068)
- Niesner, J., Jecha, D., & Stehlík, P. (2013). Biogas upgrading technologies: state of art review in European region. *Chemical Engineering Transactions*, 35(86), 517-522. [doi: 10.3303/CET1335086](https://doi.org/10.3303/CET1335086)
- NNFCCT, (2016). The Official Information Portal on Anaerobic Digestion.
- Nyakeri, E., Mwirichia, R., & Boga, H. (2018). Isolation and characterization of enzyme producing bacteria from Lake Magadi, an extreme soda lake in Kenya. *J Microbiol Exp*, 6(2), 57-68. [doi:10.15406/jmen.2018.06.00189](https://doi.org/10.15406/jmen.2018.06.00189)
- Okonkwo, U. C., Onokpite, E., & Onokwai, A. O. (2018). Comparative study of the optimal ratio of biogas production from various organic wastes and weeds for digester/restarted digester. *Journal of King Saud University-Engineering Sciences*, 30(2), 123-129. [doi:10.1016/j.jksues.2016.02.002](https://doi.org/10.1016/j.jksues.2016.02.002)
- Omitola, O. B., Abonyi, M. N., Akpomie, K. G., & Dawodu, F. A. (2022). Adams-Bohart, Yoon-Nelson, and Thomas modeling of the fix-bed continuous column adsorption of amoxicillin onto silver nanoparticle-maize leaf composite. *Applied Water Science*, 12(5), 94. [doi:10.1007/s13201-022-01624-4](https://doi.org/10.1007/s13201-022-01624-4)
- Orhorhoro, E. K., Ebunilo, P. O., & Sadjere, G. E. (2017). Experimental determination of effect of total solid (TS) and volatile solid (VS) on biogas yield. *American Journal of Modern Energy*, 3(6), 131-135. [doi:10.11648/j.ajme.20170306.13](https://doi.org/10.11648/j.ajme.20170306.13)

- Panahi, R., Vasheghani-Farahani, E., & Shojosadati, S. (2008). Determination of adsorption isotherm for l-lysine imprinted polymer. *Iran. J. Chem. Eng*, 5(4), 49-55.
- Parimal, S., Prasad, M., & Bhaskar, U. (2010). Prediction of equilibrium sorption isotherm: comparison of linear and nonlinear methods. *Industrial & engineering chemistry research*, 49(6), 2882-2888. doi:10.1021/ie9013343
- Park, H. J., Jeong, S. W., Yang, J. K., Kim, B. G., & Lee, S. M. (2007). Removal of heavy metals using waste eggshell. *Journal of environmental sciences*, 19(12), 1436-1441. doi:10.1016/S1001-0742(07)60234-4
- Patel, K., & Pamnani, A. (2017). Generation of Biogas from Kitchen Waste, Bagasse and Garden Waste. *International Journal of Latest Technology in Engineering, Management & Applied Science (IJLTEMAS)*, 6, 50-53.
- Pathak, P. D., Mandavgane, S. A., Puranik, N. M., Jambhulkar, S. J., & Kulkarni, B. D. (2018). Valorization of potato peel: a biorefinery approach. *Critical Reviews in Biotechnology*, 38(2), 218-230. doi: 10.1080/07388551.2017.1331337
- Pavi, S., Kramer, L. E., Gomes, L. P., & Miranda, L. A. S. (2017). Biogas production from co-digestion of organic fraction of municipal solid waste and fruit and vegetable waste. *Bioresource technology*, 228, 362-367. doi:10.1016/j.biortech.2017.01.003
- Persson, M. (2003). Evaluation of upgrading techniques for biogas. *Report SGC*, 142.
- Petersson, A., & Wellinger, A. (2009). Biogas upgrading technologies—developments and innovations. *IEA bioenergy*, 20, 1-19.
- Pham Van, D., Takeshi, F., Hoang Minh, G., & Pham Phu, S. T. (2020). Comparison between single and two-stage anaerobic digestion of vegetable waste: Kinetics of methanogenesis and carbon flow. *Waste and biomass valorization*, 11, 6095-6103. doi:10.1007/s12649-019-00861-0
- Piñas, J. A. V., Venturini, O. J., Lora, E. E. S., & Roalcaba, O. D. C. (2018). Technical assessment of mono-digestion and co-digestion systems for the production of biogas from anaerobic digestion in Brazil. *Renewable Energy*, 117, 447-458. doi:10.1016/j.renene.2017.10.085
- Pizzuti, L., Martins, C., & Lacava, P. (2016). Laminar burning velocity and flammability limits in biogas: A literature review. *Renewable and Sustainable Energy Reviews*, 62, 856-865. doi:10.1016/j.rser.2016.05.011
- Pliya, P., & Cree, D. (2015). Limestone derived eggshell powder as a replacement in Portland cement mortar. *Construction and Building Materials*, 95, 1-9. doi: 10.1680/jmacr.17.00003
- Puttongsiri, T., Choosakul, N., & Sakulwilaingam, D. (2012). *Moisture content and physical properties of instant mashed potato*. Paper presented at the International Conference on Nutrition and Food Science.
- Ragadhita, R., & Nandiyanto, A. B. D. (2021). How to calculate adsorption isotherms of particles using two-parameter monolayer adsorption models and equations. *Indonesian Journal of Science and Technology*, 6(1), 205-234.

- Rahman, M. A., Shahazi, R., Nova, S. N. B., Uddin, M. R., Hossain, M. S., & Yousuf, A. (2021). Biogas production from anaerobic co-digestion using kitchen waste and poultry manure as substrate—part 1: substrate ratio and effect of temperature. *Biomass Conversion and Biorefinery*, 1-11. [doi:10.1007/s13399-021-01604-9](https://doi.org/10.1007/s13399-021-01604-9)
- Ramaraj, R., & Dussadee, N. (2015). Biological purification processes for biogas using algae cultures: a review. *International Journal of Sustainable and Green Energy*, 4(1), 20-32. [doi:10.11648/j.ijrse.s.2015040101.14](https://doi.org/10.11648/j.ijrse.s.2015040101.14)
- Rani, D. S., & Nand, K. (2004). Ensilage of pineapple processing waste for methane generation. *Waste management*, 24(5), 523-528. [doi:10.1016/j.wasman.2003.10.010](https://doi.org/10.1016/j.wasman.2003.10.010)
- Ranjitha, J., & Vijayalakshmi, S. (2014). *Production of bio-gas from flowers and vegetable wastes using anaerobic digestion*.
- Rincón, B., Borja, R., Martín, M., & Martín, A. (2009). Evaluation of the methanogenic step of a two-stage anaerobic digestion process of acidified olive mill solid residue from a previous hydrolytic–acidogenic step. *Waste management*, 29(9), 2566-2573. [doi:10.1016/j.wasman.2009.04.009](https://doi.org/10.1016/j.wasman.2009.04.009)
- Rocamora, I., Wagland, S. T., Casado, M. R., Hassard, F., Villa, R., Peces, M., . . . & Bajón-Fernández, Y. (2022). Managing full-scale dry anaerobic digestion: Semi-continuous and batch operation. *Journal of environmental chemical engineering*, 10(4), 108154. [doi:10.1016/j.jece.2022.108154](https://doi.org/10.1016/j.jece.2022.108154)
- Rouquerol, J., Rouquerol, F., Llewellyn, P., Maurin, G., & Sing, K. S. (2013). *Adsorption by powders and porous solids: principles, methodology and applications*: Academic press.
- Rughoonundun, H., Mohee, R., & Holtzaple, M. T. (2012). Influence of carbon-to-nitrogen ratio on the mixed-acid fermentation of wastewater sludge and pretreated bagasse. *Bioresource technology*, 112, 91-97. [doi:10.1016/j.biortech.2012.02.081](https://doi.org/10.1016/j.biortech.2012.02.081)
- Sahu, R. C., Patel, R., & Ray, B. C. (2011). Removal of hydrogen sulfide using red mud at ambient conditions. *Fuel processing technology*, 92(8), 1587-1592. [doi:10.1016/j.fuproc.2011.04.002](https://doi.org/10.1016/j.fuproc.2011.04.002)
- Sajeena, B., Jose, P., & Madhu, G. (2013). Effect of total solid concentration on anaerobic digestion of the organic fraction of municipal solid waste. *International Journal of Scientific and Research Publications*, 3(8), 1-5.
- Saravanan, A., Kumar, P. S., Govarthanan, M., George, C. S., Vaishnavi, S., Mouliswaran, B., . . . & Yaashikaa, P. (2021). Adsorption characteristics of magnetic nanoparticles coated mixed fungal biomass for toxic Cr (VI) ions in aquatic environment. *Chemosphere*, 267, 129226. [doi:10.1016/j.chemosphere.2021.130176](https://doi.org/10.1016/j.chemosphere.2021.130176)
- Saravanathamizhan, R., & Perarasu, V. (2021). Improvement of biodegradability index of industrial wastewater using different pretreatment techniques *Wastewater treatment* (pp. 103-136): Elsevier.

- Sari, F. P., Yanto, D. H. Y., & Pari, G. (2019). Activated Carbon Derived From OPEFB by One Step Steam Activation and Its Application for Dye Adsorption: Kinetics and Isothermal Studies. *Reaktor*, *19*(2), 68-76. [doi:10.14710/reaktor.19.2.68-76](https://doi.org/10.14710/reaktor.19.2.68-76)
- Sathish, S., Chandrasekaran, M., & Solomon, G. R. (2019). Effect of total solids and agitation time on biogas yield, using rice husk. *International Journal of Ambient Energy*, *40*(1), 101-104. [doi:10.1080/01430750.2017.1372815](https://doi.org/10.1080/01430750.2017.1372815)
- Scoon, R. N., & Scoon, R. N. (2018). Lake Natron and the Oldoinyo Lengai Volcano. *Geology of National Parks of Central/Southern Kenya and Northern Tanzania: Geotourism of the Gregory Rift Valley, Active Volcanism and Regional Plateaus*, 193-206. [doi:10.1007/978-3-319-73785-0_17](https://doi.org/10.1007/978-3-319-73785-0_17)
- Shadjou, N., & Hasanzadeh, M. (2015a). Bone tissue engineering using silica-based mesoporous nanobiomaterials: Recent progress. *Materials Science and Engineering: C*, *55*, 401-409. [doi:10.1016/j.msec.2015.05.027](https://doi.org/10.1016/j.msec.2015.05.027)
- Shadjou, N., & Hasanzadeh, M. (2015b). Silica-based mesoporous nanobiomaterials as promoter of bone regeneration process. *Journal of Biomedical Materials Research Part A*, *103*(11), 3703-3716. [doi:10.1002/jbm.a.35504](https://doi.org/10.1002/jbm.a.35504)
- Shang, G., Shen, G., Liu, L., Chen, Q., & Xu, Z. (2013). Kinetics and mechanisms of hydrogen sulfide adsorption by biochars. *Bioresour. Technol.*, *133*, 495-499. [doi:10.1016/j.biortech.2013.01.114](https://doi.org/10.1016/j.biortech.2013.01.114)
- Shyamala, B., & Jamuna, P. (2010). Nutritional Content and Antioxidant Properties of Pulp Waste from *Daucus carota* and *Beta vulgaris*. *Malaysian journal of nutrition*, *16*(3).
- Sidabutar, R., & Iriany, M. S. T. (2018). Adsorption-desorption system for CO₂ removal in biogas using natural zeolite-based adsorbent. *Journal of Engineering Science and Technology*, *13*(10), 3058-3070.
- Sigot, L., Ducom, G., Benadda, B., & Labouré, C. (2014). Adsorption of octamethylcyclotetrasiloxane on silica gel for biogas purification. *Fuel*, *135*, 205-209. [doi:10.1016/j.fuel.2014.06.058](https://doi.org/10.1016/j.fuel.2014.06.058)
- Silvestre, G., Fernández, B., & Bonmatí, A. (2015). Addition of crude glycerine as strategy to balance the C/N ratio on sewage sludge thermophilic and mesophilic anaerobic co-digestion. *Bioresour. Technol.*, *193*, 377-385. [doi:10.1016/j.biortech.2015.06.098](https://doi.org/10.1016/j.biortech.2015.06.098)
- Singh, G., Kawatra, A., & Sehgal, S. (2001). Nutritional composition of selected green leafy vegetables, herbs and carrots. *Plant Foods for Human Nutrition*, *56*(4), 359-364. [doi: 10.1023/A:1011873119620](https://doi.org/10.1023/A:1011873119620)
- Siqueira, R. M., Freitas, G. R., Peixoto, H. R., Do Nascimento, J. F., Musse, A. P. S., Torres, A. E., . . ., & Bastos-Neto, M. (2017). Carbon dioxide capture by pressure swing adsorption. *Energy procedia*, *114*, 2182-2192. [doi: 10.1016/j.egypro.2017.03.1355](https://doi.org/10.1016/j.egypro.2017.03.1355)

- Smith, K. R., Bruce, N., Balakrishnan, K., Adair-Rohani, H., Balmes, J., Chafe, Z., . . . , & Pope, D. (2014). Millions dead: how do we know and what does it mean? Methods used in the comparative risk assessment of household air pollution. *Annual review of public health, 35*, 185-206. [doi:10.1146/annurev-publhealth-032013-182356](https://doi.org/10.1146/annurev-publhealth-032013-182356)
- Soeprijanto, S., Prajitno, D., Setiawan, B., Maghfiro, W., & Rohmawati, R. (2021). *Biogas production from co-digestion of water hyacinth, banana peel and water spinach wastes using a horizontal anaerobic digester*. Paper presented at the IOP Conference Series: Earth and Environmental Science.
- Song, Z., Li, Y., Yang, G., Qin, J., Ren, G., & Feng, Y. (2010). Effect of total solid concentration and temperature on biogas yields of mixture of chicken manure and corn straw. *Transactions of the Chinese Society of Agricultural Engineering, 26*(7), 260-265.
- Sreekrishnan, T., Kohli, S., & Rana, V. (2004). Enhancement of biogas production from solid substrates using different techniques—a review. *Bioresource technology, 95*(1), 1-10. [doi:10.1016/j.biortech.2004.02.010](https://doi.org/10.1016/j.biortech.2004.02.010)
- Suhartini, S., Nurika, I., Paul, R., & Melville, L. (2021). Estimation of biogas production and the emission savings from anaerobic digestion of fruit-based agro-industrial waste and agricultural crops residues. *BioEnergy Research, 14*(3), 844-859. [doi:10.1007/s12155-020-10209-5](https://doi.org/10.1007/s12155-020-10209-5)
- Sun, Q., Li, H., Yan, J., Liu, L., Yu, Z., & Yu, X. (2015). Selection of appropriate biogas upgrading technology-a review of biogas cleaning, upgrading and utilisation. *Renewable and Sustainable Energy Reviews, 51*, 521-532. [doi:10.1016/j.rser.2015.06.029](https://doi.org/10.1016/j.rser.2015.06.029)
- Syaichurrozi, I. (2018). Biogas production from co-digestion *Salvinia molesta* and rice straw and kinetics. *Renewable Energy, 115*, 76-86. [doi:10.1016/j.renene.2017.08.023](https://doi.org/10.1016/j.renene.2017.08.023)
- Syed, M., Soreanu, G., Falletta, P., & Béland, M. (2006). Removal Of Hydrogen Sulfide From Gas Streams Using Biological Processes A Review. *Canadian Biosystems Engineering, 48*, 2).
- Tan, Y., Nookuea, W., Li, H., Thorin, E., & Yan, J. (2017). Cryogenic technology for biogas upgrading combined with carbon capture-a review of systems and property impacts. *Energy procedia, 142*, 3741-3746. [doi:10.1016/j.egypro.2017.12.270](https://doi.org/10.1016/j.egypro.2017.12.270)
- Tasnim, F., Iqbal, S. A., & Chowdhury, A. R. (2017). Biogas production from anaerobic co-digestion of cow manure with kitchen waste and Water Hyacinth. *Renewable Energy, 109*, 434-439. [doi:10.1016/j.renene.2017.03.044](https://doi.org/10.1016/j.renene.2017.03.044)
- Tchobanoglus, G., Burton, F., & Stensel, H. D. (2003). Wastewater engineering: treatment and reuse. *American Water Works Association. Journal, 95*(5), 201.
- Thanakunpaisit, N., Jantarachat, N., & Onthong, U. (2017). Removal of hydrogen sulfide from biogas using laterite materials as an adsorbent. *Energy procedia, 138*, 1134-1139. [doi:10.1016/j.egypro.2017.10.215](https://doi.org/10.1016/j.egypro.2017.10.215)

- Thuy, L. B., & Chi, T. D. (2016). Application of iron-based adsorbent (FEOOH) to remove hydrogen sulfide (H₂S) from biogas. *Journal of Science and Technology*, 54(2A), 35-41.
- Toro, P., Quijada, R., Yazdani-Pedram, M., & Arias, J. L. (2007). Eggshell, a new bio-filler for polypropylene composites. *Materials letters*, 61(22), 4347-4350. doi:[10.1016/j.matlet.2007.01.102](https://doi.org/10.1016/j.matlet.2007.01.102)
- Toutian, V., Barjenbruch, M., Unger, T., Loderer, C., & Remy, C. (2020). Effect of temperature on biogas yield increase and formation of refractory COD during thermal hydrolysis of waste activated sludge. *Water research*, 171, 115383. doi:[10.1016/j.watres.2019.115383](https://doi.org/10.1016/j.watres.2019.115383)
- Traoré, K., Parkouda, C., Savadogo, A., Ba/Hama, F., Kamga, R., & Traoré, Y. (2017). Effect of processing methods on the nutritional content of three traditional vegetables leaves: Amaranth, black nightshade and jute mallow. *Food Science & Nutrition*, 5(6), 1139-1144. doi:[10.1002/fsn3.504](https://doi.org/10.1002/fsn3.504)
- Tripathi, S. K., Kaur, D., Bhardwaj, N. K., Pathak, P., & Kumar, S. (2021). Improving Biogas Production by Co-digestion of Banana Stem Juice with Agro-Based Material Washings and Digestate Along with Microbial Culture. *Waste and biomass valorization*, 12(3), 1385-1393. doi:[10.1007/s12649-020-01101-6](https://doi.org/10.1007/s12649-020-01101-6)
- Tsai, W.-T., Hsien, K.-J., Hsu, H.-C., Lin, C.-M., Lin, K.-Y., & Chiu, C.-H. (2008). Utilization of ground eggshell waste as an adsorbent for the removal of dyes from aqueous solution. *Bioresource technology*, 99(6), 1623-1629. doi:[10.1016/j.biortech.2007.04.010](https://doi.org/10.1016/j.biortech.2007.04.010)
- Uhunamure, S., Nethengwe, N., & Tinarwo, D. (2019). Correlating the factors influencing household decisions on adoption and utilisation of biogas technology in South Africa. *Renewable and Sustainable Energy Reviews*, 107, 264-273. doi:[10.1016/j.rser.2019.03.006](https://doi.org/10.1016/j.rser.2019.03.006)
- Upadhyay, A., Kovalev, A. A., Zhuravleva, E. A., Kovalev, D. A., Litti, Y. V., Masakapalli, S. K., . . . , & Vivekanand, V. (2022). Recent Development in Physical, Chemical, Biological and Hybrid Biogas Upgradation Techniques. *Sustainability*, 15(1), 476. doi:[10.3390/su15010476](https://doi.org/10.3390/su15010476)
- Vareda, J. P. (2023). On validity, physical meaning, mechanism insights and regression of adsorption kinetic models. *Journal of Molecular Liquids*, 121416. doi:[10.1016/j.molliq.2023.121416](https://doi.org/10.1016/j.molliq.2023.121416)
- Vats, N., Khan, A. A., & Ahmad, K. (2019). Effect of substrate ratio on biogas yield for anaerobic co-digestion of fruit vegetable waste & sugarcane bagasse. *Environmental Technology & Innovation*, 13, 331-339. doi:[10.1016/j.eti.2019.01.003](https://doi.org/10.1016/j.eti.2019.01.003)
- Vijayakumar, P., Ayyadurai, S., Arunachalam, K. D., Mishra, G., Chen, W.-H., Juan, J. C., & Naqvi, S. R. (2022). Current technologies of biochemical conversion of food waste into biogas production: A review. *Fuel*, 323, 124321. doi:[10.1016/j.fuel.2022.124321](https://doi.org/10.1016/j.fuel.2022.124321)

- Vinhal, J. O., Nege, K. K., Lage, M. R., Carneiro, J. W. d. M., Lima, C. F., & Cassella, R. J. (2017). Adsorption of the herbicides diquat and difenzoquat on polyurethane foam: Kinetic, equilibrium and computational studies. *Ecotoxicology and Environmental Safety*, 145, 597-604. [doi:10.1016/j.ecoenv.2017.08.005](https://doi.org/10.1016/j.ecoenv.2017.08.005)
- Wakaba, D., Ateka, J., Mbeche, R., & Oyugi, L. (2022). Determinants of Irish potato (*Solanum tuberosum*) commercialization and market participation by farmers in Nyandarua County, Kenya. *Journal of Agriculture and Food Research*, 10, 100382. [doi:10.1016/j.jafr.2022.100382](https://doi.org/10.1016/j.jafr.2022.100382)
- Wandera, S. M., Westerholm, M., Qiao, W., Yin, D., Jiang, M., & Dong, R. (2019). The correlation of methanogenic communities' dynamics and process performance of anaerobic digestion of thermal hydrolyzed sludge at short hydraulic retention times. *Bioresource technology*, 272, 180-187. [doi:10.1016/j.biortech.2018.10.023](https://doi.org/10.1016/j.biortech.2018.10.023)
- Wang, N. (2013). Adsorption of Hydrogen Sulfide on Fine Rubber Particle Media (FRPM). *Graduate Theses and Dissertations*, 13110.
- Wang, Y., Li, G., Chi, M., Sun, Y., Zhang, J., Jiang, S., & Cui, Z. (2018). Effects of co-digestion of cucumber residues to corn stover and pig manure ratio on methane production in solid state anaerobic digestion. *Bioresource technology*, 250, 328-336. [doi:10.1016/j.biortech.2017.11.055](https://doi.org/10.1016/j.biortech.2017.11.055)
- Wang, Z., Ali, S., Akbar, A., & Rasool, F. (2020). Determining the influencing factors of biogas technology adoption intention in Pakistan: The moderating role of social media. *International Journal of Environmental Research and Public Health*, 17(7), 2311. [doi:10.3390/ijerph17072311](https://doi.org/10.3390/ijerph17072311)
- Wang'ombe, J. G., & van Dijk, M. P. (2015). Sharing gains of the potato in Kenya: A case of thin governance. *International Journal of Agricultural Marketing*, 2(2), 34-45.
- Ward, A. J., Hobbs, P. J., Holliman, P. J., & Jones, D. L. (2008). Optimisation of the anaerobic digestion of agricultural resources. *Bioresource technology*, 99(17), 7928-7940. [doi:10.1016/j.biortech.2008.02.044](https://doi.org/10.1016/j.biortech.2008.02.044)
- Watanabe, S. (2021). Chemistry of H₂S over the surface of common solid sorbents in industrial natural gas desulfurization. *Catalysis Today*, 371, 204-220. [doi:10.1016/j.cattod.2020.05.064](https://doi.org/10.1016/j.cattod.2020.05.064)
- Weinlaender, C., Neubauer, R., Hauth, M., & Hochenauer, C. (2017). Removing H₂S from biogas using sorbents for solid oxide fuel cell applications. *Chemie Ingenieur Technik*, 89(9), 1247-1254. [doi:10.1002/cite.201600167](https://doi.org/10.1002/cite.201600167)
- Werkneh, A. A. (2022). Biogas impurities: environmental and health implications, removal technologies and future perspectives. *Heliyon*. [doi:10.1016/j.heliyon.2022.e10929](https://doi.org/10.1016/j.heliyon.2022.e10929)
- Witton, T. (2011). Characterization of calcium oxide derived from waste eggshell and its application as CO₂ sorbent. *Ceramics International*, 37(8), 3291-3298. [doi:10.1016/j.ceramint.2011.05.125](https://doi.org/10.1016/j.ceramint.2011.05.125)

- Xie, S., Hai, F. I., Zhan, X., Guo, W., Ngo, H. H., Price, W. E., & Nghiem, L. D. (2016). Anaerobic co-digestion: A critical review of mathematical modelling for performance optimization. *Bioresource technology*, 222, 498-512. doi:10.1016/j.biortech.2016.10.015
- Xie, S., Wickham, R., & Nghiem, L. D. (2017). Synergistic effect from anaerobic co-digestion of sewage sludge and organic wastes. *International Biodeterioration & Biodegradation*, 116, 191-197. doi:10.1016/j.ibiod.2016.10.037
- Xu, N., Liu, S., Xin, F., Zhou, J., Jia, H., Xu, J., . . . , & Dong, W. (2019). Biomethane production from lignocellulose: biomass recalcitrance and its impacts on anaerobic digestion. *Frontiers in bioengineering and biotechnology*, 7, 191. doi:10.3389/fbioe.2019.00191
- Xu, Y., Huang, Y., Wu, B., Zhang, X., & Zhang, S. (2015). Biogas upgrading technologies: Energetic analysis and environmental impact assessment. *Chinese Journal of Chemical Engineering*, 23(1), 247-254. doi:10.1016/j.cjche.2014.09.048
- Xu, Z., Cai, J.-G., & Pan, B.-C. (2013). Mathematically modeling fixed-bed adsorption in aqueous systems. *Journal of Zhejiang University Science A*, 14(3), 155-176. doi: 10.1631/jzus.A1300029
- Yagub, M. T., Sen, T. K., Afroze, S., & Ang, H. M. (2014). Dye and its removal from aqueous solution by adsorption: a review. *Advances in colloid and interface science*, 209, 172-184. doi:10.1016/j.cis.2014.04.002
- Yakub, E., Agarry, S. E., Omoruwou, F., & Owabor, C. N. (2020). Comparative study of the batch adsorption kinetics and mass transfer in phenol-sand and phenol-clay adsorption systems. *Particulate Science and Technology*, 38(7), 801-811. doi:10.1080/02726351.2019.1616862
- Yan, Y., An, Q., Xiao, Z., Zheng, W., & Zhai, S. (2017). Flexible core-shell/bead-like alginate@ PEI with exceptional adsorption capacity, recycling performance toward batch and column sorption of Cr (VI). *Chemical Engineering Journal*, 313, 475-486. doi:10.1016/j.cej.2016.12.099
- Yavini, T. D., Chia, A. I., & John, A. (2014a). Evaluation of the effect of total solids concentration on biogas yields of agricultural wastes. *Int. Res. J. Environ. Sci*, 3(2), 70-75.
- Yavini, T. D., Chia, A. I., & John, A. (2014b). Evaluation of the effect of total solids concentration on biogas yields of agricultural wastes. *Int Res J Environ Sci*, 3(2), 70.
- Yellezuome, D., Zhu, X., Wang, Z., & Liu, R. (2022). Mitigation of ammonia inhibition in anaerobic digestion of nitrogen-rich substrates for biogas production by ammonia stripping: A review. *Renewable and Sustainable Energy Reviews*, 157, 112043. doi:10.1016/j.rser.2021.112043
- Yun, Y.-M., Cho, S.-K., Kim, H.-W., Jung, K.-W., Shin, H.-S., & Kim, D.-H. (2015). Elucidating a synergistic effect of food waste addition on the enhanced anaerobic digestion of waste activated sludge. *Korean Journal of Chemical Engineering*, 32, 1542-1546. doi:10.1007/s11814-014-0271-4

Zhang, W., Deng, Q., He, Q., Song, J., Zhang, S., Wang, H., . . . , & Zhang, H. (2018). A facile synthesis of core-shell/bead-like poly (vinyl alcohol)/alginate@ PAM with good adsorption capacity, high adaptability and stability towards Cu (II) removal. *Chemical Engineering Journal*, 351, 462-472. [doi:10.1016/j.cej.2018.06.129](https://doi.org/10.1016/j.cej.2018.06.129)

APPENDICES

Appendix I: Research Output

Published Journal articles

1. **Register Mrosso**, Achisa C Mecha, and Joseph Kiplagat, 2023. Characterization of Kitchen and Municipal Organic Waste for Biogas Production: Effect of Parameters. *Heliyon* Vol 9: (2023) e16360, 1-8. <https://doi.org/10.1016/j.heliyon.2023.e16360>.
2. **Register Mrosso**, Joseph Kiplagat, and Achisa C Mecha, (2023). Anaerobic co-digestion of tuber waste and fruit waste: synergy and enhanced biogas production. *International Journal of Chemical Engineering*. Volume 2023, Article ID 6637249, <https://doi.org/10.1155/2023/6637249>
3. **Register Mrosso**, Achisa C Mecha, and Joseph Kiplagat, 2023. Biogas sweetening using new sorbent derived from Soda ash from Lake Natron, Tanzania. *Cleaner Engineering and Technology* 14 (2023) 100646 <https://doi.org/10.1016/j.clet.2023.100646>.

Accepted manuscript

1. Carbon dioxide removal using a novel adsorbent derived from calcined eggshell waste for biogas upgrading. *South Africa Journal of Chemical Engineering*, Elsevier.

Revised manuscripts submitted for publication

1. Natural and low-cost sorbents as a solution for biogas upgrading: A review. *Bioresources and Technology Report*. Elsevier.

The manuscript to be submitted

1. Hydrogen Sulfide Removal from Biogas Using Sorbent Obtained from Organic and Inorganic Material: A review

Conference presentations; accepted manuscripts

1. A new novel derived from sodium carbonate for the elimination of hydrogen sulfide from biogas. **39th JOHANNESBURG International Conference on “Chemical, Biological and Environmental Engineering” (JCBEE-23)**. November 16-17, 2023.
2. Co-digestion of Fruit and Tuber waste for Biogas Enhancement: A Synergy Effect. **39th JOHANNESBURG International Conference on “Chemical, Biological and Environmental Engineering” (JCBEE-23)**. November 16-17, 2023.

Appendix II: Plagiarism Certificate



SR357

ISO 9001:2019 Certified Institution

THESIS WRITING COURSE

PLAGIARISM AWARENESS CERTIFICATE

This certificate is awarded to

REGISTER W. MROSSO

PHD/ES/5731/21

In recognition for passing the University's plagiarism

Awareness test for Thesis entitled: **BIOGAS PRODUCTION FROM KITCHEN WASTE CO - DIGESTED WITH SELECTED MUNICIPAL SOLID WASTE AND ITS PURIFICATION USING SODA ASH FROM LAKE NATRON AND EGG SHELLS WASTE** with a similarity index of 14% and striving to maintain academic integrity.

Word count: 55037

Awarded by

Prof. Anne Syomwene Kisiu

CERM-ESA Project Leader Date: 27/10/2023